The preventive effect of greenshell mussel meat against osteoarthritis *in vivo*

A thesis presented in partial fulfilment of
The requirements for the degree of

Doctor of Philosophy

in

Health Science

At Massey University, Palmerston North,

New Zealand

Parkpoom Siriarchavatana

2021

Abstract

Osteoarthritis (OA) is identified by progressive cartilage erosion of synovial joints. One of the most prevalent OA phenotypes, metabolic OA (MetOA), is linked to metabolic syndrome (MetS). MetS is a combination of obesity, type II diabetes, hypertension, and hyperlipidemia; the effects of these disorders can lead to the development of MetOA. Osteoporosis is characterised by loss of bone mineral density and is causally linked with a decrease in systemic estrogen levels. As MetS, OA and osteoporosis are all prevalent in postmenopausal women, it is possible they may be causally linked. For example, systemic low-grade inflammation in MetS may trigger inflammation in both joints and bone, which could be further aggravated by high fat/high sugar diet (HFHS)-induced obesity and gut dysbiosis.

We hypothesized that chronic inflammation would be correlated with MetOA development and therefore decreasing inflammation would be protective. New Zealand greenshell mussel (GSM) contains anti-inflammatory properties shown to reduce OA symptoms and omega-3 fatty acids shown to reduce the development of post-menopausal osteoporosis. We hypothesized GSM could protect against both MetOA and osteoporosis reducing bone resorption, inhibiting inflammation and/or modulating beneficial gut microbes.

In vitro, non-polar GSM lipids demonstrated bone-protective properties and significantly reduced osteoclast differentiation, tartrate-resistant acid phosphatase activity, actin ring formation and gene expression of matrix metalloproteinase, cathepsin K, carbonic anhydrase and nuclear factor of activating T cells 1. *In vivo*, aging, HFHS and OVX produced a rat model mimicking human MetS. Dietary whole GSM powder provided protection by significantly reducing a biomarker of collagen degradation and subsequent joint damage, as well as improving short-term bone mineral density and lean mass accrual. GSM-induced changes in gut microbiota were not correlated with dysbiosis. No changes in inflammatory markers were found, disproving our initial hypothesis and suggesting that chronic inflammation may not be a critical factor in MetOA. In conclusion, GSM as a dietary intervention may reduce the incidence or progression of MetOA but not via altering systemic inflammation or gut dysbiosis.

Acknowledgements

The achievement of doctoral degree demands an individual endurance and determination however the supports of the following people and organization are paramount importance. Therefore, I would like to thank these people who were in part of my success.

The most importance to make this study possible was financial support from Massey University PhD Scholarship and research funding from the National Science Challenge-High value nutrition (HVN) with the collaborations of Cawthron Institute and Sanford Ltd. In addition, I have to thank Mathew Miller and Sabrina Tian, my co-supervisors from the institute and company mentioned above respectively for their contribution of knowledge and experiences in chemical analysis.

I would like to thank staff who were involved in the experiments: Aimee Hamlin and all staff in the small animal production unit of Massey University for providing animal care and husbandry; Anne Broomfield, Louise Shaw and Corrin Hulls for their contribution in surgery and the operation of Dual energy X-ray absorptiometry; Gabrielle Plimmer and Shampa De who managed to collect the biological samples from the animal studies and contributed their experiences in cell culture and molecular assays. I thank you Wei-Hang Chua who was an examiner in my PhD confirmation and being available to respond my questions on various occasions. Finally, I am very grateful to Marlena Kruger and Fran Wolber, my Massey supervisors, who gave me an opportunity to study in Massey University and have helped support me from the glorious day of my first visit in New Zealand to the hard time of the pandemics.

This thesis was written in the time of Covid-19 disease spreading from one small area in China through all nations around the world. More than 20 million people were infected and many of them lost their life. New Zealand however decided to sacrifice the country economy in order to save people life by placing the early lockdown throughout the country. During this time, I had seen an incredible spirit of Kiwis fighting the problem with full of humour, patience and kindness. Their sacrifice in helping each other and taking part in the responsibility hampered the viral transmission

in the community. Therefore, I would like to cheer all Kiwis and the government for making a right decision and keeping this country safe for everyone.

One person who I would like to address here is Anne Broomfield. She supported me not only in the experiments but also encouraged me to develop my skill for various new assays. Her generosity and humility fostered our friendship. I remembered our conversation at the beginning of my study. She mentioned that she might not see my graduation because she would get her retirement before that. So, I bet her that I would graduate before her retirement. But at the end of the day, she won and I lost. She got her lifetime retirement before my graduation and we lost her forever during the Covid lockdown.

Table of Contents

List of Figures

List of Tables

Structure of the thesis

This thesis is written according to the Graduate Research School regulations for PhD thesis by publications. The list below presents the publication status of each chapter.

Chapter 1: Thesis introduction

This chapter was written by Parkpoom Siriarchavatana as an introductory section of this thesis and is not intended for publication.

Chapter 2: Literature review

Basic concepts in the pathogenesis of osteoarthritis and others diseases in association with the development of metabolic osteoarthritis (MetOA) are discussed. Later, the current evidence of promising compounds involving GSM is mentioned. Finally, ideas and concepts of animal models used in osteoarthritis research are revealed. This literature review was written by Parkpoom Siriarchavatana and is not for publication.

Chapter 3: The inhibitory effect of greenshell mussel (*Perna canaliculus*) lipids on osteoclast differentiation (Manuscript under revision by "Marine Drugs").

Experiment contribution: Siriarchavatana P. [1.2, 3.1, 3.2], Miller MR. [3.3]
Author contribution: Siriarchavatana P. [B,C,D,E,F], Kruger MC. [A,B,E], Miller MR. [A,E], Tian HS. [A,E], Wolber FM. [A,B,E]

Chapter 4: The influence of obesity, ovariectomy and greenshell mussel supplementation on bone mineral density in rats (Manuscript under consideration of "Journal of Bone and Mineral Research Plus").

Experiment contribution: Hamlin A., and SAPU staff[1.1], Broomfield AM.[2.1, 2.2, 2.3,], Shaw L. [2.1, 2.2, 2.3], Hulls C. [2.3], De S. [2.4], Plimmer G. [2.4], Miller MR. [3.3] Siriarchavatana P. [2.1, 2.3, 2.4], Wolber FM. [2.1, 2.4]
Author contribution: Siriarchavatana P. [B,C,D,E,F], Kruger MC. [A,B,E], Miller MR. [A,E], Tian HS. [A,E], Wolber FM. [A,B,E]

Chapter 5: The preventive effects of greenshell mussel (*Perna canliculus*) on early-stage metabolic osteoarthritis in rats with diet-induced obesity. (Published in Nutrients 2019, 11(7):1601)

Experiment contribution: Hamlin A., and SAPU staffs[(1.1)], Broomfield AM.[(2.1)], Shaw L.[(2.1)], De S.[(2.4)], Plimmer G.[(2.4)], Miller MR.[(3.3)], Siriarchavatana P.[(2.4, 3.1, 3.4)], Wolber FM. [(2.1, 2.4)]

Author contribution: Siriarchavatana P. [(B,C,D,E,F)], Kruger MC. [(A,B,E)], Miller MR. [(A,E)], Tian HS. [(A,E)], Wolber FM. [(A,B,E)]

Chapter 6: Effect of greenshell mussel intake on pathological markers of multiple phenotypes of osteoarthritis in rats (Manuscript submitted to "Arthritis Research and Therapy").

Experiment contribution: Hamlin A., and SAPU staffs[(1.1)], Broomfield AM.[(2.1, 2.2, 2.3,)], Shaw L. [(2.1, 2.2, 2.3)], Hulls C. [(2.3)], De S. [(2.4, 3.2)], Plimmer G. [(2.4)], Siriarchavatana P. [(2.1, 2.2, 2.3, 2.4, 3.1, 3.2, 3.4)], Wolber FM. [(2.1, 2.4)]

Author contribution: Siriarchavatana P. [(B,C,D,E,F)], Kruger MC. [(A,B,E)], Miller MR. [(A,E)], Tian HS. [(A,E)], Wolber FM. [(A,B,E)]

Chapter 7: The influence of high fat/high sugar diets, ovariectomy and greenshell mussel supplement on the alteration of gut microbiota and relating pathological changes (Manuscript under preparation).

Experiment contribution: Hamlin A., and SAPU staff [(1.1)], Broomfield AM.[(2.1, 2.2, 2.3,)], Shaw L. [(2.1, 2.2, 2.3)], Hulls C. [(2.3)], De S. [(2.4, 3.2)], Plimmer G. [(2.4)], Siriarchavatana P. [(2.1, 2.2, 2.3, 2.4, 3.1, 3.2, 3.4)], Wolber FM. [(2.1, 2.4)]

Author contribution: Siriarchavatana P. [(B,C,D,E,F)], Kruger MC. [(A,B,E)], Miller MR. [(A,E)], Tian HS. [(A,E)], Wolber FM. [(A,B,E)]

Chapter 8: Thesis discussion and conclusion

This chapter was written by Parkpoom Siriarchavatana as a discussion section of this thesis and is not intended for publication.

Experiment contribution
Routine procedure
1.1= animal care and husbandry, 1.2=cell culture
Animal experiment
2.1=feeding, 2.2=DXA scans, 2.3=surgery, 2.4=necropsy
Analytical methods
3.1=biological analysis, 3.2=molecular analysis, 3.3=chemical analysis, 3.4=histopathological examination

Author contribution
A=conceptualization, B=methodology, C=data analysis, D=original draft, E=review and editing, F=visualization

Abbreviations

AA	arachidonic acid
ADAMTS	A disintergrin and metalloproteinase with thrombospondin type I motif
ALA	alpha linolenic acid
BMD	bone mineral density
BMC	bone mineral content
BW	body weight
C1M	connective tissue type I collagen turnover
CAII	carbonic anhydrase II
CCR2	chemokine receptor type2
CN	catalogue number
COMP	cartilage oiligomeric protein
COX	cyclooxygenase
CRP	C-reactive protein
CTX-II	C-telopeptide of type II collagen
CXCL	chemokine ligand
DHA	docosahexaenoic acid
DMSO	dimethyl sulfoxide
DPA	docosapentaenoic acid
DXA	dual energy x-ray absorptiometry
EDTA	Ethylenediaminetetraacetic acid
EPA	eicosapentaenoic acid
FA	fatty acid
FFAR	free fatty acid receptor
GAPDH	Glyceraldehyde 3-phosphate dehydrogenase
GIT	gastrointestinal tract
Glu-Gal-PYD	Glucosyl-Galactosyl-Pyridinoline
GRO-KC	growth-regulated oncogenes/keratinocyte chemoattractant
GSM	greenshell mussel
HA	hyaluronic acid
HbA1c	hemoglobin A1c

HFHS	high fat high sugar diet
HMGB1	high mobility group box 1
ICAM-1	intercellular adhesion molecule-1
IFN-γ	Interferon gamma
IL	interleukin
IP10	interferon gamma-induced protein 10
LA	linoleic acid
LC-PUFA	long chain polyunsaturated fatty acid
LPC	lysophosphatidylcholine
LPS	lipopolysaccharide
LXR	liver X receptors
MetOA	metabolic osteoarthritis
MetS	metabolic syndrome
MCP-1	monocyte chemoattractant protein-1
M-CSF	macrophage colony stimulation factor
MIP	macrophage inflammatory proteins
MMP	matrix metalloproteinase
MUFA	monounsaturated fatty acid
MTT	3-(4,5-dimethylthiazol-2-yl)-2,5-diphenyltetrazolium bromide
NAFLD	non-alcoholic fatty liver disease
n-3PUFA	omega-3 fatty acid
n-3LCPUFA	long chain omega-3 fatty acid
n-6PUFA	omega-6 fatty acid
ND	normal control diet
NFATc1	nuclear factor of activated T-cells, cytoplasmic 1
NF-κB	nuclear factor κB
NOS2	nitric oxide synthase II
NSAID	nonsteroidal anti-inflammatory drug
OA	osteoarthritis
OPG	osteoprotegerin
OVX	ovariectomy
PA	palmitic acid
PAI-1	plasminogen activation inhibitor-1
PC	phosphatidylcholine

PCR	polymerase chain reaction
PGE2	prostaglandin E2
PHA	phytohemagglutinin
PMA	phorbol myristate acetate
PLA_2	phospholipaseA_2
PPAR	peroxisome proliferator activated receptor
PUFA	polyunsaturated fatty acid
RANK	receptor activator of nuclear factor κB
RANKL	receptor activator of nuclear factor κB ligand
SCFA	short chain fatty acid
SFA	saturated fatty acid
T2D	type II diabetes
TLR	toll-like receptor
TNF-α	tumour necrosis factor alpha
TRAP	tartrate-resistant acid phosphatase
VCAM-1	vascular cell adhesion molecule-1
VEGF	vascular endothelial growth factor

Chapter 1: Introduction

1.1 Thesis background

The industrial and green revolutions of human society in the 20th century have had an impact on increasing food production and consumption worldwide (Pingali, 2012). The industrial revolution transformed the manual production methods to a new era of machinery production processes with the assists of powerful engines, iron production, and new chemical manufacturing. These further had an immense impact on the agricultural sector's so-called 'green revolution'. The use of new technologies in machines, chemical fertilizers, pesticides and irrigation systems helped increase agricultural production worldwide. As a result, the rate of population growth and the standard of living for the general population were raised in the late 20th century. Undeniably, these revolutions provide immense benefits of food security to mankind however, there have been some negative effects on human health (Graber, 1995). As a consequence, non-communicable diseases have increased globally and can be at least partially attributed to changes in lifestyles, environment and diet (Forouzanfar et al., 2016). One of these widespread diseases, osteoarthritis (OA), is associated with aging, diet and other health conditions and is of concern for public health. Its prevalence and incidence have been increasing as there is no specific treatment to stop the disease progression (Woolf & Pfleger, 2003). Palliative treatments are used to ease the pain with non-steroidal or steroidal anti-inflammatory drugs (Bijlsma et al., 2011). The World Health Organization (WHO) declared in 2017 that OA was a global burden of disease which affected 303 million people globally (Kloppenburg & Berenbaum, 2020) and predicted OA would be the fourth leading cause of disability in the year 2020 (Woolf & Pfleger, 2003). This number is expected to continue rising if there is no effective treatment for the disease. In order to control this disease burden, a new paradigm may need to be accepted to change the perspective of OA from a disease originating from cartilage tissue, which wears out over time and is unable to heal, to a disease arising from multiple causes which could possibly be prevented before it is initiated.

In Western countries, diets and cooking styles that traditionally incorporated cooking whole foods at home daily have been partially replaced with factory-processed

ready-to-eat foods. For example, people in the past mainly used to consume oil and fat from animals. When it was found that saturated fatty acid in animal fat was a cause of chronic heart disease (Kris-Etherton et al., 2007), plant oils became a preferred alternative. Plant oil, which is produced in large volumes from the agroindustry, has become a mainstream source of cooking oil in many communities. However, animal oils, especially fish oils, are rich in the long chain omega-3 fatty acids that are less prevalent in plant oils (Howe et al., 2007; Saini & Keum, 2018). Omega-3 is a particularly beneficial nutrient because its biological activities have been reported to prevent cardiovascular disease, inflammation, hypertension and cancer (Punia et al., 2019). Sourcing omega-3 to meet the global consumption demand is unlikely to be achieved from land livestock as the expansion of human activities on land will increase deforestation and environmental degradation. Therefore, an alternative source of these healthy oils from marine animals such as greenshell mussel is promising.

Having plenty of food and easy access to food are the reason for the first time in human history that more people die from over nutrition than due to starvation (Dellorto, 2012). Obesity, a contributor of premature death, is on the rise worldwide (World Health Organization, 2020). It is recognized as the predisposing cause of metabolic syndrome, type II diabetes (T2D), hypertension, and heart disease (Mitchell et al., 2011). In addition, the complex condition of OA that displays multiple phenotypes is correlated with obesity and osteoporosis in post-menopausal women (Mobasheri et al., 2017). For instance, the increased load on joints in obesity is not the only factor which causes OA. Various systemic mediators arising from adipose tissue cause inflammation centrally and locally, leading to synovitis and cartilage destruction (Collins et al., 2015b; Malfait, 2016; Azamar-Llamas et al., 2017) and bone remodeling via the activity of bone-resorbing osteoclasts (Ilich et al., 2014). It is still not conclusive whether the pathogenesis of OA is initiated on the surface cartilage layer or deeper inside the subchondral bone layer. Animal studies have indicated an increase in subchondral bone inflammation before cartilage erosion started (Li et al., 2013; Bertuglia et al., 2016; Lofvall et al., 2018). There is therefore an intimate relationship between cartilage and bone at the joints which could explain the increase in the prevalence of both osteoporosis and OA in post-menopausal women (Woolf & Pfleger, 2003), in whom bone strength is commonly reduced and adiposity is commonly increased. Therefore, both lack of estrogen and increased adiposity may have a negative effect on OA.

Adipocytes on the other hand are an alternative source of estrogen for women after the menopausal period (Rosen & Klibanski, 2009) so there remains a controversy as to whether obesity has a benefit to mitigate OA and osteoporosis.

Greenshell mussel (GSM) (*Perna canaliculus*) is an important commercial marine species of New Zealand. Its lipid fraction (total lipid extract) contain 42.4-45.6% (Miller et al., 2014a) of the long-chain omega-3 polyunsaturated fatty acids (PUFAs) eicosapentaenoic acid (20:5n-3 EPA) and docosahexaenoic (22:6n-3 DHA), as well as various types of minor fatty acids: 5,9,12,15-octadecatetrenoic acid (C18:4); 5,9,12,16-nonadecatetraenoic acid (C19:4); 7,11,14,17-eicosatetraenoic acid (C20:4); and 5,9,12,15,18-heneicosapentaenoic acid (C21:5) (Treschow et al., 2007). Long-chain omega-3 PUFAs such as EPA and DHA compounds are known to have anti-inflammatory properties (Punia et al, 2014). In particular, the GSM oil fraction extracted by a supercritical fluidic CO_2 method has been shown to have an inhibitory effect on prostaglandin E2 (PGE2) in lipopolysaccharide (LPS)-activated mononuclear cells (Whitehouse et al., 1997) via both the cyclooxygenase pathway (McPhee et al., 2007) and the lipoxygenase pathway (Treschow et al., 2007), which are the enzymatic processes used to cleave arachidonic acid into proinflammatory mediators such as PGE2, thromboxane, and leukotrienes. Its molecular mechanisms have been studied in LPS-induced RAW 264.7 cells and were found to involve the NF-κB and MAPK kinase signaling pathways (Chen et al., 2017).

This study evaluated the preventive effects of GSM in rats models of OA induced by combinations of age, diet-driven obesity, and ovariectomy, based on previous evidence which showed GSM oil has an anti-inflammatory property (Whitehouse et al., 1997; Chen et al., 2017; McPhee et al., 2007). In addition, an osteoclast differentiation assay was conducted *in vitro* to investigate cell mechanisms associated with the potential effects of GSM on osteoporosis prevention. Further, some controversial issues within the complex relationships between obesity, menopause, joint health, and bone health were explored. Finally, changes in gut microbiota due to diet and its relationship with the observed pathological changes of OA *in vivo* were explored.

1.2 Objectives and research questions

This PhD project was funded by the National Science Challenge, High Value Nutrition (HVN) “Musseling up: high-value Greenshell™ mussel foods” (UOAX1421)”

and a Massey University College of Health PhD scholarship, as collaboration between Massey University, Cawthron Institute, and Sanford Ltd. The project addressed three research questions in two objectives.

Objective 1: The main objective of this study was to evaluate the potential of GSM in MetOA prevention in rats with MetOA at two stages induced through a combination of age, ovariectomy, and/or obesity.

Question 1: Does the biological activity of GSM lipids involve the bone remodeling process?

Hypothesis: the pathogenesis of MetOA is related to subchondral bone integrity which is altered by the effect of estrogen deficiency.

Question 2: Can GSM alleviate osteoarthritis in rats induced by MetS-inducing factors (aging, obesity, and ovariectomy)?

Hypothesis: Low-grade inflammation is involved in the pathogenesis of many chronic diseases. Omega-3 fatty acids possess anti-inflammatory property and GSM contains a high amount of omega-3 fatty acid. Therefore, this compound may exert the preventive effect of MetOA.

Objective 2: The secondary objective was to reveal the involvement of MetS-inducing factors with initiating OA in rats.

Question 3: How do aging, diet, ovariectomy and GSM influence rat body weight, bone health, gut health, and knee joint health during the course of MetOA development?

Hypothesis: Obesity induced by high fat and high sugar diet in rats will develop metabolic syndrome, with concurrent chronic low-grade inflammation that should induce osteoarthritis. As the result of ovariectomy in a subgroup of rats, the rats will lack estrogen, which will accelerate obesity and bone turnover rate simultaneously. Both consequences might aggravate osteoarthritis. In addition, the alteration of gut microbiota due to those factors may associate with OA development.

1.3 Thesis introduction

Chapter 2 defines the scope of this thesis and elaborates the current knowledge about the pathogenesis of osteoarthritis and associated disorders in the disease development. The previous research of GSM in relation to be a candidate dietary

intervention for OA is summarised. Chapter 3 investigates three fractions of GSM lipids in an osteoclast differentiation assay. Chapter 4 evaluates the effect of GSM powder on body composition and bone mass in rats. Chapter 5 studies the preventive effect of GSM on early pathogenesis of OA in rats after 3 months on high energy diet. Chapter 6 studies the long-term effect of MetS-inducing factors on the development of OA in rats with the goal of identifying a specific pattern or a prognostic biomarker. The effect of GSM on MetOA is evaluated simultaneously. Chapter 7 focuses on the alteration of gut microbiota and pathological lesions in organs from MetS-inducing factors, and any mitigating effects by GSM. Chapter 8 presents a general discussion on all findings of the study, limitations, suggestions for further work, and final conclusions.

.

Chapter 2: Literature Review

2.1 Osteoarthritis (OA)

2.1.1 Definition and characteristics

OA is a chronic disease of the joints and bone with the presence of articular cartilage erosion that results in progressive pain and joint immobility. Cartilage is not the only affected tissue in this pathogenesis as muscles and tendons surrounding the joints, synovium and subchondral bone are also impacted. The comprehensive definition given by the Osteoarthritis Research Society International (OARSI) states "Osteoarthritis is a disorder involving movable joints characterized by cell stress and extracellular matrix degradation initiated by micro- and macro-injury that activates maladaptive repair responses including pro-inflammatory pathways of innate immunity. The disease manifests first as a molecular derangement (abnormal joint tissue metabolism) followed by anatomic, and/or physiologic derangements (characterized by cartilage degradation, bone remodelling, osteophyte formation, joint inflammation and loss of normal joint function), that can culminate in illness" (Kraus et al., 2015). OA can be classified into four phenotypes based on the aetiology: post-traumatic OA, age-related OA, genetic predisposition, and metabolic syndrome associated with OA (MetOA) (Kuyinu et al., 2016).

People suffering from OA experience intermittent joint pain and stiffness, especially in the morning or after a period of non-weight-bearing activities. OA causes a reduction of joint mobility, inflammation, and also joint enlargement when synovial fluid effusion is present (Bijlsma et al., 2011). Further, crepitus sounds may be detected when performing passive or active movement of a joint. In chronic cases, joint deformities can develop with the pathological lesions of cartilage destruction, subchondral bone microstructural damage, synovitis, bursitis, and inflammation of ligaments and muscles around the joints (Bijlsma et al., 2011).

2.1.2 Diagnosis and biomarkers in OA

There are many challenges in clinical practice to determine an early diagnosis of OA and provide effective treatments to prevent the progressive cartilage deterioration. Firstly, clinical signs and symptoms are not specific to the disease as the involvement of

ligament or muscle pain is common in other types of arthritis. The physical symptoms can be sufficiently minor or stable for several years during the disease progression that patients might not be aware of the serious consequences until articular cartilage loss is severe (Bijlsma et al., 2011). This late diagnosis is due to articular cartilage layers having a lack of nerve innervation and vascular access; therefore, the subsequent inflammatory mediators created by the lesions to activate pain sensation are reduced and not conveyed to the central nervous system (Litwic et al., 2013).

Another issue in the clinical diagnosis of evaluating structural changes of OA is that there are no specific tools or criteria for physical examination to identify OA with certainty at an early stage (Rousseau & Garnero, 2012). Insensitive monitoring methods are at least partly responsible for the non-corresponding relationship between clinical symptoms and pathological changes. Other invasive methods such as biopsies can give more specific information and allow histochemical assessment of cartilage, bone, and synovium but these methods have a contraindication in tissue injury and introducing joint infection. At present, the gold standard for diagnosing OA in clinical practice is imaging which includes plain radiography, computerised tomography (CT) scan and magnetic resonance imaging (MRI). Imaging can reveal the pathognomonic changes of OA such as osteophyte formation, joint-space narrowing and bone sclerosis but these are detectable only at the later stages of the disease. Therefore, a sensitive biomarker for an early detection of OA would be beneficial to the prevention and treatment of progressive OA (Bijlsma et al., 2011).

Many biomarkers have been evaluated in clinical studies (Rousseau & Garnero, 2012; Mobasheri et al., 2017). However, only a few biomarkers are reliable and highly correlated with the pathological lesions (Mobasheri et al., 2017). The studies reporting biomarkers related to OA are discussed below. First of all, cartilage metabolism or the breakdown of the articular cartilage matrix which is composed of collagens, proteoglycans, glycoprotein and chondrocytes are used to determine the degradation of cartilage. Collagen type II is the most abundant protein specific for cartilage tissue. The degradation of type II collagen may result in many fragments but the key fragment known as C-telopeptide of type II collagen (CTX-II) has been intensively used in research studies (Cheng et al., 2018). CTX-II was found to be elevated in synovial fluid and serum of early-stage OA patients (Shinmei et al., 1993). CTX-II can be measured in serum and urine samples (Mobasheri et al., 2017). Increased CTX-II in urine (uCTX-II)

correlated with radiological scores (Meulenbelt et al., 2006). Data from a 5 year cohort study of hip and knee OA showed that uCTX-II and serum COMP (cartilage oligomeric protein) were positively and consistently correlated with the presence and progression of knee OA (Van Spil et al., 2015). Similar results were also found in a Rotterdam's study (Hosnijeh et al., 2016). However, the results from a clinical trial of oral salmon calcitonin in knee OA patients indicated that reduction of uCTX-II did not correspond to WOMAC pain and radiographic responses from the patients, making it difficult for uCTX-II to be used as a sole surrogate marker for OA (Karsdal et al., 2015).

Aggrecan, an abundant proteoglycan in cartilage, undergoes extensive structural changes between the formation of foetal cartilage and the gradual development of mature cartilage; these changes manifest in the length and sulfation pattern of the chondroitin sulphate and keratan sulphate chains extending from the core protein. Increased concentration of aggrecan has been found in the serum and synovial fluid of OA patients. (Rizkalla et al., 1992; Poole et al., 1994; Wakitani et al., 2009). However, aggrecan is not currently in use as a routine diagnostic or prognostic biomarker for OA.

One of the frequently used non-collagenous protein markers for OA is cartilage oligomeric matrix protein (COMP), a group of glycoproteins that bind to type II collagen fibres. Jiao et al. (2016) found that serum COMP and hyaluronic acid (HA) were highly correlated with early cartilage erosion in knee joints observed in patient knee arthroscopies. The deamidated form (D-COMP) has been found in cartilage and serum samples, which correlated with lesions in hip OA but not in the knee (Catterall et al., 2012). Therefore the possible specificity to hip OA could be advantageous for this biomarker; however, it has been shown that COMP levels vary due to age, gender and ethnicity (Clark et al., 1999).

Synovium, the soft tissue that lines the spaces of diarthrodial joints, tendon sheaths, and bursae, is also involved with OA pathogenesis. Two possible biomarkers have been identified to detect degradation of synovial tissue: urinary glucosyl-galactosyl-pyridinoline (Glu-Gal-PYD) and hyaluronic acid (HA) (Jordan et al., 2006). The urinary excretion of Glu-Gal-PYD was found to increase in OA patients (Jordan et al., 2006). However, this post-translational modification marker of both types I and II collagen is detectable in other tissues such as bone, cartilage and tendons to a small degree (Rousseau & Garnero, 2012). Serum HA has been detected at increased concentrations in patients suffering from OA (Filková et al., 2009). However, HA is a

component of both cartilage and synovium, and liver disease can interfere with the serum HA concentration (Elliott et al., 2005); therefore, as a biomarker for OA it lacks specificity.

Inflammation is a hallmark of OA, especially synovial inflammation, which is the cause of elevated cytokine production in circulatory and synovial fluids. Many studies have evaluated a series of pro-inflammatory cytokines in association with joint lesions (Miller et al., 2014b). Patients suffering from OA have increased levels of serum tumour necrosis factor alpha (TNF-α) (Kaneko et al., 2000; Bondeson et al., 2006). Attur et al. (2015) proposed that the increased transcript levels of interleukin-1β (IL1β), TNF-α and cyclooxygenase 2 (COX-2) from peripheral blood leukocytes can predict the risk of joint space narrowing in knee OA progression. Likewise interleukin-4 (IL-4) and interleukin-6 (IL-6) were reported at higher levels in patients with OA and are highly correlated with radiographic lesions (Mabey et al., 2016). Interleukin-8 (IL-18) in synovial fluid has been correlated in relation to OA progression and severity (Denoble et al., 2011). In an animal study, Sun et al. (2017) reported that diet-induced OA in rats significantly increased serum concentrations of pro-inflammatory cytokines interferon gamma (IFN-γ) and IL-1β but decreased the anti-inflammatory cytokine interleukin-10 (IL-10). The Collins et al. (2015a) study on the other hand did not show any significant change in those cytokines; instead, changes were detected in growth-regulated oncogenes/keratinocyte chemoattractant (GRO-KC), interferon gamma-induced protein 10 (IP10), macrophage inflammatory protein 2 (MIP2) and MIPα.

A group of proteolytic enzymes have been identified as a beneficial tool in disease prognosis and evaluating efficacy of treatment in OA. These include the matrix metalloproteinase family (MMPs), which are responsible for digesting gelatinous substances, and another group known as ‘a disintergrin and metalloproteinase with thrombospondin type I motif’ (ADAMTS-4 and ADAMTS-5), which are extracellular proteolytic enzymes acting on large proteoglycans of cartilage matrix, also called aggrecanase. Production and activity of these enzymes are highly elevated during the course of OA (Denoble et al., 2011). Moreover, it has been shown that MMPs derived collagen fragments connective tissue type I collagen turnover (C1M), C2M and C-reactive protein (CRP) in blood/serum are associated with OA onset (Petersen et al., 2016).

Changes in conventional bone markers also provide some information for OA. Progressive OA patients showed CTX-I in urine at higher concentrations than non-progressive patients (Bettica et al., 2002). Osteocalcin, a non-collagenous protein hormone involving with bone mineralization process, was also found to be increased in patients with OA but the data were inconsistent (Sowers et al., 1999).

2.1.3 Pathogenesis

Despite the fact that OA is determined by cartilage erosion, all components of joints such as synovium, tendons, ligaments and muscles surrounding joints are affected. The initial pathogenesis of OA is still controversial as to whether it arises from surface cartilage itself, calcified cartilage or subchondral bone (Goldring & Goldring, 2016). The diverse pathogenesis might be dependent on different types of OA. For example, age-related OA has been associated with an increased water content in cartilage as the loss of negative charge in glycosaminoglycans leads to cartilage matrix swelling (Roberts et al., 1986; Sowers et al., 1999; Bettica et al., 2002). In post-traumatic OA, tissue trauma activates inflammation by increasing cytokine and chemokine production, so significant pathological changes such as synovial tissue expansion and inflammatory cell infiltration have been identified (Liebertha et al., 2015).

However, there is a growing interest in a possible early pathological event which is a group of proteins rising in the milieu of a joint cavity in the family of so-called ‘alarmin’. Alarmins are any endogenous proteins released from inflammation or damaged tissue (Foell et al., 2007) and may have the potential to activate specific receptors (Oppenheim & Yang, 2005). One group of alarmin is S100 proteins, which are acidic and small (10-14 kDa). Alarmin is expressed in a variety of tissues and its conformational structure is changed by calcium binding during cell injury, which enables these new epitopes to interact with various receptors (Ruse et al., 2001; Meijer et al., 2012). S100A4 is an example for cartilage protein; after the conformational changes, it binds to receptor for advanced glycation end products (RAGE), causing increased production of reactive oxygen species (ROS), protein tyrosine kinase 2β (PYK2), mitogen-activated protein kinase (MAPK), nuclear factor-κB (NF-κB) pathways, and finally MMP13 in human chondrocytes (Yammani et al., 2006). Another alarmin is High Mobility Group Box 1 (HMGB1), a 30kDa non-histone nuclear protein containing two DNA-binding boxes (Bidwell et al., 2008). Ke et al. (2015) found that

HMGB1 was overexpressed in the synovial membranes of OA patients. This protein is able to activate innate immune responses *in vitro* by binding multiple membrane receptors, cytokines and chemokines (Magna & Pisetsky, 2014). HMGB1 can be secreted from hypertrophic human chondrocytes and attract the trafficking of osteoclasts, osteoblasts and endothelial cell, resulting in endochondral ossification (Taniguchi et al., 2007).

During the course of cartilage breakdown, alarmin S100 has been shown to be produced from the cartilage matrix and to trigger synovial cells to generate other types of alarmin, such as HMGB1, to promote more pro-inflammatory mediators. S100 and HMGB1 activate chondrocytes to produce ADAMTS, MMPs, ROS, inflammatory mediators and vascular endothelial growth factor (VEGF) (Firestein, 2003). The consequences of these changes in alarmin are synovitis, cartilage breakdown, angiogenesis, hypertrophic differentiation of chondrocytes, and osteophyte formation and bone remodelling (Nefla et al., 2016). The pathological changes can be seen at macroscopic or microscopic levels by radiography or histopathological examination respectively.

As the many destructive enzymes mentioned above are released, cartilage matrix is degraded, generally initially in the superficial zone then extending to deeper areas as the disease progresses (Wu et al., 2002). This process results in the appearance of surface cartilage fibrillations, fragmented cartilage exfoliation and deep fissures into the calcified cartilage zone and subchondral bone (Zhou et al., 2016). The clonal clusters of chondrocytes, a feature of histopathological changes of non-calcified cartilage in early cartilage deterioration, also appear after degradation of cartilage matrix which is used to identify the early proliferative events (Rolauffs et al., 2010). At a late stage, the density of chondrocytes dramatically declines in the non-calcified cartilage layer and fragmentation of chondrocytes and cell apoptosis can be seen (Hwang & Kim, 2015).

Calcified cartilage and the tidemark junction between these two layers of cartilage are changed during OA progression. The pathological changes in this area are initiated by the penetration of vascular elements from fissures or microcracks at the osteochondral junction and this development is associated with VEGF as well as additional pro-angiogenic factors such as fibroblast growth factor-2 (FGF-2), platelet derived growth factor (PDGF), and angiopoietins (Goldring & Goldring, 2016). Many studies have reported that blood vessels and channels penetrate from the subchondral

bone into this calcified and non-calcified cartilage layer of OA joints (Lyons et al., 2006; Suri et al., 2007; Walsh et al., 2007).

Subchondral bone is an element under cartilage and is composed of two components, the subchondral bone plate and trabecular bone. The subchondral bone plate is a thin cortical lamella which lies beneath the calcified cartilage. The trabecular bone arises from the subchondral bone plate in a network structure of cancellous bone orientated in multi-directions to support the local mechanical loads (Burr, 2004). This internal architecture can be modified by external mechanical loadings on bone or joints and changes can affect the contour of bone in OA, which is evident by osteophyte or bone cyst formation (Bowes et al., 2016). The porous structure of the subchondral bone plate allows nutrients and mediators to cross over to the cartilage layer (Li et al., 2013). Given this ability to move nutrients and mediators both ways, subchondral bone has an important role in OA pathogenesis. For example, during subchondral bone remodeling in an animal model, prostaglandins, leukotrienes and various growth factors secreted from osteoblasts were shown to reach the overlying articular cartilage (Lajeunesse & Reboul, 2003). Similarly, osteoclast stimulating factors secreted from chondrocytes can increase bone remodeling in subchondral bone (Bellido et al., 2010). Therefore conflicting hypotheses have arisen whether early pathogenesis of OA arises from cartilage or subchondral bone. There is evidence that supports OA originating from subchondral bone including lesions in the subchondral bone such as osteophyte formation, bone remodeling, subchondral sclerosis, and attrition, which can be seen in radiography. Some of these changes not only at the final stage OA but are observed much earlier, prior to any cartilage degradation (Intema et al., 2010).

Pathogenesis of OA in humans is described in Figure 2.1. At early stages of OA increased bone remodeling and subchondral bone loss are seen (Bettica et al., 2002). In an osteoporotic rabbit model, the severity of OA was associated with increased bone remodeling and microstructural damage in subchondral bone (Bellido et al., 2010). Thinner subchondral bone plate strongly correlating with cartilage damage has been reported in dogs (Intema et al., 2010) but not in cats (Meyer et al., 2008), whereas Batiste et al. (2004) showed subchondral bone plate thickness in OA in rabbits. At late stage OA, the pathological changes of the subchondral bone include an increase in density, bone volume, subchondral bone plate thickness, and trabecular thickness in

addition to a decrease in trabecular separation, bone marrow spacing and the number of rod-shape trabecular to plate-shape trabecular (Ding, 2010).

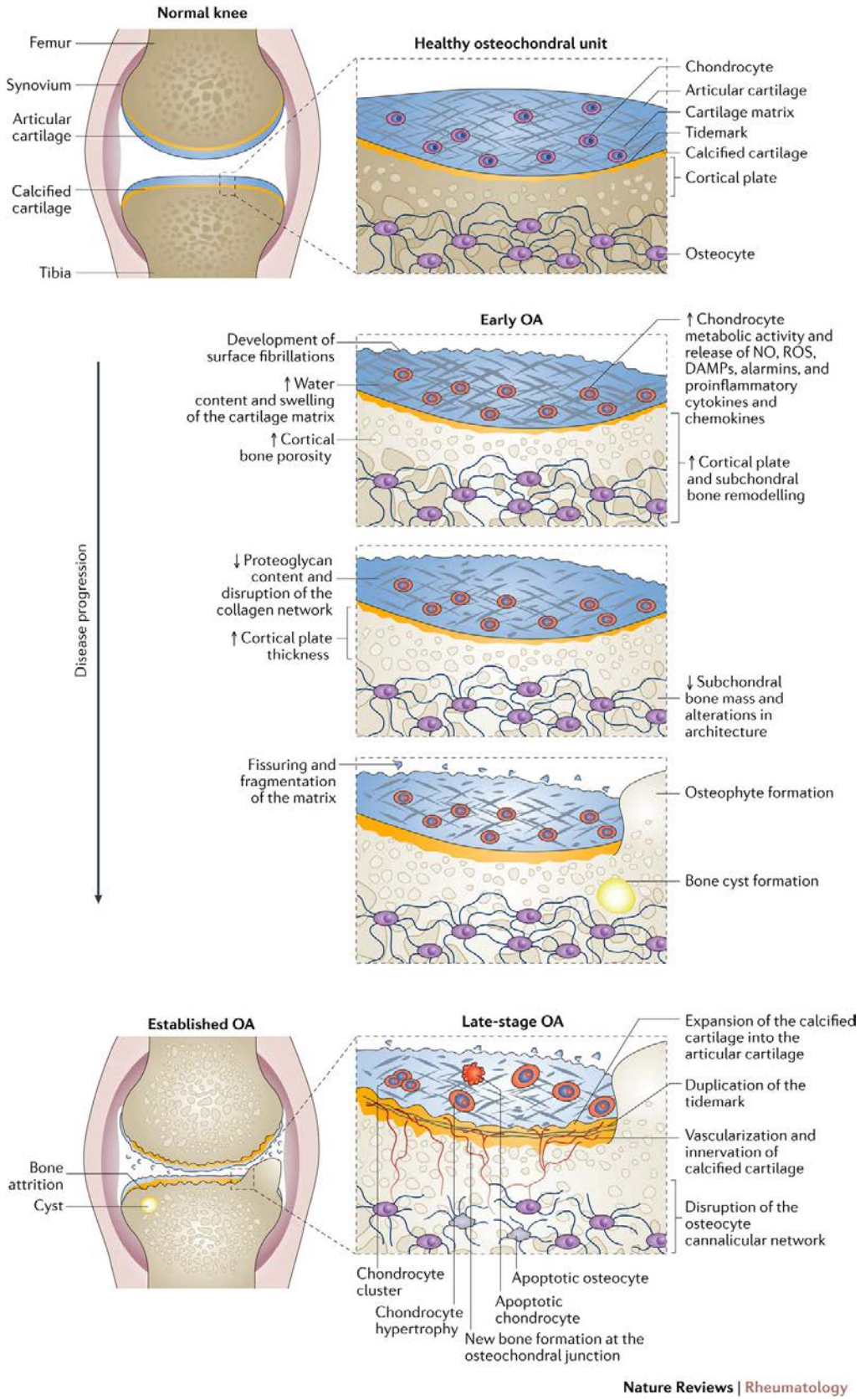

Figure 2.1: Pathogenesis of knee OA

(Source: Goldring et al, 2016, reprinted by permission of Springer Nature)
The head of the femur and tibia of a normal knee are covered with smooth articular cartilage which can be divided by tidemark junctions into a surface layer, non-calcified cartilage and deep layer, calcified cartilage. Under the cartilage is subchondral bone area, which is covered in calcified cartilage arising the thin cortical bone structure is called subchondral bone plate. From this plate, a network of cancellous bone emerges, which is called trabecular bone. This area is incorporated with bone marrow, vascular and nervous tissues. Early pathological changes in OA include increased water content in cartilage leading to swelling and increased metabolism of chondrocytes. These changes are evident by surface fibrillation and microcracks. As the disease progresses, the disruption of microarchitecture in subchondral bone is more prominent, then osteophyte and bone cyst formation are detected. At late stage OA, chondrocytes are disorganised, and some differentiated to hypertrophic chondrocytes or apoptosis. Vascularization and innervation invade from subchondral bone into calcified cartilage resulting in the thickening of calcified cartilage but reduction in the non-calcified cartilage layer. At this point, subchondral bone stiffens to replace fibrovascular tissue.

Burr and Gallant (2012) revealed that OA development and progression were related to an increase of osteoclast activity, leading to subchondral bone remodeling. Inhibiting bone resorption has a beneficial effect on cartilage but increased resorption causes cartilage destruction (Karsdal et al., 2008). Osteoclasts are being increasingly recognized in early OA at the subchondral bone plate of experimental animals (Pelletier et al., 2004; Botter et al., 2011). These findings support the notion that osteoclast function is associated with OA pathogenesis.

Osteoclasts are gigantic multinucleated cells which are able to produce bone matrix degrading enzymes such as tartrate-resistant acid phosphatase (TRAP), MMPs and cathepsin K and also carbonic anhydrase II (CAII) to achieve demineralization (Logar et al., 2007). These osteoclast functions are crucial for bone resorption during the remodeling process and endochondral ossification. Both processes are regulated by osteoblasts and osteoclasts. Osteoblasts secrete receptor activator of nuclear factor κB ligand (RANKL), which has a binding site on the osteoclast membrane, as well as osteoprotegerin (a decoy receptor of RANKL); the ratio of RANKL/OPG in the microenvironment influences the transformation of precursor cells to osteoclasts (osteoclast differentiation) (Tat et al., 2009b). Walsh et al. (2010) demonstrated that the feature of bone marrow replacement with fibrovascular tissue in subchondral bone was related to osteoclastic activity. Osteoclasts can also migrate from the subchondral area to the extended channels of subchondral bone plate and reach through non-calcified cartilage; however, this phenomenon is more frequently detected in rheumatoid arthritis than OA (Suri & Walsh, 2012).

Many lines of evidence indicate that OA is a heterogeneous disease associated with various illnesses and health disorders leading to multiple phenotypes. The relationships between other disorders and OA are described below.

2.2 Diseases associated with osteoarthritis

2.2.1 Inflammation

Inflammation is the foundation of a body defence mechanism to resolve harmful stimuli threatening body systems. The common signs of inflammatory responses are represented as redness, heat, pain and loss of function. This phenomenon is obvious in acute inflammation such as abscesses, tissue trauma, etc. However, inflammatory responses are far more complicated or even intangible in some chronic diseases. Once inflammation is established then many types of cells, pro-inflammatory mediators, cytokines, chemokines, chemo-attractants, and adhesion molecules are locally or systemically recruited in concert and display a different pattern or course for a particular disorder. These factors can modify and maintain the specialty of the inflammatory responses. It is important to have optimal inflammatory responses but inflammatory responses that lose tolerance or regulatory processes could become pathological (Calder et al., 2013).

Inflammation can be classified as acute or chronic (Table 2.1). Acute inflammation is a short-term process, initiated almost immediately after entry of harmful stimuli. The initial secretion of the primary mediators such as vasoactive amines and eicosanoids facilitate leukocyte extravasation into lesions. As a result, neutrophils and other granulocytes, monocytes and macrophages are the major cell types in classical inflammation. The objective of this response is to get rid of the triggers of inflammation. Once the triggers are removed, the resolution phase of inflammation is activated by ceasing inflammatory mediators and increasing anti-inflammatory cytokines. If the process fails to eliminate the triggers and they still persist inside the body, the course of inflammation will be prolonged. Therefore, the complexity of the inflammatory mediators, cellular biomarkers, and tissue damages can be seen as a consequence of chronic inflammation (Calder et al., 2013).

It is possible for innate and adaptive immune cells to be continuously recruited in chronic inflammation to produce a complex cascade of the inflammatory biomarkers. Some of the soluble inflammatory biomarkers which could increase systemically or

locally are the CRP, eicosanoids, leukotrienes, ROS, nitric oxide, IFN-γ, IL-1β, IL-1α, IL-6, IL-10, IL-12, IL-13, IL-17, IL-18, IL-23, TNFα, chemokine ligand2 (CCL2) (or MCP-1), CCL3, CCL5, chemokine interferon-γ inducible protein2 (CXCL-2), CXCL-8, CXCL-10. Unfortunately, these mediators cannot be used to segregate chronic inflammation from acute inflammation (Calder et al., 2013). However, chronic inflammation can be distinguished by the hallmark of tissue lesions which are fibrosis, pannus formation, tissue erosion and types of cell infiltration (Table 2.1). Recently, there have been new approaches to identify the chronic inflammation events by monitoring regulatory T cells, myeloid derived suppressor cells (MDSCs), CD274 (the MDSCs ligand for the inhibitory receptor on T-cells), and S100A8/A9 (the pro-inflammatory calcium binding proteins secreted by MDSCs) (Meirow & Baniyash, 2017). Moreover, macrophage polarization, the changing of macrophage phenotypes and functions due to an interaction of cell-to-cell or cell-to-molecules, might be the critical point in converting a simple inflammatory event to long-lasting chronic inflammation (Parisi et al., 2018).

Table 2.1 Types and characteristic of inflammations

	Acute inflammation	**Chronic inflammation**	**Low-grade chronic inflammation**
Stimuli	Pathogens, injuries	Unresolved pathogens, persistent foreign bodies, immune disorders	Metabolic disturbance, chronic infection
Responsible cells	Macrophages, monocytes, neutrophils granulocytes; T cells later	Macrophages, neutrophils, development of adaptive immune response; T and B cells resolution; fibroblasts	Mononuclear cells (monocytes, macrophages, T cells, B cells), neutrophils, adipocytes (if adipose tissue involved)
Primary mediators	Vasoactive amines, eicosanoids; complement system	Cytokines, chemokines, eicosanoid, growth factors, reactive oxygen species, hydrolytic enzymes	Cytokines, chemokines, adipokines (if adipose tissue involved), eicosanoids, reactive oxygen species, hydrolytic enzymes
Onset/ duration	Immediate/2-3 days	Delayed/more than 30 days	Delayed/ more than 30 days
Pathological finding	Heat, redness, pain, swelling	Tissue and structure damages, fibrosis necrosis, pannus formation	No overt pathology, tissue (vascular) damage, increased insulin resistance, intracellular lipid accumulation

Chronic inflammation can be further categorized into a low grade or high grade subtype, based on the detectable concentration of inflammatory biomarkers in systemic circulation. It has been seen that in some chronic conditions (rheumatoid arthritis, inflammatory bowel disease, atopic dermatitis, psoriasis, asthma and obesity) the presence of the inflammatory biomarkers is minimal or even absent (Calder et al., 2013). Hence, these disorders are recognized as a low grade-chronic inflammation.

Low-grade inflammation is suggested to be a factor relating to many diseases (Dinh, 2019). For example, Alzheimer patients who presented with TNF-α serum levels of >4.2 pg/ml at baseline showed a 4-fold greater cognitive decline in the 6-month-study compared to patients <2.4 pg/ml (Holmes, et al., 2009). Obesity is another health condition associated with low-grade inflammation. Increasing adipose tissue is the key factor of producing pro-inflammatory markers such as leptin, adiponectin, IL-6, and CRP. A study in metabolically obese elderly subjects found that means of circulating IL-6 levels were 2.23, 2.39 and 2.61 pg/ml which were associated with BMI at <25.08, 25.08-27.79 and >27.79 kg/m^2 respectively (Wannamethee et al., 2007), and these also correlated with CRP levels. Many research studies have shown that increased CRP levels of >10 mg/L in blood circulation consistently indicate systemic inflammation (Calder et al, 2013; Anzar, et al. 2016; Ellulu et al., 2017). CRP levels in healthy people are $\leq$1.0 mg/L; levels 2-3 fold greater than this indicates a heightened risk of cardiovascular diseases (Ellulu et al., 2017). Dinh et al. (2019) suggested that a range of circulating CRP levels between 3-10 mg/L could represents low-grade inflammation in patients with mental and physical fatigue. In aging, several systemic inflammatory mediators were found to be elevated 2-4 fold when compared with young adults (Fagiolo, 1993). However, other studies showed that some key inflammatory markers such as TNF-α, IL-1β, serum amyloid A, and IL-8 were less consistently correlated with age (Di Iorio et al., 2003; Morrisette-Thomas et al., 2014). Collated data from Calder et al. (2017) demonstrates that plasma levels of some inflammatory markers are higher in elderly such as CRP, IL-6, IL-18, and fibrinogen (Table 2.2).

Table 2.2 Levels of circulating inflammatory markers in young and old adults

Parameters	Young adults (18-30 years old)	Elderly (>65 years old)	Data expression
CRP (mg/dl)	Not detectable	0.1 ± 0.2	Arithmetic means of log transformed values±SD
IL1RA (pg/ml)	112 (100-125)	133 (124-141)	Means (95% confidence intervals)
IL-6 (pg/ml)	0.69 (0-1.09)	38 (0.7-20.4)	Geometric mean (2.5-97.5 percentile)
IL-10 (pg/ml)	13.13 (2.15-156.60)	6.00 (1.94-81.50)	Median (range)
IL-15 (pg/ml)	1.73 ± 0.05	1.94 ± 1.32	Mean ± SD
IL-18 (ng/ml)	0.19 ± 0.02	0.26 ± 0.03	Mean ± SEM
MIP-1β (pg/ml)	32 (6-1107)	32 (11-200)	Median (range)
sGP130 (ng/ml)	230 (195-263)	263.9 (263.3-300.4)	Median (25-75 percentile)
sTNFR-I (ng/ml)	0.60 ± 0.12	1.0 ± 0.29	Mean ± SD
sTNFR-II (ng/ml)	1.22 ± 0.27	1.75 ± 0.34	Mean ± SD
Fibrinogen (mg/dl)	297.19 ± 68.60	336.75 ± 89.87	Mean ± SD

(Modified from Calder, 2017)

2.2.2 Obesity

The overweight and obese populations have dramatically increased worldwide over the last 5 decades (Blüher, 2019). Hence, obesity is often referred to as a global epidemic even within the scientific community: the phrase ‘obesity epidemic’ elicits >3500 results in a PubMed search. The basic criteria used in categorisation is body mass index (BMI), a height to body weight ratio in which the BMI ranges of 25-29.9 kg/m^2 and ≥30 kg/m^2 are overweight and obesity respectively (World Health Organization, 2006) . In 2016, more than 1.9 billion adults worldwide were overweight and over 650 million of these were obese (World Health Organization, 2020). Obesity has been proven as a risk factor for non-communicable diseases such as atherosclerosis, cardiovascular diseases, hypertension, T2D, hepatic steatosis and certain types of cancer (Blüher, 2019). Therefore, obesity-associated chronic diseases and metabolic disorders have put significant workload and financial pressure on public health systems globally (Bluher, 2019).

In addition, obesity has been associated with OA. Coggon et al. (2001) showed that obese people were 6.8 times more likely to develop knee OA than normal-weight

people. Further, weight loss in obese patients by surgical manipulation improved physical function and reduced joint pain after 6 months, which correlated with the reduction of serum COMP (Richette et al., 2011). Similarly, a meta-analysis study by Christensen et al. (2007) found that physical disability was reduced in knee OA patients after weight loss. Although body weight seems to be related to OA, increased weight bearing on to the joints is not the only causal factor of OA as the systemic elements of OA also develop in non-weight bearing joints such as fingers, hands, wrists and temporomandibular joints (Cicuttini et al., 1996). The collective data found that BMI was only correlated with knee OA in non-obese patients but insulin resistance was highly correlated with both non-obese and obese patients (King et al., 2013). These findings reveal that there may be an OA-driving cause for OA in the systemic circulation, but as not all joints in an individual are equally affected there are also likely to be localised changes in specific joints.

In obese diabetes patients, an array of pro-inflammatory cytokines including TNF-α, IL-6, IL-1β, and MCP-1 are increased in various tissues (Shoelson et al., 2006). Unlike the inflammation from trauma or the acute phase of immune responses in which systemic levels of pro-inflammatory cytokines are highly elevated, obesity inflammation presents with only modest levels of circulatory cytokines as reported in animals and humans (Gregor & Hotamisligil, 2011), which is also known as low-grade inflammation. Inflammation is a cell-mediated event and thus the inflammatory changes in the joint microenvironment may not be matched by those in the systemic circulation. Xu et al. (2003) demonstrated that obese mice fed a high fat diet increased macrophage infiltration into adipose tissues which significantly upregulated the mRNA expression of inflammatory cytokines. Further, Weisberg et al. (2006) showed that deletion of chemokine receptor type 2 (CCR2) in mice fed a high fat diet could reduce macrophage infiltration into adipose tissue and also improved insulin sensitivity. On the contrary, overexpression of MCP-1 in adipocytes resulted in the increase of macrophage infiltration, insulin resistance, and hepatic steatosis (Kamei et al., 2006; Kanda et al., 2006). These lines of evidence reveal that macrophages are locally responsible in obesity inflammation and metabolic disarrangement.

Increased body adiposity is a significant feature of obese subjects, although this may not completely correlate with BMI. In true obesity both the number and sizes of adipocytes are extremely elevated. Adipocytes are capable of producing many types of

pro-inflammatory cytokines and chemokines such as TNF-α, IL-1, IL-6, IFN-γ, MIP-1, GRO-α, and RANTES (CCL5) (Collins et al., 2016). Moreover, they also secrete adipokines into the blood circulation. One of the significant adipokines is leptin, which has responsibility in regulating appetite and satiety via a hypothalamus mechanism (Richter et al., 2015). Leptin production is highly and positively correlated with BMI and fat mass (Neumann et al., 2016). In obese animals and humans, increased leptin levels however do not inhibit appetite because of the reduction of leptin transport across the blood-brain barrier and reduced signalling transduction (Montague et al., 1997). This situation is known as "leptin resistance". Leptin in addition has an influence on inflammation. Leptin stimulates innate immunity by activating macrophage proliferation, phagocytosis, NK cells and upregulates TNF-α, IL-6, and IL-12 production (Vadacca et al., 2011). In OA patients, leptin was detected in chondrocytes, synoviocytes, osteophytes, infrapatellar fat pad (Francin et al., 2011) and synovial fluid (SF) (Bas et al., 2014). SF leptin levels are correlated with joint pain (Bas et al., 2014), radiographic severity with pro-inflammatory cytokines, and MMPs in OA patients (Karvonen-Gutierrez et al., 2013).

Obesity in laboratory animals can be manipulated by monogenic mutations in the leptin pathway in which the defect of either the leptin gene (ob/ob mice) or the leptin receptor gene (db/db mice) results in animal models used in obesity research (Lutz & Wood, 2012). These two genetically modified strains of leptin knockout mice, ob/ob and db/db, were shown to have massive expansion of adiposity but no pathological changes in inflammatory cytokines in knee joints (Griffin et al., 2009). Leptin injection directly into the rat knee joint on the other hand resulted in cartilage degradation which showed the depletion of proteoglycan in articular cartilage and the increased gene expression of ADAMTS-4 and -5. In addition, both gene expression and protein levels of MMP-2, MMP-9, cathepsin D, and collagen II were elevated (Bao et al., 2010). This revealed that local leptin also has a critical role in OA activation. Zhao et al. (2016) demonstrated that leptin at 50-100 ng/mL decreased the migration of chondrogenic progenitor cells but increased the production of pro-inflammatory cytokines, MMP 1,2,3,9,13 expression, and chondrocyte senescence by activating the p53/p21 pathway and nitric oxide, with all these resulting in chondrocyte hypertrophy and apoptosis, chondrocyte phenotype loss and cartilage degradation.

The most abundant adipokine produced by white adipose tissue is adiponectin (Fain et al., 2008). It is normally present in blood circulation at high concentrations (5-10 µg/mL) in humans. A reduction in serum adiponectin levels was reported in association with obesity, T2D and cardiovascular disease while increase of adiponectin production was detected in weight loss (Kopp et al., 2005; Inadera, 2008; Ashley et al., 2011; Reverchon et al., 2014). It seems that adiponectin has negative relationships with BMI or body fat but there is no significant correlation among those parameters (Hernandez-Morante et al., 2006). On the contrary, some conditions showed positive association of circulating adiponectin with body fat. For instance, women have a higher percentage of body fat and also higher plasma adiponectin concentrations than men (Chandran et al., 2003). Further, postmenopausal women who tend to have increased visceral fat or adiposity have greater adiponectin levels than premenopausal women (Lubkowska et al., 2014). These findings imply that adiponectin levels might be influenced by sex hormones. Moreover, a positive relationship of adiponectin with adiposity can be found in the obese population who are metabolically healthy (Guenther et al., 2014). Kadowaki and Yamauchi (2005) revealed that adiponectin has a role in regulating insulin. Injection of adiponectin into normal or lipoatrophic mice caused a reduction of plasma glucose levels and improvement of insulin sensitivity by inhibiting hepatic gluconeogenesis and activating fatty acid oxidation in skeletal muscles.

The anti-inflammatory role of adiponectin is still debated. On one hand, it exhibits an anti-inflammatory effect by inhibiting TNF-α, IL-6, MCP-1, intercellular adhesion molecule-1 (ICAM-1), vascular cell adhesion molecule-1 (VCAM-1), and endothelial-leukocyte adhesion molecule 1 (ELAM-1) expression, oxidation, and fibrosis in adipose tissues through NF-kB activation (Ouchi et al., 2000). Further, the production of superoxide radicals in endothelial cells was reduced and the alteration of a T cell subpopulation and macrophage polarization to the resting state were evident in cell culture studies (Ohashi et al., 2010). Moreover, administration of adiponectin in collagen-induced arthritis mice showed a reduction of cartilage damage in histological scores as well as mRNA levels of pro-inflammatory cytokines (Ebina et al., 2009). On the other hand, adiponectin levels are elevated in association with most chronic inflammatory and auto-immune diseases including inflammatory bowel disease, systemic lupus erythematous, type I diabetes, rheumatoid arthritis and OA (Fantuzzi, 2008). In addition, adiponectin showed a detrimental effect on cartilage development by

inducing MMP-(3 and 9), NOS2 and MCP-1 in chondrocytes (Lago et al., 2008). To explore this, the current study will assess the change of plasma adiponectin levels in relation to body weight or body fat in a MetOA rat model (chapter 5-6).

2.2.3 Osteoporosis

The relationships between osteoporosis, obesity and metabolic syndrome (MetS) are still controversial in clinical studies. Some studies showed positive effects of obesity on osteoporosis by increasing bone mineral density (BMD). For example, the retrospective study of Kinjo et al. (2007) in 8194 subjects aged over 20 years old in the USA found that people with MetS showed higher BMD at the femoral neck when compared to subjects without MetS. This finding is supported by another study by El Maghraoui et al. in 2014, who found that women with MetS showed higher BMD at hip and spine, suggesting a protective effect of MetS on bone. However, other studies showed negative effects of MetS on osteoporosis. von Muhlen et al. (2007) found that the total hip BMD was lower in MetS patients, similar to the findings of a study in a T2D population (Yaturu et al., 2009). Hwang and Choi (2010) also demonstrated that MetS related bone loss could be detected in the vertebral column. Finally, Zhao et al. (2007) study showed no association between MetS and BMD.

Theoretically, obesity should have many negative influences on the pathological mechanisms of osteoporosis. Firstly, adipocytes and osteoblasts are derived from the common precursor mesenchymal stem cell in bone marrow. Thus, the occurrence of adipogenesis bias can compromise osteoblastogenesis and result in the reduction of bone formation (Rosen & Klibanski, 2009). This theory is supported by bone marrow of obese mice having more adipocyte infiltration (Xu et al., 2013). Additionally, obesity is relevant to chronic-low grade inflammation as it correlates with an increase in IL-6, MCP-1, TNF-α and CRP (Guri & Bassaganya-Riera, 2011). The elevation of these inflammatory cytokines result in the expression of RANKL in osteoblasts (Campos et al., 2012). RANKL is essential for driving osteoclast differentiation and eventually increasing bone resorption. On the contrary, obesity might have some benefits for osteoporosis. For instance, increased mechanical loading on bone can inhibit apoptosis and increase proliferation of osteoblasts and osteocytes (Felson et al., 1993; Ravn et al., 1999; Robling et al., 2006). This is probably activated via the Wnt/β-catenin signalling pathway (Duan & Bonewald, 2016). Disuse or lack of loading resulting in reduction of convective fluid flow in bone tissue causes an acceleration of bone loss, which is

evident by programmed cell death in osteocytes (Nobel et al., 2003). Increased mechanical loading on bone facilitates the extracellular fluid flow in bone canaliculi to osteocyte lacunae, which generates mechanical signals including drag force, fluid shear stress and streaming potential. These forces can activate bone cells such as osteocytes and osteoblasts to secrete nitric oxide and PGE2. PGE2 has anabolic effects which are important in bone matrix synthesis. Nitric oxide plays a role in bone resorption by suppressing the recruitment of osteoclasts via RANKL/OPG system. Mechanical loading also increases hydrostatic pressure in bone marrow, which may activate preosteoblastic marrow stromal cells to reduce expression of RANK-L, which in turn decreases osteoclast differentiation and number (Robling et al., 2006).

Another possibility of obesity being beneficial for bone health is that aromatase in adipocytes is an alternative source producing estrogen in women, (Rosen & Klibanski, 2009) so this would be beneficial to obese postmenopausal women for mitigating bone loss due to estrogen deficiency. However, the outcome in that population may not be explicit because the total estrogen production is still insufficient. In figure 2.2, it is shown that estrogen suppresses IL-6 production in bone marrow stromal cells and osteoblastic cells (Jilka et al., 1992) so the increase of IL-6 in obese postmenopausal women could activate osteoclastogenesis resulting in an increase in bone resorption (Tamura et al., 1993).

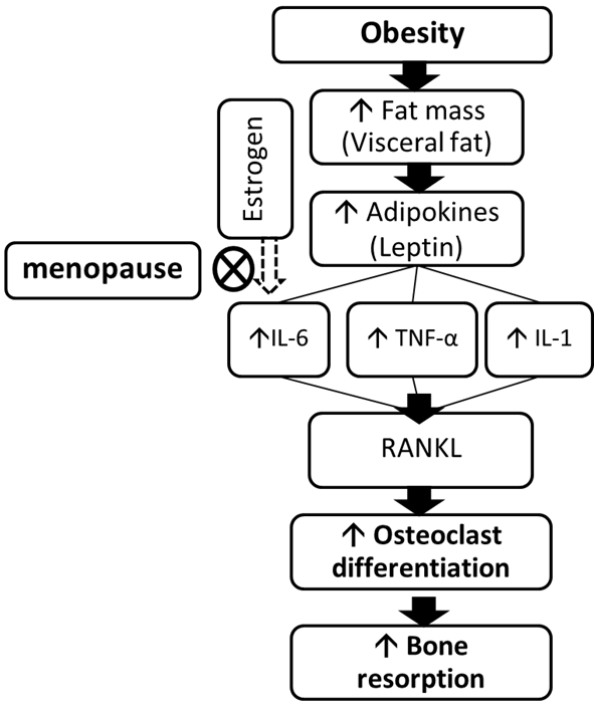

Figure 2.2: The association of obesity and menopause in bone loss due to excessive osteoclast activity

The relationships between MetS, obesity, menopause and osteoporosis are complicated. Moreover, these relationships are also likely to be associated with OA based on the fact that the prevalence of OA in women increases after the postmenopausal period. Therefore, OA in postmenopausal women is a heterogeneous disease with various pathophysiologic drivers leading to multiple phenotypes. Most of the *in vivo* OA studies in animal models have employed surgical and chemical induction methods which obviously represent a post-traumatic OA phenotype rather than MetOA. Recently, a few studies have been used high fat and/or high carbohydrate diets to generate OA, which more closely mimics the majority of MetOA problems in humans. However, the results in many parameters and aspects are still ambiguous and need to be clarified. In the animal study (chapter 4) we will conduct a multifaceted approach to imitate the most common OA population characteristics including age related OA, metabolic OA, obesity, and menopause.

2.3 Intestinal microflora in osteoporosis and osteoarthritis

Humans have co-evolved with microorganisms to form a complex relationship with their microbiome. This relationship can be recognized as symbiosis or parasitism. The interrelationship is stitched into human DNA. For example, mitochondria of human cells have independent sets of genomes that originated from bacteria (Johnston & Williams, 2016). Human gut microbiota includes bacteria, fungi, archaea, viruses and protozoans. Bacteria are the major population in which the most abundant phyla are *Fermicutes* and *Bacteroidestes* while *Actinobacteria*, *Verrucomicrobia* and *Proteobacteria* are less abundant (Marchesi et al., 2016). Billions of symbiotic microorganisms living in the human alimentary tract have a role in supporting biological functions, performing like an additional organ (Baquero & Nombela, 2012). The symbiosis of human's intestinal microflora starts developing at the beginning of life when new-born babies are first exposed to the natural environment and then later evolves during food ingestion (Cani & Dezenne, 2011).

The evolution of intestinal microflora is modifiable and has a huge impact on the human body involving the digestive, endocrine, immune, cardiovascular, and musculoskeletal systems. For example, most indigestible components of the human diet are degraded by intestinal microflora so that nutrients can be absorbed into the body (Sonnenburg et al., 2005). It has been shown that germ-free mice who receive intestinal

microflora obtained from conventional mice resulted in a significant increase in body weight within 10-14 days, although the mice consumed less food when compared to the control (Fredrik et al., 2004). This study revealed the beneficial association of gut microbes to improve the digestive system and harvest extra energy and nutrients which is beyond the host capability. Further, the alteration of gut microbiota in animals has resulted in pathological changes including inflammation of various tissues, changing gut barrier function and altering osteoclastogenesis (Cani et al., 2012; Galvao et al., 2018); each of these phenomena are described in more detail below.

Turnbaugh et al. (2006) transferred gut/faecal microbes from obese or lean-conventional mice into germ-free mice and showed that the germ-free mice that received the obese gut microbiota gained significantly more body fat compared to mice that received gut microbes of the lean phenotype. However, the differences in microbial and other components of the faecal content between lean-mouse faeces and obese-mouse faeces have not been fully elucidated. Subsequent animal studies of obesity induced by a high fat diet have confirmed the discrepancy of gut microbial profiles in animals fed different diets. The results showed that the obese animals increased the ratio of *Firmicutes/Bacteroides* abundance and decreased *Bifidobacterium spp.* when compared to the lean animals fed the control diet (Ley et al., 2005; Patrone et al., 2012; Ravussin et al., 2012; Collins et al., 2015a). The high fat diet mimics a Western-type diet; it causes obesity in animals and also changes systemic inflammatory markers related to MetS and T2D (Collins et al., 2015a). Many studies have hypothesized that the gut microbiome-induced low-grade inflammation is the cause of metabolic disorders and a few possible mechanisms have been theorized including toll-like receptor (TLR) activation (Shi et al., 2006), and changing gut barrier function via tight-junction proteins or the endocannabinoid system (eCB) (Muccioli et al., 2010).

Fatty acids (such as saturated fatty acids (SFAs)) in a high fat diet are able to directly activate TLR-4 on adipocytes and macrophages (Shi et al., 2006; Suganami et al., 2007). Reducing gut microbial abundance using antibiotics can inhibit the development of glucose intolerance, insulin resistance, inflammation and oxidation stress (Cani et al., 2008). This evidence suggests that gut microbes have an independent effect on developing MetS. Lipopolysaccharide (LPS) from bacterial cell walls, a natural ligand for TLR-4, is probably the central messenger linking gut microbes with MetS. Many studies found that increased plasma LPS levels with a reduction in

Bifidobacterium spp., *Bacteroides* and *Eubacterium rectale-Clostridium coccoides* in high–fat diet fed mice are linked to microbial-dysbiosis induced endotoxemia leading to MetS (Cani & Delzenne, 2011).

Cani et al. (2008) found that chronic administration of LPS induced inflammation and insulin resistance and later it was identified that these disorders were mediated by changing gut barrier function (Cani & Delzenne, 2011). Similarly, feeding a HF diet to rats caused the disruption of the tight-junction proteins zonula occludens-1 and occludin, which eventually altered the gut barrier function (Cani et al., 2012). Furthermore, the eCB system, which is composed of G protein-coupled receptors (CB_1R, and CB_2R) and lipid ligands (the most studied being anandamide and 2-arachidonoylglycerol), is physiologically related to various gastrointestinal functions including gut motility and gut permeability (Cani et al., 2012). The eCB system in the colon was revealed to have an interaction with gut microbiota resulting in the change of epithelial barrier permeability. For instance, the activation of CB_1R by the gut microbiota in mice caused an increase in plasma LPS levels (DiPatrizio, 2016) and also the expression of CB_1R (Cani et al., 2012).

Along with diet and environmental impacts, the gut microbiota is altered during aging and is generally characterized by a decrease in bacterial diversity, a variation of the dominant species and a reduction in beneficial bacteria (Salazar et al., 2014). Odamaki et al. (2016) demonstrated that specific groups of bacteria changed during aging including lower levels of *Firmicutes* (*Clostridium cluster XIVa* and *Faecalibacterium prausnitzii*) and *Actinobacteria* (*Bifidobacteria*) but increased levels of *Proteobacteria* .

There is growing evidence that shows the host microbiome is also associated with osteoporosis. Germ-free mice exhibited greater bone mass and lower osteoclast numbers in trabecular bone as well as fewer osteoclast precursor cells in bone marrow (Sjögren et al., 2012). Transfer of gut microbes from normal mice to the germ-free mice increased osteoclast bone resorption leading to normal BMD (Sjögren et al., 2012). In other studies, the inhibition of intestinal bacteria by a low dose of antibiotics showed an increase in the BMD in younger and adult mice (Cho et al., 2012; Cox et al., 2014). On the other hand, bacterial replenishment with some specific prebiotics/probiotics in both male and ovariectomised (OVX) rodents resulted in an increase in bone mass and changes in the gut microbial profile. More specifically, in one study giving

Lactobacillus reuteri in OVX mice found reductions of TRAP5 and RANKL mRNA expression in bone (Rodrigues et al., 2012). This complements another OVX mouse study (Britton et al., 2014), which utilized a mixture of *Lactobacillus* strains to show an increase in OPG expression and bone mineral content while reducing TNF-α and IL-1β gene expression (Ohlsson et al., 2014). This evidence demonstrates a possible role of gut microbes in altering osteoclastogenesis.

The relationship of gut microbes with OA has been studied in monosodium iodoacetate (MIA) induced arthritis rat models. Rats given oral doses of *Lactobacillus casei* with type II collagen (CII) and glucosamine (GS) were more effective than CII and GS alone in reducing pain, cartilage destruction and lymphocyte infiltration (So et al., 2011). Additionally, the expression of pro-inflammatory cytokines and matrix metalloproteinases were decreased while anti-inflammatory cytokines IL-10 and IL-4 were upregulated (So et al., 2011). Some studies have proposed possible pathological mechanisms by which gut microbes directly affect OA such as the infection of *Streptococococus* spp. (Boer et al., 2019) and *Mycoplasma synoviae* in chicken chondrocytes (Dušanić et al., 2009). The notion that gut microbes are causing or promoting OA was demonstrated in a study that identified the occurrences of *Porphyromonas* and *Bacteroides* DNA in synovium and synovial fluid of rheumatoid arthritis and OA (Berthelot et al., 2019). However, this finding is debatable whether the DNA was live bacteria from the gut or bacterial fragments in phagocytes trafficking from intestinal mucosae.

One of the most significant classes of molecules produced by bacteria in the gut is short chain fatty acids (SCFAs) which have an influence on human health. SCFAs are fatty acids with less than six carbon chains and include acetic acid, propionic acid, butyric acid and valeric acid. They provide not only additional energy sources to the body but also have a role in regulating physiological functions (Morrison & Preston, 2016). About 70% of energy utilized by epithelial cells lining in the colon is from SCFAs, particularly butyric acid (Scheppach, 1994). Acetic acid and other SCFAs are absorbed from the colon before being metabolized in the liver and presenting in blood circulation mostly as acetic acid (Cummings et al., 1987), later used to synthesise glutamine, glutamate, beta hydroxybutyric acid (Dagher et al., 1996) and cholesterol (Rittenberg & Bloch, 1945). With regards to their physiological functions, butyric acid is able to regulate cellular gene expression by inhibiting histone deacetylase

(Krautkramer et al., 2016); propionic acid reduces low-grade inflammation in the gut and inhibits fatty acid production in humans (Al-Lahham et al., 2010). A group of G protein coupling receptors (GPR) for SCFAs has also been discovered on various cell types which are free fatty acid receptors including FFAR2 (GPR43) and FFAR3 (GPR41) (Kimura et al., 2020).

It has been recognised that SCFA profiles are associated with gut microbiota. Groups of bacteria such as *Akkermansia muciniphila, Bacteroides spp., Bifidobacterium spp., Ruminococcus spp., Blautia hydrogenotrophica, Prevotella spp, Clostridium* spp., and *Streptococcus* spp., produce acetic acid from pyruvate through acetyl-CoA and the Wood–Ljungdahl pathway (Louis et al., 2010). *Bacteroides* spp., *Dialister* spp., *Veillonella* spp., *Megasphaera elsdenii, Coprococcus catus, Salmonella* spp., *Roseburia inulinivorans*, and *Ruminococcus obeum* are the producers of propionic acid via succinate, acrylate, and propanediol pathways (Scott et al., 2006). Groups of *Firmicutes* such as such as *Faecalibacterium prausnitzii, Anaerostipes* spp., *Eubacterium rectale, Eubacterium hallii, Coprococcus catus, Roseburia* spp. are bacteria producing butyric acid via the phosphotransbutyrylase/butyrate kinase and the butyrylCoA:acetate CoA-transferase routes (Duncan et al., 2002).

Presently it is unresolved whether SCFAs are an inducer or protector in relation to obesity and insulin resistance. It is also possible that they are a consequence rather than a cause of obesity and insulin resistance. As mentioned above, SCFAs are an extra energy source for humans; however, the activation of FFAR2 and FFAR3 on enteroendocrine cells (L-cells) by SCFAs causes the secretion of glucagon-like peptide (GLP-1, GLP-2), pancreatic peptide YY3–36 and oxyntomodulin, thereby resulting in reduction of nutrient absorption from the intestine, increase of insulin secretion and promotion of satiety (Chambers et al., 2015). In addition, signaling FFAR3 on enteric neurons and sympathetic ganglia activates intestinal movement and gluconeogenesis, reduces hepatic glycolysis, and increases energy expenditure (Priyadarshini et al., 2016). This is a recent and active area of research and more research is needed in order to understand the relationship of SCFAs, gut microbiota associated with human physiology and disease, particularly with OA and MetS.

2.4 Promising active compounds from marine animals

A long list of nutrients has been studied in the past decade as dietary supplements for treating OA. Systematic reviews or meta-analysis found the following nutrients and active compounds that may aid in OA: glucosamine, chondroitin sulphate, diacerein, avocado soybean unsaponifiables, vitamin D and E, collagen hydrolysate, *Boswellia serrata* extract, methylsulfonylmethane, pine bark extract, curcumin, *Artemisia annua* extract, and polyunsaturated fatty acids (Vista & Lau, 2011; Senftleber et al., 2017; Liu et al., 2018). Among those, glucosamine and chondroitin sulphate, the components of cartilage, are advertised to delay knee OA progression, with many formulations and commercial products available in markets (Messina et al., 2019).

Liu et al. (2018) did a meta-analysis of dietary supplements for treating OA. This report focused on randomised controlled clinical trials which provided comparisons of oral supplements with placebo in hand, hip or knee OA. The mean age of subjects ranged from 48-69 years with 65% being women. Standardised mean differences (SMD) of clinical improvement were reported and classified as small to large size effects for individual supplements. The result of this meta-analysis found that among 20 types of supplements investigated in 69 eligible studies, glucosamine and chondroitin sulphate were the most frequently studied nutrients (18 and 14 trials respectively). However, their short-term to long-term use showed very low effect size and less than the minimal clinically significant difference. On the contrary, avocado/soybean unsaponifiables, undenatured type II collagen and greenshell mussel (GSM) extract showed a high effect size exceeding the acceptable criteria in both short- and long-term administration. GSM extracts were also reported to be clinically effective in pain reduction with medium-term use.

Many clinical research studies have focused on the anti-arthritis potential of oil from GSM and other marine animals. Senftleber et al. (2017) reviewed 42 trials using whole fish, cod liver oil, mussel extracts, seal oil, or krill oil as a treatment for rheumatoid arthritis or OA from for periods ranging from 2 weeks to 18 months. The study suggested that overall marine oils have a small effect on reducing pain in arthritis patients. Mussel oil however showed a significant relationship by meta-regression analysis with reducing pain; however, this effect was more evident in rheumatoid arthritis rather than OA.

Perna canalisculus is a species of bivalve shellfish which is known by various names including the common term ‘green-lipped mussel’ and the seafood industry term ‘green-shelled mussel’ (GSM). It is endemic in New Zealand and accepted as being part of a health promoting diet by Mātauranga Maori (traditional Maori knowledge). As it has been intensively cultivated along the coastlines of New Zealand, the trademark name “Greenshell^{TM} mussel” was established to specify that the mussels were cultured in the natural environment of New Zealand, providing similar quality and species specification. Therefore, this research study using the test substances from these mussels will utilise the term greenshell mussel or GSM in abbreviation.

The biological activities of GSM have been reported since 1975 which revealed mixed results with regards to health benefits (Whitehouse et al., 1997). GSM contains a large range of nutrients and bioactives including marine proteins and peptides, complex carbohydrates, lipids, naturally chelated minerals, nucleic acids and mucopolysaccharides (glycosaminoglycans), which could promote healthy bone and joints structure. The lipid fraction (~2% of the green weight of the mussel) is the most intensively-studied part. The lipid fraction is composed of polyunsaturated fatty acids (PUFAs) including long-chain (C≥ 20) omega-3 fatty acids, especially eicosapentaenoic acid (EPA, 20:5n-3) and docosahexaenoic acid (DHA, 22:6n-3) (Miller et al., 2014a; Singh et al., 2008). Apart from those well-known fatty acids, some minor lipid components present are non-methylene-interrupted (NMI)-FA, plasmalogens, and phytosterols which are not found in fish oil but only in GSM oil (Miller et al., 2011b; Wakimoto et al., 2011). *In vitro* studies have shown that GSM oil extracted by a supercritical carbon dioxide fluidic (CO_2-SFE) method inhibited prostaglandin E2 (PGE2) in LPS-activated mononuclear cells (Whitehouse et al., 1997). Likewise, McPhee et al. (2007) and Treschow et al. (2007) showed the anti-inflammatory mechanism of GSM oil is related to the cyclooxygenase pathway and lipoxygenase pathway.

The pioneer preclinical study in animals (Whitehouse et al., 1997) assessed the adjuvant-induced arthritis model in female Wistar rats fed GSM. Rats were subcutaneously injected in the rear paw with inactivated *Mycobacterium tuberculosis* dispersed in oil (Freud’s adjuvant). The inflammatory response at the paw developed from day 10 onward after induction. The intensity of inflammation was evaluated by measuring the paw’s thickness. GSM oil extracted by CO_2-SFE and other test

substances were orally introduced one day before injection and continued for 16 days. The result at 15 days after adjuvant injection demonstrated that 15 mg/kg GSM oil effectively resolved the paw swelling in the rats when compared to a negative control. The anti-inflammatory effect of 15 mg GSM oil/kg body weight was shown to have more potency than doses of 25 mg naproxen, 50 mg ibuprofen or 300 mg aspirin. Furthermore, no gastrotoxicity was found in rats fed 300 mg/kg GSM oil while aspirin caused severely gastric haemorrhage at this dose.

Similarly, Singh et al. (2008) conducted a study using an adjuvant-induced arthritis model in Long Evan rats to compare the anti-inflammatory potency of different components of GSM oil. The study found that giving 100 mg/kg of crude GSM lipid from CO2-SFE for 15 days significantly reduced paw swelling by 34% but when administered for only 5 days failed to alleviate the swelling. On the other hand, administration of 30 mg/kg free fatty acid fraction for 5 days dramatically reduced paw swelling by 74%. This evidence suggests that the main active compound of GSM oil is in the free fatty acid fraction which could infer the well-known anti-inflammation bioactivity of DHA and EPA.

Another study proposed a different active agent, furan fatty acid, in a commercial GSM oil product (mixed 1:3 with olive oil) (Wakimoto et al., 2011). This study employed the adjuvant-induced arthritis model in female Wistar rats and gave rats furan fatty acids for five days after day 10, post arthritis induction. The result showed that 5 mg/kg of furan fatty acid significantly reduced rat paw swelling. This study reported the lowest effective dose of any anti-inflammatory substances found in GSM; however, furan fatty acid is present in small amounts, difficult to extract, and unstable, making it less attractive in research of this area. Other detailed analysis on GSM has yet to identify furan fatty acids, although it does occur in olive oil (Boselli et al., 2000).

Most of the animal studies used for assessing activity of GSM used an adjuvant-induced arthritis model and evaluated the changes in paw swelling. It could be argued that the measured effect was an anti-inflammatory rather than anti-arthritic property as no joint histopathological examination was undertaken. A systematic review by Vandeweerd et al. (2012) revealed inconsistent therapeutic effects of nutraceuticals to alleviate clinical signs of OA in various animals. Twenty-two studies involving horses, dogs, and cats were investigated and most of them were randomized controlled trials. Four studies using GSM powder in dogs have been completed (Bierer & Bui, 2002;

Dobenecker et al., 2002; Bui & Bierer, 2003; Pollard et al., 2006). One study, which was not funded by the GSM nutraceutical industry, showed no improvement of clinical symptoms evaluated by dog owners or veterinarians. The others, which were financially supported by GSM producers, reported positive effects; however, no objective assessment such as a force plate was performed in these studies. An additional four studies investigating omega-3 fatty acid in OA, which weren't supported by an industry sponsor, reported positive effects. It is known that GSM extracts, particularly the oil products contains very high amounts of omega-3.

Vandeweerd et al. (2012) recommended not to use GSM powders for OA. On the contrary, a more recent systematic review showed more consistently positive results across dog, cat and horse studies using doses ranging between 20-49, 18-30 and 25 mg/kg/day respectively (Eason et al., 2018). Even though these two systematic reviews arrived at different outcomes of the use of GSM in OA, there was an agreement about difficulties of collecting data from inconsistent methodology provided in different studies and the limited numbers of high-quality trials in animals. Therefore, research studies in this area are still required to elucidate the benefits or lack of benefits of GSM in OA.

Commercial GSM extracts use resulted in health claims for relief of arthritis symptoms for more than four decades now, based on human clinical trials. A GSM oil product known as Lyprinol showed 50-80% of OA symptomatic improvement (pain relief and joint function) after 4-8 weeks of the product intake (Cho et al., 2003). Cobb and Ernst (2006) gathered data in their systematic review which included the commercial product names Seatone, Perna capsule and Perna plus. The authors found that the results of trials were mixed, with two out of six studies revealing beneficial effects (pain relief and increased joint function) of the supplements in rheumatoid and OA patients (Gibson & Gibson, 1998; Gibson, 2000). Studies which used the supplements for less than 3 months showed no significant difference between placebo and treat groups (Huskisson et al., 1981; Caughey et al., 1983). All this evidence suggests that the therapeutic efficacy of GSM in OA is unstable or inconclusive, and the previous preclinical studies in animal models do not have enough strong evidence to ensure whether GSM has potential as anti-arthritis supplements. Therefore, further animal studies, such as the one outlined in chapter 5 and 6, is needed to reinvestigate the effect of GSM in greater detail.

2.5 Animal models in osteoarthritis research

Animal models are important in OA research as the complex nature of the disease is impossible to fully replicate in *in vitro* studies. Further, there are also several limitations of knowledge acquired from human clinical studies, such as variations between the onset of the symptoms and the disease and the chronic nature of the disease with a range of variability in the rate of the disease progression, that make it difficult to have an accurate interpretation. Without animal studies these obstacles would have hampered the advancement of understanding and treatments of OA. Many species of animals can be used to develop OA with similarity to the pathogenesis of human OA. However, rodents are commonly used in OA research for the shorter time frame, cost efficiency and manageability. This review and thesis will be focused mostly on rat models.

There are two main categories of animal models for studying the pathogenesis of the disease or proving the effectiveness of treatments: spontaneous models and induction models. These are described in detail below.

2.5.1 Spontaneous animal models

In the perspective of this degenerative disease, aging is a major cause of the most common form of OA. Some species of laboratory animals develop a course of OA similar to humans and thus are useful tools for investigating natural OA pathogenesis. A mouse inbred strain, C57BL/6, normally develops knee OA at around 17 months old (Wilhelmi & Faust, 1976). Another strain of mouse called STR/ort is prone to developing articular cartilage destruction when it reaches 12-20 weeks old (Poulet et al., 2013). Dunkin Hartley guinea pigs are another species is well-known for their use for age-related OA studies and probably the best representation of primary OA in human as they develop similar pathological lesions. The early events of OA can be seen within 3 months of age of Dunkin Hartley guinea pigs and the lesions continuously increase in severity which is noticeable in 18 months (Jimenez et al., 1997). Furthermore, genetic mouse models for OA have been developed, particularly since *ex vivo* studies of human tissues and inducible OA in animal models revealed a similarity of the pathogenesis with genes. 80 gene mutations or single nucleotide polymorphism (SNPs) confirmed the association with OA. As an example, Col2a1, Col9a1 and Col11a1 are important to the extracellular matrix and cartilage structure so deletion of collagen type IX alpha 1 gene in Col9a1$^{-/-}$mice created a spontaneous OA model (Säämänen et al., 2007). These

transgenic mouse models are efficient to target a specific mechanism of OA development. However, the results from therapeutic efficacy of treatments targeting these specific genes might be meaningless in clinical trials because there are other genes which are simultaneously influential on the pathogenesis of this disease.

2.5.2 Induction animal models

There are two major types of OA induction animal models in experimentation, which are acute and chronic models.

Acute models: The main disadvantage of spontaneous animal models in OA is that they are time consuming. Therefore an induction model is favourable in mimicking the OA destructive process of articular cartilage due to its consistency, robustness and time efficiency. Many agents can be used for intra-articular injection protocols which produce a significant inflammation or OA lesions in the injected joints. The inflicted animals subsequently show pain and clinical signs, making it convenient to monitor the results of treatments; in addition, the pathological lesions of the whole joint structure can be explored. The list of the agents utilised in the literature include Freud adjuvant (Little & Zaki, 2012; Lampropoulou-Adamidou et al., 2014), papain (Scharstuhl et al., 2003), iodoacetate (Janusz et al., 2004) and collagenase (Vogel & Vogel, 1997). Despite the advantages of inducing OA in a short period of time, the chemical induction produces a severe inflammatory response and rapid chondrocyte death which is unlikely to appear in human OA. Thus, they are mainly used for studying pain mechanisms and drugs targeting pain pathways (Lampropoulou-Adamidou et al., 2014). Another method used to fabricate OA in animals is physical immobilization. The method was reported in rats, rabbits, and dogs (Vanwanseele et al., 2002) which shows a 9% decrease in overall cartilage thickness after 11 weeks of immobilization. This model showed chondrocyte atrophy and necrosis rather than chondrocyte cloning and subchondral bone changes which represent the hallmark of human OA (Goldring & Goldring, 2016). Surgical destabilization of anterior cruciate ligament or meniscus is the most common method for OA induction and widely used in laboratory animals (rats and mice). Anterior cruciate ligament transection in mice induces mild cartilage destruction at 8 weeks and subsequent subchondral bone damage (Zhen et al., 2013). The meniscal tear approach on the other hand generates more severe OA showing significant cartilage destruction with subsequent osteophyte formation (McCoy, 2015). The surgically induced OA animal model is a useful tool for explaining the pathological mechanisms in post-

traumatic OA in human but not for MetOA. Moreover, inflammation caused by infection and tissue trauma after the operation process can be a confounding factor resulting in significant variability.

Chronic models: joint instability may not be the sole pathological mechanism of the cartilage destruction as the majority of human OA is heterogeneous and involves multifactorial causes, especially metabolic diseases. Recently, metabolic OA has become more prevalent than other types of OA, making it more important to find a suitable animal model for further study. It is known that the replenishment of damaged cartilage is difficult, and treatments should be provided at the earliest stage of the disease to prevent cartilage loss. Hence, the study of early stage OA is crucial in order to establish a new approach of prevention methods in clinical trials. Most induction models are not able to provide early stage OA in particular as the inflammation progresses rapidly at the post-induction event. Furthermore, the slow development process of a chronic model gives the opportunity to detect the pathological changes in the early events. To construct a similar pathological disease model like MetOA is challenging as a number of variables involved in the induction process causes different severities in clinical signs and pathological lesions.

One recognised rat model which has been established within the last decade and is still being optimised is obesity-induced OA (Collins et al., 2015b). The pathological mechanism of OA is thought to involve chronic low-grade inflammation and metabolic disorder (Thijssen et al., 2014). High energy diets such as fat and sugar can be used to increase animal weight similar to the modern Western diets causing obesity in the human population. However, the success rate of OA induction varies upon many factors. The work of de Visser et al. (2017) suggested that high energy diets might not be able to produce a successful OA induction. His study in male Wistar rats compared 12 weeks of a high fat diet with a high fat diet plus groove surgery. The latter method induced pathological features of OA at the surgical knee joint while the rats without groove surgery showed only initial synovitis without cartilage erosion. It was concluded that a high fat diet itself is incapable of driving the relevant MetOA in animal models over a 12 week period. On the contrary, (Collins et al., 2015b) used male Sprague Dawley rats to successfully demonstrate a similar pathological pattern of MetOA over 28 weeks of high fat diet group compared with the same diet induction incorporated with groove surgery. The same research group showed that the diet-induced-OA model

in rats presented the elevation of leptin, MIP-2, MIP-1α, MCP-1, IL18, VEG-F, IL12, TNF-α, IL-4, IL-17 and fractalkine in blood circulation and a dramatic increase of IL-6, IL-1β and IL-12 in synovial fluid (Collins et al., 2015a). Recently, another research group conducted a 16 week-diet-induced MetOA model in male Wistar rats and showed significantly pathological changes in articular cartilage and synovium, increased IFN-γ and IL1-β in serum, and decreased IL-10 in serum. Moreover, the lipid profile, insulin and liver function parameters were also increased (Sun et al., 2017). Therefore, obesity-induced OA can initiate the combination of systemic inflammation and glucose/lipid metabolism derangements.

Numerous factors affect the success of MetOA animal model establishment. Sekar et al. (2017) induced OA by diet in male Wistar rats age 9-10 weeks old by feeding them with different types of SFA for 16 weeks and demonstrated differing degrees of OA pathological lesions. These results revealed that rats fed 20% beef tallow (trans fat, high molecular weight), stearic acid (C18:0), palmitic acid (C16:0) or myristic acid (C14:0) developed varying degrees of metabolic syndrome, cartilage degradation and subchondral changes depending on the molecular weight of the fat. The longer the chain length of SFA, the more severe the lesions. Thus, the source of fat, the fatty acid profile of the fat and the proportion of fat in the diet will influence the appearance of OA symptoms.

Genetic background and gender are other crucial factors in MetOA induction. For instance, outbred stock Sprague Dawley rats have been found to respond differently to high fat/high carbohydrate diets (Schemmel et al., 1970). Approximately two-thirds of the population have shown to be highly prone to obesity but the rest show an obese resistant phenotype (Schemmel et al., 1970). Male rats can increase weight faster than females and have more tendencies for obesity in induced OA models. Female rats have a protective effect from estrogen and less potential to develop OA unless ovariectomy is performed. The mechanism by which estrogen exerts the protective effect is still unknown. It is probably related to the fact that estrogen receptors are found on chondrocytes of rats along with many other species (Oestergaard et al., 2006). Another possibility is that estrogen has an inhibitory effect on subchondral bone turnover (Ham & Carlson, 2004). The lack of estrogen in OVX female rats results in an alteration of subchondral bone remodeling, which can change load distribution on the bearing joint and eventually compromise the joint integrity and cause cartilage damage. Based on this

evidence, OA can be induced by ovariectomy and this rat model has been used in research for decades (Høegh-Andersen et al., 2004). OVX does not only disrupt bone metabolism but also stimulates the accumulation of body fat mass resulting in an increase of adipokines, inflammatory cytokines which aggravate metabolic syndrome (Kang et al., 2015). Therefore, the OVX-induced OA model mimics the real circumstances of OA in women, in which the prevalence is higher after menopause.

The animal model utilised in this thesis has been designed to recapitulate the facets relating to MetOA in women using a combination of factors including spontaneous aging, diet-induced obesity and ovariectomy-induced OA and osteoporosis in a rat model, in order to explore and identify the influence of each factor on the disease. In addition, GSM is, for the first time, intensively investigated in this MetOA model. This thesis reveals the effect of GSM on not only OA protection but also bone health and the alteration of gut microbiota.

2.6 Aim and research objectives

Although there have been some research studies on the use of GSM supplementation in animals, all of them used surgical and chemical induction methods such as adjuvant-induced arthritis. These models only represent the conditions and pathological mechanisms that are relevant to post-traumatic OA or acute-arthritis-like symptoms. This study focuses on a possible prevention or treatment for MetOA, which is the most prevalent type of OA in the global population. Therefore, a novel animal experiment was established, using a high fat/ high sugar diet for long period of time (48 weeks) to disrupt the female rat's metabolic regulation and eventually initiate the cartilage destruction process without artificial or surgical intervention. OVX to increase obesity and induce osteoporosis was also a new addition to this model. In addition, previous studies have used only GSM lipids, where the thesis research presented in this thesis utilised whole dried GSM containing a number of interesting compounds such as glucosamine, chondroitin, hyaluronic acid and also a potential range of undiscovered bioactive compounds. As various dietary factors can influence many aspects of inflammation or illnesses, a preventive treatment for MetOA by using nutritional approaches should be considered so that alteration of dietary components may improve global health. Based on the previous evidence, anti-inflammation and analgesia are the only actions have been proposed so far to mitigate OA by the effect of GSM. Our study

has addressed another possible mechanism of GSM in the prevention of the disease development.

Apart from the main objective mentioned above, there has been some evidence about metabolic disorders which show a complicated relationship between obesity, menopause, gut microbiota, and OA. This ambiguous issue is still debated and more scientific evidence is needed to reach a conclusion. Therefore, the experimental design and some relevant parameters to the aforementioned context were elaborated to clarify some ambiguities and collect more supportive evidence for the scientific community. More specifically, this study proposed the following objectives.

1. To investigate which fraction(s) of GSM lipid have anti-osteoclastogenesis activity *in vitro*. (Chapter 3)

2. To unravel the complex relationship of aging, obesity and estrogen deficiency on bone loss in rats of which the effect could contribute to the development of OA (Chapter 4)

3. To investigate the preventive effect of GSM on early development of MetOA in rats (Chapter 5)

4. To evaluate the long-term effect of GSM supplementation on multiple phenotypes of OA in rats (Chapter 6)

5. To explore the influence of high-fat-high-sugar diets, ovariectomy and GSM supplementation on the change in the number and/or types of beneficial intestinal bacteria and their products, short chain fatty acids (Chapter 7)

MASSEY UNIVERSITY
GRADUATE RESEARCH SCHOOL

STATEMENT OF CONTRIBUTION
DOCTORATE WITH PUBLICATIONS/MANUSCRIPTS

We, the candidate and the candidate's Primary Supervisor, certify that all co-authors have consented to their work being included in the thesis and they have accepted the candidate's contribution as indicated below in the *Statement of Originality*.

Name of candidate:	Parkpoom Siriarchavatana
Name/title of Primary Supervisor:	Dr. Wolber Fran
Name of Research Output and full reference:	
Siriarchavatana P, Kruger MC, Miller MR, Tian HS, Wolber FM: The inhibitory effect of greenshell mussel (Perna canaliculus) lipids on osteoclast differentiation	
In which Chapter is the Manuscript /Published work:	Chapter 3
Please indicate:	
• The percentage of the manuscript/Published Work that was contributed by the candidate:	85%
and	
• Describe the contribution that the candidate has made to the Manuscript/Published Work:	
Study design, methodology optimisation, labwork/technical experiments, formal analysis, investigation, data curation, original draft preparation, review and co-editing, visualization.	
For manuscripts intended for publication please indicate target journal:	
Marine Drugs	
Candidate's Signature:	Parkpoom Siriarchavatana Digitally signed by Parkpoom Siriarchavatana DN: cn=Parkpoom Siriarchavatana, o=Massey University, ou=College of Health, email=blueno...@gmail.com, c=NZ Date: [illegible]
Date:	24 July 2020
Primary Supervisor's Signature:	Fran Wolber Digitally signed by Fran Wolber Date: 2020.07.27 14:43:07 +12'00'
Date:	27 July 2020

(This form should appear at the end of each thesis chapter/section/appendix submitted as a manuscript/ publication or collected as an appendix at the end of the thesis)

Chapter 3: The inhibitory effect of greenshell mussel (*Perna canaliculus*) lipid on osteoclast differentiation

This is the only chapter in which the experiments were solely conducted *in vitro*, using the murine macrophage cell line RAW 264.7 precursor cells transformed into bone resorptive osteoclasts. The model mimics the event of active bone resorption process in either cortical bone or cancellous bone in subchondral bone area. The lipid component of GSM has been recognized for its biological activity for a long time but no data from subfractionation are available. To elucidate the mechanisms by which GSM lipids influence bone cell activity, it is necessary to more precisely identify the bioactive component(s). Therefore, we studied subfractions of GSM lipid to identify which class(es) of lipids may have bioactivity. Three fractions of GSM lipid: total lipid, polar lipid, and non-polar lipid, were introduced into the cell culture to evaluate their inhibitory effect on osteoclast differentiation and function. The results of these experiments could predict or explain how GSM might exert any preventive effects against osteoporosis in the animal studies carried out in parallel in this thesis.

Abstract

The osteoclast-dependent bone resorption process is a crucial part of the bone regulatory system. The excessive function of osteoclasts can cause diseases of bone, joint, and other tissues such as osteoporosis and osteoarthritis. Nutritional interventions such as an increased intake of long chain omega-3 polyunsaturated fatty acids (n-3LCPUFAs) are now recommended to help prevent many chronic illnesses. GSM oil, a good source of LCn-3PUFAs, was fractionated into total lipid, polar lipid, and non-polar lipid components and their anti-osteoclastogenic activity tested in RAW 264.7 cell cultures. Osteoclast differentiation process was achieved after 5 days of incubation with RANKL in 24-well culture plates. Introducing the non-polar lipid fraction into the culture caused a lack of cell differentiation, and a reduction in tartrate-resistant acid phosphatase (TRAP) activity and TRAP cell numbers, in a dose-dependent manner, demonstrating that non-polar but not polar lipids from GSM can prevent progenitor cells from differentiating into bone-resorbing osteoclasts. At 20 µg/mL, the non-polar fraction reduced TRAP enzyme and TRAP cell numbers by approximately 50% ($p<0.001$). Moreover, actin ring formation was significantly diminished by non-polar lipids at 10 - 20 µg/mL. The bone digestive enzymes released by osteoclasts into the pit formation were also compromised by downregulating gene expression of cathepsin K, carbonic anhydrase II (CA II), matrix metalloproteinase 9 (MMP-9), and nuclear factor of activated T-cells, cytoplasmic 1 (NFATc1). This study revealed that the non-polar lipid fraction of GSM oil contains bioactive substances which possess potent anti-osteoclastogenic activity.

3.1 Introduction

Greenshell mussel (GSM) or *Perna canaliculus*, a species of bivalve shellfish that is endemic to New Zealand, has solid demonstrated evidence of providing health benefits. Its biological activity has been reported since 1975 (Whitehouse et al., 1997). GSM lipids, the most well-researched component, contain a high proportion of long-chain polyunsaturated fatty acids (LCPUFAs) including EPA and DHA (Miller et al., 2014; Singh et al., 2008). These are renowned as having potent anti-inflammatory activity, as they both inhibit the production of pro-inflammatory compounds and can be converted into resolvins, protectins and maresins which protect against tissue inflammation and organ injury. Most studies using GSM oil extracted by supercritical fluid CO2 method support its anti-inflammatory property showing inhibition of prostaglandin E2 (PGE2) in LPS-activated mononuclear cells (Whitehouse et al., 1997), which relates to both cyclooxygenase and lipoxygenase pathways (McPhee et al., 2007; Treschow et al., 2007). Both enzymatic pathways are responsible for cleaving arachidonic acid into many species of inflammatory mediators including a family of prostaglandins and leukotrienes (Calder et al., 2013). Later clinical studies in animals or humans were mainly focused on GSM's anti-inflammatory and anti-arthritis property (Brien et al., 2008; Cobb & Ernst, 2006; Eason et al., 2018; Zawadzki et al., 2013). Our study of metabolic osteoarthritis (OA) in rats fed a high-energy diet found that GSM prevented the early occurrence of OA pathological markers (Siriarchavatana et al., 2019). The early pathogenesis of metabolic OA is hypothetically associated with subchondral bone remodeling (Burr & Gallant, 2012; Goldring & Goldring, 2016).

Bone remodeling is a physiological function occurring continuously through human life. It is driven by two processes, osteoblast-mediated bone formation and osteoclast-mediated bone resorption in which the equilibrium is a key factor to maintain bone health. Theoretically, bone-resorbing osteoclasts create an empty space for osteoblasts to reconstruct new microarchitecture in response to the microdamage caused by load-bearing stress on the bones and joints (Li et al., 2013). Excessive osteoclast function leads to skeletal disorders, so osteoclasts currently are considered to be a target for drugs such as bisphosphonates in the treatment of osteoporosis (Mastaglia et al., 2006). Osteoclasts, large multinucleated cells, are derived from hematopoietic stem cells of monocyte lineage (Marino et al., 2014). The osteoclast differentiation of the precursor

cells or murine macrophage cell line (RAW 264.7) of this study is established by an osteoblast-secretory factor called RANKL (Collin-Osdoby & Osdoby, 2012).

The increased number of osteoclasts in the subchondral bone plate is evident in early-stage OA in animals (Botter et al., 2011; Pelletier et al., 2004). Suppression of the bone resorption process in a preclinical study improved cartilage health, whereas increased resorption caused more severe cartilage deterioration (Karsdal et al., 2008). Moreover, osteoclasts probably have a direct involvement in cartilage degradation (Knowles et al., 2012) as chondrocytes, similar to osteoblasts, produce a great abundance of RANKL (Tat et al., 2009; Xiong et al., 2011). A study in equines demonstrated that osteoclasts were recruited to the subchondral bone plate of post-traumatic OA and their density was highly correlated with the expression of RANKL in the hyaline cartilage layer (Bertuglia et al., 2016). An in vitro model also proved that osteoclasts are able to resorb cartilage and calcified cartilage by the means of MMP and cathepsin K (Lofvall et al., 2018). In addition, a subset of osteoclasts, arising at the subchondral bone plate or near calcified cartilage, was recognized as chondroclasts (Knowles et al., 2012; Lewinson & Silbermann, 1992). Both cells are morphologically similar and positive by TRAP staining; however, a recent study has showed the distinction of metabolic genes between those cells (Khan et al., 2020). This revealed a pathogenic relationship between bone and cartilage.

Despite the fact that DHA and EPA have consistent evidence of anti-inflammatory and anti-osteoclastogenic effects leading to a therapeutic option for bone and joint diseases (Kim et al., 2017; Rahman et al., 2008), no study has addressed the potential of GSM oils in association with bone or osteoclasts. This current study hypothesized that GMS oil could have an anti-osteoclastogenic effect as it contains omega 3 fatty acid. To investigate this, we conducted experiments using an osteoclast differentiation assay and analysed TRAP cell number, enzymatic activity, actin ring formation and gene expression. This is the first study using GSM oil in osteoclast differentiation. The results reveal a new perspective of using GSM for the treatment or prevention of skeletal disorders.

3.2 Methodology and Research Design

3.2.1 Reagents and materials

Dulbecco's Modified Eagle Medium (DMEM) was purchased from GE Life sciences (Pittsburgh, PA, USA). Heat inactivated fetal bovine serum (FBS) and antibiotic solution was supplied by GIBCO (Invitrogen, Corp., Victoria, Australia). RANKL (#462-TEC) was acquired from Research and Diagnostic Systems (R&D Systems, Minneapolis, MN, USA). Docosahexaenoic acid (DHA), napthol-AS-BI phosphate, 4-nitrophenyl phosphate, pararosaniline, hematoxylin, Phalloidin-Atto® 488, and Hoescht 33342 were obtained from Sigma-Aldrich Inc. (St. Louis, MO, USA). RNA extraction kit (Direct-zol™ RNA Miniprep Plus) was purchased from Zymo Research (Tustin, CA, USA). SuperScript™ IV First-Strand Synthesis System and primers were bought from Invitrogen (Life Technologies, New Zealand). SYBR™ Green Master Mix was purchased from Bio-Rad Laboratories (New South Wales, Australia). 24-well culture plates were obtained from Greiner Bio-one (Kremsmünster, Austria).

3.2.2 Greenshell mussel (GSM) extraction and identification

All the extraction and identification process were carried out by the Food Testing Laboratory of Cawthron Analytical Services (Nelson, NZ). Live GSM, shipped overnight on ice from the Marlborough Sounds NZ, were shucked and meat was homogenized and extracted by a modified Bligh Dyer procedure (Bligh & Dyer, 1959), providing a total lipid fraction. Later, it was separated into 2 different fractions, polar-lipid and non-polar lipid, by silica column running mobile phase with ether and hexane respectively. After evaporating the solvent, all fractions were treated with lipases (*Candida antarctica*: lipase B (CALB) Novozyme 435, Sigma Aldrich) at 40°C for 5 hours (Kahveci & Xu, 2011), extracted by a modified Bligh dyer, dried under nitrogen then kept at -20°C for in vitro assay. To prevent lipid oxidation, the sample vials were filled with nitrogen gas before capping. The lipid compositions were identified as follows: 1 mL of analytical samples were made from lipid extracts with an internal injection standard (C19:0 methyl nonadecanoate; NuCheck Elysian, MN, USA) and external standards (Supelco 37 Component FAME Mix, Merck, Auckland, NZ) then analysed by gas chromatography – flame ionised spectroscopy (GC-FID) according to AOAC 963.22 (Association of Official Agricultural Chemists (AOAC)).

3.2.3 Cell culture maintenance

Murine macrophage cell line RAW 264.7 (#TIB71) was purchased from the American Type Culture Collection (ATCC, Rockville, MD, USA). The cells were maintained in DMEM with 10% FBS, 100 U/mL penicillin and 100 µg/mL streptomycin and incubated at 37°C with 5% CO_2. Cells in flasks were passaged or harvested for the assay when reaching 90% confluence and a scraping technique was used to prepare a single-cell suspension. All GSM lipid fractions and DHA were dissolved in DMSO at various concentrations and stored at -20 °C prior to introducing into the culture wells. The final concentration of DMSO in culture media was equal to 0.1%.

3.2.4 MTT assay

The cytotoxicity of the test substances were determined by assessing the presence of metabolically active RAW 264.7 macrophages using MTT assay (Ferrari et al., 1990). The optimisation study comparing 1 day with 6-day-incubation periods found no differences in the interpretation of cytotoxic levels (Table A1 of Appendix B); therefore, the incubation period for the main study was selected to be a shorter time point. Cells were seeded on 96-well culture plates at 10,000 cells per well for 24 hours prior to new media replacement together with induction of test substances in duplicate wells. The concentrations of all GSM lipid fractions were tested at 5-80 µg/mL while DHA as the positive control was evaluated at 5-20 µg/mL. After a 48-hour incubation period, 10 µl of 5 mg/mL MTT (purchased from Sigma-Aldrich Inc.) was added to each well and incubated further for 3 hours at 37 °C. Then the media from each well was replaced with 100 µl of DMSO. After 5 mins, the plates were shaken until the formazan colour was homogeneous and the absorbance measured at 550 nm on a microplate reader (Multiskan FC, Thermo Fisher Scientific, Vantaa, Finland). Data were normalised and reported as percentage compared to the vehicle control (DMSO treatment only). Three independent experiments were conducted, each in duplicate wells, and the data pooled.

3.2.5 Measurement of Tartrate Resistant Acid Phosphatase (TRAP) activity

The pilot study of this assay tested the GSM oil at the concentrations of 1.25-20 µg/mL but concentrations lower than 2.5 µg/mL showed no effect. In subsequent assays the test concentrations were limited to 5-20 µg/mL (Figure A1 of Appendix B). The

assay was performed according to Boeyens, *et al.* (Boeyens et al., 2014). Briefly, RAW 264.7 cells were routinely prepared as describe above. 1 mL of cell suspension at density of $1.5X10^4$ cells/mL was seeded in each well of 24 well plates. The GSM lipid fractions at three concentrations (5, 10, and 20 µg/mL) were introduced into the culture on day 1 simultaneously with RANKL at 15 ng/mL. 10 µg/mL of DHA were used as a reference for the assay. Each treatment was performed in triplicate. At day 4, new media and test substances were replaced. At day 6, culture medium from each well was collected separately and kept at -80 C for further enzymatic activity measurement. TRAP enzyme from the culture media was measured by enzymatic methods. Briefly, 30 µl of test sample was added into 96 well plates followed by 170 µl of assay reagent (4-nitrophenyl phosphate in tartrate-acetate buffer). The reaction was stopped by adding 50 µl of 1 M NaOH after 1 hour of incubation period at 37°C. This incubation period was selected to avoid an increase of non-specific reaction in the assay (Figure A2 of Appendix B). Optical density was read at 405 nm. The percentage of the enzymatic activity compared to the control was reported. The osteoclast differentiation assay was done in duplicate with three separate experiments.

3.2.6 Tartrate Resistant Acid Phosphatase (TRAP)-positive cell staining

The 24-well culture plates from the osteoclast cultures were processed for TRAP cell staining immediately. The method was modified from Boeyens, *et al*. (Boeyens et al., 2014). Briefly, the cells were fixed with fixative buffer then washed with warm deionized water. A 500 µl of 0.125 mg/mL naphthol-AS-BI phosphate in acetate-tartrate buffer was added and incubated at 37° C for 30 minutes. Then, pararosaniline dye in acetate-tartrate buffer was added and incubated for 15 minutes. Haematoxylin was used for counter staining. All TRAP-positive multinucleated cells containing more than 4 nuclei in each well were counted as osteoclasts under 10X objective lens of an inverted microscope (Olympus CK40). Images were taken with an Olympus camedia C-5060 camera.

3.2.7 Actin ring formation staining

RAW 264.7 cells were seeded at 15,000 cells per well in 24-well culture plates together with 15ng/mL RANKL and test substances. The process of cell maintenance was similar to the above. After the end of incubation period, cells were washed with PBS and fixed with 3.75% formaldehyde solution in PBS for 15 minutes. Later, cell permeabilization was done by 0.5% Triton X-100 in PBS for 10 minutes. Actin ring

formation was stained with 0.5 nmol/mL fluorescent phalloidin conjugate solution (Phalloidin-Atto® 488, Sigma-Aldrich) for 40 minutes and nuclei were stained with 5 µg/mL Hoescht 33342. Actin ring formation was visualized using an inverted microscope (Olympus IX-71) with dual filters: Hoescht (dichromatic filter 400 nm); Phalloidin (dichromatic filter 505 nm) and images were taken using Olympus camera XC 50.

3.2.8 Quantification of mRNA expression using RT-PCR

RAW 264.7 cells were grown and assessed similarly as the above osteoclast differentiation studies. At the end of incubation period, cells in osteoclast culture were lysed by Trizol reagent and then RNA was separated using the RNA extraction kit (Direct-zol™ RNA Miniprep Plus, Zymo Research, USA). cDNA was synthesised from the total RNA according to manufacturer's protocol using SuperScript™ IV First-Strand Synthesis System (Invitrogen, USA). Real-time quantitative PCR, using SYBR™ Green Master Mix, was performed on LightCycler® 480 Real-Time PCR instrument (Roche Applied Science). Four genes were quantitatively measured: cathepsin K, NFATc1, MMP-9, and CA II; each was normalized to GAPDH. The relative quantification was calculated using ($2^{--\Delta\Delta CT)}$ method. The conditions for the PCR process and primer sequences are presented in Table 3.1 and 3.2 respectively. More information can be seen in Figure A3 of Appendix B.

Table 3.1 Protocol for quantitative RT-PCR

Programs	Temperature	Duration	Cycles
Pre-incubation	95 °C	10 min	1
Amplification (3 steps)	95 °C	20 s	35
	60 °C	20 s	
	72 °C	20 s	
Melting	95 °C	5 s	1
	65 °C	1 min	

Table 3.2 Primer sequences

Gene description		Sequences	Length (bp)	TM(°C)	GC%
GAPDH	Forward	5'-AGGTCGGTGTGAACGGATTTG-3'	21	60.88	52.38
	Reverse	5'-TGTAGACCATGTAGTTGAGGTCA-3'	23	58.59	43.48
NFATc1	Forward	5′-GTGGAGAAGCAGAGCAC-3	17	54.77	58.82
	Reverse	5′- ACGCTGGTACTGGCTTC-3	17	56.45	58.82
CathepsinK	Forward	5′-CTGGAGGGCCAACTCAAGA-3′	19	58.93	57.89
	Reverse	5′-CCTCTGCATTTAGCTGCCTT-3′	20	58.24	50.00
MMP-9	Forward	5′-GTCATCCAGTTTGGTGTCGCG-3	21	62.11	57.14
	Reverse	5′-AGGGGAAGACGCACAGCTC-3	19	61.95	63.16
CAII	Forward	5′-GAGTTTGATGACTCTCAGGACAA-3	23	58.11	43.48
	Reverse	5′-CATATTTGGTGTTCCAGTGAACCA-3	24	59.48	41.67

3.2.9 Statistical analysis

Data were analysed by one-way ANOVA and least significant difference test, using IBM statistics software (SPSS) version 25 (Armonk, NY, USA). A p-value of <0.05 was considered statistically significant.

3.3 Results

3.3.1 GSM lipids and composition

Three lipid fractions were recovered from GSM lipids (Table 3.3). Fatty acid profiles of all three lipid fractions were almost equivalent in term of total recovery. They were rich in PUFA (37.68-45.07 g/ 100 g) rather than SFA (22.42-28.80 g/100 g) and also contained a high proportion of omega 3: omega 6 (~ 9: 1). The three fatty acids found in high abundance were palmitic acid (13.50-16.70 g/ 100 g), EPA (13.60-20.10 g/ 100 g) and DHA (14.40-15.40 g/ 100 g). Despite the equivalence of fatty acids contained in those lipid fractions, the lipid classes of each lipid fraction were obviously distinct depending on their polarity. Phospholipids (PL) were highly present in the polar lipid fraction (79.50 g/ 100 g) but completely absent in the non-polar lipid fraction. Triglycerides on the other hand were highly present in the non-polar lipid fraction (35.40 g/100 g) but absent in the polar lipid fraction. Free fatty acids were also pronounced in the non-polar fraction (34.80 g/100 g) and the total lipid fraction (15.40 g/100 g) but only small amount was detected in the polar lipid fraction (3.90 g/100g).

As free fatty acids are well-recognized molecules influencing biological mechanisms, the amount of the fatty acids in free form was retrieved by calculating data in lipid profiles against percentage of free fatty acids in the lipid class; the results are shown in the last three columns of Table 3.3. The non-polar lipid fraction contained the highest amount of at least three free fatty acids, which were palmitic acid (5.81 g/100g), EPA (6.99 g/100g) and DHA (5.01 g/100g). The total lipid fraction showed around 50% lower abundance of those free fatty acids, and those fatty acids were only minimally present in the polar lipid fraction. Interestingly, although the three fractions were similar in quantities of total SFA, n-3 PUFA and n-6 PUFA as noted above, in free form these differed markedly across the fractions. The non-polar fraction contained over ten-fold more of each of these components in free form compared to the polar fraction, and at least two-fold more compared to the total lipid fraction.

Table 3.3 GSM lipid composition

	Fatty acid in GSM oil (g/100g)			The amount of fatty acid in free form (g/100g)		
	Total lipid	**Polar**	**Non-polar**	**Total lipid**	**Polar**	**Non-polar**
				(15.4%)	**(3.9%)**	**(34.8%)**
Fatty acid						
C14:0 myristic acid	4.50	1.60	6.30	0.69	0.06	2.19
C15:0 pentadecanoic acid	0.71	0.31	0.83	0.11	0.01	0.29
C16:0 palmitic acid	16.10	13.50	16.70	2.48	0.53	5.81
C16:1 palmitoleic acid	5.60	2.20	8.80	0.86	0.09	3.06
C18:0 stearic acid	4.40	5.20	3.60	0.68	0.20	1.25
C18:1n7 vaccenic acid	2.20	0.91	3.00	0.34	0.04	1.04
C18:2n6c linoleic acid	1.80	1.70	1.90	0.28	0.07	0.66
C18:3n3 alpha linolenic acid (ALA)	1.10	0.79	1.40	0.17	0.03	0.49
C18:3n6 gamma linolenic (GLA)	0.22	0.12	0.33	0.03	0.00	0.11
C18:4n3 stearidonic acid (SDA)	2.10	0.80	3.40	0.32	0.03	1.18
C20:1 gadoleic acid	1.80	2.30	1.40	0.28	0.09	0.49
C20:4n6 arachidonic acid (AA)	1.90	3.00	1.00	0.29	0.12	0.35
C20:5n3 eicosapentaenoic acid (EPA)	16.90	13.60	20.10	2.60	0.53	6.99
C22:5n3 docosapentaenoic acid (DPA)	1.30	1.60	1.00	0.20	0.06	0.35
C22:6n3 docosahexaenoic acid (DHA)	15.00	15.40	14.40	2.31	0.60	5.01
∑SFA	27.21	22.42	28.80	4.19	0.87	10.02
∑MUFA	10.72	6.10	14.72	1.65	0.24	5.12
∑PUFA	41.40	37.68	45.07	6.38	1.47	15.68
- ∑n-3 PUFA	36.71	32.31	40.83	5.65	1.26	14.21
- ∑n-6 PUFA	4.14	4.97	3.49	0.64	0.19	1.21
Lipid class (%)						
TAG	5.10	n.d.	35.40			
FFA	15.40	3.90	34.80			
Sterols	9.80	15.80	13.10			
MAG & DAG	4.90	2.90	9.80			
PL	62.30	79.50	n.d.			

Greenshell mussel was extracted as described in Methods section 3.2.2 and three lipid fractions (total, polar, and non-polar lipid) were obtained. The total composition of fatty acid in each individual lipid fraction is presented in g/100g and shown in the first three data columns. Lipid classes as the percentage of each fraction are indicated at the bottom of the table. The amount of fatty acid in free form was calculated using the fatty acid profile multiple by the percentage of lipid class and the results are shown in the last three data columns. SFA = saturated fatty acid, MUFA = monounsaturated fatty acid, PUFA = polyunsaturated fatty acid, n-3 = omega-3 fatty acid, n-6 = omega-6 fatty acid, TAG = triacylglycerol, DAG = diacylglycerol, MAG = monoacylglycerol, FFA = free fatty acid, PL= phospholipid nd = not detectable

3.3.2 Cell viability

RAW 264.7 cells were incubated for 48 hr with individual fractions of GSM lipids at concentrations of 5-80 µg/mL, or with DHA at concentrations of 5-20 µg/ml. The relative numbers of metabolically active cells per well, assumed to equate to viable cells, were determined by MTT assay. The result showed that all GSM fractions and DHA were not cytotoxic at the concentrations of 5-20 µg/mL; however, the percent cell viability when treated with non-polar lipid at 80 µg/mL was lower than 95% indicating

mild cytotoxicity (Figure 3.1). Therefore, the concentrations of 5, 10, and 20 µg/mL for all lipids fractions were selected for subsequent study in an osteoclast differentiation assay.

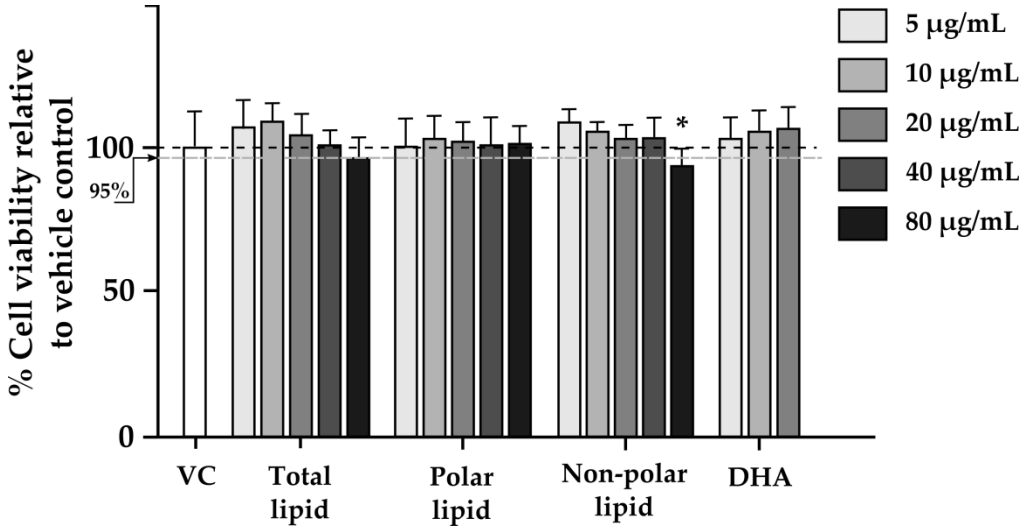

Figure 3.1: Cell viability

RAW 264.7 cells were incubated with different fractions of GSM lipids at concentration of 5-80 µg/mL or docosahexaenoic acid (DHA) at concentrations of 5-20 µg/mL in 96-well plates for 48 hrs. The viability of the cells was measured by MTT assay. Bar chart represents mean ±SD to demonstrate intra- and inter-experimental variability of percent cell viability from three independent experiments each conducted in duplicate. Individual fractions were compared with the vehicle control (VC) using one-way ANOVA followed by LSD post hoc test. Asterisk * indicates significantly different when compared to vehicle control at $p<0.05$.

3.3.3 TRAP enzymatic activity

As can be seen in Figure 3.2, only non-polar lipid GSM reduced the TRAP enzyme in a dose dependent manner by which the highest concentration displayed approximately 50% reduction (% change = 47.66 ± 2.20, $p < 0.001$) when compared to the vehicle control. At the highest concentration the total lipid fraction, which included the non-polar lipids, slightly reduced TRAP. The polar lipids had no effect. The positive control (DHA) significantly reduced percent change of TRAP enzyme.

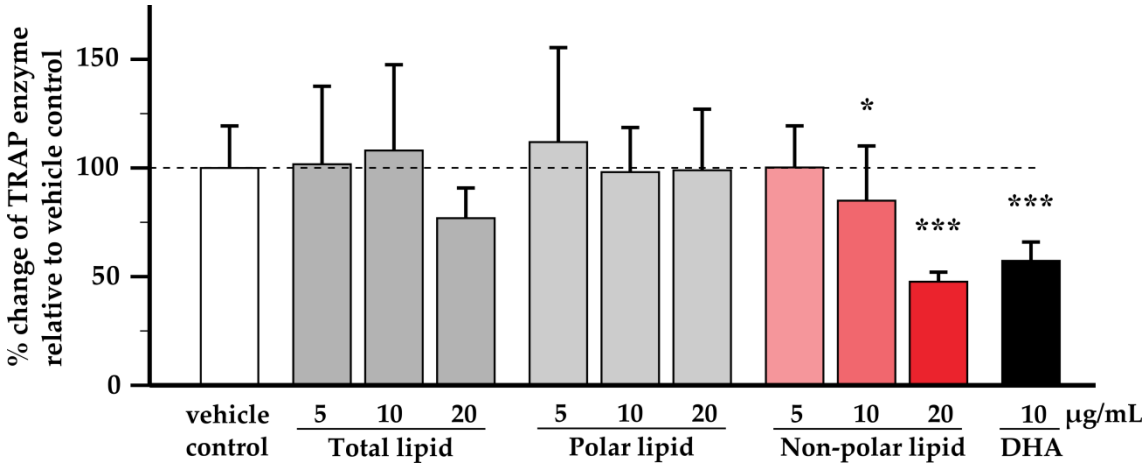

Figure 3.2: Effect of greenshell mussel lipid on TRAP enzymatic activity

The three fractions of GSM lipids at the concentration range from 5-20 µg/mL were tested in osteoclast differentiation assay and 10 µg/mL of docosahexaenoic acid (DHA) was used as a positive control for anti-osteoclastogenesis. The amount of TRAP was measured in supernatants by enzymatic activity. Bar chart shows mean±SD of percentage of differences between the test substances and the vehicle control (n=3 per condition). Individual fractions were compared with the vehicle control using one-way ANOVA followed by LSD post hoc test. Asterisk * and *** indicate significant different when compared to vehicle control at $p< 0.05$ and 0.001 respectively.

3.3.4 TRAP-positive cell counting

Excessive osteoclast activity due to increasing of osteoclast numbers is a pathological mechanism of bone associated diseases. As shown in Figure 3.3, RAW264.7 cells without RANKL could not transform into osteoclasts, which appear morphologically as large multinucleated cells with red staining in the cytoplasm that demonstrates the presence of the TRAP enzyme. The positive control DHA significantly inhibited the number of RANKL-induced osteoclasts as expected (Boeyens et al., 2014) and reduced the number of red-staining TRAP-positive cells. Non-polar lipid extract at 5-20 µg/ml showed an inhibitory effect in a dose dependent manner and at the highest concentration halved the number of osteoclasts when compared to the vehicle control. The total lipid, in which the non-polar lipids were present, at the highest concentration also significantly reduced the number of TRAP positive cells by approximately 20% ($p <0.05$). The polar lipid did not show an inhibitory effect similar to its lack of effect in the TRAP enzymatic assay. As the result of these findings, only the non-polar lipid was investigated in subsequent assays.

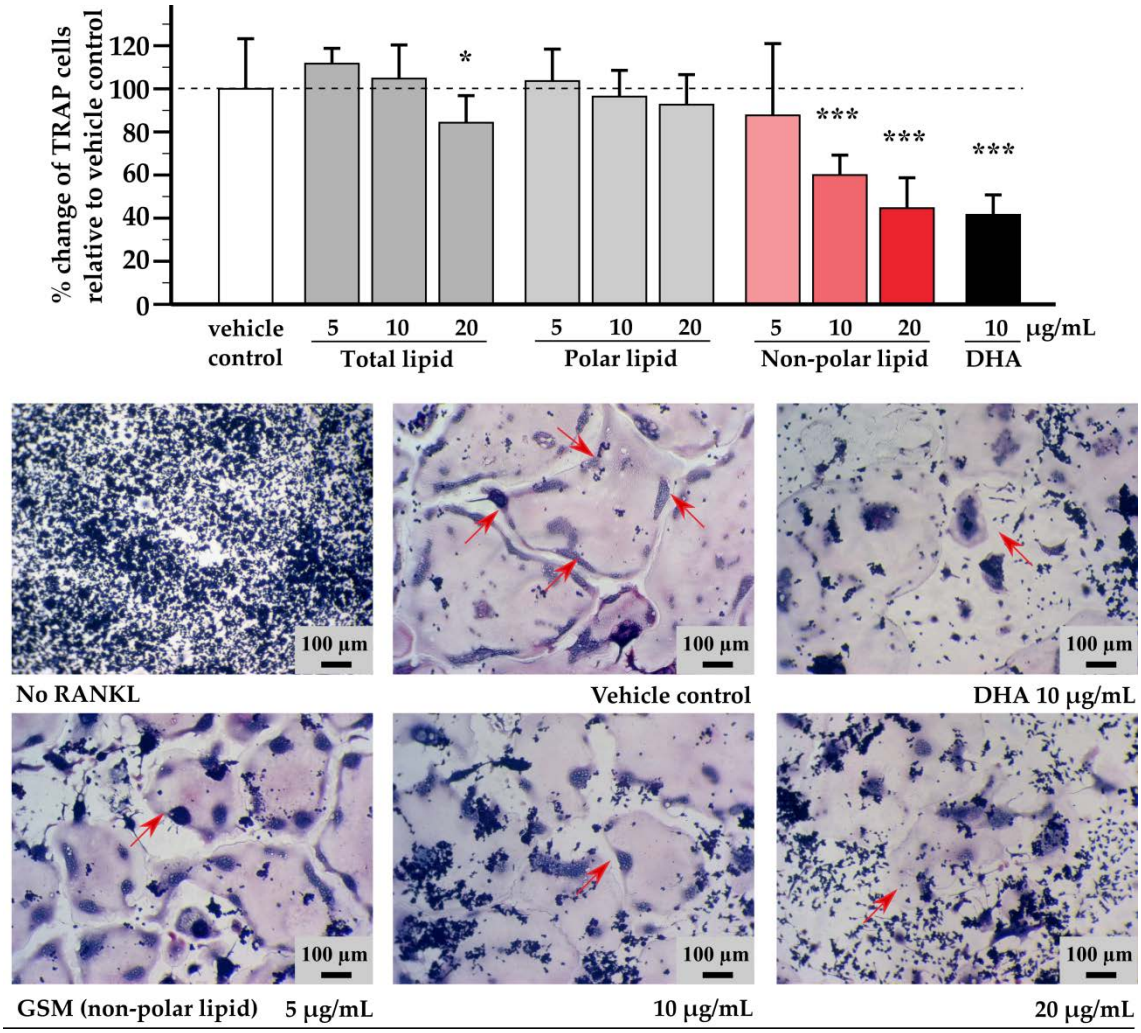

Figure 3.3: Effect of greenshell mussel lipid on TRAP-positive cell counting

The three fractions of GSM lipids at the concentration ranging from 5-20 µg/mL were tested in osteoclast differentiation assay. All cultures but "No RANKL" were treated with 15 ng/mL RANKL to induce osteoclastogenesis; vehicle control represents the negative control with RANKL only while 10 µg/mL of docosahexaenoic acid (DHA) was used as a positive control for anti-osteoclastogenesis. All treatments, including No RANKL, contained the vehicle (0.1% DMSO). TRAP positive cells with more than four nuclei were visually counted in each well under a microscope and expressed as percentage. Bar chart shows mean±SD of percentage of differences between the test substances and the vehicle control (n=3 per condition). Individual fractions were compared with the vehicle control using one-way ANOVA followed by LSD post hoc test. Asterisk * and *** indicate significant differences when compared to vehicle control at $p < 0.05$ and 0.001 respectively. Representative images show the effect of non-polar lipid GSM on anti-osteoclastogenesis in dose dependent manner. The red arrows identify the border of fusion osteoclasts (Vehicle control) or an osteoclast (the other images).

3.3.5 Actin ring formation

Active osteoclasts create actin rings which are an essential element in the bone resorption process. By incubation with RANKL, RAW 264.7 cells transformed to active osteoclasts showing actin rings, which are large rings of cytoskeletal elements that stained in green due to phalloidin's ability to bind selectively to filamentous actin but

not actin monomers (Figure 3.4). Inclusion of non-polar lipid reduced the number and size of actin ring formation in a dose-dependent manner. As expected, the positive control (DHA) showed only a few, small sized actin rings.

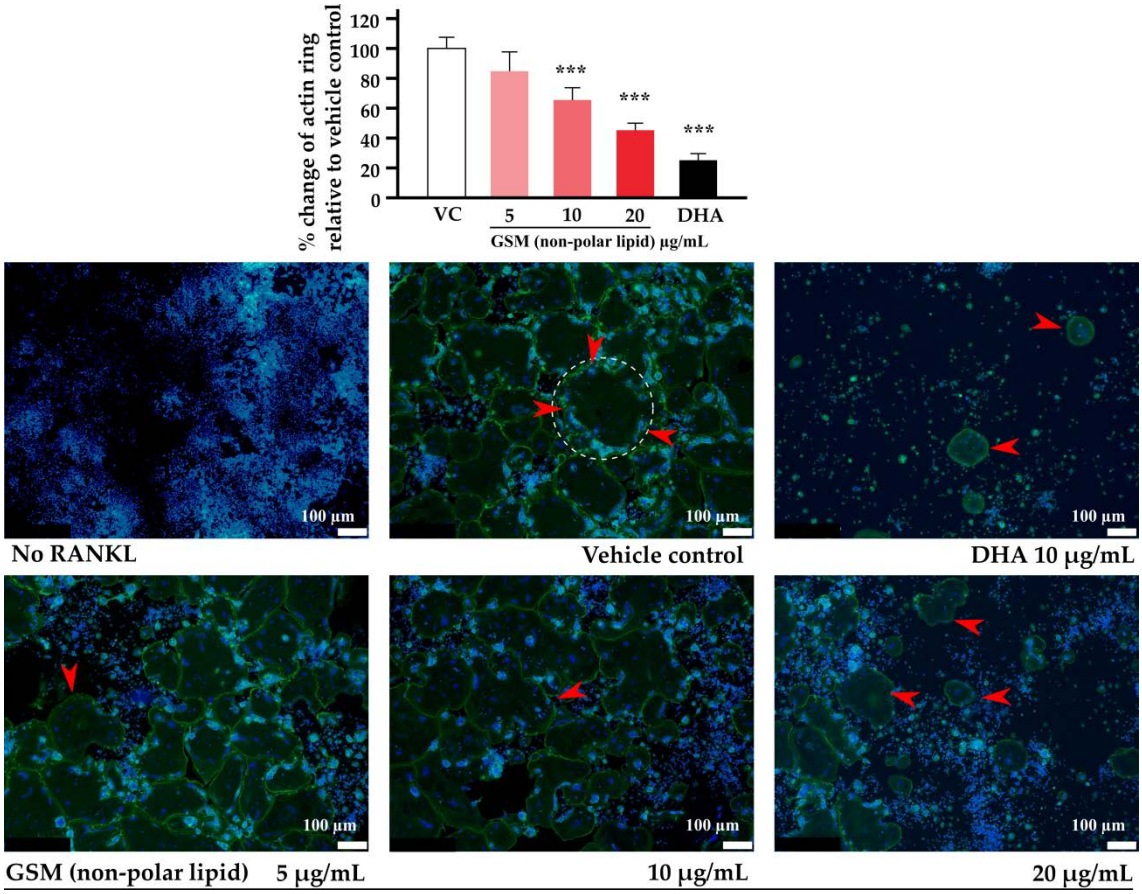

Figure 3.4: Effect of non-polar lipid GSM on actin ring formation

RAW 264.7 cells were seeded on 24-well culture plates at a density of $1.5X10^4$ cells per well with various concentrations of non-polar lipid GSM and 15 ng/mL RANKL. After 5 days of incubation, the cultures were stained with fluorescent dyes phalloidin (green) for actin and Hoechst 3324 (blue) for nuclei and then actin rings were counted in each well. Bar chart shows mean±SD of percentage of differences between the test substances and the vehicle control (n=3 per condition). Individual fractions were compared with the vehicle control using one-way ANOVA followed by LSD post hoc test. Asterisk *** indicate significant differences when compared to the vehicle control at $p<0.001$. A demonstration of one actin ring is enclosed with a circle in the vehicle control and red arrows indicate actin ring formation. GSM = greenshell mussel, DHA = docosahexaenoic acid. Scale bars = 100 µm.

3.3.6 Gene expression

MMP-9, cathepsin K, carbonic anhydrase II and NFATc1 were expressed at detectable but low levels in undifferentiated cells (data not shown). RANKL-induced osteoclasts however highly upregulated those genes, thus relative quantification using $2^{-\Delta\Delta CT}$ method was compared with non-RANKL control. MMP-9 and carbonic anhydrase

II were consistently inhibited by non-polar lipids. Cathepsin K was downregulated at the highest concentration of non-polar lipid (Figure 3.5).

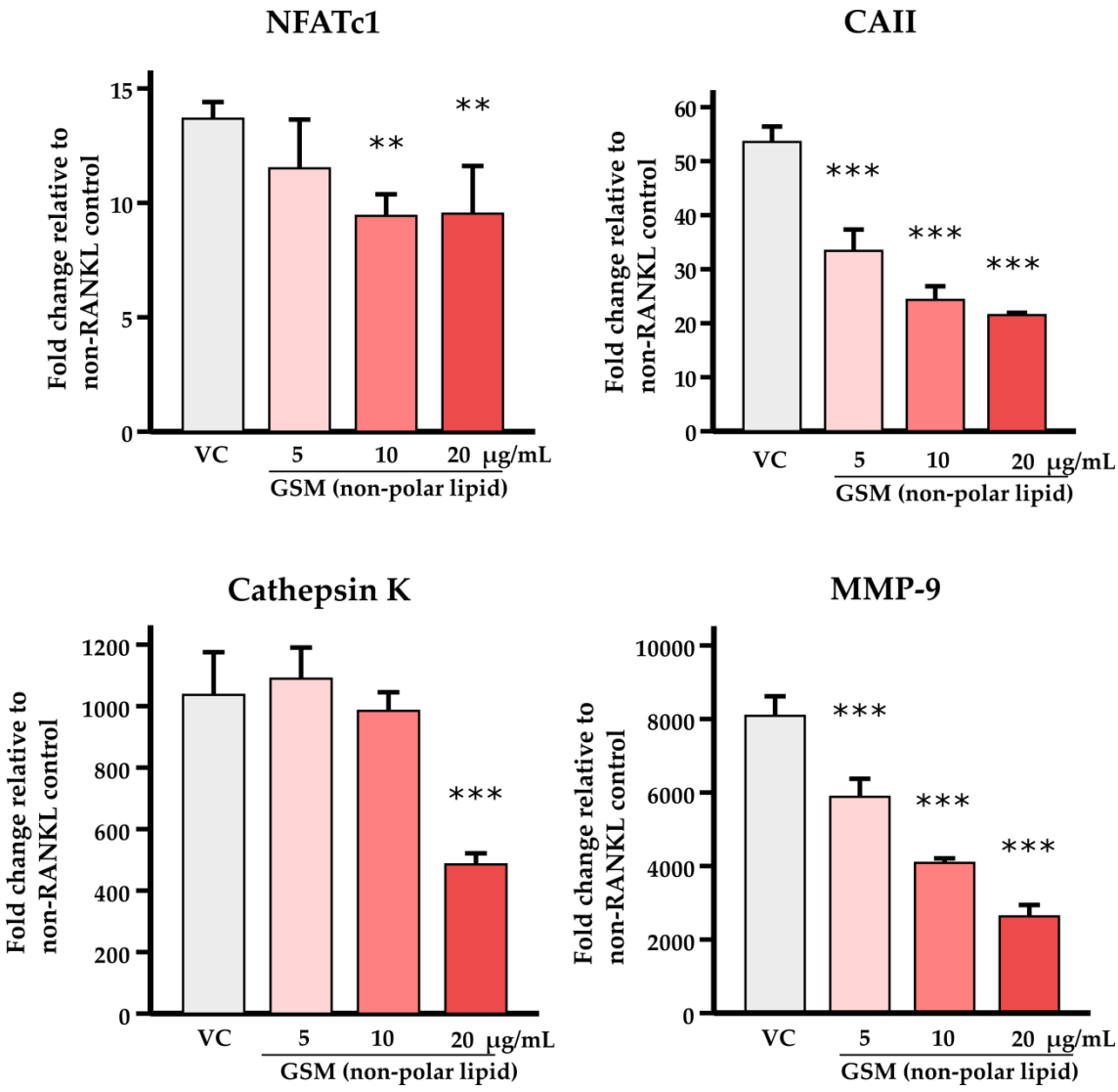

Figure 3.5: Effect of non-polar lipid GSM on gene expression

RAW 264.7 cells were seeded on 24-well culture plates at a density of $1.5X10^4$ cells per well with various concentrations of non-polar lipid GSM and 15 ng/mL RANKL for 5 days. The specific mRNA expression of gene relevant for osteoclast function was determined by quantitative RT-PCR. Relative quantification to non-RANKL vehicle-only control (0.1% DMSO) was calculated in fold change. The data are shown as mean ±SD (n=3 per condition). Asterisk * and ** indicate significant differences of each concentration when compared to the vehicle control (VC) using one-way ANOVA followed by LSD post hoc test at $p<0.01$ and 0.001 respectively. MMP-9 = Matrix metallopeptidase 9, Cat K = Cathepsin K, CAII = Carbonic anhydrase, NFATc1 = Nuclear Factor of Activated T Cells 1

3.4 Discussion

There has been an increasing interest of using marine animals as a source of n-3 PUFA to supply the omega3 requirement in health markets since many health authorities have recommended a daily dose intake to prevent many chronic diseases (Punia et al., 2019). Therefore, aqua-cultured GSM is a focus as it is sustainable and some health benefits are scientifically evident. This current study has proved another pharmacological activity of GSM which is anti-osteoclastogenesis.

The total lipid in this study was a parent fraction in which the most abundant lipid class was PL (62%). The further separation steps gave rise to the other two daughter fractions, polar and non-polar lipid. By the processes, PL was enriched in more hydrophilic phase, which was the polar lipid fraction, and triglyceride was concentrated in hydrophobic phase, the non-polar lipid. At the end of the oil extraction process, all lipid fractions were enzymatically treated with lipase. This enzymatic process had hydrolysed ester bonds of triglyceride chemical structure and then released fatty acid branches into free form. However, not all units of triglyceride had been digested through this enzymatic reaction as the large amounts of triglycerides still remained in those fractions. The activity of lipase in this study was not able to cleave ester bonds in PL thus; small amount of free fatty acid was present in the polar lipid which probably obtained from the reaction with mono-diacylglycerols or naturally occurred by partial hydrolysis (Buri et al., 2012). Normally, PL could be digested by another effective enzyme which is pancreatic phospholipase A_2 (Buri et al., 2012). Therefore, the lipase treatment in our study had enriched fatty acid in free form significantly especially in the non-polar lipid.

Our results showed that GSM non-polar lipid fraction contained a higher percentage of free fatty acids (34.8%) than the polar fraction (4%) in which the most abundant of PUFAs was n-3 PUFA, especially EPA (20%) and DHA (14%). Free form of the fatty acids was calculatedly extrapolated in order to estimate the approximate amounts of bioactive molecules in the assay. The data showed that the non-polar lipid contained the highest amount of PUFA especially EPA and DHA and also contained the highest of SFA such as palmitic acid, palmitoleic acid, and myristic acid. At the highest concentration (20 µg/mL) of the tested lipids in the assay, the non-polar lipid would contain approximately 2.8 µg of n-3PUFA (mainly composed of 1 µg of DHA and 1.4 µg of EPA), and 2 µg of SFA (mainly composed of 1.2 µg of palmitic acid and 0.6 µg

of palmitoleic acid). These would equate to total DHA at 2.88 µg/mL and EPA at 4 µg/mL, or free-form DHA at 1 µg/mL and free-form EPA at 1.4 µg/mL in the assay conditions using the non-polar fraction at 20 µg/mL. DHA and EPA have been shown to individually significantly decrease TRAP-positive cells in this assay in a linear dose-response fashion in concentrations from 5-20 and 10-20 µg/mL respectively (Boeyens et al., 2014) and for DHA to be significantly effective when present as low as 3.2 µg/mL (Rahman et al, 2008). Thus it is reasonable to speculate that the anti-osteoclastic activity observed with the non-polar fraction is due to largely to the combination of DHA and EPA, with the former being more bioactive. This is discussed further below.

In contrast, the total lipid could contain less than half of the free fatty acid found in the non-polar lipid and no individual species of free fatty acid would be available over 0.1 µg in the polar lipid. In the non-polar fraction, approximately a third of the DHA and EPA were present in the free form. This finding leads to the possibility that fatty acid in free form could be at least partially responsible for the biological response with non-polar lipids in this assay.

Free fatty acids possibly activate molecular signaling cascades via free fatty acid receptors (FFARs), the orphan receptors of G protein coupling receptors, of which FFAR1, 2, 3 and 4 have been identified. In RAW264.7 cells, DHA-activated FFAR4 showed inhibition of both TLR4- and TNF-α- mediated inflammatory responses by intervening with transforming growth factor-β activated kinase 1 (TAK1), resulting in abolishment of all downstream signal transduction from LPS or TNF-α (Oh et al., 2010). This identifies at least one mechanism of the anti-inflammatory property of n-3 fatty acids in the treatment of low-grade chronic inflammation. FFAR4 is also expressed in osteoclasts and osteoblasts. A recent study showed that DHA or EPA inhibited osteoclast formation via FFAR4 activation, but the same activation in osteoblasts enhanced signaling transduction resulting in an increase of bone formation. These results from both cell types support the health benefits of DHA and EPA as a bone protective effect (Kasonga et al., 2019). In this study, 10 µg/ml of DHA in free form was used as a reference and clearly exhibited the anti-osteoclastogenic effect. It is possible that DHA could activate FFAR4 because FFAR4 is highly expressed in RAW264.7 cells (Tazoe et al., 2008) and DHA possesses the highest binding affinity to this receptor among other FAs (Kimura et al., 2020).

Although it is known that molecules of free fatty acid are able to activate cellular mechanisms, whether via free fatty acid receptors (FFARs) on cell membranes (Itoh et al., 2003; Hirasawa et al., 2005) or intracytoplasmic receptors such as peroxisome proliferator-activated receptor alpha (PPARα) (Komprda, 2012), FFA are not the only lipid molecules which have an identified receptor in the signal transduction process. There are other recognised receptors for various lipid ligands such as cannabinoids, sterols, leukotrienes, platelet-activating factors, prostanoids, lysophospholipid (lysophosphatidic acid and sphingosine 1-phosphate) (Audet & Stevens, 2019). Therefore, all of these molecules which might be present in the GSM oil need to be considered as candidate bioactives, especially the PLs.

There has been an increased interest in comparing efficacy between marine n-3 LC-PUFA in triglyceride form versus PL form. It was assumed that PL form may have advantages over triglyceride form in oral bioavailability. In the intestine, PLs are less dependent on bile salts to facilitate absorption, but they do require pancreatic phospholipase A_2 (PLA_2) to break down the bond at the sn-2 position, which finally returns free fatty acid and lysophosphatidylcholine (LPC). These forms can be taken up by the enterocytes, after which PL is rapidly incorporated on the chylomicron surface and subsequently transferred to high-density lipoprotein (HDL) (Buri et al., 2012). Schuchardt et al., (2011) found that there was a higher incorporation of EPA, DHA, and total n-3 PUFA into plasma PLs after ingestion of krill oil (a rich source of PLs), compared with consuming re-esterfied triglycerides derived from fish oil, although the differences failed to meet statistical significance. Sugasini et al., (2019) studied the effects of dietary DHA of triglyceride, phosphatidylcholine (PC) and LPC on enrichment of brain DHA and found that DHA of triglyceride and PC (sn-2 position) were not suitable for brain enrichment, but sn-1 and sn-2 of LPC and sn-1 PC were functionally effective. However, a pharmacokinetic study comparing different formats of GSM found inconclusive data of explaining the beneficial absorption of n-3 LC-PUFA bounded PLs (Miller et al., 2020). The authors suggested that there were various factors affecting the distribution of lipid classes in test diets derived from marine animals such as food format and processing, sex of animals, animal feed intake, and season, which present additional challenges for normalising the lipid classes in the experiment.

Even though the advantage of PL on bioavailability or therapeutic efficacy is still not conclusively demonstrated in animal or clinical trials, studies at the cellular level can avoid those confounding factors and possibly offer feasible interpretations external to the complicated issue of lipid absorption in body systems. The result of our *in vitro* study can compare the effects of n-3 LC-PUFA in different lipid forms, especially between PL and free fatty acid. There is no doubt these molecules are bioactively capable and cellular-permeable. Both lipid structures have access to their specific receptors, and also their molecules are involved with many steps of cell signaling pathways. For example, in the case of PL, phosphatidylcholines, phosphoinositides and sphingolipids are capable of regulating nuclear receptors in cell models as well as mouse models (Crowder el al., 2017). The prevalence of phospholipid between the polar and the non-polar lipid fractions of our study was totally distinct. The polar lipid contained mainly PL (79%) but little free fatty acid (4%). On the other hand, the non-polar lipid contained no detectable PL but showed large amounts of free fatty acid (34.8%). Interestingly, the results showed that the polar lipid exerted no biological activity while the non-polar lipid dramatically inhibited the differentiation of osteoclasts in term of cell numbers, TRAP enzymatic activity, actin ring formation, and the gene expression relating to bone digestive enzymes. The remarkable performance of the non-polar lipid could possibly be attributed to free fatty acid which is a main component of this lipid fraction and is known to have available the specific receptors. It is unlikely that triglyceride, diacylglycerol and monoacylglycerol were responsible for the observed biological response because of a lack of existent receptors for those molecules. Sterol such as oxysterol is a ligand for liver X receptors (LXR) which are important regulators of cholesterol, fatty acid and glucose homeostasis. There is evidence relating LXR activity to the pathogenesis of metabolic disorder, hyperlipidemia and atherosclerosis (Wollam & Antebi, 2011) however, sterol would not be a strong candidate in this study as sterol was almost equally distributed across all three lipid fractions.

Despite the fact that many lines of evidence support biological activities of PLs via receptor activation, PL in the polar lipid extract failed to perform any biological modification in this osteoclast assay at the concentrations tested. It might be that because PL in GSM oil has no actual anti-osteoclastic bioactivity; conversely, PL in GSM oil may need to be activated by the physiological digestion, absorption and

distribution processes to expose its functional properties. To address this ambiguity, it would be of interest to re-assess the polar lipid extract using specific enzymatic treatments prior to testing and comparison.

Changes in bioavailability due to lipid form may have minimal impact on therapeutic effects as the efficacy and potency of most lipid bioactives are likely to remain similar. On the other hand, the effect of multiple bioactives working in concert can modify the biological response with marked shifts in efficacy or potency. In this experiment, the free form of DHA at the concentration of 10 µg/mL was used as a reference and it produced the strongest biological response in the assay. Treatment with 20 µg/mL of the non-polar lipid exerted a nearly equivalent effect to the reference in the TRAP cell count but was less effective than DHA in the actin ring assay. DHA in the 20 µg/mL non-polar lipid was present at less than a third of the reference for total DHA and one-tenth for free DHA; however, this treatment contained other free fatty acids such as EPA, palmitic acid, palmitoleic acid, and myristic acid. Anti-osteoclastogenic effects have been reported in studies for many lipids such as EPA, GLA, AA (Boeyens el al., 2014), steric acid, palmitic acid (Cornis et al., 2008), palmitoleic acid (Van Heerden et al., 2017) and myristic acid (Bao et al., 2020). Despite the obvious evidence of the effects of individual free fatty acid on osteoclasts, it is not clear what the biological response of a fatty acid combination would be as there is no supporting evidence currently available. However, different fatty acids may activate different receptors, pathways or mechanisms and consequently may modulate the biological response in an additive or even synergistic manner. In addition, allosteric modulation of lipid receptors such as GRP40 (FFAR1) has been reported in which a simultaneous activation of the orthosteric and allosteric binding sites by different fatty acids can modulate the response (Audet et al., 2019). There are still many gaps to be filled in order to elucidate which and how fatty acids in the non-polar lipid extract used in this study exerted its activity. Meanwhile we postulate that free fatty acids in the non-polar lipid extract were responsible for some or all of the anti-osteoclastogenic effect, as this extract was found to be high in n-3 LC-PUFAs, DHA and EPA.

DHA (C22:6, n-3) and EPA (C20:5, n-3) can be synthesized from ALA (C18:3, n-3) in humans using desaturation, elongation and β-oxidation process. However, ALA is required from external sources as humans lack the Δ15 desaturases to convert omega6 LA (C18:2, n-6) to omega3 ALA (C18:3, n-3) (Ruiz-Lopez et al., 2015). Most vegetable

oils contain small amounts of ALA but some particular plants such as flax seed, canola (rapeseed) and chia seed contain a higher proportion of ALA. Even though by intrinsic biosynthesis the essential fatty acid ALA from plant oil can be converted into effective anti-inflammatory DHA, the conversion ratio of ALA to DHA is very limited in human adults (Brenna et al., 2009) and thus not likely to be physiologically relevant. Hence, acquiring DHA and EPA from external dietary sources is necessary and recommended.

Substantial evidence supports that regular intake of n-3PUFAs, particularly DHA and EPA, can protect against bone loss whether by increasing calcium bioavailability (Kruger & Schollum, 2005) or by inhibiting the proliferation of osteoclast precursors and survival of mature osteoclasts (Haissam et al., 2019; Kim et al., 2017). Bone health is regulated by two processes, bone resorption and bone formation. Osteoclasts are responsible for bone resorption but excessive activity can cause deterioration in bone strength, leading to skeletal and mobility disorders (Bertuglia et al., 2016; Chen et al., 2018). Activation of osteoclast precursor differentiation can be mediated by the RANKL/OPG system produced by osteoblasts. Osteoprotegerin (OPG) is a decoy receptor for RANKL and the ratio between OPG and RANKL is crucial to drive the differentiation of osteoclasts in the microenvironment. RANKL directly participates by binding to receptors on osteoclasts (RANK) and initiates the signaling cascade via tumor necrosis factor receptor-associated factor 6 (TRAF6) to activate NFκB and finally stimulate NFATc1 (Boyce et al., 2015). The completed differentiation results in giant multinucleated cells. The cells are capable of producing the TRAP enzyme, which presents as red colouration in a specific staining assay. Our results showed that the amount of TRAP enzyme and the numbers of TRAP positive cells were significantly reduced by the non-polar lipid fraction and partially reduced by the total lipid fraction at the highest concentration, the latter being relative to the different proportions of non-polar and free fatty acids in its lipid compositions

Factors initiating osteoblasts to upregulate RANKL expression have a downstream influence on osteoclast activation and bone resorption. Pro-inflammatory cytokines such as IL-6 and TNF-α have been found to activate RANKL expression in osteoblasts via TLR4 receptors (Campos et al., 2012). Leptin also indirectly manipulates osteoclast differentiation by activating macrophage proliferation, phagocytosis, and NK cells and by upregulating TNF-α, IL-6, and IL-12 production (Azamar-Llamas et al., 2017). Obesity and menopause, both conditions which escalate leptin production, result

in low-grade inflammation that can lead to bone and articular cartilage attrition. Obesity is an established risk factor for many chronic diseases and in addition to causing increased load bearing upon bone and joints, its other systemic factors are correlated with increased risk fracture of the proximal humerus, upper legs, and ankles (Compston et al., 2011; Prieto-Alhambra et al., 2012). Estradiol was shown to inhibit IL-6 production in vitro, and loss of estrogen by ovariectomy enhances the number of colony-forming units for granulocytes and macrophages, resulting in an increased osteoclast number in trabecular bone (Jilka et al., 1992). Lack of estrogen in post-menopausal women results in the expansion of adiposity highly correlating to increased plasma leptin. These relevant circumstances indicate that osteoclasts have a complicated association with many health conditions. Thus, inhibition of osteoclast activity might be a versatile therapeutic approach for osteoporosis and other bone-associated diseases.

Actin ring formation is the essential cytoskeleton structure of active osteoclasts and is also considered as a functional marker (Teitelbaum, 2000). The formation of this structure is the foundation for osteoclasts to attach to the bone surface prior to the excavation of bone matrix. Bioactive compounds capable of disrupting actin ring foundation in osteoclast development could be beneficial in prevention of bone-related diseases. The GSM non-polar lipid extract at a concentration of 5-20 µg/ml effectively inhibited actin ring formation, showing a reduction in both size and number of rings. The positive control treatment DHA at the concentration of 10 µg/mL similarly inhibited the differentiation and actin ring formation of osteoclasts. This evidence is consistent to a previous study using 20 µg/ml of DHA which completely inhibited the actin ring formation (Boeyens et al., 2014).

NFATc1, the master transcription factor of osteoclast differentiation, regulates gene expression of TRAP, cathepsin K, calcitonin receptor, and osteoclast-associated receptor (OSCAR) through cooperation with microphthalmia-associated transcription factor (MITF) and c-Fos (Kim & Kim, 2014). The GSM non-polar lipid suppressed the expression of NFATc1 and the downstream functional enzymes (CAII, cathepsin K and MMP-9) active in bone digestion. All these findings confirm that the non-polar lipid fraction of GSM oil has a potent anti-osteoclastogenic property involving several genes.

We speculated that the inhibition of osteoclasts was related to free fatty acid composition in GSM oil but it is not possible to specify which of these free fatty acids were responsible for the biological response. Further, it is too soon to reject the

biological activity of PL in osteoclast differentiation assay as our study was not designed to address this question. Therefore, our study concluded that the non-polar lipid relating to free fatty acid of GSM oil inhibited osteoclast differentiation and function in vitro. This bioactivity may reduce the bone resorption process and increase bone formation in humans. Finally, while the results of the in vitro studies shed initial light, there is a need for more evidence in animal studies to confirm whether GSM could improve bone mass in cortical or cancellous bone and have health benefits relating to osteoporosis and osteoarthritis prevention.

MASSEY UNIVERSITY
GRADUATE RESEARCH SCHOOL

STATEMENT OF CONTRIBUTION
DOCTORATE WITH PUBLICATIONS/MANUSCRIPTS

We, the candidate and the candidate's Primary Supervisor, certify that all co-authors have consented to their work being included in the thesis and they have accepted the candidate's contribution as indicated below in the *Statement of Originality*.

Name of candidate:	Parkpoom Siriarchavatana
Name/title of Primary Supervisor:	Dr. Wolber Fran
Name of Research Output and full reference:	
Siriarchavatana P, Kruger MC, Miller MR, Tian HS, Wolber FM: The influence of obesity, ovariectomy and greenshell mussel supplementation on bone mineral density in rats.	
In which Chapter is the Manuscript /Published work:	Chapter 4
Please indicate:	
• The percentage of the manuscript/Published Work that was contributed by the candidate:	90%
and	
• Describe the contribution that the candidate has made to the Manuscript/Published Work:	
Part of animal study work, statistical analysis of bone mineral density data, remaining data analysis, data curation, original draft preparation, review and co-editing, visualization.	
For manuscripts intended for publication please indicate target journal:	
Journal of Bone and Mineral Research Plus	
Candidate's Signature:	Parkpoom Siriarchavatana Digitally signed by Parkpoom Siriarchavatana DN: cn=Parkpoom Siriarchavatana, o=Massey University, ou=College of Health, email=blueno...@gmail.com, c=NZ Date:
Date:	24 July 2020
Primary Supervisor's Signature:	Fran Wolber Digitally signed by Fran Wolber Date: 2020.07.27 14:47:40 +12'00'
Date:	27 July 2020

(This form should appear at the end of each thesis chapter/section/appendix submitted as a manuscript/ publication or collected as an appendix at the end of the thesis)

Chapter 4: The influence of obesity, ovariectomy and greenshell mussel supplementation on bone mineral density in rats

The previous chapter showed that GSM, non-polar lipid, effectively inhibited osteoclast differentiation and functions that are hallmarks of osteoporosis. This led to the hypothesis that some positive biological effects of GSM powder on bone health in this rat study would be observed. As age, estrogen status, diet and obesity can also impact the development of osteoporosis, these factors were incorporated into the design of the rat model. This chapter will explain the effects of age, HFHS (high fat/high sugar) diet, and OVX on the changes of body composition and bone mineral density using DXA scans. MetS will be established in the animals by the aforementioned challenges, and then the study will observe how inclusion of GSM in the diet could affect changes in bone mass and body composition.

Abstract

Obesity is considered to impair long-term health by disturbing multiple physiological functions. However, incremental deposition of fat with aging is considered normal, and some types of fat tissues are beneficial to health. This controversy has been reported in many research studies, particularly in association with osteoporosis in post-menopausal women. The aims of this study were to investigate the relationships between obesity and bone mass under conditions of ovarian hormone deficiency in an animal model and to evaluate the potential health benefits of greenshell mussel (GSM) on bone health. A total of 144 adult female Sprague-Dawley rats were fed from age 12 weeks on one of four diets: normal (ND), ND + GSM, high fat/high sugar (HFHS), or HFHS + GSM (N = 36 per diet). At age 20 weeks, following a dual energy X-ray absorptiometry (DXA) scan, 12 of the rats on each diet underwent ovariectomy (OVX) and the remaining rats were left intact. 12 of the intact rats in each diet group were culled at age 26 weeks (short-term cohort). The remaining rats were culled at age 48 weeks (long-term cohort). Rats were DXA scanned to measure whole-body and location-specific bone mineral density (BMD) as well as total body lean and fat mass prior to cull, and then selected fat pads were dissected. The results revealed that HFHS rats and OVX rats dramatically increased body weight and fat deposition, both of which correlated with circulating leptin concentrations. At the end of the long-term cohort study, HFHS rats (535.38 g ± 27.16) weighed more than ND rats (403.89 g ± 17.30) ($p<0.001$), and OVX HFHS rats (633.35 g ± 34.01) weighed more than OVX ND rats (499.20 g ± 18.56) ($p<0.001$) In long term cohort, vertebral spine BMD rapidly declined after OVX. Significantly higher BMD was found in OVX rats fed HFHS diet when compared to ND but this difference was not recapitulated in intact rats. BMD of right femur was significantly increased 5-10% by GSM in short term cohort. The data demonstrated that obesity can be beneficial by increasing bone mass in OVX rats, and this may extrapolate to post-menopausal women as adipocyte-produced estrogen may slightly compensate for the reduction in ovarian hormones. Finally, the data showed that GSM may be beneficial to bone health by increasing BMD accrual.

4.1 Introduction

The incidence of obesity has increased worldwide in the last five decades (Litwic et al., 2013). It has been recognized as a predisposing cause for many chronic diseases including hypercholesterolemia, hypertension, cardiac disease, and T2D, giving it the status of a global public health burden (Litwic et al., 2013). Osteoporosis is a disease of aging, and it shares a complex relationship with obesity. It used to be considered that obesity had a positive effect on osteoporosis based on a positive correlation between bone mineral density (BMD) and body mass index (BMI) (Zhao et al., 2008; Reid, 2010; Yang & Shen, 2015), and evidence from computed tomography showing that obese people have higher BMD in cortical and trabecular bone as well as increased trabecular bone at the distal radius and tibia (Sornay-Rendu et al., 2013; Evans et al., 2015). Further support from a meta-analysis study showed that low BMI correlated with hip fracture risk (De Laet et al., 2005) with obese adults having lower risk of hip fracture (Tang et al., 2013). However, despite strong evidence of increased BMD in obese adults, the incidence of bone fracture is increased in obese children (Dimitri et al., 2012). Further, there is an increased fracture risk in obese people at the proximal humerus, upper legs and ankles (Compston et al., 2011; Prieto-Alhambra et al., 2012), particularly in post-menopausal women (Compston, 2015). However, the fracture risk in these bone sites might be attributed to impairment of muscular function causing instability of movement in obesity (Scott et al., 2015; Scott et al., 2016). While obesity in older adults is accepted as being at least partly protective against osteoporosis, it is also clearly a risk factor for other chronic disorders such as osteoarthritis, diabetes, cardiovascular disease, and metabolic syndrome. These contradictions in the benefits versus detriments of obesity have given rise to the term “obesity paradox” (Fassio et al., 2018).

Homeostasis of bone structure and function is the equilibrium between bone formation supported by osteoblasts and bone remodeling driven by osteoclasts. From a perspective of cell origin, adipogenesis bias could threaten bone formation and result in bone loss because adipocytes and osteoblasts share a common precursor mesenchymal stem cell in bone marrow (Rosen & Klibanski, 2009). This notion is evidenced by the fact that bone marrow of obese mice has more adipocyte infiltration (Xu et al., 2013). However, the increase of mechanical loading on bone in obesity can inhibit apoptosis and increase the numbers of osteoblasts and osteocytes (Felson et al., 1993; Ravn et al.,

1999; Robling et al., 2006) by activation of the Wnt/β-catenin signaling pathways (Duan & Bonewald, 2016). This could result in an increase in bone formation.

Another controversial factor is leptin, an adipokine secreted from adipocytes, which is significantly increased in the blood of obese people. On one hand, leptin has osteogenic effects by increasing osteoblastogenesis and suppressing adipocytic differentiation in human marrow stromal cells (Thierry et al., 1999). Strong evidence supports the role of leptin in increasing bone mass. Steppan et al. (2000) demonstrated that leptin administration resulted in an increase in femoral bone length, bone mineral content, and BMD in leptin-deficient mice (ob/ob mice). Injection of leptin mitigated cancellous and trabecular bone loss in ovariectomised rats (Burguera et al., 2001). However, other studies suggested that the effect of leptin on the central nervous system was different from its effect on peripheral tissues, resulting in the reduction of bone mass (Wong et al., 2008; Gérard & Mathieu, 2012). Moreover, leptin indirectly activates osteoclastogenesis by activating macrophages to produce pro-inflammatory cytokines (Azamar-Llamas et al., 2017). These cytokines in turn increase RANKL expression in osteoblasts, which directly activates the process of osteoclast differentiation and subsequent bone resorption (Campos et al., 2012). Finally, adipocytes in large numbers, as occurs in obesity, can themselves increase the pro-inflammatory cytokines TNF-α, IL6, IL1β, IFN-γ, MIP-1, GRO-α, and RANTES (Collins et al., 2016).

The relationship between obesity and bone mass is further complicated under post-menopausal circumstances. Estrogen deficiency is associated with not only fat deposition but also bone loss leading to osteoporosis. In addition to the lack of estrogen causing calcium loss from bone, parathyroid levels are elevated correlating with body weight (BW) in obese menopausal women (Bolland et al., 2006; Pitroda et al., 2009) while circulating 25-hydroxyvitamin D levels are low in obese people (Wortsman et al., 2000; Drincic et al., 2012). This evidence supports a correlation between bone loss and obesity in post-menopausal women. However, an increase in adiposity has a benefit on estrogen replacement because aromatase in adipocytes has the ability to produce estrogen as an alternative source for post-menopausal women (Rosen & Klibanski, 2009). The controversy remains a highly debated subject and is unlikely to reach a consensus in clinical research. The current study addressed the issues described above by using an obese rat model compounded with the multiple challenges (high fat/high

sugar diet, OVX, metabolic dysregulation) and followed serial stages of the life cycle in order to further understand the changes in BMD in the context of obesity, post-menopause and aging.

Supplements containing components of greenshell mussel (GSM) have been widely reported to be a rich source of omega-3 fatty acids (Treschow et al., 2007; Miller et al., 2014a), and to have beneficial anti-inflammatory and anti-arthritis effects (Whitehouse et al., 1997; McPhee et al., 2007; Treschow et al., 2007). Omega-3 fatty acids have been shown to protect against osteoporosis (Kruger & Schollum, 2005), although there is no published information to date regarding any potential benefits of GSM on bone health. The current study assessed whether GSM could benefit bone health by increasing BMD in growing rats or reducing bone loss in ovariectomised rats under either normal or obese conditions. The findings from this study, combined with additional studies using a rat model as a tool for preclinical studies assessing the effect of GSM on obesity-related disorders, may clarify some of the ambiguities in the BMD-obesity relationship and as well as in the obesity paradox.

4.2 Materials and methods

4.2.1 Greenshell mussel and diet composition analyses

Flash-dried powder from whole GSM meat was produced by Sanford Ltd (ENZAQ facility, Blenheim, New Zealand) using standard manufacturing processes and assessed for proximate composition in a commercial testing laboratory (Food Testing Laboratory of Cawthron Analytical Services; Nelson, New Zealand). To measure the stability of the diets, samples from each of the experimental diets used in the study were collected and frozen after mixing with mussel powder, and the nutritive value analysed according to the Association of Official Analytical Chemists (AOAC) methods for crude protein (AOAC 981.10), total fat (AOAC 948.15), moisture at 105 °C (AOAC 950.46) and ash (AOAC 920.153). Carbohydrate content was determined by calculation (100% − % crude protein – % total fat – % moisture – % ash). An aliquot of the total lipid extract from the GSM powder was trans-methylated in methanol/chloroform/hydrochloric acid (10:1:1, v/v/v) for 1 h at 100 °C. After the addition of water, the mixture was extracted three times with hexane/chloroform (4:1, v/v) to obtain fatty acid methyl esters (FAME). Samples were made up to 1 mL with an internal injection standard (19:0 FAME) and analysed by gas chromatography mass

spectrometry (GC-MS) according to AOAC 963.22. At the end of the study, base diets without GSM after long-term storage were assessed for proximal analysis by the IANZZ-accredited Massey University Nutrition Laboratory using methods as described above.

4.2.2 Animals and study design

One-hundred-forty-four female Sprague-Dawley rats aged 12 weeks were obtained from the Small Animal Production Unit at Massey University (Palmerston North, New Zealand), randomized into groups, and fed test diets for 14 weeks (short-term cohort, 48 rats) or 36 weeks (long-term cohort, 96 rats) after a one week acclimatization period. Animals were maintained in conventional systems and singly housed in plastic "shoe box" cages with high-top wire lids, using heat-treated aspen wood shavings as bedding. The rat rooms were kept at 22 ±1 °C, 45-55% humidity and a 12/12 hour light-dark cycle. The numbers of rats per test group was selected calculating a power (1-β) of 0.8 and a type 1 error rate (α) of 5% for the key parameter of bone mineral density using data from our research group's previous rat studies. All aspects of the study were approved by Massey University Animal Ethic Committee (MUAEC protocol/approval 16/112).

Normal versus high-fat high-sugar diets were used to allow comparisons between normal-weight and obese rats groups that these diets generated. Each base diet type (Specialty Feeds, Glen Forrest, Western Australia) was obtained as a single batch, colour-coded and number-coded, packaged in vacuum-sealed plastic pouches containing 4.5 or 5 kilos within a cardboard box, and used within 9 months of receipt. Diets were stored frozen until needed. All diets were designed to contain 15% protein as is standard for AIN-93M. The proportion of GSM was selected on the assumption that, extrapolated to the human diet, one meal out of each three meals per day would source the protein from GSM; therefore, for the rat diets one-third of the protein was sourced from GSM for the GSM-containing diets. After thawing a pouch in the refrigerator, diets designed to incorporate GSM had GSM powder added in a ratio of 1 part GSM: 9 parts base diet. Diets were then stored refrigerated during the week of use. Subsamples of each diet were taken periodically for further chemical analysis.

Each day, uneaten diet from each individual feeder was weighed and discarded, and feeders were cleaned and filled with new food, which was weighed and recorded to

measure food intake. The test diets, designed to meet or exceed all AIN-93M requirements, were:

(1) normal control diet (ND) containing 5% total fat (from soy oil), 5% sucrose, and 15% total protein (from casein); “yellow diet”

(2) normal control diet supplemented with GSM (ND + GSM) containing 5% total fat (84% from soy oil/16% from GSM), 5% sucrose, and 15% total protein (66% from casein/33% from GSM); “orange diet”

(3) high-fat high-sugar diet (HFHS) containing 30% total fat (50% from soy oil/50% from lard), 30% sucrose, and 15% total protein (from casein); “pink diet”

(4) high-fat high-sugar diet supplemented with GSM (HFHS + GSM) containing 30% total fat (49% from soy oil/49% from lard/1% from GSM), 30% sucrose, and 15% total protein (66% from casein/33% from GSM) “green diet”.

4.2.3 Dual–energy X-ray absorptiometry (DXA) scans

DXA whole-body and regional scans to generate bone mineral density and fat mass/lean mass data in the short-term cohort were performed at baseline (age 12 weeks) and after 8 and 14 weeks on the experimental diets (age 20 and 26 weeks). The long-term cohort schedule was similar to the short-term cohort but with an additional scan after 36 weeks on the experimental diets (age 48 weeks). For both cohorts, after the baseline DXA scan rats were randomised into diet groups, ensuring that there were no significant differences between groups in basal body weight, no significant differences in lumbar spine and whole body bone mineral densities, and that littermate sisters were distributed as evenly as possible across groups within a cohort. A total of 24 dams provided the rats for these studies; the number of daughters per litter ranged from 1 – 12 (mean = 6.6). Rats in the long-term cohort were further randomised into surgical groups within their diet groups, with randomisation again based on eliminating significant differences in body weight and bone mineral density.

Anaesthesia and DXA scans were carried out as described previously (Kruger & Morel, 2016). BMD was evaluated with a Hologic Discovery, a bone densitometer (Bedford, MA). Quality control checks were performed before scanning the animals and the acceptance of coefficient of variance was 0.98-1.01. Rats were positioned supine with right angles between the spine and femurs. All scans used a high resolution mode.

4.2.4 Surgical procedures and euthanasia

In the long-term cohort, at the age of 20 weeks, half of each group (12 of 24 rats) underwent ovariectomy, and the other half a sham surgery as described previously (Kruger & Morel, 2016). At the end of each cohort, all rats were subjected to euthanasia by undergoing deep anaesthesia followed by exsanguination. Samples including different fat pads (inguinal fat, interscapular brown fat, retroperitoneal fat and perigonadal fat) were dissected and weighed.

4.2.5 Plasma leptin measurement

A sandwich ELISA method, Quantikine Mouse/Rat leptin (R&D Systems, Minneapolis, USA), was used to measure plasma leptin concentrations. Samples were performed in duplicates and reactions were measured using a microplate reader (Multiskan FC, ThermoFisher Scientific, Vantaa, Finland)

4.2.6 Data analysis

The food consumption and body weight of different time point from the intact rats (sham) and the ovariectomised rat (OVX) in different diet groups are summarised as mean ± SE. The significant different across all conditions of diets and surgical procedures were determined by one-way ANOVA followed by a multiple comparison test of the least significant difference method. $P < 0.05$ is used to determine the statistical significance.

Body fat mass and body lean mass measured by DXA scans from serial time points were calculated into percent change compared to each individual animal's baseline data. In this case, T1 = the difference between the baseline data and the 20-week-old rats' data (before surgery); T2 = the difference between the baseline data and the 28-week-old rat's data (6 weeks after surgery); T3 = the difference between the baseline data and the data at the end of the study. The percent change was compared using two-way ANOVA with repeated measure method. Time was assigned as a within-subject effect in the analysis; a single or multiple effects of diet, GSM, and OVX were assigned as a between-subject effect. The post-hoc test used was the least significant difference to identify the significant influence of those effects within the same time point. $P<0.05$ was taken to determine statistical significance.

Selected white and brown fat pads were harvested and weighed at the termination of each cohort. To compare the effects of different diet conditions, means of each group

and each cohort were separately analysed by one-way ANOVA and the least significant test. OVX rats and sham rats in the long term study were also divided in the analysis. To compare the effect of time or OVX, independent T test was used to test the differences across those conditions but within the same diet condition. All statistical significance was determined by p values less than 0.05.

Data from serial DXA scans were calculated in percent change according to T1-T3 as aforementioned and data were adjusted for body weight to control for the confounding effect of body weight on bone mineral density. Two-way ANOVA with repeated measure statistical analysis was used to identify the influence of three effects -- diet (ND/HFHS), GSM (yes/no) and surgical procedure (OVX, sham) -- as described above for body fat mass and body lean mass. One-way ANOVA and least significant difference methods were used to analyse data between groups within one particular time point. Pearson correlation was used to evaluate relationships between body composition and bone mineral density. Statistical analysis was performed using IBM statistic software (SPSS) version 25 (Armonk, NY, USA) and differences were considered significant at $p<0.05$. Statistically significant differences are discussed in the text; however, non-significant changes and observable trends are also noted as these may provide important evidence in animal studies when the number of animals per group precludes these changes reaching statistical significance.

4.3 Results

4.3.1 Analysis of diet composition

Protein was equivalent in ND and HFHS diets (Table 4.1), but the partial substitution of carbohydrate with fat in the HFHS and HFHS + GSM diets increased the energy levels to 24.9 and 22.9 kilojoules per gram (kj/g) compared to the ND and ND + GSM diets (16.9 and 16.8 kj/g respectively). Added fat in the HFHS diet increased saturated fatty acid (SFA) and monounsaturated fatty acid (MUFA) but not polyunsaturated fatty acid (PUFA). Two omega-3 fatty acids particularly associated with bone-health protection, DHA and EPA, were increased in diets containing GSM, but there was no change in the omega-6 fatty acids (linoleic acid and arachidonic acid) (Table 4.1). Ash content of GSM powder contains high amounts of inorganic substances including sodium, and calcium. Inclusion of GSM powder to the base diets resulted in an increase of 2-4% ash in those diets. The protein content in HFHS+GSM diet was 1%

lower than other diets, which can likely be attributed to minor errors in mixing, subsampling, and/or analytical method; it was observed that after the base diets had been in storage for 9 months, proximal analysis carried out by a different laboratory found ND to have 6.7% fat, 4.2% ash, 8.7% moisture, 12.4% protein and 68.0% carbohydrate, and HFHS to have 42.9% fat, 2.4% ash, 2.6% moisture, 11.7% protein and 40.5% carbohydrate .

Table 4.1 Nutritive value of the four different diets in the study

	ND	ND+GSM	HFHS	HFHS+GSM
Proximate composition (g/100g)				
Fat	5.4	5.1	31.3	30.1
Ash	2.9	4.7	2.7	4.1
Moisture	8.3	8.2	3.7	3.3
Crude Protein	13.5	13.3	13.5	12.6
Carbohydrate	69.9	68.7	48.8	49.9
Fatty acid profile (%Fatty acids)				
C16:0 palmitic acid	11.2	12.1	18.2	17.8
C18:0 stearic acid	4.8	4.7	10.4	10
C18:1n7 vaccenic acid	1.5	1.7	1.9	1.9
C18:1n9c oleic acid	21.9	20.6	28.2	27.8
C18:2n6c linoleic acid	48.6	45.5	31.7	31.6
C18:3n3 alpha linolenic acid (ALA)	6.2	5.8	4.1	4.2
C20:4n6 arachidonic acid (AA)	<0.1	<0.1	<0.1	<0.1
C20:5n3 eicosapentaenoic acid (EPA)	<0.1	1.2	<0.1	0.31
C22:6n3 docosahexaenoic acid (DHA)	<0.1	0.93	<0.1	0.21
∑SFA	16	16.8	28.6	27.8
∑MUFA	23.4	22.3	30.1	29.7
∑PUFA	54.8	53.43	35.8	36.32
- ∑n-3 PUFA	6.2	7.93	4.1	4.72
- ∑n-6 PUFA	48.6	45.5	31.7	31.6

Diet samples were taken during the experimental period and sent to Cawthron Institute at the end of the study. The analysis was performed according to the Association of Official Analytical Chemists (AOAC) methods. ND=normal control diet, HFHS=high fat/high sugar diet, GSM=greenshell mussel powder, ∑SFA = sum of saturated fatty acids; ∑MUFA = sum of monounsaturated fatty acids; ∑PUFA = sum of polyunsaturated fatty acids; ∑n-3 PUFA = Omega-3 polyunsaturated fatty acids; ∑n-6 PUFA= Omega-6 polyunsaturated fatty acids

4.3.2 Body weight gain and food consumption

Time 0 (T0) designates the period of growing rats on standard chow from age 4 weeks to 12 weeks, during which the rate of BW gain of almost 3 g/day was similar across all groups in the long-term cohort (Figure 4.1 and Table 4.2). The experimental diets were introduced to the animals at week 12th (the end of T0). At this time point, the range of mean BW across all groups (Table 4.2) was 267.37-280.84 g with no significant difference between groups (p =0.911). The rate of mean BW gain in the following periods (T1-T3) declined consecutively, especially in intact rats on the normal control diet (ND), while BW gain in the OVX rats increased immediately after the surgical procedure (T2) before returning to the rate of gain observed in T1.

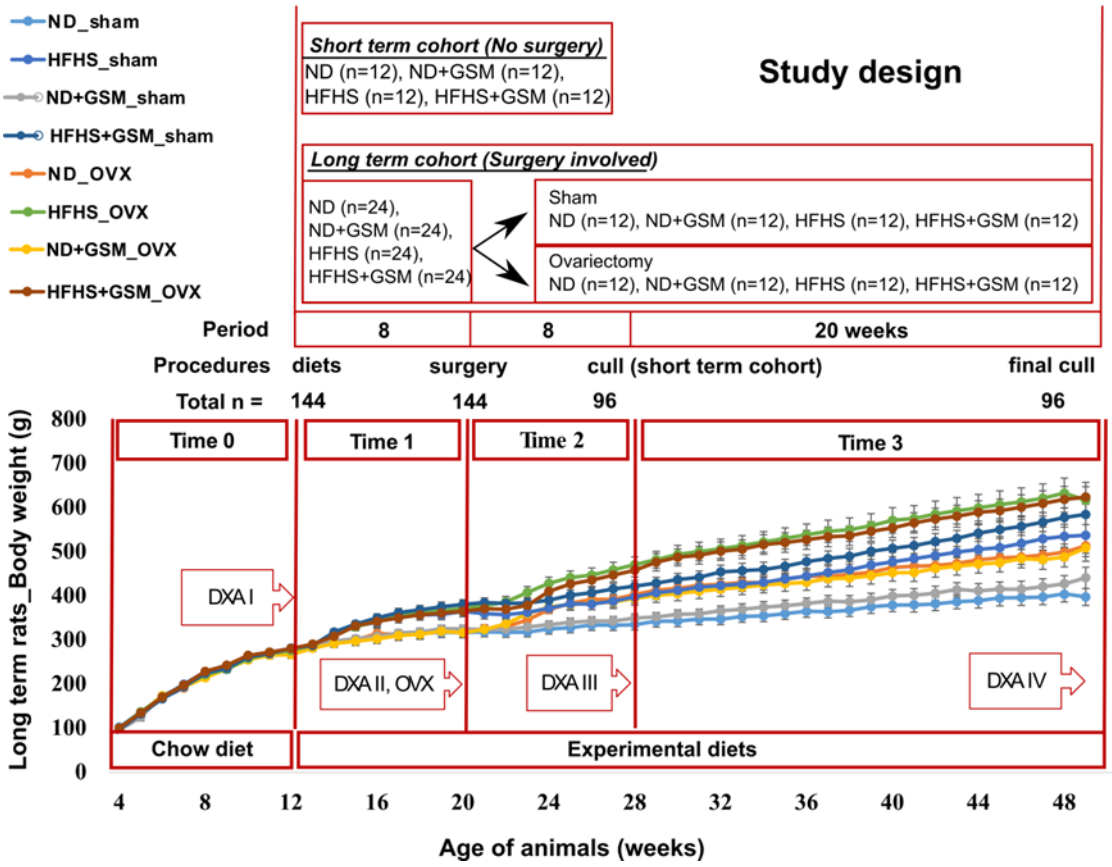

Figure 4.1: Study plan and BW gain in rats along the long term cohort:

Individual rat body weights were recorded in grams every week. Group means + SE are shown plotted in the line graph. Groups: ND= normal control diet, HFHS=high-fat-high-sugar diet, OVX=ovariectomy, DXA= Dual energy X-ray absorptiometry scanning. The periods of the study were specified as "Time"; Time 0 = rat growing period on standard chow, Time 1 = experimental diets provided for 8 weeks, Time 2 = 8 weeks after the surgical procedures, Time 3 = termination of the study.

During the first 8 weeks on the experimental diets prior to surgery (T1), rats fed HFHS consumed 20% less food by weight than those fed ND but had a 12% higher kilojoule intake per day due to the HFHS diets being more energy-dense (Table 4.2). As a result, the HFHS rats had an 82% higher rate of mean daily BW gain compared to ND rats. Inclusion of GSM during this period slightly increased weight gain but this was not significant. Following sham operation or ovariectomy (OVX) at the end of T1, during the next 8 week period (T2) feed intake, energy intake and BW gain were significantly higher in OVX rats compared to sham rats (BW gain in sham = 0.54-0.70 g/day versus OVX 1.32-1.89 g/day, $p<0.001$). For the last period of the study (T3), voluntary food consumption rate by OVX rats reduced to a similar rate as sham rats but their BW gain continued to be higher than sham rats and subsequently OVX rats had higher BW at the

end of the study, especially those fed HFHS. The OVX procedure increased total final BW by 24% and 18% respectively in rats fed ND and HFHS compared to their sham counterparts ($p<0.001$), but only 14% and 7% respectively in rats fed ND+GSM and HFHS+GSM, suggesting that regardless of diet type the inclusion of GSM showed a trend to partially mitigate the weight gain caused by OVX although this did not reach statistical significance.

Table 4.2 Changes in food consumption and body weight

	Sham				OVX				
	ND	**ND+GSM**	**HFHS**	**HFHS+GSM**	**ND**	**ND+GSM**	**HFHS**	**HFHS+GSM**	P values
BW 12th week	273.73±8.53	276.06±6.20	280.84±7.01	281.62±7.54	275.64±8.20	267.37±8.96	276.51±7.93	280.70±6.41	NS
BW 20th week	317.30±10.82^{ab}	325.39±8.69^{abcd}	365.21±12.28^{bcde}	380.91±10.97^{e}	320.58±7.72^{abc}	316.68±11.37^{a}	372.09±13.61^{de}	365.50±11.78^{cde}	< 0.001
BW 28th week	335.54±12.40^{a}	349.75±9.63^{ab}	397.77±13.73^{bc}	422.59±12.54^{cde}	403.13±11.05^{bcd}	394.58±15.24^{abc}	470.91±17.97^{e}	458.34±14.92^{de}	< 0.001
BW the end	403.89±17.30^{a}	428.18±18.05^{a}	535.38±27.16^{bc}	578.15±21.78^{bc}	499.20±18.56^{ab}	488.27±22.36^{ab}	633.35±34.01^{c}	619.05±29.34^{c}	< 0.001
Weight gain (g/day)									
Time 0	2.71±0.11	2.85±0.10	2.91±0.09	2.93±0.09	2.82±0.09	2.65±0.14	2.80±0.10	2.85±0.11	NS
Time 1	0.65±0.08^{a}	0.67±0.08^{a}	0.99±0.10^{ab}	1.37±0.14^{b}	0.66±0.07^{a}	0.70±0.15^{a}	1.26±0.20^{ab}	1.26±0.27^{ab}	< 0.001
Time 2	0.54±0.05^{a}	0.56±0.06^{a}	0.70±0.09^{a}	0.69±0.09^{a}	1.78±0.10^{bc}	1.32±0.10^{b}	1.74±0.15^{bc}	1.89±0.17^{c}	< 0.001
Time 3	0.48±0.05^{a}	0.55±0.06^{ab}	0.87±0.10^{bcd}	0.94±0.09^{cd}	0.68±0.07^{abc}	0.64±0.05^{abc}	1.10±0.14^{d}	1.06±0.11^{d}	< 0.001
Feed intake (g/day)									
Time 1	16.72±0.53^{c}	15.90±0.56^{bc}	12.71±0.47^{a}	13.76±0.37^{ab}	16.97±0.51^{c}	15.55±0.68^{bc}	13.28±0.54^{a}	12.57±0.41^{a}	< 0.001
Time 2	16.17±0.44^{b}	15.79±0.56^{b}	11.94±0.42^{a}	12.13±0.38^{a}	19.53±0.48^{c}	18.61±0.62^{c}	14.76±0.47^{b}	14.36±0.48^{b}	< 0.001
Time 3	16.19±0.48^{b}	16.22±0.53^{b}	12.86±0.46^{a}	13.43±0.43^{a}	16.81±0.45^{b}	16.48±0.37^{b}	13.61±0.58^{a}	13.68±0.49^{a}	< 0.001
Energy intake (Kcal/day)									
Time 1	59.93±1.91^{ab}	57.00±2.00^{a}	63.81±2.38^{ab}	69.08±1.84^{b}	60.82±1.83^{ab}	55.75±2.45^{a}	66.64±2.71^{b}	63.08±2.04^{ab}	< 0.001
Time 2	57.96±1.58^{ab}	56.60±2.01^{a}	59.94±2.11^{ab}	60.89±1.90^{ab}	70.02±1.71^{c}	66.71±2.21^{bc}	74.07±2.34^{c}	72.08±2.39^{c}	< 0.001
Time 3	58.03±1.72^{a}	58.16±1.88^{a}	64.54±2.30^{abc}	67.39±2.15^{bc}	60.27±1.61^{abc}	59.09±1.34^{ab}	68.31±2.90^{c}	68.65±2.44^{c}	< 0.001

The food consumption and body weight of different time points from the intact rats (sham) and the ovariectomised rats (OVX) in different diet groups are summarized. Values are mean±SE. The significant differences across all conditions (diets and surgical procedures) were determined by one-way ANOVA and p values are indicated in the last column. In case, no statistical significance (NS) was found then no multiple comparison performed. Significance is recognized when p values less than 0.05 and superscript letters indicate the least significant difference test. Values that do not share the same superscript letters are significantly different. Time 0 = rat growing period on standard chow, Time 1 = experimental diets provided for 8 weeks, Time 2 = 8 weeks after the surgical procedure, Time 3 = termination of the study. Group: ND=normal control diet, HFHS=high fat/high sugar diet, OVX=ovariectomy, GSM=greenshell mussel.

4.3.3 Changes in body composition

In the long-term cohort (Figure 4.2A), body fat mass of all rats increased significantly over time. Both HFHS and OVX independently caused significant increases in the acquisition of body fat mass. During T1 (age 12 weeks to 20 weeks), body fat mass approximately doubled in ND groups and tripled in HFHS groups. This increase was recapitulated during T2 following surgery (age 20 weeks to 28 weeks), and was even more pronounced during T3 (age 28 – 48 weeks), when body fat mass increased nearly 10-fold; the effect was greatest in OVX rats fed HFHS. Interestingly, OVX caused a significant increase in body lean mass over eight weeks (T2) but no further gains in lean mass occurred during the twenty week T3 period. There was a significant interaction effect of diet and GSM on body lean mass with time. At T2, HFHS reduced the increase in lean mass acquired by ND rats. Adding GSM in ND caused a reduction in lean mass while being combined with HFHS resulted in a slight increase in lean mass. However, the latter two findings were trends and did not reach statistical significance.

At the end of the short-term and long-term studies, all rats were subjected to necropsy and both visceral and subcutaneous fat pads were harvested and weighed (Figure 4.2B). Data from the short-term cohort who did not undergo sham or OVX surgery were compared with the sham rats of the long-term cohort while the OVX rats were compared against the sham rats in the same cohort. As expected, feeding HFHS diets to rats for 14 weeks or 36 weeks resulted in a significant increase in retroperitoneal (32.84 ± 3.17) and perigonadal (21.52 ± 1.43) as well as inguinal (subcutaneous) white fat pad weights (17.76 ± 2.48) compared to ND, but did not consistently alter the much smaller pad of interscapular brown fat (1.15 ± 0.08); the weight of the brown fat differed significantly only between the ND and HFHS+GSM groups in the short-term cohort and the long-term sham cohorts. Likewise, age significantly increased the weight of the white but not brown fat pads. OVX significantly increased the abdominal fat pads only in rats fed ND, but significantly increased the subcutaneous fat pad weight in all four diet groups. (Figure 4.2B; Table A5 of Appendix B)

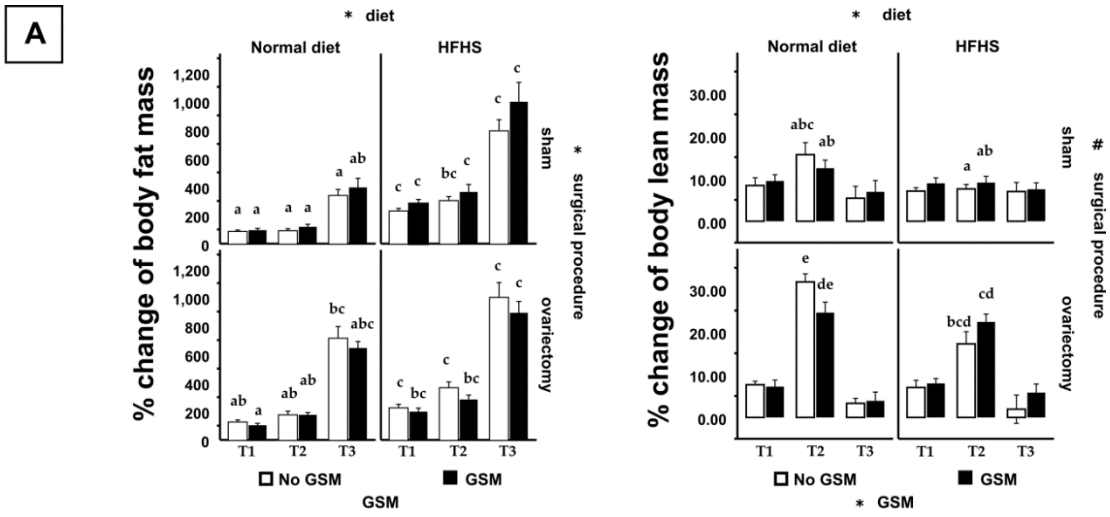

Percent change	time	time * diet	time * GSM	time * OVX	time * diet * GSM	time * diet * OVX	time * GSM * OVX	time * diet * GSM * OVX
WB_Fatmass	<0.001	<0.001	0.693	<0.001	0.464	0.040	0.098	0.508
WB_Leanmass	<0.001	<0.001	0.105	<0.001	0.004	0.327	0.586	0.344

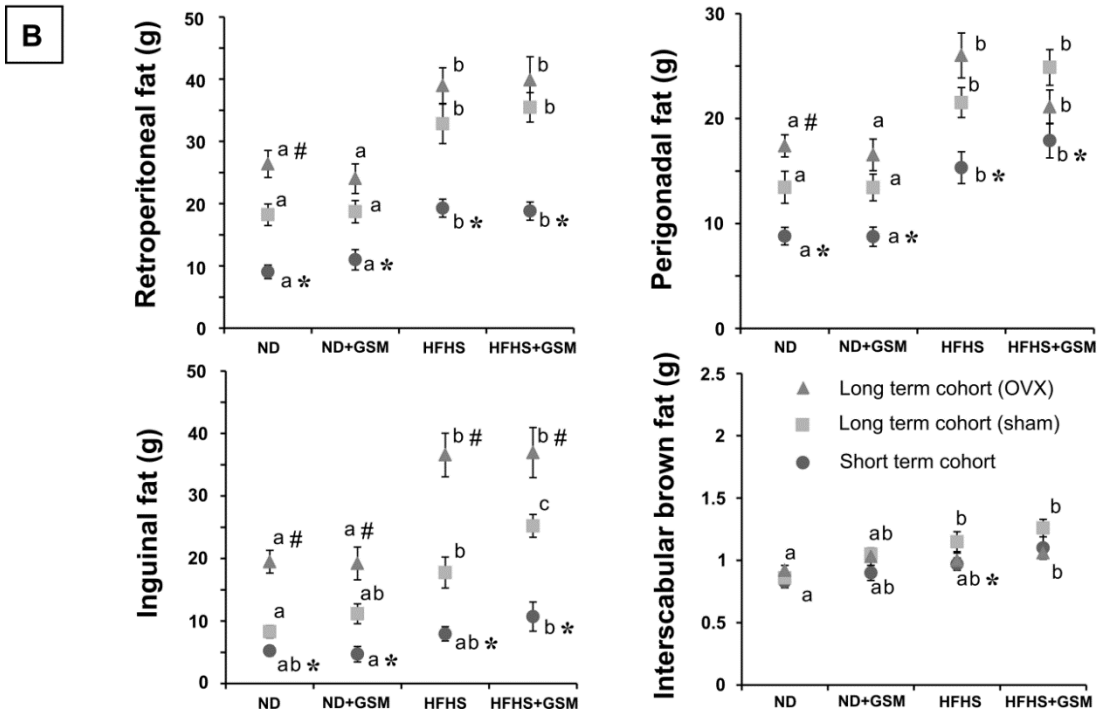

Figure 4.2: Changes in body composition

Body composition was measured by Dual energy X-ray absorptiometry in the long-term cohort rats (12-48 weeks old) (A). Then data were statistically analysed by repeated measured method and a summary of p value was reported in the table. The signs (* or #) adjacent to the name of the effects (diet, surgical procedure, GSM) indicate significant differences. In case of there is an interaction effect, the same sign is present on those effects. One-way ANOVA and a multiple comparison (least significant different test) were also used to analyse the data across all groups. The differences of letters indicate significant differences. At the end of each study, all rats were sacrificed and each type of fat pad was harvested and weighed (B). Data were summarized in box-whisker graphs which represent mean± SE. One-way ANOVA and the least significant difference test were used to analyse data across the groups then different superscript letters were given to indicate statistical significance. Independent T test was used to

compare the data in the same diet condition. An asterisk * shows significant difference when compared the short-term cohort with the long-term (sham). Hashtag # was used instead for comparison between the sham rats and OVX rats. All statistical significance was determined by P value less than 0.05. Group: ND=normal control diet, HFHS=high fat/high sugar diet, OVX=ovariectomy, GSM=greenshell mussel. Legend: Short term cohort=non-operated rats sacrificed at 26 weeks of age, Long term cohort (sham)=intact rats sacrificed at 48 weeks of age, Long term cohort (OVX)=ovariectomised rats sacrificed at 48 weeks of age.

4.3.4 Changes in bone mineral density

Bone mineral density was measured in three different scans: whole body, lumbar spine, and right femurs. In the short-term cohort (Figure 4.3), whole body BMD increased with time between baseline (age 12 weeks) to age 20 weeks (T1) and 26 weeks (T2) regardless of diet or GSM. Changes in BMD of spine and femurs were proportionally greater than whole body BMD. Of interest was the finding that inclusion of GSM in the HFHS diet significantly increased femur BMD during the final 6 weeks of the study (T2).

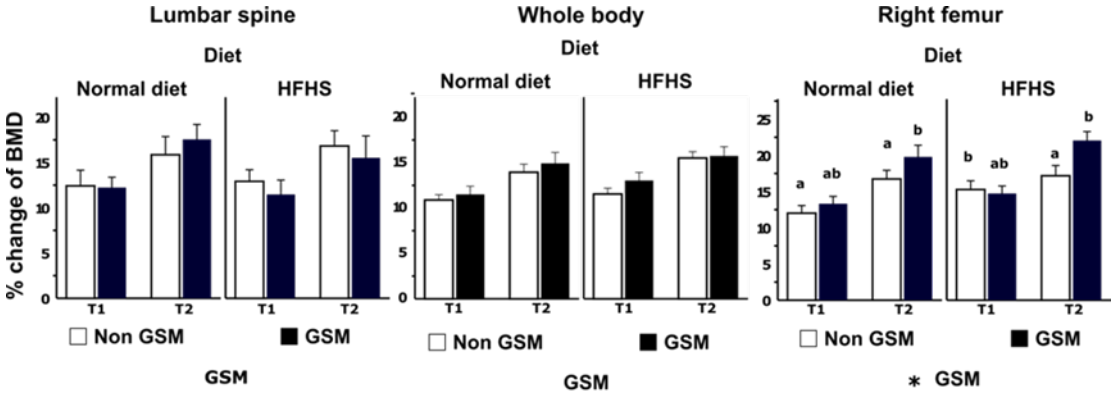

Percent change of Bone mineral density	Time	Time* Diet	Time* GSM	Time* Diet* GSM
Right femur	<0.001	0.334	0.001	0.076
Lumbar spine	<0.001	0.775	0.475	0.537
Whole body (WB)	<0.001	0.880	0.483	0.210

Figure 4.3: Percent change of bone mineral density in short-term-cohort rats (12-26 weeks old)

The individual chart represents the different bone sites which are lumbar spine (L1-L4), whole body (WB) and right femur. Bars and error bars represent mean and SE (n=12) of percent change between the baseline of bone mineral density (BMD) at week 12th and the particular time point (T1 or T2, which is week 20th and week 26th respectively). Repeated measure analysis was used to analyse statistically significant differences between the time points and those two effects (diet and GSM). An asterisk is indicated on graphs next to the name of the effect when the effect is significant. Letters; a or b or ab are provided as possible if there is a statistical difference when compared the mean of the different groups of rats in the same period by one-way ANOVA and least significant difference method was used for multiple comparison test. A table summary from repeated measured analysis shows p values which are significant at <0.05. Group: ND=normal control diet, HFHS=high fat/high sugar diet, OVX=ovariectomy, GSM=greenshell mussel.

In the long-term cohort, OVX was the main determinant causing BMD to fail to increase in tandem with body mass; in particular, only OVX rats lost bone mineral density in the lumbar spine and the right femur (Figure 4.4). GSM showed a trend to increase whole body, lumbar spine, and right femur BMD at T1 in all groups but ND sham rats, and a significant difference was detected in sham rats on HFHS at T2 of the whole body scan. There was an interaction effect between diet and surgical procedure in the lumbar spine bone mineral density changes during T3. All sites of BMD in sham rats fed ND tended to be higher compared to sham HFHS rats, but the opposite effect was observed in OVX rats, although these differences did not reach statistical significance. Likewise, in the right femurs, only OVX had a significant effect, resulting in a significant reduction in BMD during T3

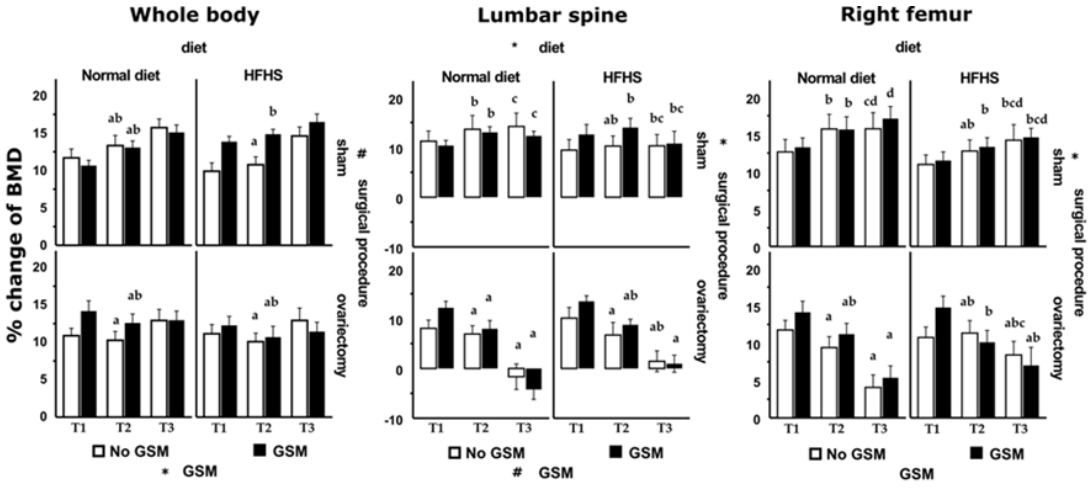

Percent change	time	time * diet	time * GSM	time * OVX	time * diet * GSM	time * diet * OVX	time * GSM * OVX	time * diet * GSM * OVX
WB_BMD	<0.001	0.483	0.002	<0.001	0.640	0.692	0.185	0.370
RF_BMD	0.001	0.143	0.134	<0.001	0.281	0.149	0.125	0.28
LS_BMD	<0.001	0.347	0.003	<0.001	0.866	0.015	0.231	0.527

Figure 4.4: Percent change of bone mineral density in long-term cohort rats (12-48 weeks old)

The individual chart represents bone mineral density (BMD) of the different bone sites which are whole body (WB), lumbar spine (L1-L4), and right femur. Bars and error bars represent means and SE (n=12) of percent change between the baseline of bone mineral density (BMD) at week 12th and the particular time point (T1 or T2 or T3, which is week 20th, 28th, and 48th respectively). Repeated measure analysis was used to analyse statistically significant differences between the time points and those three effects (diet, GSM and OVX). A sign (asterisk* or hashtag#) was labelled close to the name of the effects when statistical significance of the main effect was detected. The similar sign showed on different effects means the significance of the interaction effect between those. One-way ANOVA and least significant difference methods were used to analyse data between groups within one particular time point then differences of superscript letters show statistical significance. A table summary from repeated measured analysis shows *p* values which is significant at less than 0.05. Group: ND=normal control diet, HFHS=high fat/high sugar diet, OVX=ovariectomy, GSM=greenshell mussel.

4.3.5 Relationships between obesity and bone mass

To understand the relationship between obesity and BMD, data from T3 were interrogated and the correlations between BMD of individual bone sites and BW, fat mass, lean mass or leptin were graphed (Figure 4.5).

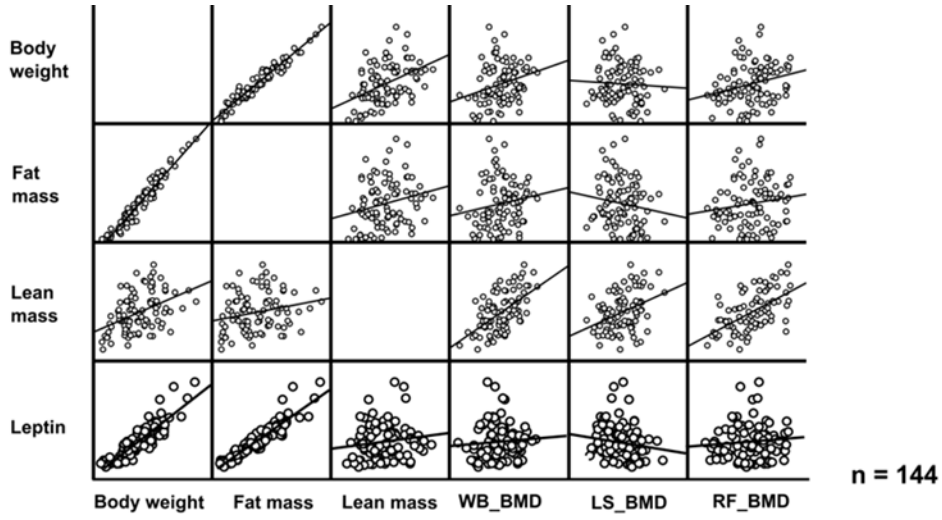

		Body weight	Body fat mass	Body lean mass	WB_BMD	RF_BMD	LS_BMD
Body weight	Pearson Correlation	1	0.971**	0.445**	0.280**	0.268**	-0.053
	Sig. (2-tailed)		< 0.001	< 0.001	0.006	0.009	0.612
Body fat mass	Pearson Correlation	0.971**	1	.233*	0.152	0.131	-0.173
	Sig. (2-tailed)	< 0.001		0.023	0.142	0.206	0.093
Body lean mass	Pearson Correlation	0.445**	0.233*	1	0.566**	0.572**	0.363**
	Sig. (2-tailed)	< 0.001	0.023		< 0.001	< 0.001	< 0.001
Leptin	Pearson Correlation	0.872**	0.927**	0.138	0.071	0.087	-0.148
	Sig. (2-tailed)	< 0.001	< 0.001	0.189	0.502	0.412	0.159

Figure 4.5: Correlation of body weight or fat mass or lean mass or leptin against bone mineral density of different bone sites

The data at the final time point (T3) from all rats of the long-term cohort was pooled together and analysed. Correlation is presented in both figures and values from Pearson correlation method. Statistical significance was set at p <0.05 and asterisk* was indicated. ** and *** mean p<0.01 and 0.001 respectively. WB=whole body, LS=lumbar spine, RF=right femur.

BW had minimal correlation with whole body and right femur BMD at 0.280 and 0.268 respectively. Extracting BW into fat mass and lean mass resulted in a higher correlation of body lean mass with BMD in all scans, whereas body fat mass correlated poorly with BMD. Leptin, an adipokine produced by adipocytes, was highly correlated with fat mass (0.927, p <0.001) but showed no correlation with any BMD scans. Then BMD data were segregated into each group and correlation curves of BMD against BW or plasma leptin were depicted (Figure 4.6 and Table A2 of Appendix B). As can be seen in the graphs, there were tightly positive correlations between BMD and BW in

only the sham rats on ND. Introducing other interventions of GSM, HFHS or OVX caused some modification of this pattern and possibly explained the interference of their effect on BMD. In the whole body BMD, the positive correlation as showed by trend line turned downward in OVX rats on HFHS and similar downturns were also seen in most group of lumbar spine BMD.

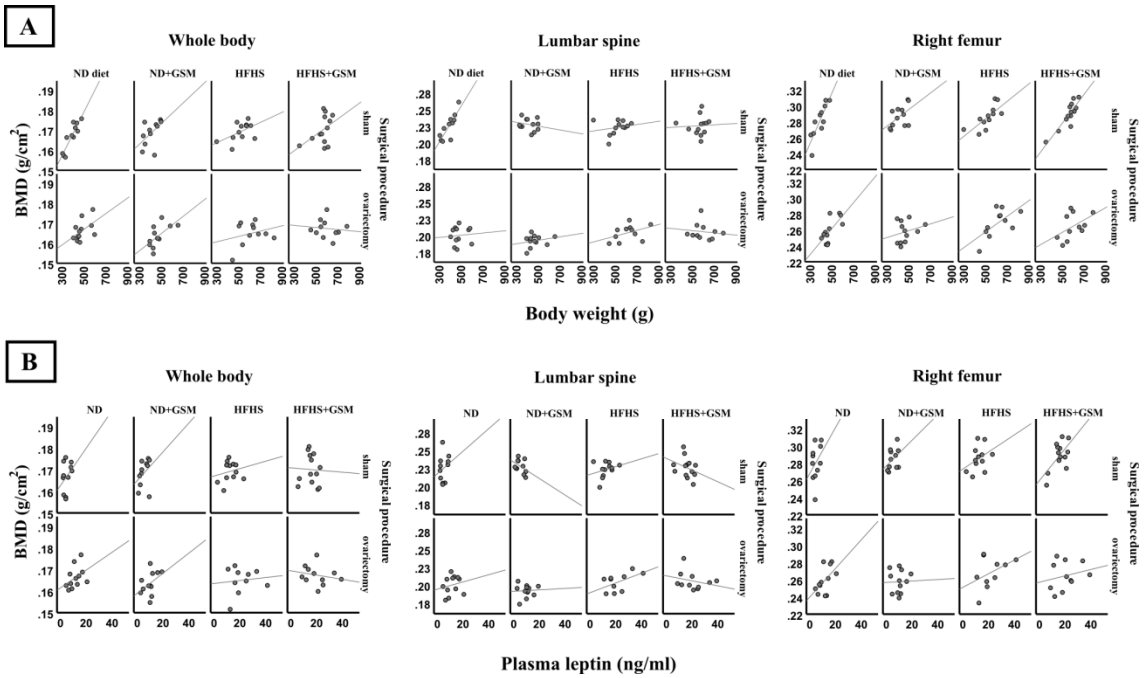

Figure 4.6: Correlation of body weight or leptin with bone mineral density in the individual group

Data at the final time point (T3) of the long-term cohort was stratified in the different condition groups and correlation analysis was performed. Correlation between body weight and bone mineral density (BMD) or between leptin and BMD is present in A and B respectively.

4.4 Discussion

Our study showed that GSM supplementation increased BMD of the right femur especially in rats in the short-term cohort. The statistically significant difference of this data is consistent even after adjusting BMD with BW. However, the effect was very mild (only 5% differences when compared to non GSM diet), inconsistent with comparative BMD in other body sites, and transient as this effect disappeared at the same time (T2) and the later time (T3) in the long-term cohort. It is possible that with this very small effect size, a larger sample size would be needed to reveal a consistent result. On the other hand, it might be irrelevant to expect more than a minor change of BMD in physiologically normal rats as body homeostasis regulates the optimal levels of minerals in bone. Any values undergoing extreme changes may represent pathological

stages rather than a beneficial effect. Another explanation is that a higher dose of bioactives may be required for being effective; the dosage levels on a per-kg body weight basis would be reduced when the food intake did not proportionally increase with increased body weight.

In addition, the bioactives in GSM may not be potent enough to prevent severe bone loss from OVX. Our results seem to support the benefit of omega-3 rather than omega-6 because the composition of the diets supplemented with GSM contained DHA and EPA while these omega-3 fatty acids were not present in the GSM-free diets. Arachidonic acid is an omega-6 fatty acid and was not present in all diet formulae. The total amount of DHA and EPA in ND+GSM was approximately 2 g/ 100 g. If the average daily feed intake of the rats was 20 g and the mean body weight was 500 g then each rat would receive the combination of DHA and EPA at a dose of 800 mg/kg. This dose level is higher than the daily dosage recommended for humans (Punia et al., 2019) and reached the therapeutic doses of GSM in animal studies (Whitehouse et al., 1997; McPhee et al., 2007; Treschow et al., 2007), although these studies did not specifically assess bone health. Thus, it would be predicted that the daily intake in the current study would at least maintain the effective dose of DHA and EPA for anti-inflammation in the rats. However, as individual lipids were not tested in this study, the bioactive factor(s) cannot be definitively identified. It is also noted that GSM diets contained more ash, and therefore it is possible that the beneficial effects of GSM included additive or synergistic effects between lipids, proteins and peptides, and/or minerals such as calcium.

Feeding rats with HFHS induced obesity; even though these animals consumed a lower volume of food due they had a higher overall energy intake due to the HFHS diet being energy-sense. This resulted in a greater rate of weight gain per day. Weight gain and BW increased in accordance with both feed intake and energy intake in all groups except the sham rats on ND+GSM. Although those rats consumed less food than their paired diet group and even though the GSM diets provided slightly lower energy source (fat, protein and, carbohydrate) the rats' BW still increased significantly.

There was no significant change in the feed intake in all sham rats throughout the study. OVX rats however increased their food intake after the surgical procedure for a short period within 2 months, and then the consumption rate reduced to these rats' baseline intake and matched the same level as sham animals. The modified food intake

in OVX rats had significant effects on their weight gain and increased BW. This main effect resulted in OVX rats being the most obese in the study; the brief period of increased food intake is likely due to the fact that ovarian hormones have direct effects on adipose tissues and indirect effects on regulation of feed intake and energy expenditure via hypothalamus (Cooke & Naaz, 2004; Rosaria et al., 2004) although those specific parameters were not tested in the current study. Similar results were also found in other animal studies (Roy & Wade, 1977; Fonseca et al., 2012) and corresponding human studies in which post-menopausal women increased their food intake and weight a few years after the onset of menopause (Lovejoy et al., 2008), alterations in metabolism that likely can be attributed to hormonal changes.

Fat mass was the source of BW gain in the older rats as can be seen in the consecutive increases of percent change of body fat mass by DXA scans. Also, all main white fat pads harvested during necropsy (retroperitoneal, perigonadal and, inguinal fat pad) significantly increased from 6-month-old rats to 12- month-old rats. Inguinal fat, which is subcutaneous fat situated around groin and inguinal regions, was present as only a half of that perigonadal fat mass. There was a significant increase of interscapular brown fat due to feeding HFHS diet but this effect was not present in OVX rats. This finding probably indicates that estrogen deficiency reduces the effect of diet on brown fat tissue.

As expected, HFHS and OVX showed cumulative effects on the expansion of these fat pads; therefore, the OVX rats on HFHS accumulated more fat tissue compared to the other groups. Interestingly, the inguinal fat pad, a type of subcutaneous fat composed of mixed functional (white and brown) adipocytes in OVX rats accelerated its expansion in a more pronounced fashion than retroperitoneal and perigonadal fat pad which are visceral fat composed of white adipocytes. This revealed that OVX influenced shifting the course of fat accumulation from visceral fat to inguinal fat. OVX did not only influence fat deposition but also significantly increased lean mass in a short period of time after surgery. It is possible that the observed increase in feed intake directly after ovariectomy supported an increase in body lean mass through increased protein intake. More importantly, the instant loss of estrogen due to ovariectomy would result in a higher androgen:estrogen ratio. The relative increase in androgen could enhance body lean mass and also influence the shift of fat distribution. This finding corroborates with Morita et al. (2006) reporting a short-term increase of body lean mass

in women after menopause and a shift of fat distribution from leg-groin area to the upper part of body and abdominal cavity. There was an interaction effect of diet and surgical procedure which could possibly explain the different effects of OVX on the significant increase of fat mass only in ND groups but not HFHS groups at T3. Body fat tended to increase in sham rats but reduced in OVX rats when adding GSM into the diets, although these differences did not reach statistical significance. In contrast, body lean mass increased and reached the peak at the middle age of the animals then declined at the older age.

Loss of BMD in OVX rats was observed consistently in the lumbar spine and femur scans. However, the whole body scan, which is less accurate for detecting bone loss in subjects with high body fat compared to the other scans, did not show reduced BMD at the end of the study in OVX rats. Thus using the whole body scan to interpret the relationship between body compositon and bone mineral density in the context of the obesity paradox is inappropriate. More information about whether the rats in this study could reasonably be categorised as normal, overweight or obese can be found in Appendix A (Addendum).

The other DXA scans revealed that the deposition of calcium in the femur, the long bone, takes precedence over the lumbar spine in rats as percent changes of BMD in femurs were higher compared to lumbar spines. Even though most bone sites showed significant bone loss in response to ovariectomy, the lumbar spine is the most sensitive bone site to detect the early bone loss in OVX rats. This finding seems to be different from the study of human trials indicating the total hip is the most reliable site for detecting osteoporosis or predicting hip fracture (Sheu & Diamond, 2016). This discrepancy might be due to the fact that our study scanned the whole femur which is composed more of cortical bone rather than the cancellous bone found in the femoral head and pelvic part of the total hip region. However, the same study also recommended using spinal BMD for monitoring treatment. At around 6 months after OVX, estrogen deficiency may cause bone fragility in the lumbar spine as the BMD was lower than the baseline and in clinical practice, low BMD at hip is used for predicting hip fracture (Sheu & Diamond, 2016). It has been posited that the expansion of adipocytes in obesity may have an advantage on bone in post-menopausal women by being an alternative source of estrogen. Unfortunately, estrogen levels were not measured in this study and

thus this cannot be confirmed, and a significant positive correlation between fat mass and BMD was not observed.

To explore some aspects of the complex relationship between obesity and bone and whether obesity has any benefit on to BMD, relevant parameters of all rats at the end point data were pooled and correlation analysis was done. The data generally showed that it was not BW and fat mass but only lean mass that had a high correlation with BMD, although we observed significant correlations between fat mass and lean mass as well as between BW and fat mass and between BW and lean mass. These findings demonstrate the complexity of defining "obesity" and might raise the question of whether BW needs to be adjusted for, in correlation with BMD in obese populations as these subjects are likely to have increased fat mass proportionally higher than lean mass.

High levels of fat mass correlated with increased leptin production in the rats, which in turn was highly correlated with BW and fat mass, but leptin still failed to show a correlation with BMD. The data were stratified into groups and the correlations were re-evaluated. Surprisingly, a highly positive correlation of BW and BMD in ND/Sham rats was detected in all bone site scans and a similar result was found in the correlation with leptin. Therefore, in our model increased BW and leptin correlated with an observed positive influence on BMD within the normal weight range. We hypothesise that there are likely to be causal relationships between some of these parameters but this has not yet been demonstrated conclusively.

Many findings in this animal study are in accordance with the evidence in post-menopausal women. In women, bone growth during childhood and adolescence contributes to the achievement of peak bone mass resulting in bone strength of later life (Ho & Kung, 2005). Attainment of peak bone mass depends on a variety of nutritional and endocrine factors (Whiting et al., 2004). Many studies have reported the benefits of PUFA consumption however omega-3 and omega- 6 are debated in context of anti-inflammation (Tortosa-Caparrós et al., 2017) and bone health (Abdelhamid et al., 2019). The increase in BMD theoretically is related to increased calcium deposition in the bone matrix and this might be due to the capability of enhanced calcium absorption in duodenum by DHA and EPA (Haag et al., 2003)

However, some discrepancies between rodents and humans were evident in this study or have been reported elsewhere. For instance, women have two main parts of

subcutaneous fat all located at the lower part of the body, which is gluteofemoral and abdominal fat depot. Gluteofemoral fat in women has been considered as a healthy fat associated with lower triglycerides (Snijder et al., 2005) and higher concentration of high-density lipoprotein cholesterol (Bos et al., 2005), producing lower pro-inflammatory cytokines than visceral fat (Manolopoulos et al., 2010) whereas abdominal fat has detrimental effects associated with insulin sensitivity similar to visceral fat (Kelley et al., 2000; Smith et al., 2001). A rat's subcutaneous fat, on the other hand is divided into cranial and caudal part which are interscapular fat and inguinal fat respectively. Both fat pads have common type of beige adipocytes and different from white adipocytes of visceral fat. In post-menopausal women, preferential site of fat deposition is shifted from subcutaneous fat depot to visceral fat depot (intra-abdominal fat) regardless of age (Toth et al., 2000) but this study showed that OVX rats increased inguinal fat mass more pronounced than visceral fat when compared with sham rats and probably, total subcutaneous fat may greater than visceral fat in OVX rats. Furthermore, women reach the peak of bone mass at the hip by approximately 20 years old (Dimitri et al., 2012) followed by a decline, while rats are sexually mature by 2.5 months of age but bone growth still remains until 10 months of age (Lelovas et al., 2008). BMD at all bone sites measured in the sham rats in this study increased over time hence the data may not extrapolate to human bone loss in advancing age. However, bone growth in this rat model provided an opportunity to investigate the effect of GSM on enhancement of calcium acquisition in bone.

In conclusion, our data has partially unravelled the ambiguity of the obesity paradox identified in humans and enabled inference with human bone health by establishing correlations between a number of parameters. Firstly, increased BW appears to enhance bone mineral density to some extent as long as the weight gain is associated with an increase in lean mass. High fat mass in general was not beneficial to bone density in these rats although it has been reported to have some advantages of increased bone mass in post-menopausal women. Moreover, consumption of GSM was correlated with increased acquisition of bone mineral density in younger age rats but had no effect on increased BMD in ovarian hormone deficiency. Taken together these findings suggest that the bioactive components in whole GSM are slightly beneficial to bone density accrual throughout the adult lifespan, and suggest that whole GSM as well as concentrated marine lipid extracts could be marketed for bone healt

MASSEY UNIVERSITY
GRADUATE RESEARCH SCHOOL

STATEMENT OF CONTRIBUTION
DOCTORATE WITH PUBLICATIONS/MANUSCRIPTS

We, the candidate and the candidate's Primary Supervisor, certify that all co-authors have consented to their work being included in the thesis and they have accepted the candidate's contribution as indicated below in the *Statement of Originality*.

Name of candidate:	Parkpoom Siriarchavatana
Name/title of Primary Supervisor:	Dr. Wolber Fran
Name of Research Output and full reference:	
Siriarchavatana P, Kruger MC, Miller MR, Tian HS, Wolber FM: The Preventive Effects of Greenshell Mussel (Perna canaliculus) on Early-Stage Metabolic Osteoarthritis in Rats with Diet-Induced Obesity. Nutrients 2019, 11(7):1601.	
In which Chapter is the Manuscript /Published work:	Chapter 5
Please indicate:	
• The percentage of the manuscript/Published Work that was contributed by the candidate:	90%
and	
• Describe the contribution that the candidate has made to the Manuscript/Published Work:	
Part of animal study work, all formal analysis, investigation, data curation, original draft preparation, review and co-editing, visualization.	
For manuscripts intended for publication please indicate target journal:	
published (Nutrients)	
Candidate's Signature:	Parkpoom Siriarchavatana Digitally signed by Parkpoom Siriarchavatana DN: cn=Parkpoom Siriarchavatana, o=Massey University, ou=College of Health, email=blueno...@gmail.com, c=NZ Date:
Date:	24 July 2020
Primary Supervisor's Signature:	Fran Wolber Digitally signed by Fran Wolber Date: 2020.07.27 14:56:39 +12'00'
Date:	27 July 2020

(This form should appear at the end of each thesis chapter/section/appendix submitted as a manuscript/ publication or collected as an appendix at the end of the thesis)

GRS Version 4– January 2019

Chapter 5: The preventive effects of greenshell mussel (*Perna canaliculus)* on early-stage metabolic osteoarthritis in rats with diet-induced obesity

The previous chapter showed that inclusion of greenshell mussel (GSM) powder in the short term rats' diets (26 weeks of age, with dietary intervention beginning at age 13 weeks) had an influence by increasing bone mineral density. The effect might be related to anti-osteoclastogenesis or increased calcium absorption from the gastrointestinal tract. This chapter will assess the early events of osteoarthritis pathogenesis in the short term rats and identify whether GSM powder can protect against the development of osteoarthritis in rat knee joints. If so, the findings may simultaneously support the anti-osteoclastogenesis activity of GSM observed in the cell culture study and localise the initial mechanism of MetOA to the subchondral bone.

Abstract

The prevalence of osteoarthritis (OA) is rising worldwide, with the most pronounced increase being in the category of metabolic-associated osteoarthritis (MetOA). This is predicted to worsen with the global rise in aging societies and obesity. To address this health burden, research is being conducted to identify foods that can reduce the incidence or severity of MetOA. Oil from the greenshell mussel (*Perna canaliculus*) (GSM), a native New Zealand shellfish, has been successfully used to reduce OA symptoms. The current study assessed the effect of including flash-dried powder from whole GSM meat as part of a normal (control) or high-fat/high-sugar (HFHS) diet for 13 weeks on the development of MetOA in rats. Rats fed a HFHS diet developed metabolic dysregulation and obesity with elevated plasma leptin and HbA1C concentrations. Visible damage to knee joint cartilage was minimal, but plasma levels of C telopeptide of type II collagen (CTX-II), a biomarker of cartilage degradation, were markedly higher in HFHS-fed rats compared to control-fed rats. However, rats fed the HFHS diet containing GSM had significantly reduced serum CTX-II. Inclusion of GSM in rats fed the control diet also lowered CTX-II. These findings suggest that dietary GSM can reduce the incidence or slow the progression of early MetOA.

5.1 Introduction

Osteoarthritis (OA) is a chronic disease of joints featuring articular cartilage erosion resulting in progressive pain and joint immobility. It affects 3.7% of the global population, equating to approximately 268 million people (Briggs et al., 2016). The prevalence increases by age group. OA can be classified into four subtypes based on its pathogenesis: post-traumatic, genetic predisposing, ageing, and metabolic-associated osteoarthritis (MetOA). It is projected that MetOA incidence will continue to increase in parallel with the incidence of obesity (Zhuo et al., 2012).

The relationship between obesity and osteoarthritis is not due simply to the physical demands caused by additional body weight; this is evident because frequently osteoarthritis in obese patients occurs in non-weight bearing joints such as the fingers, hands, wrists and temporomandibular joint (Cicuttini et al., 1996). Instead, systemic factors associated with low-grade chronic inflammation are implicated. In animals fed high-energy diets, this is indicated by the presence of inflammatory cells, especially macrophages, in adipose tissue (Gregor & Hotamisligil, 2011). Obese rats display a significant increase both in the volume of white adipose tissue in the body and in the size of individual adipocytes. Adipocytes are capable of producing many types of pro-inflammatory cytokines and chemokines such as tumour necrosis factor-α (TNF-α), interleukin 1 (IL-1), interleukin 6 (IL-6), interferon-γ IFN-γ, macrophage inflammatory protein-1 (MIP-1), growth-related oncogene-α (GRO-α), and regulated on activation, normal T cell expressed and secreted (RANTES) (Collins et al., 2016). Moreover, they secrete adipokines into the blood circulation. One of the most significant adipokines is leptin, which has an influence on chronic inflammation (Eun-Young et al., 2012) and may contribute to the development of osteoarthritis caused by obesity (Teichtahl et al., 2005; Barboza et al., 2017; Pearson et al., 2017).

The greenlipped or Greenshell™ mussel (GSM) (*Perna canaliculus*) is an important commercial marine species of New Zealand. Its lipid fraction contains high amounts of long-chain omega-3 polyunsaturated fatty acids (EPA (20:5n-3) and DHA (22:6n-3)) as well as various types of interesting minor fatty acids: 5,9,12,15-octadecatetraenoic acid (C18:4); 5,9,12,16-nonadecatetraenoic acid (C19:4); 7,11,14,17-eicosatetraenoic acid (C20:4); and 5,9,12,15,18-heneicosapentaenoic acid (C21:5) (Treschow et al., 2007). Long-chain omega-3 polyunsaturated fatty acids such as EPA and DHA compounds are known to have anti-inflammatory properties. In particular, the

GSM oil fraction extracted by supercritical fluidic CO2 method has been shown to have an inhibitory effect on prostaglandin E2 (PGE2) in lipopolysaccharide (LPS)-activated mononuclear cells (Whitehouse et al., 1997) via both the cyclooxygenase pathway (McPhee et al., 2007) and the lipoxygenase pathway (Treschow et al., 2007). Its molecular mechanisms have been studied in LPS-induced RAW 264.7 cells and found to involve the NF-κB and MAPK kinase signaling pathways (Chen et al., 2017).

In a study employing an adjuvant-induced arthritis rat model, a GSM oil extract of 15 mg/kg BW had more potent anti-inflammatory effects than doses of 25 mg naproxen, 50 mg ibuprofen, 300 mg aspirin or 300 mg dried mussel (Whitehouse et al., 1997). This mussel oil at a dose of 300 mg/kg caused no gastrointestinal toxicity, a common side effect of aspirin, or any other negative side effects in the animals. It also had an analgesic effect at the initial phase of inflammation; *ex vivo* splenocytes reduced production of the pro-inflammatory cytokines, TNF-α and IFN-γ, but increased the anti-inflammatory cytokine IL-10 (Chi-Ho et al., 2009). Pre-clinical veterinary studies involved with GSM have also been recently reviewed. Most of these studies were predicated on the hypothesis that anti-inflammatory activity of mussel lipids would be due to long-chain polyunsaturated fatty acids (LC-PUFAs), omega-3 or furan fatty acid (Wakimoto et al., 2011). Although there remains strong evidence supporting the health benefits of mussel oil in arthritis via regulation of inflammatory processes (Whitehouse et al., 1997; McPhee et al., 2007; Treschow et al., 2007), animal model studies published to date have been carried out only in post-traumatic osteoarthritis models by using chemical or surgical induction to destabilize the joints. The current study was designed to focus specifically on MetOA, which is a chronic disorder and the most common debilitating affliction in the obese population.

5.2 Materials and methods

5.2.1 Analysis of GSM composition

The analysis methods are described in section 4.2.1.

5.2.2 Animal study

Forty-eight female Sprague Dawley (SD) rats aged 11 weeks reared on standard chow were obtained from the Small Animal Production Unit at Massey University (Palmerston North, New Zealand) and the study was conducted in the same animal facility as approved by the Massey University Animal Ethics Committee (MUAEC

protocol/approval 16/112). The animal room environment was set at 22 ± 1 °C, with 45%–55% humidity and a 12/12 light-dark cycle throughout the study. The rats were singly housed in conventional cages with heat-treated aspen wood shavings as bedding. After a one-week acclimatization period, the rats were randomized into test groups and fed one of four diets (Specialty Feeds, Glen Forrest, Western Australia) for 13 weeks:

(1) normal control diet (ND) containing 5% total fat (from soy oil), 5% sucrose, and 15% total protein (from casein);

(2) normal control diet supplemented with GSM (ND + GSM) containing 5% total fat (84% from soy oil/16% from GSM), 5% sucrose, and 15% total protein (66% from casein/33% from GSM);

(3) high-fat high-sugar diet (HFHS) containing 30% total fat (50% from soy oil/50% from lard), 30% sucrose, and 15% total protein (from casein);

(4) high-fat high-sugar diet supplemented with GSM (HFHS + GSM) containing 30% total fat (49% from soy oil/49% from lard/1% from GSM), 30% sucrose, and 15% total protein (66% from casein/33% from GSM).

Fresh food was provided daily and the previous day's food intake was measured. At the end of the study, rats were food-deprived overnight. All rats were anesthetized and subjected to dual energy X-ray absorptiometry scanning (DXA) as described elsewhere (Kruger & Morel, 2016) to measure lean mass and fat mass. Plasma was collected from EDTA-anticoagulated blood samples drawn by cardiac puncture and stored at −80 °C until analysis. Retroperitoneal, perigonadal, inguinal, and interscapular fat pads were individually dissected and weighed. Knee joints were dissected out and stored in formalin prior to further processing as described below.

5.2.3 Plasma analysis

Duo-set kits for rat IL10 (Catalogue number (CN) DY522), TNF-alfa (CN DY510) , IL-6 (CN DY506), IL1β (CN DY501), Quantikine Mouse/Rat leptin (CN MOB00) and Quantikine Rat total adiponectin/Acrp30 kits (CN RRP300) were obtained from R&D System, Minneapolis, USA. CTX-II assay kit (CN CEA686Ra) was obtained from Cloud-Clone Corp, TX, USA. HbA1C assay kit (CN ER1030) was obtained from (Fine Test, Wuhan Fine Biological Technology, Wuhan, China). All assays were carried out following the manufacturer's instructions and the optical density

was measured using a microplate reader (Multiskan FC, Thermo Fisher Scientific, Vantaa, Finland).

5.2.4 Histopathological assessment

After the knee joints were dissected, each of them was separately submersed in 10% buffer formalin fixative followed by a decalcification process in 10% EDTA buffer for four weeks. Knee joints were cut along the coronal plane at the middle of the collateral ligament and embedded in paraffin. Two sections were cut at a thickness of 3 µm and stained with safranin-O. Articular cartilage at the tibial plateau was evaluated by 14-point Mankin score criteria (Mankin et al., 1971), which evaluates the formality of structure, cellularity, matrix staining, and tidemark.

5.2.5 Data analysis

Statistical analysis was performed using IBM statistics software (SPSS) version 25 (Armonk, NY, USA). Data were analysed by one-way ANOVA or Student's t-test. Multiple comparisons were analysed by the least significant difference test. Data from the pathological study of knee joint scoring was an ordinal scale; therefore, a non-parametric statistic, the Mann–Whitney U test, was applied to compare groups in the study. A p value <0.05 was considered statistically significant.

5.3 Results

5.3.1 GSM composition

The GSM powder used to supplement the rat diets was comprised of approximately 43% protein, 22% carbohydrate, 21% ash, 8% fat, and 6% moisture (Table 5.1). The fatty acids were equally represented by saturated and polyunsaturated fatty acids, with monounsaturated fatty acids being present at much lower levels.

Table 5.1 Nutritive value of greenshell mussel (GSM) powder and the composition of fatty acids.

Proximate composition (g/100 g)	
Fat	8.1
Crude protein	43
Carbohydrate	21.9
Moisture	5.8
Ash	21.2
Fatty acid profile (% fatty acids)	
C14:0 myristic acid	5.9
C16:0 palmitic acid	20.3
C17:0 heptadecanoic acid	1.2
C18:0 stearic acid	4.9
C18:1n7 vaccenic acid	3.2
C18:1n9c oleic acid	2.1
C18:2n6c linoleic acid	2.1
C18:3n3 α-linolenic acid (ALA)	1.4
C18:3n4 octadecatrienoic acid	1.3
C18:4n3 stearidonic acid (SDA)	2.5
C20:1 gadoleic acid	2.6
C20:4n6 arachidonic acid (AA)	1.0
C20:5n3 eicosapentaenoic acid (EPA)	13.5
C22:5n3 docosapentaenoic acid (DPA)	1.0
C22:6n3 docosahexaenoic acid (DHA)	10.7
∑SFA	34.29
∑MUFA	8.23
∑PUFA	34.20
∑n-3 PUFA	29.4
∑n-6 PUFA	3.5

∑SFA = sum of saturated fatty acids; ∑MUFA = sum of monounsaturated fatty acids; ∑PUFA = sum of polyunsaturated fatty acids; ∑n-3 PUFA = Omega-3 polyunsaturated fatty acids; ∑n-6 PUFA= Omega 6 polyunsaturated fatty acids

5.3.2 Animal study

After 13 weeks on the test diets, HFHD-fed rats had significantly higher BW gain than ND-fed rats, as expected. Body composition data revealed the weight gain was due to additional fat deposition in the body, as percent body fat was almost double in HFHS-fed rats compared with ND-fed rats. Retroperitoneal and perigonadal fat masses rose from approximately 10 g each in ND-fed rats to nearly 20 g in HFHS-fed rats, corresponding with the approximate doubling in percent total body fat. The inguinal fat pad, although smaller, also showed a near-doubling between ND and HFHS rats, with GSM inclusion in the HFHS diet resulting in a significant increase. Only the interscapular fat pad showed a minor difference in weight between the diet groups, although the gain was statistically significant in the HFHS + GSM group (Table 5.2).

Table 5.2 Body weight and fat deposition of the rats at the end of the study.

Weight (g)	ND	ND + GSM	HFHS	HFHS + GSM	*p*-Value
BW (week 0)	277.14 ± 8.24	280.47 ± 10.48	280.78 ± 6.53	276.28 ± 9.43	NS
BW (week 13)	343.00 ± 45.70[a]	351.80 ± 51.00[a]	400.80 ± 50.43[b]	417.2 ± 88.08[b]	0.010
% BW gain	24.05 ± 7.95[a]	25.44 ± 8.62[a]	42.42 ± 9.56[b]	48.22 ± 15.72[b]	<0.001
%body fat (week 0)	11.16 ± 3.48	11.36 ± 4.62	11.24 ± 3.64	12.83 ± 4.03	NS
%body fat (week 13)	21.2 ± 5.43[a]	22.88 ± 7.90[a]	34.39 ± 4.80[b]	36.46 ±7.52[b]	<0.001
%body fat gain	101.13 ± 65.10[a]	112.48 ± 60.96[a]	232.89 ± 98.82[b]	193.91 ± 51.78[b]	<0.001
Lean mass(week 0)	237.68 ± 22.77	236.28 ± 27.05	234.44 ± 20.73	227.39 ± 21.92	NS
Lean mass(week 13)	269.62 ± 32.55	275.29 ± 29.86	266.68 ± 26.49	266.04 ± 29.97	NS
% lean mass gain	13.34 ± 6.52	16.89 ± 8.10	13.77 ± 6.30	17.01 ± 6.54	NS
Retroperitoneal	9.05 ± 3.90[a]	11.14 ± 5.89[a]	19.28 ± 5.01[b]	18.81 ± 5.10[b]	<0.001
Perigonadal	8.80 ± 3.04[a]	9.04 ± 3.17[a]	15.31 ± 5.25[b]	17.90 ± 5.73[b]	<0.001
Inguinal	5.23 ± 2.87[a]	4.98 ± 4.42[a]	7.95 ± 3.95[a]	10.71 ± 8.09[b]	0.023
Interscapular	0.83 ± 0.18[a]	0.90 ± 0.23[a]	0.97 ± 0.19[a]	1.10 ± 0.31[b]	0.033

Data are shown as mean ± SD of n = 11–12 rats per group and were analysed by one-way ANOVA or by the least significant difference test for multiple comparison tests. Different superscript letters indicate significant difference at $p \leq 0.05$. NS = no significance difference, BW = body weight, ND = normal control diet, HFHS = high-fat high-sugar diet

Plasma analytes are shown in Table 5.3. Plasma cytokines were detected at low (picogram/mL) concentrations with high variability between subjects, and showed no trends or statistical differences between test groups. HbA1C (glycated hemoglobin), a biomarker for high blood glucose, was elevated in HFHS-fed rats, with a significant difference in the HFHS + GSM group when compared to ND-fed rats. Leptin was highly variable between individuals; however, leptin levels in rats fed either of the NDs were <9 ng/mL while the HFHS diets resulted in more than double those levels. Adiponectin was present in very high (µg/mL) concentrations but did not differ between groups. Only leptin was highly correlated with BW, percent body fat, and specific fat pads; leptin was not correlated with lean mass (Figure 5.1).

Table 5.3 Inflammatory and metabolic markers in rat plasma at the end of the study.

Analysts	ND	ND + GSM	HFHS	HFHS + GSM	*p*-Value
IL-1β (pg/mL)	23.90 ± 39.34	4.93 ± 7.45	6.95 ± 15.23	13.46 ± 36.93	NS
IL-6 (pg/mL)	21.90 ± 19.23	29.40 ± 19.67	16.23 ± 22.27	19.56 ± 20.27	NS
IL-10 (pg/mL)	3.36 ± 7.16	7.33 ± 13.11	14.31 ± 38.74	2.39 ± 5.03	NS
TNF-α (pg/mL)	0.16 ± 0.58	0.35 ± 0.81	1.25 ± 3.30	0.00 ± 0.00	NS
HbA1C(ng/mL)	252.25 ± 50.46[a]	227.10 ± 41.59[a]	275.44 ± 67.73[a]	326.76 ± 120.24[b]	0.044
Leptin (ng/mL)	7.71 ± 5.62[a]	8.47 ± 5.52[a]	18.26 ± 10.94[b]	21.72 ± 14.59[b]	0.002
Adiponectin (µg/mL)	8.17 ± 1.97	7.85 ± 2.94	7.92 ± 1.94	9.51 ± 0.96	NS

Rat plasma analytes were measured by ELISA in duplicate wells. Data are shown as mean ± standard deviation and were assessed by one-way ANOVA; NS = no significant difference. Least significant difference method was applied for multiple comparison tests. Different superscript letters indicate significant difference at $p \leq 0.05$.

	Body weight	Lean mass	% Fat	Retro-peritoneal	Epididymal	Inguinal	Inter scapular	Total fat pad
Pearson Correlation	0.856**	0.277	0.832**	0.812**	0.789**	0.835**	0.685**	0.902**
p-Value	<0.001	0.057	<0.001	<0.001	<0.001	<0.001	<0.001	<0.001

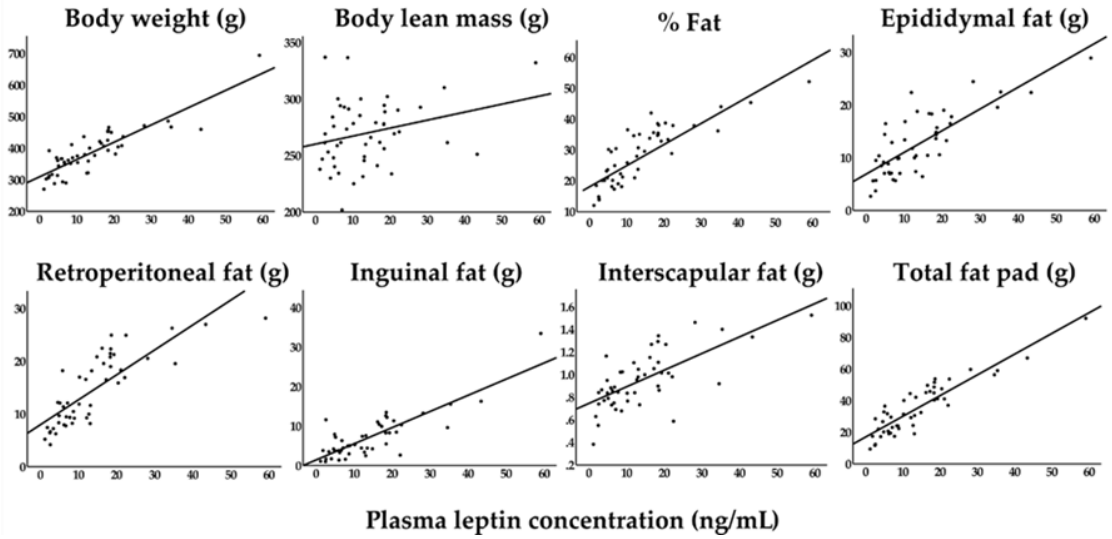

Figure 5.1: Correlation of plasma leptin with body composition and fat pads

The data was evaluated by the Pearson correlation method. Asterisks indicate a significant difference. "Total fat pads" is the summation of retroperitoneal, perigonadal, inguinal, and interscapular fat pad. Scatter plot charts represent the correlation of plasma leptin with each individual parameter.

To evaluate the presence of early osteoarthritis in the rats' joints, cartilage degradation was measured using the plasma biomarker C-terminus telopeptide of type II collagen (CTX-II). The results showed that rats fed the HFHS diet had a higher level of CTX-II than rats fed either of the NDs. Interestingly, including GSM in the diet slightly reduced CTX-II in the ND rats and significantly reduced CTX-II in the HFHS rats (Figure 5.2).

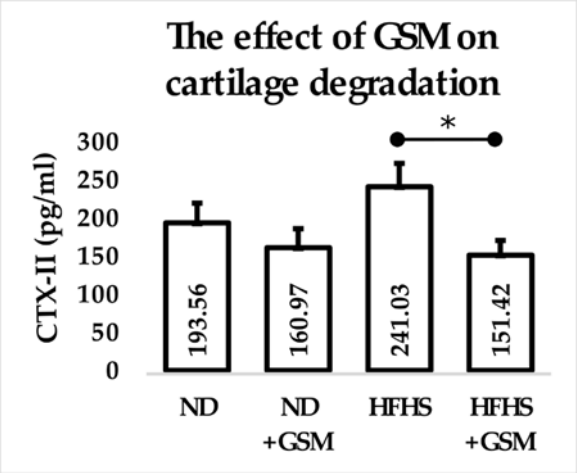

Figure 5.2: Modulation of cartilage degradation by diet

Plasma samples were assessed in duplicate for C-terminus telopeptide of type II collagen (CTX-II) by competitive ELISA. Data are shown as mean + standard deviation of n = 11–12 rats per group, and the mean values inserted into each bar. * $p \leq 0.05$ between the groups within a diet by Student's t-test.

As the CTX-II data indicated the presence of cartilage degradation at least in the HFHS group, the rat knee joints were assessed. The cartilage layers were microscopically examined in accordance with the Mankin scoring system (Figure 5.3A). All histological sections presented a normal appearance with similar thicknesses of cartilage layers and homogeneous colour stains (Figure 5.3C–F). A small amount of irregularity of articular surface was observed only in the knee joints of rats fed the HFHS diet (Figure 5.3B) but these were not statistically significant when the Mankin scores were analysed using a Mann–Whitney U test. However, there was an observable trend for the HFHS rats to have a higher Mankin score than the ND diet rats, and for this to be reduced when GSM was added to the HFHS diet.

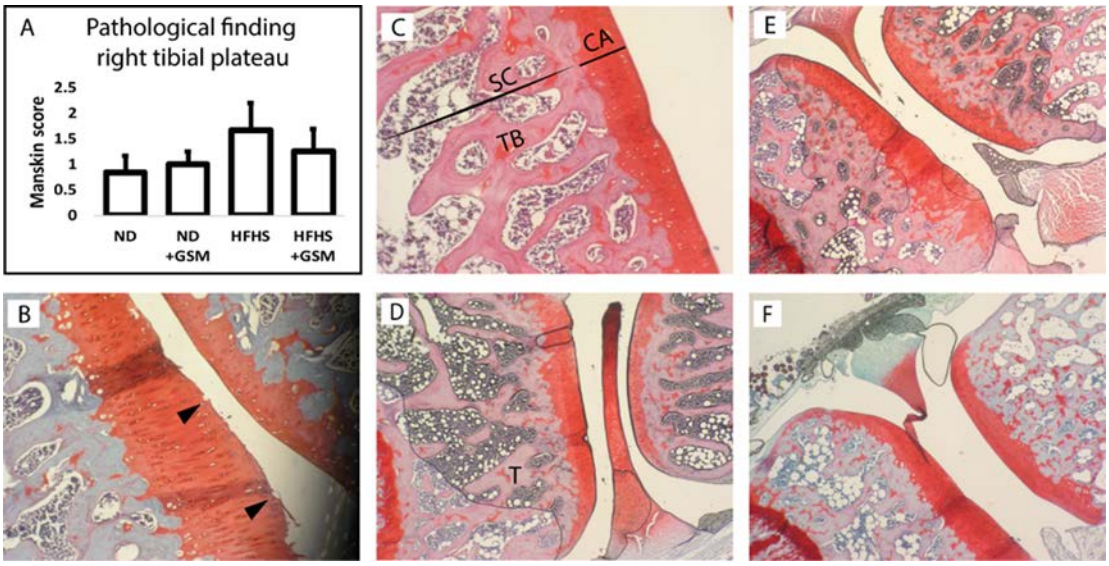

Figure 5.3: Histopathological assessment of osteoarthritis in right knee joints

Mankin scores were used to measure the severity of osteoarthritis at the tibial plateau (**A**). Scores for each histological aspect were summed for each individual. Data are shown as mean + standard error of mean of n = 11–12 rats per diet group. No significant difference was detected by analysing with the Mann–Whitney U test. Knee joint at microscopic levels, 40X (C, E, D, F) and 100X magnification (B): Dark red staining represents cartilaginous layers (CA), which have similarity in colour and thickness across all groups. Most of the slices have smooth surface cartilage and seem to be normal articular cartilage. Surface irregularities were found in some tissue samples from HFHS as indicated by black arrowheads (**B**). Articular cartilage of tibia bone (T) from each group, ND (**C**), ND + GSM (**D**), HFHS (**E**), and HFHS + GSM (**F**). SC= subchondral bone, TB = trabecular bone

5.4 Discussion

Obesity is associated with the progression of OA due not only to increasing weight-loading but also to the many systemic factors produced as part of a chronic inflammatory process. Recent preclinical studies have achieved the establishment of OA in diet-induced animal models without surgical manipulation (Collins et al., 2015a), more closely mimicking the human condition common in the elderly in which OA occurs due to aging, body weight, and/or general 'wear and tear' on the joints rather than the less common type of OA that occurs due to an acute injury and is more often seen in young athletes (Amoako & Pujalte, 2014) This animal model represents one particular subtype of human OA, MetOA, and shares with the human both abnormal metabolic markers and pathological changes in articular joints. These markers are associated with reduction of glycemic control, alterations in lipid metabolism, and increases in mediators such as adipokines and cytokines linked with low-grade chronic inflammation (Collins et al., 2016; Pearson et al., 2017; Sun et al., 2017; Teichtahl et al., 2005). The current study used a similar HFHS diet but assessed MetOA after only

13 weeks rather than 28 weeks. CTX-II was significantly elevated in the HFHS group compared to both of the ND groups, identifying this biomarker as being an early indicator of MetOA prior to the presence of frank cartilage erosion in this model. Importantly, addition of GSM to the HFHS diet significantly ameliorated CTX-II production, establishing this model and the 13 week time point as being suitable for assessing intervention strategies to prevent or slow the initial stages of joint pathology.

HbA1c was elevated in the HFHS groups compared to both of the ND groups, suggesting that insulin resistance was beginning to be established at this time point, although the difference only reached statistical significance in the HFHS+GSM group. HbA1c was significantly lower in the HFHS group compared to HFHS+GSM, even though the HFHS group had a higher Mankin score and CTX-II. This suggests that HbA1c is unlikely to be a useful early biomarker to predict MetOA development. It is unclear whether or how GSM may have contributed to the increase in HbA1c, as this has never been reported in the literature. Instead, various mussel preparations fed to obese rodents have been shown to reduce rather than increase insulin resistance (Zhou et al., 2017) and dyslipidemia (Vaidya et al., 2017a; Vaidya et al., 2017b), contradicting the rather surprising finding in the current study.

Variations in outcomes when using this model are likely to depend on the source and proportion of fat in the diet as well as the induction period and the sex of the animals (de Visser et al., 2017; Sekar et al., 2017). In the current study, diets containing 30% fat and 30% sucrose in diets induced significantly more weight gain than diets containing 5% fat and 5% sucrose. However, the differences in weight gain and mean BW between diet groups were less than some other published studies. Sun et al. (2017) demonstrated accelerated BW gain, cytokine concentration, and progressive articular cartilage lesions at the joint after 16 weeks of the HFHS diet in male Wistar rats. Collins et al. (2015a) identified obvious cartilage destruction, severe obesity, and high concentrations of pro-inflammatory cytokines in both blood and synovial fluid after 28 weeks in male Sprague Dawley rats. Both of these studies used higher sucrose in the diet as well as different sources of fat, with the latter study having a higher concentration of fat in the diet as well. The differences in magnitude in weight gain and other parameters between the current study and previously published studies are likely to be due to testosterone in male rats combined with a higher-energy diet, both of which would influence progression and severity of MetOA (Ma et al., 2007). However, using

female rats and lowering the fat in the diet slowed the progression of joint disease and allowed for the assessment of preventive effects of GSM powder on the early events of the disorder's pathogenesis, and was also necessary in order to make direct comparisons with the long term cohort as OVX requires female animals.

Three types of adipocytes with different functionality are situated in various fat depots: brown adipocytes in interscapular fat, beige adipocytes in inguinal fat, and white adipocytes in visceral fat (Ràfols, 2014). They produce a range of adipokines, including leptin and adiponectin, which are known to correlate with obesity. White adipocytes release the most leptin into the blood circulation; thus, the amount of visceral fat is highly correlated with plasma leptin concentration (Large et al., 2004). In the current study, the BW gain in HFHS-fed rats correlated with percent total body fat and in particular with the mass of visceral (perigonadal and retroperitoneal) fat, whereas interscapular fat mass was unaffected by diet. Correspondingly, plasma leptin and adiponectin were markedly increased in the HFHS-fed rats. The role of adiponectin and its contribution to the obesity microenvironment has not yet been fully elucidated, as some human and animal studies have shown adiponectin in obesity to be lower than normal (Kopp et al., 2005; Ashley et al., 2011; BrahmaNaidu et al., 2014; Reverchon et al., 2014), suggesting production of adiponectin may be influenced by age, sex, location of excess adipose deposits, or overall health status.

In contrast, consistent evidence indicates that leptin is an initiator for systemic and local inflammation in obesity. Leptin activates toll-like receptor 4 (TLR-4) on innate immune cells such as macrophages and natural killer (NK) cells, resulting in an upregulation of cell proliferation, phagocytosis function, and production of TNF-α, IL-6, IL-1β, and IL-12 (Azamar-Llamas et al., 2017). However, the expression of those serum pro-inflammatory cytokines in rats is variable, dependent upon many factors (Viney & Riley, 2017) and unlikely to have an established reference value. Some studies showed the serum levels of IL-1β, TNF-α, IL-6, and IL-10 in control rats to be around 2–6, 1–11, 0–93, and 6–12 pg/mL respectively (Chin & Ima-Nirwana, 2017; Lu et al., 2017; Ferreira et al., 2018). The result of these cytokines in this study is similar to Collin's study (2015a), which showed no significant difference between rats fed a normal diet, and rats fed the HFHS diet. An increase in plasma pro-inflammatory cytokines was not observed in the current study in rats fed a HFHS diet, corresponding with little evidence of synovial damage and thus likely the lack of increase was due to

the rats being in the early pathological stage of MetOA. Our study also measured some pro-inflammatory cytokines (TNF-α, IL-1β, IL-16 and IL-10) from synovial fluid by using joint lavage techniques, injecting 1 ml of phosphate buffer saline in each knee joint and draw the fluid back form the joint cavity. This fluid was kept at -80ª C until analysis. However, we were not able to detect measurable levels of those cytokines (data not shown), although it could not be determined whether no cytokines were present in synovial fluid or the synovial fluid was diluted too much during the collection process.

Inflammatory marker status varies widely and may in fact be minimal or absent in chronic diseases caused by low-grade inflammation such as rheumatoid arthritis, inflammatory bowel disease, atopic dermatitis, psoriasis, and asthma (Calder et al., 2013). Aging is also recognized as a low-grade inflammation status. In elderly human subjects, there was no increase in serum inflammatory marker levels but rather an increase in the production of IL-1β, IL-6, and TNF-α in *ex vivo* culture by mononuclear white blood cells activated with phytohemagglutinin (PHA) plus phorbol myristate acetate (PMA) (Fagiolo et al., 1993; Pietschmann et al., 2003). Thus, low-grade chronic inflammation may not be reflected by changes in serum pro-inflammatory cytokines, but may instead demonstrate changes in discrete microenvironments both in cell function and soluble factors. In the current study, it is reasonable to speculate that low-grade inflammation was successfully established due to leptin upregulation and plasma glucose elevation, which indicate initiation of a metabolic disorder.

Currently, most OA is diagnosed by clinical symptoms and radiographic imaging, at which point significant cartilage damage has already occurred. Early detection of OA is crucial to slow or halt progressive cartilage loss before it becomes debilitating, and this requires early prognostic markers that can both detect early OA and monitor intervention treatment efficacy (Kemp et al., 2018). C-telopeptide collagen type II (CTX-II) is a metabolic fragment from cartilaginous matrix released by cartilage degradation. It is considered to be one of the most reliable markers for early OA detection and is accurate in predicting further cartilage destruction (Garnero et al., 2003). It is possible to detect CTX-II in urine as well as serum, and the latter is a commonly used sampling technique in clinical studies as it is less invasive than blood sampling.

The current study showed an increase in plasma CTX-II in HFHS-fed rats but this significantly diminished when the diet was supplemented with GSM. This finding provides further evidence that GSM is protective against OA, and in the absence of changes in inflammatory markers suggests that GSM's effects may be localized to the cartilage microenvironment. Interestingly, even though the cartilage degradation marker was detected in the blood, the knee joint histopathological findings appeared visually normal. This may be due in part to the fact that CTX-II in the blood circulation represents cartilage degradation events throughout the whole body, whereas histology was conducted on only a single joint. In addition, circulatory CTX-II detection is sensitive and thus measurable levels can likely be identified prior to a cartilage lesion being detectable histologically. A similar finding was observed in a study using a papain-induced osteoarthritis rat model, in which a significant increase of serum CTX-II was detected within a day after inducing papain into the knee joints; CTX-II plateaued at week 2 and remained constant until the study concluded at week 4 (Khan et al., 2014). Murat et al. (2007) also used the papain model and observed that CTX-II increased within 1 week, but significant changes in Mankin scores in the knee joints did not occur until week 4. Thus, in the rat there is a consensus that CTX-II increases significantly prior to the cartilage lesion becoming explicit.

As whole GSM was fed in this study, it cannot be determined at this time which component(s) of the GSM powder was responsible for the significant decrease in CTX-II. GSM contains high levels of polyunsaturated fatty acids, especially the omega-3 PUFAs DHA and EPA. The anti-inflammatory (Teitelbaum & Allan Walker, 2001; Wall et al., 2010; Tortosa-Caparrós et al., 2017; Layé et al., 2018) and anti-arthritis (Lee et al., 2012; Norling & Perretti, 2013; Rajaei et al., 2015) effects of omega-3 PUFAs are well established. There is limited evidence that omega-3s are important compounds in GSM with potential as anti-inflammatory and anti-arthritis bioactives, although much work remains to be done before a consensus can be reached. However, peptides alone from blue mussel have been shown to reduce myriad parameters of metabolic syndrome in obese mice (Zhou et al., 2017; Vaidya et al., 2017b), and therefore the potential for proteins or peptides in the GSM to have directly affected the changes observed in CTX-II in the current study cannot be dismissed.

The results of the current study demonstrate that GSM significantly reduced the CTX-II elevation induced by a HFHS diet, and slightly reduced CTX-II in normal rats.

This may indicate protective effects of GSM against the initial stages of MetOA development, as evinced by a slight decrease in Mankin score of knee joints from rats fed the HFHS diet. However, to date this effect has only been demonstrated in the early stage of a MetOA model; long-term effects of GSM and its potential ability to treat exacerbated OA are still unknown and should be the subject of further investigation. Such work may reveal additional biomarker changes to confirm ongoing MetOA and identify biomarkers useful for monitoring treatment.

MASSEY UNIVERSITY
GRADUATE RESEARCH SCHOOL

STATEMENT OF CONTRIBUTION
DOCTORATE WITH PUBLICATIONS/MANUSCRIPTS

We, the candidate and the candidate's Primary Supervisor, certify that all co-authors have consented to their work being included in the thesis and they have accepted the candidate's contribution as indicated below in the *Statement of Originality*.

Name of candidate:	Parkpoom Siriarchavatana
Name/title of Primary Supervisor:	Dr. Wolber Fran
Name of Research Output and full reference:	
Siriarchavatana P, Kruger MC, Miller MR, Tian HS, Wolber FM: (2020). Effects of greeshell mussel intake on pathological markers of multiple phenotypes of osteoarthritis in rats.. Applied Sciences , 10, 6131.	
In which Chapter is the Manuscript /Published work:	Chapter 6
Please indicate:	
• The percentage of the manuscript/Published Work that was contributed by the candidate:	90%
and	
• Describe the contribution that the candidate has made to the Manuscript/Published Work:	
Part of animal study work, all formal analysis, investigation, data curation, original draft preparation, review and co-editing, visualization.	
For manuscripts intended for publication please indicate target journal:	
Published (Applied Sciences)	
Candidate's Signature:	Parkpoom Siriarchavatana Digitally signed by Parkpoom Siriarchavatana DN: cn=Parkpoom Siriarchavatana, o=Massey University, ou=Colllege of Health, email=bluenoo@gmail.com, c=NZ Date:
Date:	24 July 2020
Primary Supervisor's Signature:	Fran Wolber Digitally signed by Fran Wolber Date: 2020.07.27 15:10:54 +12'00'
Date:	27 July 2020

(This form should appear at the end of each thesis chapter/section/appendix submitted as a manuscript/ publication or collected as an appendix at the end of the thesis)

Chapter 6: Effects of greenshell mussel intake on pathological markers of multifactorial-induced phenotypes of osteoarthritis in rats

The previous chapter showed that greenshell mussel reduced CTX-II and may have limited cartilage breakdown during early-stage metabolic osteoarthritis (MetOA) in younger rats. However, a long term rat study is needed to verify the findings and to extend them to MetOA under conditions of estrogen deficiency. Such pre-clinical findings could identify GSM as a good candidate for a subsequent human trial. The rats in this long term cohort received metabolic syndrome (MetS)-inducing factors for a longer period when compared to the short term rats and, in addition, some groups of rats underwent ovariectomy to induce simulated menopause. MetS was assessed by measuring pro-inflammatory cytokines, adipokines, and hyperglycemia. The MetS was also compounded by other factors and induced multi-factorial OA, which was shown by reduced bone mineral density and histopathological lesions of the rats' knee joints.

Abstract

Background: The prevalence of metabolic osteoarthritis has been increasing worldwide, particularly among women. The aim of this study was to investigate the effects of greenshell mussel (GSM) on osteoarthritis prevention in a rat model.

Methods: Ninety-six female rats aged 12 weeks were divided into 4 test groups, containing 24 rats each. Each test group received one of the four experimental diets: normal control diet (ND); normal control diet supplemented with GSM (ND+GSM); high fat/high sugar diet (HFHS); or high fat/high sugar diet supplemented GSM (HFHS+GSM), for 36 weeks (end of the study). After 8 weeks on the experimental diets, half of each group was subjected to ovariectomy (OVX) and the remaining half received a sham operation (ovaries left intact). The study evaluated body composition, bone mineral density (BMD), plasma cytokines, adipokines, HbA1c, and knee joint histopathology. Groups were in addition compared to younger rats from a previous study using the same diets to assess age-related differences.

Results: The HFHS diet and OVX significantly induced BW gain which positively correlated with leptin production. The rats' BMD was not significantly changed by diet; however, rats that underwent OVX showed 10% lower BMD in both lumbar spine and femur when compared with sham rats. There were no statistical differences in the group comparison of plasma cytokines except MCP-1 which was significantly upregulated in the OVX rats. Likewise, adiponectin and HbA1c also increased in the OVX rats. Inclusion of GSM did not alter the aforementioned parameters except increasing adiponectin levels. Knee joint pathological scores were pronounced in the aged rats and particularly in OVX rats fed HFHS, but cartilage damage was significantly mitigated by GSM supplementation. In conclusion, the induced OA in the rat model demonstrated that a cluster of metabolic inducing factors caused OA in rats and GSM might be beneficial in the prevention of OA joint damage.

6.1 Introduction

Osteoarthritis affects people worldwide, especially those in advanced age. Currently, the global prevalence of knee OA is 3.7% of the population, which means 268 million people are suffering from OA in this particular joint (Briggs et al., 2016). But OA can occur in any joints including hip, fingers, hands, wrist, and tempomandibular joints (Cicuttini et al., 1996); thus the total prevalence of OA is greater than the previous estimation. The United Nations and the World Health Organization predicted this burden to be the fourth leading cause of disability in 2020 (Woolf & Pfleger, 2003).

The disease is characterised by articular cartilage deterioration, which progresses slowly and appears initially at a subclinical level, making it difficult to be detected at an early stage (Bijlsma et al., 2011). Therefore, patients diagnosed with OA already have some severity of cartilage erosion. Treatment is also challenged by the fact that avascular tissue such as cartilage has less ability to regenerate itself (Karuppal, 2017). Moreover, microstructural damage to subchondral bone is replaced by fibrous tissue resulting in less porosity of the subchondral bone plate, which limits the nutrient supply to the cartilage layers (Suri & Walsh, 2012; Li et al., 2013). The ideal strategies to alleviate the disease burden would focus on both prevention and halting disease progression rather than relieving pain by anti-inflammatory drugs. Effective treatments need to target the underlying causes of disease but the aetiology of OA is very complicated, especially in the case of metabolic osteoarthritis (MetOA) which is largely defined as OA that presents in a patient within the context of metabolic syndrome. It is not clear whether OA is a single disease itself or a nebula of several diseases which have no specific markers to identify them.

There are many animal models to study OA, including both spontaneous OA and induction of OA models. The spontaneous OA model, using animals which are genetically prone to develop OA in advancing age (Jimenez et al., 1997; Poulet et al., 2013), theoretically mimics the pathological mechanisms for age-related OA in humans, whereas surgical induction OA models mimic post-traumatic OA (Kuyinu et al., 2016). The incidence of MetOA has been increasing due to the global expansion of obesity and related chronic diseases (Teichtahl et al., 2005; Pradhan, 2007), increasing the importance of developing and optimising a reliable animal model for this OA phenotype. The use of a high energy diet due to increased fat or sugar proportion

successfully induces obesity in rat models; however the effectiveness of this model to generate OA is controversial. Some studies have revealed that high-fat alone was inadequate to cause cartilage lesions in a rodent model unless groove surgery was incorporated (Wilhelmi & Faust, 1976; de Visser et al., 2017). However, other studies demonstrated that the pathological lesions of MetOA were successfully established in rats by feeding a high fat diet for 16 or 28 weeks (Collins et al., 2015a; Collins et al., 2015b; Sun et al., 2017). The success of these studies might be related to the gender as male rats are prone to osteoarthritis because of the influence of testosterone while female rats become prone to the disease only when they undergo a significant decrease in estrogen (Ma et al., 2007). In addition, the variation in success rates also depends on the type and quantity of fat in the diet (Sekar et al., 2017). It therefore remains inconclusive whether OA is inducible in female rats by a high energy diet or ovariectomy.

This study focused on the MetOA in a female population which is both the most prevalent phenotype and the most complicated. There is no established set of biomarkers to distinguish the phenotype or subtypes of OA. We hypothesized that different causes could activate MetOA in unique pathways resulting in distinguishable pathological patterns. Hence, the experiment was designed to find the differences in pathological markers from individual causes and as well as additive causes. In addition, greenshell mussel (GSM), a rich source of omega-3 fatty acids (Treschow et al., 2007; Miller et al., 2014a) showed some evidence supporting its use for anti-inflammation and arthritis (Whitehouse et al., 1997; McPhee et al., 2007; Singh et al., 2008), however, the previous animal studies that have been conducted using GSM oil employed chemical or surgical induction methods which obviously represent a post-traumatic OA phenotype rather than MetOA (Whitehouse et al., 1997; Singh et al., 2008) which differ in cause and pathogenesis (Zhuo et al., 2012; Wen et al., 2014; Chen et al., 2017). Our study hypothesized that a flash-dried powder preparation of GSM, which would be more economically accessible for people compared to expensive oil extracts and which may contain other unknown bioactive compounds, could prevent MetOA induction or slow MetOA progression using a model that more closely mimics the human condition.

The animal model was designed to simulate the broad range of MetOA severity that occurs in aging, obese, and/or postmenopausal women by feeding the rats a Western-style diet high in sugar and high in saturated fat, and by ovariectomising some

of the animals to induce menopause. The GSM intervention was designed to mimic a reasonable human consumption pattern of 1 meal of mussels per day providing approximately one-third of the person's protein intake. The results of the study provide insight in how single versus multiple causes could affect the pathological pattern in the rat model and identify the potential of GSM in preventing MetOA.

6.2 Materials and methods

6.2.1 Greenshell mussel (GSM) powder

Flash-dried powder from whole GSM meat was produced by Sanford Ltd (ENZAQ facility, Blenheim, New Zealand) using standard manufacturing processes and assessed for proximate composition in a commercial testing laboratory (Food Testing Laboratory of Cawthron Analytical Services; Nelson, New Zealand). The GSM powder contains 8.1% fat, 43% crude protein, 21.9% carbohydrate, 5.8% moisture and 21.2% ash. The fat contains 29.4% omega3 fatty acid and 3.5% omega6 fatty acid.

GSM powder in the normal control diet (ND+GSM) and high fat/high sugar diet (HFHS+GSM) was included at a final concentration of 100 g/kg. The diet formulae were predetermined in order to normalize the energy in the diet counterpart. All diets were stored at -20°C until used as described in previous chapters.

6.2.2 Animal study

The overall experimental plan is presented in Figure 6.1. One hundred and eight female Sprague Dawley (SD) rats aged 11 weeks reared on standard chow were obtained from the Small Animal Production Unit at Massey University (Palmerston North, New Zealand) and the study was conducted in the same animal facility as approved by the Massey University Animal Ethics Committee (MUAEC protocol/approval 16/112). The animal room environment was set at 22 ± 1 ◦C, with 45%–55% humidity and a 12/12 light-dark cycle throughout the study. The rats were singly housed in conventional cages with heat-treated aspen wood shavings as bedding. After a one-week acclimatization period, the rats were randomized into test groups and fed one of four diets (Specialty Feeds, Glen Forrest, Western Australia) designed as shown in Table 6.1.

Table 6.1 Test diets composition

		ND	ND + GSM	HFHS	HFHS + GSM
Total sugar		**5 %**	**5 %**	**30 %**	**30 %**
	sources	*- sucrose 100%*	*- sucrose 100%*	*- sucrose 100%*	*- sucrose 100%*
Total protein		**15 %**	**15 %**	**15 %**	**15 %**
	sources	*- casein 100%*	*- casein 66%* *- GSM 33%*	*- casein 100%*	*- casein 66%* *- GSM 33%*
Total fat		**5 %**	**5 %**	**30 %**	**30 %**
	sources	*- soy oil 100%*	*- soy oil 84%* *- GSM 16%*	*- soy oil 50%* *- lard 50%*	*- soy oil 49%* *- lard 49%* *- GSM 1 %*

After 8 weeks on the experimental diets (age 20 weeks), 96 rats were subjected to surgery: half of them were ovariectomised and the rest were left with ovaries intact as sham control animals. The surgical procedure and anaesthesia were performed as described previously (Kruger & Morel, 2016). These surgically manipulated rats were on their experimental diets through to the end of the study (age 48 weeks) before termination and biological samples being collected. Twelve rats from a previous study which did not undergo any surgery that were fed the ND were included in the data set in order to compare knee joint scoring between rats of different ages. These were sacrificed at 26 weeks of age and knee joints were collected for histopathological slide preparation. All rats were euthanized by exsanguination following anaesthesia.

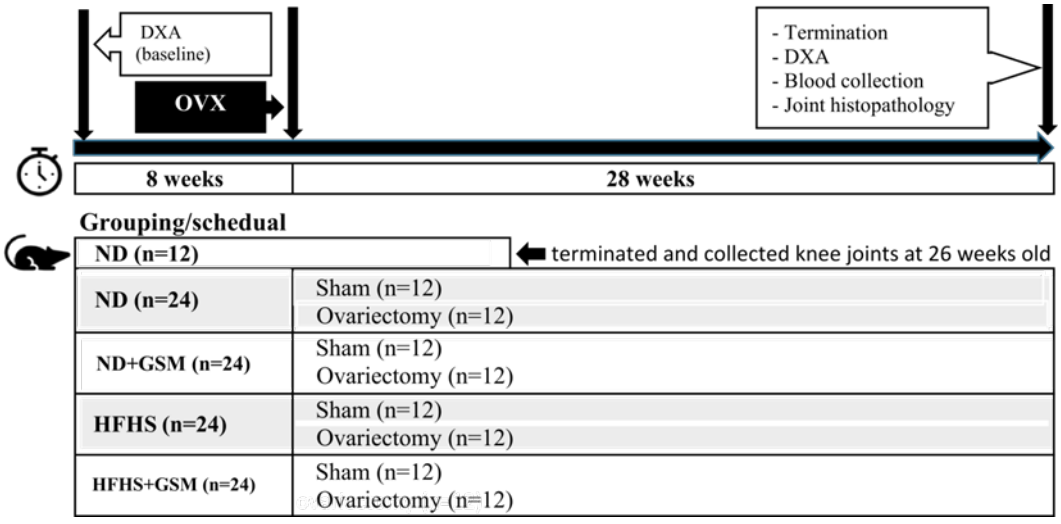

Figure 6.1: Experimental schedule

The figure shows the experimental schedule for obesity-induced osteoarthritis in the rat model with greenshell mussel. DXA= Dual X-ray energy absorptiometry; OVX = ovariectomy

6.2.3 Dual-energy X-ray absorptiometry (DXA) scans

In vivo percent whole body fat and BMD from lumbar spine and right femur were evaluated using a Hologic Discovery scanner (Hologic, Bedford, Massachusetts), at the beginning of the study and the end (age 48 weeks). Anaesthesia was provided prior to DXA scans as described previously (Kruger & Morel, 2016). Daily quality control (QC) scans were run prior to the scanning; the coefficient of variation (CV) for the spine was 0.98%-1%, and the CV for the femur was 0.85%-0.92%. Rats were positioned supine with right angles between the spine and femur. Three high resolution scans were applied for the individual bone sites of whole body, lumbar spine, and right femur.

6.2.4 Plasma analysis

At the end of the study, anaesthetized rats underwent cardiac puncture. Blood was drawn and collected in EDTA-anticoagulant tubes. Plasma was separated by centrifugation at 1050 g (Heraeus Megafuge 1.0R, Thermofisher) and kept at -80 °C until analysis. All analytes were measured by ELISA methods with different kits. IL1β, IL-6, IL-10, and TNF-α were assessed using Duo-set® kits (R&D system, Minneapolis, USA). MCP-1, adiponectin and leptin were assessed using Quantikine® kits (R&D). PGE2 was assessed using PGE2 ELISA kit (Invitrogen, Vienna, Austria). CTX-II assay kit was obtained from Cloud-Clone Corp, TX, USA. HbA1C assay kit was obtained from Fine Test, Wuhan Fine Biological Technology, Wuhan, China. Assays were performed following the manufacturers' instruction and optical density measured using a microplate reader (Multiskan FC, Thermo Fisher Scientific, Vantaa, Finland). The other inflammatory cytokines; INF-γ, CXCL-1, IL-12, IL-17, IL-18, IL-33 were measured by LEGENDplex^{TM} (BioLegend®, San Diego, USA) using a Gallios Flow Cytometer (Beckman Coulter, USA). The concentrations of the analytes were calculated against their standard curves accordingly to individual kits. All tests were performed in duplicate.

6.2.5 Leptin gene expression

Rats were dissected and perigonadal fat was harvested then immediately frozen in liquid nitrogen prior to storage in -80°C until analysis. Tissue homogenization was performed as follows: 200 mg of fat tissue in 2 mL tubes with 1 mL of Tri reagent® was dissociated in a homogenizer (Precellys Evolution Homogenizer, Bertin). 200 µl chloroform was added in the homogenate then shaken vigorously prior to centrifuging

at 12,000 x g for 15 min at 4°C. The clear upper part of the homogenate was recovered and further subjected to the column of the RNA extraction kit (Direct-zol™ RNA Miniprep Plus, Zymo Research, USA). cDNA was synthesised from the total RNA according to manufacturer's protocol using SuperScript™ IV First-Strand Synthesis System (Invitrogen, USA). Real-time quantitative PCR, using SYBR™ Green Master Mix, was performed on LightCycler® 480 Real-Time PCR instrument (Roche Applied Science). The specific primers for leptin were NM_013076.3 CCAGGATCAATGACATTTCACA (forward); AATGAAGTCCAAACCGGTGA (reverse). The PCR reaction was initialized with 1 cycle of 95°C for 10 min, followed by 35 cycles of denaturation step at 95°C for 20 s and extension step at 72°C for 20 s. Expression levels were calculated relative to the mean of ND sham rats and GAPDH expression (Primers XM_017593963.1 forward_CTGCACCACCAACTGCTTAG; reverse_TGATGGCA TGGACTGTGG) was used as the internal control. Quantitative measurements were determined using the ($2^{-\Delta\Delta Ct}$) method. Amplification of specific transcripts was confirmed by melting curve analysis.

6.2.6 Histopathological examination of knee joints

At the termination, knee joints were harvested and fixed in 10% buffer formalin followed by decalcification in 10% ethylenediaminetetraacetic acid and were later embedded in paraffin and sectioned. Coronal section was applied from the medial collateral ligament and stained with safranin-O. The pathological changes of the knee joints were assessed using the Mankin scoring method as described previously (Mankin et al., 1971) in a blinded fashion. A single veterinary pathologist conducted the scoring; this was an unfortunate but necessary limitation of the study as limited funding for the thesis project did not allow for the hiring of additional veterinary pathologists to reproduce the work. Both medial and lateral tibia were examined and the cumulative data of both were analysed.

6.2.7 Statistical analysis

Two-way ANOVA was used to evaluate the effects of diet or GSM or OVX on the following parameters: body composition, BMD, plasma analytes and leptin gene expression. One-way ANOVA was also applied to identify the differences across all groups and in case a significant difference was detected, a multiple comparison test Tukey test, followed. As data from scoring systems is an ordinal, therefore a non-parametric statistical analysis, Mann-Whitney U test, was used for evaluating knee joint

pathology. All analyses were performed using IBM statistic software (SPSS) version 25 (Armonk, NY, USA) and *P*-values < 0.05 were considered to be significant. All data are presented as mean ± SE.

6.3 Results

6.3.1 Changes in body composition

At the beginning of the study, the mean BW of all rat groups ranged from 267.37-281.62 g with no significant differences (Table 6.2). Increased BW of all rats was observed at the end of the 36-week study period and as expected, HFHS alone significantly increased both BW and body fat gain. Likewise, ovariectomy alone resulted in significantly higher weight gain and even greater changes in percent body fat. The success of ovariectomy was confirmed by regression of uterus weight at necropsy process (data not shown). The combination of ovariectomy and HFHS diet had additive effects and resulted in the greatest increases in body fat.

Table 6.2 Body composition of the rats at 48 weeks of age

	Sham				**OVX**				
	ND	**ND+GSM**	**HFHS**	**HFHS+GSM**	**ND**	**ND+GSM**	**HFHS**	**HFHS+GSM**	P values
BW 12th week	273.73±8.53	276.06±6.20	280.84±7.01	281.62±7.54	275.64±8.20	267.37±8.96	276.51±7.93	280.70±6.41	0.911
BW the end	403.89±17.30^{a}	428.18±18.05^{a}	535.38±27.16^{bc}	578.15±21.78^{bc}	499.20±18.56^{ab}	488.27±22.36^{ab}	633.35±34.01^{c}	619.05±29.34^{c}	**<0.001**
Change of BW (%)	49.01±4.74^{a}	54.55±3.97^{ab}	89.68±6.97^{cd}	105.51±6.86^{cde}	80.99±3.34^{bc}	83.41±7.66^{bc}	129.03±10.51^{e}	118.15±7.44^{de}	**<0.001**
Change of %body fat (%)	185.55±25.75^{a}	221.94±35.14^{ab}	344.14±33.06^{bc}	377.30±41.02^{c}	328.88±43.10^{abc}	303.18±18.48^{abc}	357.20±27.90^{bc}	338.88±37.36^{bc}	**0.001**
Statistical analysis by two-way ANOVA with three effects									
	diet	**GSM**	**OVX**	**diet * GSM**	**diet * OVX**	**GSM * OVX**	**diet * GSM * OVX**		
BW 12th week	0.217	0.964	0.579	0.615	0.944	0.74	0.518		
BW the end	**<0.001**	0.538	**<0.001**	0.824	0.807	0.176	0.748		
Change of BW (%)	**<0.001**	0.498	**<0.001**	0.874	0.642	0.119	0.217		
Change of %body fat (%)	**<0.001**	0.792	**0.042**	0.966	**0.011**	0.243	0.913		

Body composition of the rats was reported as mean ± SE (n=11-12). Rat's bodyweight was measured on scales at the beginning of the study and at the end and percent change of BW was calculated accordingly. Similarly, % body fat at the start and end from DXA scanning was reported as percent change. The statistically significant differences across all groups were analysed using One-way ANOVA and p values were reported in the last column. In case there was a significant difference, multiple comparison tests, using Tukey method, was applied and the differences of superscript letters indicated the statistical significance. Two-way ANOVA was used to analyse the influence of diet, GSM and ovariectomy (OVX) on the body composition. These three effects were treated as fixed effects in general linear models. The p values were summarized in the table below. Statistical differences is applied when $P<0.05$.

6.3.2 Bone mineral density (BMD) of lumbar spine and femur

BMD from anesthetized rats was measured using DXA at the end of the study (Figure 6.2). Lumbar spine displayed lower BMD than both sides of femur in all rats. In general, OVX rats had lower BMD than sham rats in all bone sites. Lumbar spine BMD in all sham rats was around 0.22 g/cm^2 while OVX rats displayed only 0.20 g/cm^2. Similarly, both left and right femur BMD in sham rats was ≥ 0.28 g/cm^2 while OVX rats showed ≤0.27 g/cm^2 and ≤0.26 g/cm^2 in the left and right femur respectively. The significant differences were only observed due the effect of OVX on all bone sites. No significant differences of the single effects were detected comparing the cluster of no GSM with GSM fed rats or the cluster of ND with HFHS fed rats. However, there was an interaction effect of diet and OVX in the lumbar spine scan. As can be seen, feeding HFHS in sham rats seemed to reduce lumbar spine BMD when compared with their paired diet group, but the opposite was observed in OVX rats.

	Sham				OVX			
BMD (g/cm^2)	ND	ND+GSM	HFHS	HFHS+GSM	ND	ND+GSM	HFHS	HFHS+GSM
Lumbar spine	0.225	0.229	0.223	0.225	0.200	0.192	0.204	0.206
SE	0.006	0.003	0.003	0.004	0.004	0.003	0.004	0.004
Left femur	0.285	0.292	0.290	0.290	0.257	0.257	0.271	0.264
SE	0.006	0.004	0.004	0.003	0.005	0.004	0.006	0.005
Right femur	0.281	0.287	0.285	0.289	0.259	0.258	0.269	0.265
SE	0.006	0.004	0.004	0.004	0.004	0.004	0.005	0.005

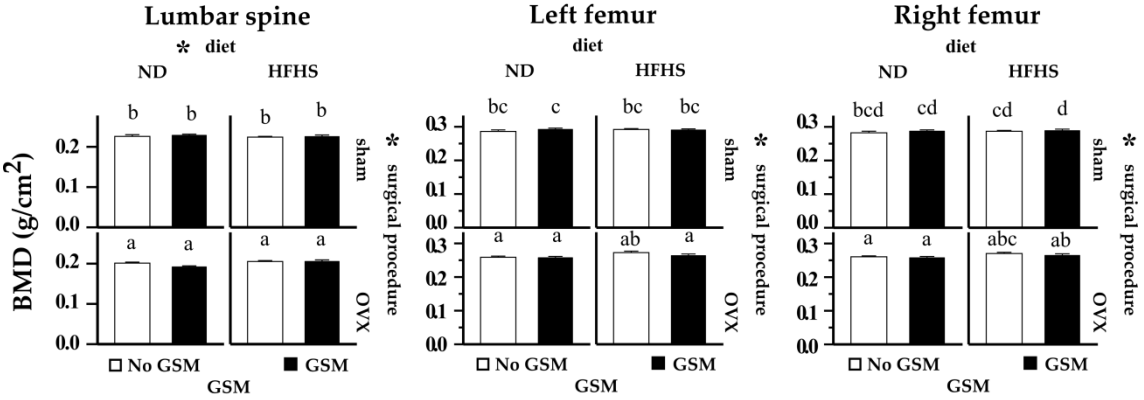

Percent change of bone mineral density	diet *	GSM	OVX	diet * GSM	diet * OVX	GSM * OVX	diet * GSM * OVX
Lumbar spine	0.224	0.995	<0.001	0.433	0.032	0.202	0.291
Left femur	0.069	0.962	<0.001	0.248	0.217	0.258	0.997
Right femur	0.083	0.724	<0.001	0.649	0.414	0.238	0.973

Figure 6.2: Bone mineral density in lumber spine and femur

Bone mineral density (BMD) was evaluated using Dual energy X-ray absorptiometry at the end of the study (age 48 weeks). Bar graphs and error bars show means and SE respectively (each group n=11-12) and the accurate numbers of mean and SE are also provided in the upper table. Two-way ANOVA was

used to evaluate the influence of effects; diet, surgical procedure and GSM. If the effect was statistically significant, the asterisk * is indicated. One-way ANOVA was used to identify significant differences across all groups. In case data reached the criteria, a multiple comparison test is performed using Tukey method, and then letters are indicated on the bar. Groups showing different letters are significant differences. Table in the figure shows p values calculated from two-way ANOVA analysis. P values less than 0.05 was used to determine statistical significance in all methods.

6.3.3 Analysis of inflammatory markers in systemic circulation

All inflammatory markers are presented in Table 6.3. Most pro-inflammatory and anti-inflammatory cytokines in plasma were present at very low concentrations and not influenced independently by diet, GSM or surgery. MCP-1 however was significantly increased in the OVX rats when compared to the sham rats. Moreover, the increased MCP-1 levels in the ovariectomised rats fed HFHS were different from ND although a significant diet effect was not detected. There was also an interaction effect of GSM and OVX on IL-17. The result showed that inclusion of GSM resulted in an increase of IL-17 in the sham rats but levels were decreased in the OVX rats.

Table 6.3 Analysis of inflammatory markers in systemic circulation

	Sham				OVX				
	ND	ND+GSM	HFHS	HFHS+GSM	ND	ND+GSM	HFHS	HFHS+GSM	P values
IL1β (pg/ml)	8.68±3.63	7.03±3.91	5.93±1.77	4.48±1.44	4.23±1.61	7.50±2.00	6.57±1.68	3.73±0.88	0.8
IL6 (pg/ml)	32.96±4.53	26.79±5.04	28.91±5.35	27.69±4.60	36.96±9.36	32.44±3.87	27.88±4.27	28.75±4.05	0.9
IL10 (pg/ml)	0.28±0.29	1.27±1.04	0.34±0.24	0.07±0.05	0.44±0.32	0.46±0.22	0.87±0.58	0.17±0.17	0.47
TNFα (pg/ml)	1.08±0.18	1.88±0.28	1.78±0.28	2.09±0.18	1.53±0.31	2.04±0.84	1.89±0.17	1.88±0.56	0.75
MCP1(pg/ml)	340.65±49.76^{ab}	387.69±53.60^{ab}	320.93±55.72^{a}	376.20±71.69^{ab}	483.26±81.78^{ab}	559.44±69.88^{ab}	574.41±122.81^{ab}	732.36±163.99^{b}	**0.02**
PGE2 (pg/ml)	1254.75±187.65	1314.51±234.97	1263.81±212.19	1155.18±237.85	1446.57±221.96	1017.02±123.24	1323.19±313.98	1683.71±321.77	0.66
IFNγ (pg/ml)	241.55±35.38	279.23±40.09	222.36±27.98	241.99±35.16	263.20±30.81	226.20±33.19	217.63±33.88	249.71±26.38	0.695
CXCL1 (pg/ml)	23.65±6.42	19.74±5.36	16.83±3.54	19.31±4.88	32.09±7.27	17.44±4.71	19.71±6.31	18.55±4.82	0.283
IL18 (pg/ml)	136.10±48.45	159.41±55.21	163.36±76.23	112.23±29.89	111.33±13.87	119.65±41.65	99.90±16.12	130.33±27.99	0.974
IL12 (pg/ml)	40.30±13.65	48.85±11.20	34.60±4.77	48.33±5.69	51.25±5.78	35.09±0.76	65.66±3.36	53.98±5.35	0.804
IL17 (pg/ml)	43.72±8.31	50.58±10.12	33.37±6.78	43.40±7.56	53.26±4.60	33.08±5.47	41.89±10.90	34.59±4.41	0.428
IL33 (pg/ml)	612.27±68.81	598.94±95.12	622.62±111.93	516.23±60.95	650.36±42.59	577.06±80.56	584.99±46.44	617.76±58.09	0.85

Statistical analysis by two-way ANOVA with three effects

	diet	GSM	OVX	diet * GSM	diet * OVX	GSM * OVX	diet * GSM * OVX
IL1β (pg/ml)	0.316	0.689	0.54	0.379	0.563	0.597	0.347
IL6 (pg/ml)	0.297	0.468	0.525	0.497	0.528	0.805	0.977
IL10 (pg/ml)	0.375	0.97	0.995	0.085	0.256	0.22	0.646
TNFα (pg/ml)	0.338	0.171	0.661	0.39	0.542	0.607	0.982
MCP1 (pg/ml)	0.367	0.193	**0.001**	0.727	0.253	0.609	0.775
PGE2 (pg/ml)	0.565	0.863	0.48	0.363	0.311	0.976	0.163
IFNγ (pg/ml)	0.4	0.573	0.76	0.583	0.712	0.504	0.35
CXCL1 (pg/ml)	0.233	0.267	0.593	0.2	0.794	0.354	0.646
IL18 (pg/ml)	0.858	0.925	0.343	0.651	0.868	0.565	0.405
IL12 (pg/ml)	0.436	0.871	0.333	0.778	0.262	0.161	0.984
IL17 (pg/ml)	0.189	0.609	0.69	0.438	0.711	**0.036**	0.639
IL33 (pg/ml)	0.659	0.468	0.719	0.951	0.828	0.719	0.37

Plasma was recovered from the rat's blood at termination (48 weeks of age). Technically, ELISA methods were employed to quantify the concentration levels of all inflammatory cytokines. Data were present as mean±SE (n=11-12). The statistically significant differences across all groups were analysed using One-way ANOVA and p values were reported in the last column. In case there was a significant difference, multiple comparison tests, using Tukey method, was applied and the differences of superscript letters indicated the statistical significance. Two-way ANOVA was used to analyse the influence of diet, GSM and ovariectomy (OVX) on the cytokines. These three effects were treated as fixed effects in general linear models. The p values were summarized in the table below. Statistical differences were applied at $P<0.05$.

6.3.4 Analysis of adipokines in systemic circulation and fat tissue

Adiponectin was the most abundant adipokine in the blood circulation (Figure 6.3). In sham rats, the lowest concentration (6.37±0.59 µg/mL) was found in the ND group, and the highest concentration (7.64±0.38 µg/mL) in the HFHS+GSM group. OVX significantly increased adiponectin production in all diet groups (>9 µg/mL). GSM also increased adiponectin in OVX rats fed the ND but not the HFHS diet.

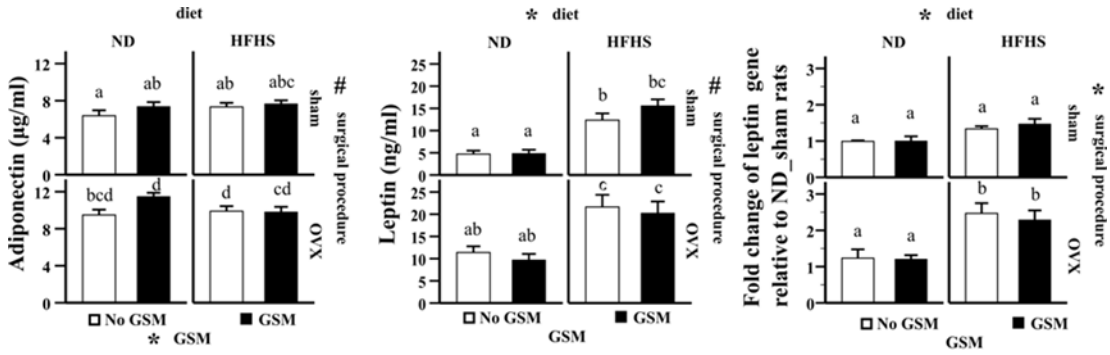

Analysts	diet	GSM	OVX	diet * GSM	diet * OVX	GSM * OVX	diet * GSM * OVX
Adiponectin	0.989	**0.026**	**<0.001**	0.057	0.082	0.683	0.300
Leptin	**<0.001**	0.957	**<0.001**	0.483	0.617	0.185	0.565
Leptin mRNA	**<0.001**	0.896	**<0.001**	0.959	**0.005**	0.494	0.589

Figure 6.3: Analysis of plasma adipokines and leptin mRNA expression

Plasma adiponectin and leptin concentrations were measured using ELISA method (n=11-12 per group). The quantification of Leptin mRNA expression was performed in perigonadal fat using qRT-PCR method (n=7). Bar graphs and error bars show means and SE respectively. Two-way ANOVA was used to evaluate the influence of effects; diet, surgical procedure and GSM. If the effect was statistically significant then, the asterisk * or hashtag # was indicated. Having similar asterisk on the both effects means the interaction effect detected. One-way ANOVA was used to identify significant differences across all groups. In case data reached the criteria, a multiple comparison test is performed using Tukey method, and then letters are indicated on the bar. Groups showing different letters are significant differences. The table shows p values calculated from two-way ANOVA analysis. $P<0.05$ was used to determine statistical significance in all methods.

The effect of HFHS diet on plasma leptin was more distinct than adiponectin. Rats fed HFHS had increased levels of leptin at more than two-fold compared to their ND counterparts and OVX also increased leptin production similar to its effect on adiponectin. GSM however had no significant effect on leptin. To confirm the source of leptin production, the perigonadal fat pad, which attaches along the female reproductive tract, was harvested and leptin mRNA from the adipocytes was quantitatively measured. The result showed a corresponding pattern to the plasma leptin levels (Figure 3). Feeding HFHS in sham rats resulted in a measurable increase in leptin mRNA compared to the sham rats fed ND, and significantly increased leptin mRNA to more

than double those of the OVX rats compared to ND OVX. The interaction of diet and OVX had an additive effect on leptin gene expression and subsequent leptin production.

6.3.5 Analysis of cartilage degradation and glucose metabolism

A significant alteration in glucose metabolism in OVX rats was detected by increased plasma HbA1c, a red blood cell marker correlating with long term glycemic control (Figure 6.4). OVX, diet and GSM did not independently or additively influence the cartilage degradation marker, CTX-II.

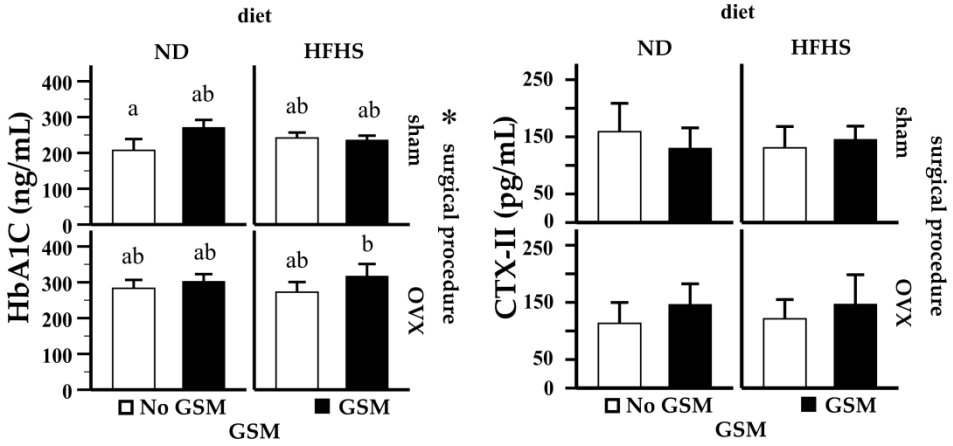

Analytes	diet	GSM	OVX	diet * GSM	diet * OVX	GSM * OVX	diet * GSM * OVX
HbA1C	0.926	0.083	**0.002**	0.522	0.949	0.929	0.172
CTX-II	0.935	0.428	0.494	0.509	0.697	0.185	0.353

Figure 6.4: Analysis of cartilage and glucose metabolism in systemic circulation

Plasma analysis was measured in the rats at 48 weeks of age. Bar graphs and error bars show means and SE respectively (n=11-12, per group). Two-way ANOVA was used to evaluate the influence of effects; diet, surgical procedure and GSM. If the effect was statistically significant, the symbol * is indicated. One-way ANOVA was used to identify significant differences across all groups. In case data reached the criteria, a multiple comparison test is performed using Tukey method, and then letters are indicated on the bar. Groups showing different letters are significant differences. The table shows p values calculated from two-way ANOVA analysis. $P<0.05$ was used to determine statistical significance in all methods.

6.3.6 Pathological changes in knee joints

Total Mankin score of knee joints examined histologically was compared in rats of different ages fed a similar diet (ND) (Figure 6.5). Younger rats (26 weeks old) showed lower scores than the aged rats (48 weeks old), demonstrating that age alone in the absence of HFHS diet or OVX resulted in significant knee joint damage.

Age	Knee joint scoring			
	Structure	Cellularity	Matrix	Tide mark
Young rats	0.53±0.31	0.30±0.13	0.00±0.00	0.00±0.00
Aged rats	0.80±0.29	1.40±0.16	1.20±0.36	1.00±0.26

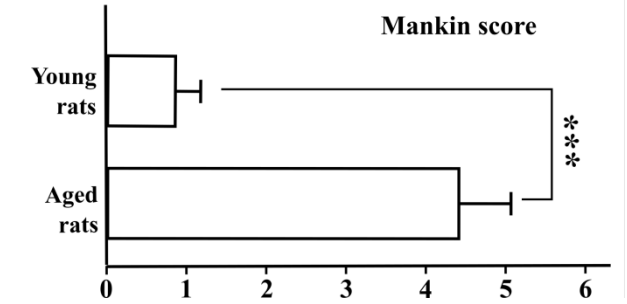

Figure 6.5: Comparison of knee joint scores between young rats and aged rats

Rats on normal control diet at age of 26 weeks (young rats, n=12) and 48 weeks (aged rats, n=10) were sacrificed and knee joints were processed to pathological slide preparation stained with safranin-O. The criteria of Mankin score were used to evaluate articular cartilage and then summed into mean±SE presented in the bar chart. Mann-Whitney U test was used to analysed statistical differences between young rats and aged rats as which asterisk *** shows significance at $p<0.001$

Figure 6.6 demonstrates the pathological findings of knee joints in the 48 week old rats from each of the test groups, with images selected to visually represent the various criteria used to inform the Mankin score. Severity of cartilage erosion was graded from 0-14 with the higher scores corresponding to more severe deterioration. As can be seen, all rat groups had only modest severity (4-5) except the OVX rats fed HFHS; this group expressed a Mankin score of approximately 7 which is considered being moderate severe disease. Rats on the ND developed only modest OA with no significant differences due to other interventions. Rats on the HFHS diet who did not undergo OVX likewise had only moderate scores, although the score was decreased slightly but not significantly with GSM addition. Thus, neither OVX nor HFHS diet alone induced additional joint damage, but the combination resulted in a greater effect causing moderate damage. Of greatest interest was the observation that inclusion of GSM in the OVX rats fed HFHS resulted in complete mitigation of the induced pathological lesions (Figure 6.6).

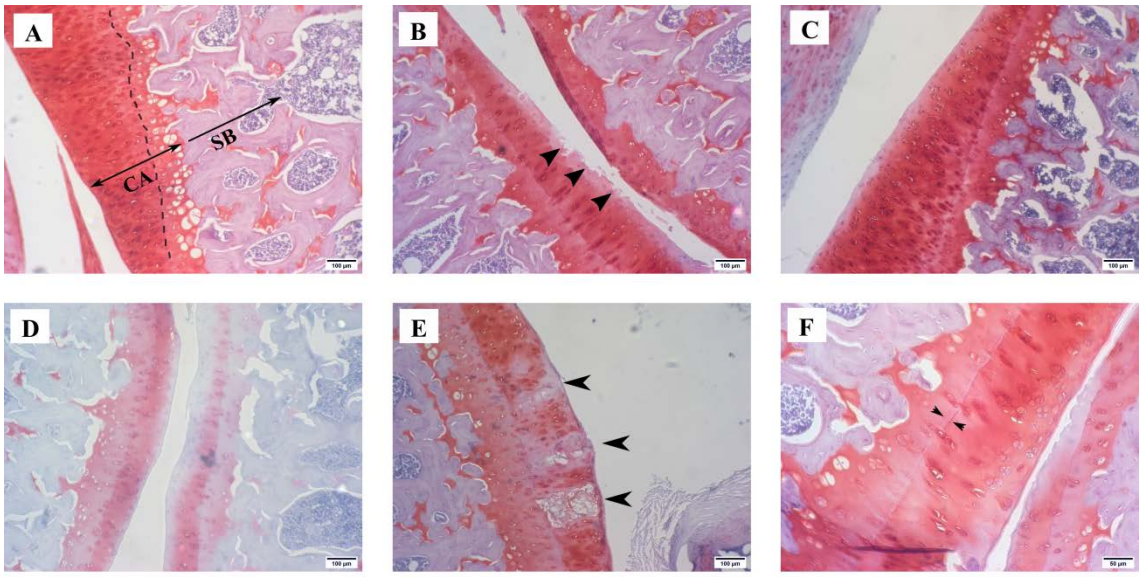

G

Group	n	Knee joint scoring			
		Structure	Cellularity	Matrix	Tide mark
Sham					
ND	10	0.80±0.29	1.40±0.16	1.20±0.36	1.00±0.26
ND+GSM	12	1.91±0.75	0.50±0.19	1.33±0.45	0.50±0.19
HFHS	12	1.41±0.35	1.66±0.28	1.66±0.28	0.41±0.14
HFHS+GSM	12	1.00±0.25	1.75±0.28	0.58±0.19	0.50±0.14
Ovariectomy					
ND	9	0.77±0.32	1.11±0.26	1.22±0.46	0.66±0.23
ND+GSM	9	0.66±0.37	1.44±0.24	1.66±0.55	0.77±0.22
HFHS	10	2.40±0.61	2.10±0.31	1.70±0.47	0.90±0.18
HFHS+GSM	12	1.58±0.46	1.08±0.19	1.25±0.21	0.33±0.18

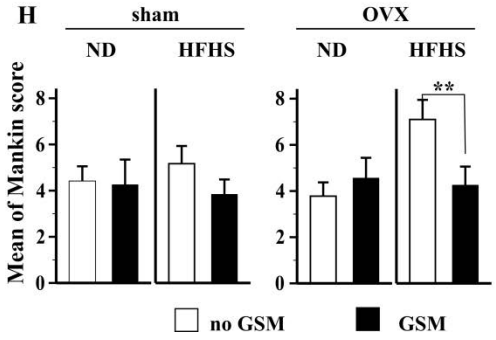

Figure 6.6: Pathological changes in rat's knee joints at 48 weeks of age.

Knee joints from rats at the end of the study were dissected, formalin-fixed and decalcified prior to processing tissue slides. Slides were stained with safranin-O showing in A-F. Image (A) shows normal features of rat tibia bone as which articular cartilage is stained red (CA) and subchondral and trabecular bone are pink (SB). The cartilage can be divided by tide mark (dotted line) into two zones; non calcified cartilage (from the surface area to tide mark junction) and calcified cartilage (under tidemark to subchondral bone plates). The abnormality of articular cartilage can be marked as surface irregularity (black arrows in B), cloning and clusters of chondrocytes (C), pale staining of cartilage matrix (D), degeneration and necrosis of chondrocytes (black arrow in E), and duplicated tide mark (F). Mankin score criteria was used to grade the severity of cartilage lesion in each group and mean ±SE is showed in the table (G). Finally, all criteria were summed and presented as a mean±SE of Mankin score in the bar chart (H). Mann-Whitney U test was used to analysed statistical differences between groups and asterisk ** shows significance at $p<0.01$.

6.4 Discussion

The increased prevalence of OA over the past decade is attributed to the expansion of both an aging society and the consumption of a "western-type" high energy diet leading to increased obesity (Heidemann et al., 2008). In addition, menopause is considered one of the most significant causes of OA in women (Woolf & Pfleger, 2003). This study's experimental design was intended to assess which of these

factors (aging, diet, OVX) independently or synergistically cause OA and how they determine the disorder's signature pathological pattern. This study successfully established the multi-factorial induced OA in a female rat model by using the mixed factors of aging, obesity and ovariectomy.

Interestingly, GSM consumption directly alleviated cartilage destruction without modulation of the predisposing factors including obesity, hyperglycaemia, and bone loss due to oestrogen deficiency. We speculated that the biological activity of GSM can be mainly attributed to omega-3 fatty acids, DHA and EPA, which are abundant in GSM powder (Siriarchavatana et al., 2019) and well known to have anti-inflammatory properties (Wall et al., 2010; Knott et al., 2011; Cai et al., 2014; Rajaei et al., 2015; Layé et al., 2018). However, GSM also contains other nutrient compositions such as a series of unusual lipids (non-methylene interrupted FAs and plasmalogens), proteins, carbohydrates and insoluble fibre which are not well clarified in their biological activity (Miller et al., 2011a; Saltzman et al., 2017) but these may contribute partially to some effects observed in this study. Therefore, the flash-dried GSM used in the current study may produce an anti-arthritis effect as effectively as GSM oil has been shown to do in previous studies (Whitehouse et al., 1997; Singh et al., 2008). It was observed in the current study that in the early cohort rats, whole GSM powder significantly reduced CTX-II (Siriarchavatana et al., 2019), an early prognostic biomarker for OA. Similarly, in the late cohort rats, whole GSM powder significantly reduced OA in rats with a high Mankin score, which was the only definitive diagnostic marker for OA.

Diet induced obesity models have been used in rats for many decades. Feeding a diet with high proportions of fat and sugar accelerates bodyweight gain. The main bodyweight gain is attributed to an increase in body fat, the characteristic of obesity. Interestingly, inclusion of GSM in the diet of sham rats resulted in increased bodyweight but it was opposite in the OVX rats. It is possible that some components in GSM might be able to facilitate the digestion or absorption of macronutrients in the gastrointestinal tract resulting in an increase of nutrient bioavailability (Haag et al., 2003). However, the mechanism of GSM on weight reduction in the OVX rats due to less fat mass gain cannot be explained by the current available information.

Obese rats have a substantially increased proportion of body fat, mainly in the abdominal cavity (visceral fat) and under the skin (subcutaneous fat) (Pranprawit et al., 2013). Visceral fat is composed of white adipocytes which are responsible for adipokine

production (Ràfols, 2014). Leptin, one of the adipokines, highly correlated with body fat mass, and is known to be a critical mediator that initiates low-grade chronic-inflammation by activating Toll-like receptors on macrophages (Azamar-Llamas et al., 2017). Subsequently, activated macrophages release various types of pro-inflammatory cytokines into the circulatory system, manifesting inflammatory responses (Li et al., 2015). In this study, plasma leptin was dramatically elevated in the HFHS fed rats proportional to bodyweight gain.

Oestrogen deficiency had an explicit influence on increased bodyweight and plasma leptin (Lizcano & Guzmán, 2014). To confirm the source of leptin production, the perigonadal fat pad, one portion of visceral fat, was assessed for leptin mRNA expression. A similar incremental pattern between plasma leptin and gene expression was revealed in all groups, indicating that perigonadal fat is one of the main sources of circulating leptin production in obesity which corroborates with previous rat studies (Villafuerte et al., 2000; Mulet et al., 2003). Plasma adiponectin levels in ND sham rats were high (around 7µg/mL) and similar to those found in humans under matching physiological conditions (5-10 µg/mL) (Inadera, 2008). Both increased and decreased adiponectin levels correlating with obesity have been reported. Moreover, the controversy of adiponectin's effect on systemic chronic inflammation and joint inflammation is still a matter of debate (Stofkova, 2009). Our study revealed that adiponectin was less sensitive in responding to the increased bodyweight or body fat but ovariectomy significantly elevated adiponectin. Increased adiponectin can induce NOS2, IL-6, MMP-3, MMP-9 and MCP-1 expression in chondrocytes (Lago et al., 2008), influencing the pathophysiology of osteoarthritis.

Theoretically, low-grade inflammation in obesity is characterized by a systemic influx of adipokines (leptin, adiponectin, resistin) and an increase of pro-inflammatory cytokines (IL-1β, IL-6, TNF-α, MCP-1) in small quantities, and thus linked to many chronic inflammatory diseases (BrahmaNaidu et al., 2014; Ilich et al., 2014). In one published study, rats fed high fat and high carbohydrate diets were shown to have significantly increased serum IFN-γ and IL-1β, and decreased serum IL-10, concurrent with synovitis and cartilage destruction (Sun et al., 2017). Collins et al. (2015a) study on the other hand showed that serum IFN-γ, Il-10, IL-12, IL-13, IL-17a, IL-18, IL-1β, Il-2, IL-6TNF-α and MCP-1 were not significantly different between diet-induced-obese rats and normal-diet fed rats; however, most of the pro-inflammatory cytokines

were elevated in synovial fluid and related to joint pathological lesions. It is possible that low-grade inflammation might be obscured at the systemic level but is definitively altering immune responses at local tissue or cellular function levels (Fagiolo et al., 1993). The evidence showed that activation of macrophage functions at local tissue sites such as synovial membrane is related to OA or rheumatoid arthritis (Culemann et al., 2019). Our results concurred with this previous work.

We did not see modulation of pro-inflammatory cytokines in plasma in response to HFHS, and only increased plasma MCP-1 was detected in response to ovariectomy. MCP-1, a chemokine produced by adipocytes, macrophages, and endothelial cells, can regulate macrophage polarization and infiltration, insulin sensitivity and lipid metabolism (Nio et al., 2012). Hence, it can contribute to local inflammation such as arteriosclerosis and coronary heart disease (Kanda et al., 2006) and may be involved in osteoarthritis. Interestingly, plasma MCP-1 theoretically is associated with adiposity (Kouyama et al., 2007) but our data revealed that MCP-1 was modified by the effect of ovariectomy, not obesity. The male rats in Collin's study (Collins et al., 2015a) gained even more weight than our female rats, but no change of plasma MCP-1 levels was detected. This evidence indicates that MCP-1 is distinctly different in females and might be a crucial modulator of MetOA in post-menopausal women; if so, then it could be used as a biomarker to diagnose or monitor disease progression in this population. It may also be of interest to determine whether drugs that target MCP-1 are more potent against this specific OA phenotype.

Further, the change in plasma IL-17 influenced by the interaction effect between GSM and OVX was irrelevant to other results. IL-17 is recognized as a T cell activator of neutrophil mobilization and activation, mediating innate immunity and being involved with the pathogenesis of inflammatory diseases such as psoriasis and rheumatoid arthritis (Zenobia & Hajishengallis, 2015). Therefore, IL-17 would have been expected to increase in the OVX rat fed HFHS which showed pathological joints. However, a previous study revealed no relation of IL-17 to HFHS diets (Collin et al., 2015b). Despite a lack of explanation to this occurrence, we speculate that this change may be related to an alteration of gut microbiota due to GSM and OVX, or possibly an as-yet unexplored interaction between GSM, diet, and estrogen levels.

The result at the end of this study showed that the average BMD in OVX rats was 10% lower than sham rats at all bone sites. OVX resulting in oestrogen deficiency

caused the significant reduction of BMD in both lumbar spine and femurs. Lack of oestrogen changes the course of bone remodeling and induces excessive osteoclast activity which reduces calcium deposition in bone, resulting in weakening of the trabecular bone that forms the porous bone network beneath calcified cartilage to support load-bearing by the joints. However, changing the microscopic structure in some areas of bone can also cause the development of bone cysts, osteophyte formation, flattening and deforming of the subchondral articular contour: all these features are recognized as OA (Goldring & Goldring, 2016). The loss of estrogen that accompanies menopause is therefore also a critical risk factor for OA in women, changing from the low prevalence in females at age under 50 years old to prevalence greater than males after the postmenopausal period (Woolf & Pfleger, 2003). Interestingly, weight gain induced by HFHS caused slight reduction of lumbar spine BMD in sham rats but increased BMD in OVX rats. This reveals that adipocytes may play an important role as an alternative source for producing estrogen after ovariectomy.

Despite the fact that the rat model does not completely mimic human OA because of differences in growth plate activity during adulthood, patterns of cartilage loading, and spontaneous intrinsic healing of cartilage lesions (Cook et al., 2014), rats in addition to mice and rabbits (McCoy, 2015) are the main animal models used in OA research. Their main advantages are cost efficiency and manageability, and the rat model provides crucial evidence for further study in other larger animals. This species is not considered as a spontaneous OA model like guinea pigs, STR/1N mice or C57/BL mice, but it is commonly used in a chemical induction model using intraarticular injection of adjuvant, collagen, iodoacetate or papain (Vogel & Vogel, 1997; McCoy, 2015;). Just in the last decade, high-energy-diet-induced OA models have been developed, firstly in mice (Griffin & Guilak, 2008), then rabbits (Brunner et al., 2012) and most recently rats (Collins et al., 2015b). As a new animal model, evidence is still inconsistent. Our study revealed interesting and novel information about this model. Firstly, young female rats (26 weeks of age) did not spontaneously evolve explicit pathological lesions in knee joints; however, the older rats (48 weeks of age) revealed some pathological changes by the Mankin score. Even though the lesions in the cartilage layers appeared to be only a modest feature of OA, the changes were significant after time; a similar finding has been reported (Ferrandiz et al., 2014). This means that age also contributes to OA development at subclinical levels in the rat

models. At 48 weeks of age, all rats showed at least mild features of cartilage attrition. As low-grade inflammation due to HFHS diet and bone loss from oestrogen deficiency progressed, cartilage destruction became more pronounced and distinct only in one particular group. This cumulative evidence can explain the multi-factorial causes of osteoarthritis observed in this rat model.

Interestingly, plasma concentrations of CTX-II, the cartilage degradation marker, did not correlate with the pathological changes in the knee joints in older rats. In a matching study, we did detect a significant increase of CTX-II in younger rats correlating with obesity and the initiation of Met-OA (Siriarchavatana et al., 2019). A similar study showed that serum CTX-II dramatically increased in OVX rats within 3 weeks of surgery, then declined to the baseline level six weeks later OVX (Oestergaard et al., 2006). Likewise, Høegh-Andersen et al. (2004) monitored serum CTX-II in 5-month-old ovariectomised rats and found that CTX-II transiently increased by approximately 50% within 2 weeks after surgery and then declined afterward to 50% below baseline at week 8. CTX-II in the sham rats also declined to the same level of the OVX rats. This indicates that the sensitivity of serum CTX-II as a cartilage marker is of less value in rats older than 6 months or when OA has progressed further. However, cartilage degradation would have progressed though the development of OA as can be seen in the knee joint sections. This ambiguity is likely due to the limitation of the model, as mature rats retain growth plate function. To overcome this drawback, CTX-II levels should be monitored immediately after the second week of surgery. Another limitation of this study is due to the lack of revelation in the precise pathological mechanisms driving the development of the disease and the anti-osteoarthritis effect of GSM. This may be an interesting gap for other studies in the future. However, no adverse effects of GSM were noted, suggesting that the findings in the current pre-clinical study warrant clinical trials with whole GSM powder.

In conclusion, our data support the hypotheses that diet and OVX independently increase weight gain via body fat gain. Ageing, HFHS diet and OVX-induced oestrogen deficiency together cause low-grade-chronic inflammation via leptin, adiponectin and MCP-1 upregulation. OVX-induced bone resorption can further accelerate joint instability resulting in the cartilage destruction observed in OA. Finally, GSM independently has a potential role in OA prevention.

Chapter 7: The influence of high fat/high sugar diets, ovariectomy and greenshell mussel supplement on the composition of gut microbiota and related pathological changes

The complex relationship between MetS-inducing factors (age, HFHS and OVX) and OA was explored in the previous chapters. However, growing lines of evidence showed that the alteration of gut microbiota may play an important role in the pathogenesis of these disorders and in addition, a gut microbiota signature has been correlated with some diseases. This chapter focuses on this context, to determine whether the results could show any alteration of selected species of beneficial gut bacteria in rat's caecal contents in relation with those MetS-inducing factors and the disorders established in rats.

Abstract

The increased prevalence of non-communicable diseases such as obesity, T2D and metabolic syndrome is a burden to global public health which can be attributed in part to aging, high fat and/or high sugar diets, and sedentary life style. However, emerging knowledge of gut microbiota has extended our understanding of disease pathogenesis and could potentially be a solution for these problems when microbes in the gut ecosystem are properly managed. Prebiotics, a group of nutrients, are intentionally used for enhancing the growth of beneficial microbes in the gastrointestinal tract. The objective of this study was to evaluate the effect of greenshell mussel on selected beneficial bacteria in rats affected with metabolic syndrome. A total of 144 adult female Sprague-Dawly rats were fed on one of four diets (normal; normal+GSM; high fat/high sugar (HFHS); HFHS+GSM; N=36 per diet) from age 12 weeks. At age 20 weeks, 12 of the rats on each diet underwent ovariectomy and the remaining rats were left intact. 12 of the intact rats in each diet group were culled at age 26 weeks (short term cohort). The remaining rats were culled at age 48 weeks (long term cohort). At the termination of each cohort, blood, internal organs and caecal samples were collected during necropsy. The results showed that HFHS and OVX rats displayed obesity, hyperglycemia, and dyslipidemia condition which represent MetS. Hepatic steatosis, a pathological feature of MetS was frequently detected in HFHS and OVX rats. In the short term rats, the number of rats affected by hepatic steatosis increased from 8% in rats receiving the normal diet to around 30% in HFHS fed rats. Hepatic steatosis in the long term rats exceeded an overall 50% prevalence, but differed by group as it was present in only 50-64% of sham rats but 70-100% of OVX rats. The quantification of gut bacterial DNA in a pilot exploratory study measuring four common bacterial types showed no significant changes in total bacterial numbers between the groups of the same cohort or different cohorts; however, the proportion of *Lactobacillus acidophilus* was negatively affected by age (reduction ~ 12%) and HFHS (reduction ~ 8%, 11%, 10% in the short term cohort, sham rats and OVX rat respectively). Interestingly, *Akkermansia muciniphila* was significantly reduced by approximately 3% due to GSM. The change of this bacteria's proportion in the caecum correlated with changes in the proportion of propionic acid (a short chain fatty acid produced by gut microbes). Propionic acid was

significantly reduced by HFHS but increased by GSM in both cohorts. Finally, an inverse correlation between *Akkermansia muciniphila* and propionic acid was detected in normal diet rats. In conclusion, aging, HFHS diet and OVX had a collective effect on the development of MetS in rats. GSM did not improve the clinical biochemistry profile or pathological lesions of MetS in rats; however, it changed the proportion of *Akkermansia muciniphila*. Yet it is not possible to have a consensus whether this change is beneficial to general health and it would be of interest to carry out a more in-depth assessment of the caecal bacterial profile.

7.1 Introduction

The rise of obesity, T2D, and metabolic syndrome worldwide could be attributed to the changes in human diet and lifestyle after the agro-industrial revolution as their prevalence were temporally correlated (Ranasinghe et al., 2017). It has been recognized that these largely preventable disorders similarly expanded in both developed and developing countries over the last two decades (Cornier et al., 2008). In 2015, the survey found that obesity has occurred across 195 countries, with an estimated 604 million adults and 108 million children being obese (Saklayen, 2018). In the same year, 415 million people were living with T2D and it is expected that the prevalence will increase to 642 million in 2040 (Saklayen, 2018). As metabolic syndrome is more common than diabetes, by extrapolation, metabolic syndrome could afflict people more than 3 times the diabetes population which is estimated to be 20-25% of the global population. A regional study showed that the prevalence of MetS were 12-37% and 12-26% in Asia and Europe respectively (Sigit et al., 2020).

Metabolic syndrome (MetS) is characterized as a cluster of at least three out of five concomitant abnormalities which are obesity, hyperglycemia, hypertriglyceridemia, low HDL-cholesterol, and hypertension (Grundy et al., 2005; Alberti et al., 2009). MetS, as a multifactorial disease, has the risk factors of other non-communicable diseases, such as cardiovascular disease, T2D, cancer, non-alcoholic fatty liver disease (NAFLD) and osteoarthritis (Zhuo et al., 2012; Patell et al., 2014; Wong et al., 2018). In addition, osteoporosis may be associated with MetS due to the disturbance of the bone remodeling process (El Maghraoui et al., 2014); commonly in postmenopausal women bone resorption outpaces bone building and results in osteoporosis with decreased bone mineral density and increased bone fragility that may impact adjacent joints.

Many factors are possibly involved with the pathogenesis of MetS. For example, genetic predisposition has some contribution to the disease as can be seen in the different prevalences among ethnic groups (Sigit et al., 2020). The Western type diet which contains a high amount of fat and sugar is known as a significant cause of the obesity pandemic leading to MetS (Cani et al., 2007). Further, aging has an impact on the host's metabolism, gastrointestinal function and gut microbiota (Vemuri et al., 2019).

Growing evidence suggested that alteration of gut microbiota is crucial in the development of obesity, low-grade inflammation, diabetes, hypertension and metabolic

syndrome (Turnbaugh et al., 2006; Cani et al., 2012). For example, without translocation of gut microbes, germ free mice fed a high fat diet (HF) are not able to gain weight (Fredrik et al., 2004). It has been shown that HF disrupts the balance of gut microbiota by diminishing levels of gut barrier protecting bacteria such as *Bifidobacterium* spp. but promoting the proliferation of endotoxin producing bacteria (Cani et al., 2007). In addition, the gut dysbiosis is revealed as an increased ratio of *Fermicutes/bacteroides* (Cani et al., 2012). These changes cause increased plasma lipopolysaccharide levels (Cani et al., 2008) and eventually result in fatty liver degeneration and MetS (Grabherr et al., 2019).

Perna canaliculus is a species of bivalve shellfish which is known as greenshell mussel (GSM). It is endemic in New Zealand and recognized as a health promoting dietary component by Mātauranga Maori (traditional Maori knowledge). The main implication of GSM in previous research was mainly focused on its anti-inflammation or anti-arthritis effects (Whitehouse et al., 1997; McPhee et al., 2007; Treschow et al., 2007; Brien et al., 2008; Eason et al., 2018) however, oral administration of GSM in osteoarthritis patients found not only significant improvement of joints but also gastrointestinal tract (GIT) symptoms (Coulson et al., 2012) which could be a result from a long term use of analgesic drugs (NSAID). Coulson et al. (2013) postulated that the alleviation of GIT symptoms could be related to the prebiotic activity of GSM but this work only showed a trend in gut bacterial alteration which was *Clostridia* spp. reduction. To date, the evidence of GSM relating to gut microbiota is very limited. Therefore, our study also aimed to carry out a pilot study to assess the impact of GSM on selected beneficial gut bacterial types in rats, with the intention of assessing additional beneficial species as well as neutral and pathogenic species in later studies if warranted by the results of this limited exploratory study. We hypothesised that GSM could have benefits to prevent or limit the gut dysbiosis induced by HFHS diet and this in turn may reduce the prevalence or progression of MetS. The bacterial species selected for assessment were chosen based on the prevalence of data available in publication.

7.2 Materials and methods

7.2.1 Greenshell mussel and diet composition

Flash-dried powder from whole GSM meat was produced by Sanford Ltd (ENZAQ facility, Blenheim, New Zealand) using standard manufacturing processes and

assessed for proximate composition in a commercial testing laboratory (Food Testing Laboratory of Cawthron Analytical Services; Nelson, New Zealand). 10% of GSM powder was included in the experimental diets; normal control diet (ND+GSM) and high fat/high sugar diet (HFHS+GSM). All diets were stored at -20°C until used.

7.2.2 Animals and study design

The study design is described in section 4.2.2.

7.2.3 Plasma analysis

The rat whole blood samples were collected in EDTA-anticoagulant tubes and then centrifuged at 1050 g (Heraeus Megafuge 1.0R, Thermofisher) for 5 mins. The subsequent plasma was kept at -80 °C until analysis. Glucose, triglyceride, total cholesterol, high density lipoprotein (HDL-C) were analysed using Randox kits with Daytona Plus clinical analyser at Nutrition Laboratory, Massey Institute of Food Science and Technology, NZ.

7.2.4 Histopathological study

During necropsy, the internal organs (liver, uterus, pancreases, heart, kidneys and caecum) were dissected and weighed. Caecum and caecal contents were weighed separately. The organs were immediately submerged in 10% buffer formalin for tissue slide preparation and subsequently embedded in paraffin. Tissue sections were made at 3 µm thickness and stained using haematoxylin and eosin (H&E).

7.2.5 Quantification of gut microbes

The frozen caecal contents were used to quantify the number of microbes. Firstly, bacterial DNA was extracted using Isolate Faecal DNA kit (Bioline, NSW, Australia). 150 mg of caecal contents with 750 µl lysis buffer were mixed in a tube containing bashing beads. The tube was incubated at 95°C in a water bath for 5 mins in order to rupture the bacterial membranes followed by the procedure written in the kit's instruction. The faecal DNA was eluted from the columns and kept at -80°C until analysis. The concentration of DNA was evaluated using Nanodrop and all samples were normalized by appropriate dilution. Real-time quantitative PCR, using SYBR™ Green Master Mix, was performed on LightCycler® 480 Real-Time PCR instrument (Roche Applied Science). The specific primers for bacteria are provided in Table 7.1

Table 7.1 Primers for gut microbes

Bacteria	Forward primers	Reverse primers
Total bacteria (16SRNA)	TCCTACGGGAGGCAGCAGT	GGACTACCAGGGTATCTAATCCTGTT
A.muciniphila	CAGCACGTGAAGGTGGGGAC	CCTTGCGGTTGGCTTCAGAT
Bifidobacterium	GGG ATG CTG GTG TGG AAG AGA	TGC TCG CGT CCA CTA TCC AGT
L. acidophilus	GAA AGA GCC CAA ACC AAG TGA TT	CTT CCC AGA TAA TTC AAC TAT CGC TTA
Bacteroides/ Prevotella	TCCTACGGGAGGCAGCAGT	CAATCGGAGTTCTTCGTG

7.2.6 Measurement of short chain fatty acids in caecal contents

Rat caecal contents (~1g) were received and analysed for short chain fatty acids (SCFA). Approximately 100 mg of sample was extracted in 400 µL of deionised water (type II) and vortexed. The pH was adjusted with HCl to pH of 2-3. An internal standard (50 µl Hexanoic acid @ 1000 µg/mL) was added to each tube and then mixed for 10 minutes in an orbital shaker. The samples were centrifuged at 4000 g for 20 minutes at room temperature and 1 mL of the supernatant was put through a 0.22 µm disposable filter. Analytical grade chemicals used as references were purchased from Sigma Aldrich. Standard curves were made for Acetic (CN 71251), Propanoic (CN 94425), iso-Butyric (CN 96499), n-butyric (CN 19215) and n-Valeric (CN 75054) acids. The GC-MS conditions were taken from Zhao et al. (2006). Briefly, 1µL was injected on Agilent 7890 GC system equipped with both flame ionised detection (FID) and mass spectroscopy. Identification of samples was confirmed by mass spectra but integration was done on chromatograms from the FID data. A fused-silica capillary column with a free fatty acid phase (ZB-FFAP) of 30 m × 0.25 mm i.d. coated with 0.25 µm film thickness was used. The initial oven temperature was 100°C, maintained for 0.5 min, raised to 180°C at 8°C/min and held for 1.0 min, then increased to 200°C at 20°C/min, and finally held at 200°C for 5 min.

7.2.7 Data analysis

Body and organ weights of each rat's cohort were collected at the end of the studies. Means of each group with SE from the short term and the long term cohort were calculated and analysed using one-way ANOVA or two-way ANOVA respectively. As there were substantial differences of BW among the groups of animals in the long term cohort and increased BW has an influence on organ weights, therefore a covariate factor of BW was applied in two-way ANCOVA for the statistical analysis of the long term cohort and one-way ANCOVA for the analysis of the differences across both cohorts.

The multiple comparison test was used Tukey test and statistical differences were determined at $p<0.05$.

The plasma parameters of glucose and lipid metabolism was measured in only the long term cohort rats and the statistical analysis was performed using two-way ANOVA followed by Tukey method as post hoc test. Statistical differences were applied at $p<0.05$.

The histological findings from liver, kidneys, heart, and pancreas were qualitative data, recording a frequency of the incidence. The number of animals found particular lesions in each group was summarised as a percentage. To identify a factor effecting the pathological changes, data were analysed using non-parametric statistics (Mann-Whitney U test). Mean rank was calculated according to each comparison. The data from the short term rats were compared against the sham rats of the long term cohort in order to test the effect of age. Only data from the long term cohort were used to analyse the effect of diet, GSM, and OVX. For example, in order to evaluate the effect of diet, data from the four groups of rats fed ND were compared with the four groups of rats fed HFHS. Statistical differences were determined at $p<0.05$.

The abundance of microbes in caecal contents are presented in log scale. The short and the long term cohorts were analysed using one-way or two-way ANOVA respectively. Statistical differences between the cohorts were assessed using Independent T test. The multiple comparison test was used Tukey test and statistical differences were determined at $p<0.05$.

The amount of SCFA recovered from caecal contents of each rat group is reported in Table A6 of Appendix B. Each species of SCFA data was converted to relative values compared to the total SCFA and it is reported in Figure 7.2. The similar statistical analysis used with the gut microbial data was applied to the analysis of SCFA. In addition, Pearson correlation was used to find a significant relationship between the gut microbes and SCFA.

7.3 Results

7.3.1 Body/organ weights

At the end of the short term cohort, both groups of ND-fed rats had increased their BW around 25% from the beginning (12 weeks old) while HFHS-fed rats doubled their BW increase when compared to ND-fed rats (Table 7.2). Inclusion of GSM into the

diets had no significant impact on the BW increase in both diet groups. The long term rats at the end of the study were similar to the short term rats in which the BW increase significantly corresponded with HFHS and in addition, ovariectomy also had a dramatic impact on the BW increase.

All organ weights of the short term rats had no significant changes across all groups except for the caecum and caecal contents (Table 7.2). Both masses had 23-32% reduction in response with feeding HFHS. Interestingly, adding GSM to the HFHS diet slightly increased caecum and caecal contents but without significant differences.

In order to exclude the influence of BW on the organ weight in older rats or the other test effects (diet, GSM, OVX) BW was assigned as a covariate factor in the ANCOVA analysis. The result showed that advanced age seemed to have an influence on the weight reduction of two particular organs. One was liver, consistently reduced in all diet groups (percent reduction between both cohorts, ND≈10%; ND+GSM≈7%; HFHS≈7%; HFHS+GSM≈3%). Secondly, caecum weight of ND fed rats was almost significantly reduced ($p = 0.058$) when compared between the short and the long term cohort. Giving HFHS for longer period of time seemed to increase heart and kidney weight (11.60%, and 12.59% respectively in the HFHS group and they were 16.36%, and 23.13% respectively in the HFHS+GSM group) but this was not significant when accounting for the increasing BW of older rats.

In the long term cohort in which half of the rats were ovariectomised, the success of the procedure was clearly confirmed by the reductions of uteri weight and OVX also had a significant negative impact on pancreas weight (Table 7.2). Similar to the short term rats, caecum and caecal contents in the long term rats were significantly reduced due to HFHS feeding analysed using two-way ANCOVA. Interestingly, adding GSM into the diets increased caecum weight. Liver weight was increased by HFHS but reduced by OVX. Heart and kidney weight seemed to be influenced by HFHS especially in sham rats which was recognized by one-way ANOVA however the global analysis using two-way ANCOVA rejected the differences.

Table 7.2 Body/organ weights of the rats in both cohort studies

Short term cohort (26 weeks old)	ND (n=12)	ND+GSM (n=11)	HF/HS (n=12)	HF/HS+GSM (n=12)	P value
% Change BW	24.05±2.12^{a}	26.09±2.46^{a}	42.42±2.75^{b}	48.22±4.36^{b}	<0.001
Pancreas (g)	0.77±0.03	0.88±0.06	0.85±0.08	0.84±0.05	0.501
Uterus	1.29±0.11	1.24±0.07	1.32±0.08	1.22±0.01	0.876
Caecum	2.90±0.15$^{b*?}$	2.84±0.14^{b}	1.96±0.13^{a}	2.20±0.09^{a}	<0.001
Caecal contents	1.77±0.12^{b}	1.89±0.08^{b}	1.25±0.09^{a}	1.36±0.07^{a}	<0.001
Liver	10.25±0.50***	10.95±0.41***	11.07±0.61***	11.55±0.72***	0.442
Heart	1.03±0.03	1.10±0.04	1.12±0.04	1.10±0.05	0.415
Kidneys (both)	2.36±0.08	2.40±0.10	2.62±0.11	2.68±0.13	0.129

Body and organ weights of the long and short term rats were collected at the end of the studies. The difference of body weight from the start to the end was calculated as percent change. Data are shown as mean±SE. One-way ANOVA followed by Tukey post hoc test were used in the statistical analysis and different letters were indicated significant. Two-way ANCOVA (covariated with BW) additionally was applied for testing the significant effects of the long term cohort. The differences across the cohorts were used ANCOVA and *** indicated P<0.001 All statistical significance was determined by *P value* less than 0.05. Group: ND=normal control diet, HF/HS=high fat/high sugar diet, OVX=ovariectomy, GSM=Greenshell mussel.

Long term cohort	Sham				OVX				
(48 weeks old)	ND (n=11)	ND+GSM (n=12)	HF/HS (n=12)	HF/HS+GSM (n=12)	ND (n=12)	ND+GSM (n=12)	HF/HS (n=11)	HF/HS+GSM (n=11)	P value
% Change BW	48.29±4.09^{a}	56.00±4.31^{ab}	91.02±6.96^{cd}	109.49±7.62^{cde}	82.48±3.59^{bc}	86.32±8.18^{c}	131.07±10.50^{e}	119.38±7.13^{de}	<0.001
Pancreas (g)	0.77±0.06^{ab}	0.78±0.05^{ab}	0.90±0.04^{ab}	0.88±0.05^{ab}	0.68±0.03^{a}	0.75±0.05^{ab}	0.92±0.07^{ab}	0.88±0.06^{b}	0.01
Uterus	1.41±009^{b}	1.33±0.07^{b}	1.38±0.10^{b}	1.60±0.11^{b}	0.17±0.01^{a}	0.16±0.01^{a}	0.18±0.01^{a}	0.29±0.09^{a}	<0.001
Caecum	2.48±0.10^{bc}	2.98±0.19^{c}	2.02±0.16^{ab}	2.21±0.14^{ab}	2.58±0.16^{bc}	2.57±0.19^{bc}	1.81±0.10^{a}	2.12±0.13^{ab}	<0.001
Caecal contents	1.50±0.09^{bc}	1.85±0.14^{c}	1.23±0.10^{ab}	1.22±0.11^{ab}	1.49±0.10^{bc}	1.50±0.13^{bc}	0.94±0.09^{a}	1.10±0.13^{ab}	<0.001
Liver	9.19±0.45^{a}	10.17±0.30^{ab}	10.26±0.54^{ab}	11.24±0.38^{b}	9.49±0.44^{ab}	9.18±0.46^{a}	10.10±0.61^{ab}	9.98±0.49^{ab}	0.04
Heart	1.06±0.04^{a}	1.15±0.02^{ab}	1.25±0.04^{b}	1.28v0.04^{b}	1.12±0.04^{ab}	1.11±0.04^{ab}	1.19±0.05^{ab}	1.22±0.05^{ab}	<0.001
Kidneys (both)	2.58±0.09^{a}	2.86±0.07^{ab}	2.95±0.12^{ab}	3.30±0.10^{b}	2.55±0.06^{a}	2.63±0.16^{a}	2.91±0.09^{ab}	2.86±0.13^{ab}	<0.001

Statistical analysis by two-way ANOVA with three effects

	diet	GSM	OVX	diet * GSM	diet * OVX	GSM * OVX	diet * GSM * OVX
% Change BW	<0.001	0.538	<0.001	0.824	0.807	0.176	0.748
Pancreas	0.414	0.83	0.017	0.218	0.245	0.425	0.694
Uterus	0.09	0.263	<0.001	0.058	0.598	0.784	0.399
Caecum	<0.001	0.03	0.087	0.987	0.955	0.491	0.137
Caecal contents	<0.001	0.12	0.19	0.546	0.868	0.606	0.118
Liver	<0.001	0.366	<0.001	0.867	0.582	0.206	0.276
Heart	0.434	0.329	<0.001	0.687	0.21	0.823	0.175
Kidneys (both)	0.403	0.043	<0.001	0.709	0.567	0.218	0.552

7.3.2 Dysregulation of glucose and lipid metabolism

Glucose, triglyceride, cholesterol and HDL levels were measured in plasma samples from the long term rats (Table 7.3). The results showed that increased glucose levels were influenced by HFHS (17%) and GSM (20%) but not OVX. The OVX rats had increased plasma cholesterol levels but interestingly rats fed HFHS showed a reduction in all lipid profiles including cholesterol, triglycerides and HDL.

In the pancreas, the obvious pathological changes were fatty infiltration and the degeneration and necrosis of acinar cells as shown in Figure 7.1 (G, H, I). All groups and cohorts showed fatty infiltration of pancreas to some extent with no obvious impact from HFHS or GSM or OVX. Acinar cells on the other hand obviously revealed differences in degeneration/necrosis between the short and the long term rats as the lesions did not appear in the younger rats.

Normal cardiac muscle fibers were revealed in the short-term fed ND rats (Figure 7.1 J). Feeding HFHS increased the percentage of rats having myocardial hypertrophy (Figure 7.1 K) in both short and long term cohorts when compared to ND fed rats (Table 7.4). Similar to the effect of HFHS, OVX also increased the number of rats having myocardial hypertrophy which was around 80% in the OVX rats fed HFHS.

Table 7.3 Measurement of glucose and lipid metabolism in the long term cohort rats

	Sham				OVX				
	ND (n=11)	**ND+GSM (n=12)**	**HF/HS (n=12)**	**HF/HS+GSM (n=12)**	**ND (n=12)**	**ND+GSM (n=12)**	**HF/HS (n=11)**	**HF/HS+GSM (n=11)**	**P values**
Glucose (mmol/l)	10.42 ± 1.04^{a}	13.46 ± 0.88^{ab}	12.87 ± 0.75^{ab}	15.00 ± 1.41^{b}	11.27 ± 0.91^{ab}	11.03 ± 0.91^{ab}	12.66 ± 0.91^{ab}	14.25 ± 1.09^{ab}	0.02
Cholesterol (mmol/l)	2.31 ± 0.17^{abc}	2.21 ± 0.12^{abc}	1.86 ± 0.13^{ab}	1.71 ± 0.08^{a}	2.75 ± 0.26^{c}	2.35 ± 0.10^{bc}	2.12 ± 0.13^{ab}	1.99 ± 0.10^{ab}	<0.001
Triglyceride (mmol/l)	0.76±0.09	0.94±0.10	0.82±0.09	0.80±0.09	0.91±0.08	0.87±0.10	0.62±0.05	0.71±0.07	0.17
HDL (mmol/l)	0.58 ± 0.04^{cd}	0.58 ± 0.03^{d}	0.42 ± 0.03^{a}	0.42 ± 0.03^{a}	0.57 ± 0.05^{bcd}	0.57 ± 0.02^{bcd}	0.44 ± 0.03^{ab}	0.44 ± 0.02^{abc}	<0.001

Statistical analysis by two-way ANOVA with three effects

	diet	**GSM**	**OVX**	**diet * GSM**	**diet * OVX**	**GSM * OVX**	**diet * GSM * OVX**
Glucose (mmol/l)	**0.004**	**0.027**	0.384	0.753	0.829	0.189	0.345
Cholesterol (mmol/l)	**<0.001**	0.053	**0.007**	0.568	0.932	0.492	0.444
Triglyceride (mmol/l)	**0.033**	0.383	0.375	0.812	0.13	0.615	0.18
HDL (mmol/l)	**<0.001**	0.964	0.766	0.949	0.567	0.979	0.922

Plasma was recovered from the rat's blood at termination (48 weeks of age). Data are presented as mean±SE. The statistically significant differences across all groups were analysed using One-way ANOVA and p values were reported in the last column. In case there was a significant difference, multiple comparison tests, using Tukey method, was applied and the differences of superscript letters indicated the statistical significance. Two-way ANOVA was used to analyse the influence of diet, GSM and ovariectomy (OVX) on the particular parameters. These three effects were treated as fixed effects in general linear models. The p values are summarized in the lower table. Statistical differences were applied at $P<0.05$. Group: ND=normal control diet, HFHS=high fat/high sugar diet, OVX=ovariectomy, GSM=Greenshell mussel.

7.3.3 Histopathological changes

The tissue slides of liver, kidneys, pancreas, and heart were prepared using H&E staining as shown in Figure 7.1. The pathological findings in the animals were recorded in each group and the number of animals showing a particular lesion was reported as percentage in Table 7.4. The statistical differences were reported in Table 7.5. The result showed that obesity either due to HFHS or OVX caused fatty degeneration in hepatocytes. Mild degree (affected 5%-33% of the tissue section) of the periportal fatty change (Figure 7.1A) could be detected in the short term rats fed ND at a low percentage (8%). This mild-degree lesion significantly increased ($p<0.001$) with advancing age with around 50% in the ND-sham rats. HFHS obviously had an influence on the fatty changes which increased the severity (accumulation of fat vesicles) in the periportal area (Figure 7.1B), and the number of the affected animals. The percentage in HFHS fed rats with fatty liver rose from ~30% in the short term to ~50% in the long-term sham rats and to ~80% in the OVX rats (Table 7.4). As the result, OVX had a significant effect ($p=0.024$) on the increase of periportal fatty changes. The hyperplasia of the periportal bile ductules also increased due to HFHS feeding but this was only obvious in the short term cohort.

Only mild pathological changes in the kidneys were detected in three features (Figure 7.1 D, E, F). Firstly, the vascular congestion at the corticomedullary region showed a low percentage in the short term cohort (<50%) especially, the ND-fed rats (<17%) while all the long term rats were commonly found at around 80%. Secondly, vacuolation/degeneration of renal tubules was not found in the short-term fed ND rats but the percentage increased in the HFHS fed rats especially, in the long term rats. Thirdly, mild hypercellularlity at the glomerular pole was not detected in the short-term fed ND rats but the percentage increased correspondingly due to HFHS, advancing age, and OVX (Table 7.4). As the results show, age had significant effects on all three pathological findings; diet had significant effects on vacuolation and mild hypercellularity of glomerular pole; OVX had a significant effect on mild hypercellularity of glomerular pole.

The prevalence of myocardial hypertrophy was significantly increased due to both diet and OVX effect ($p<0.001$ and $p=0.006$ respectively). In the pancreas, acinar cell degeneration/necrosis were not detected in the short term rats and around 50% of this cohort found fatty infiltration. On the other hand the long term cohort showed higher

prevalence in both pathological lesions. The statistical analysis showed the significant effect of age on both lesions ($p<0.001$ and $p=0.037$ respectively).

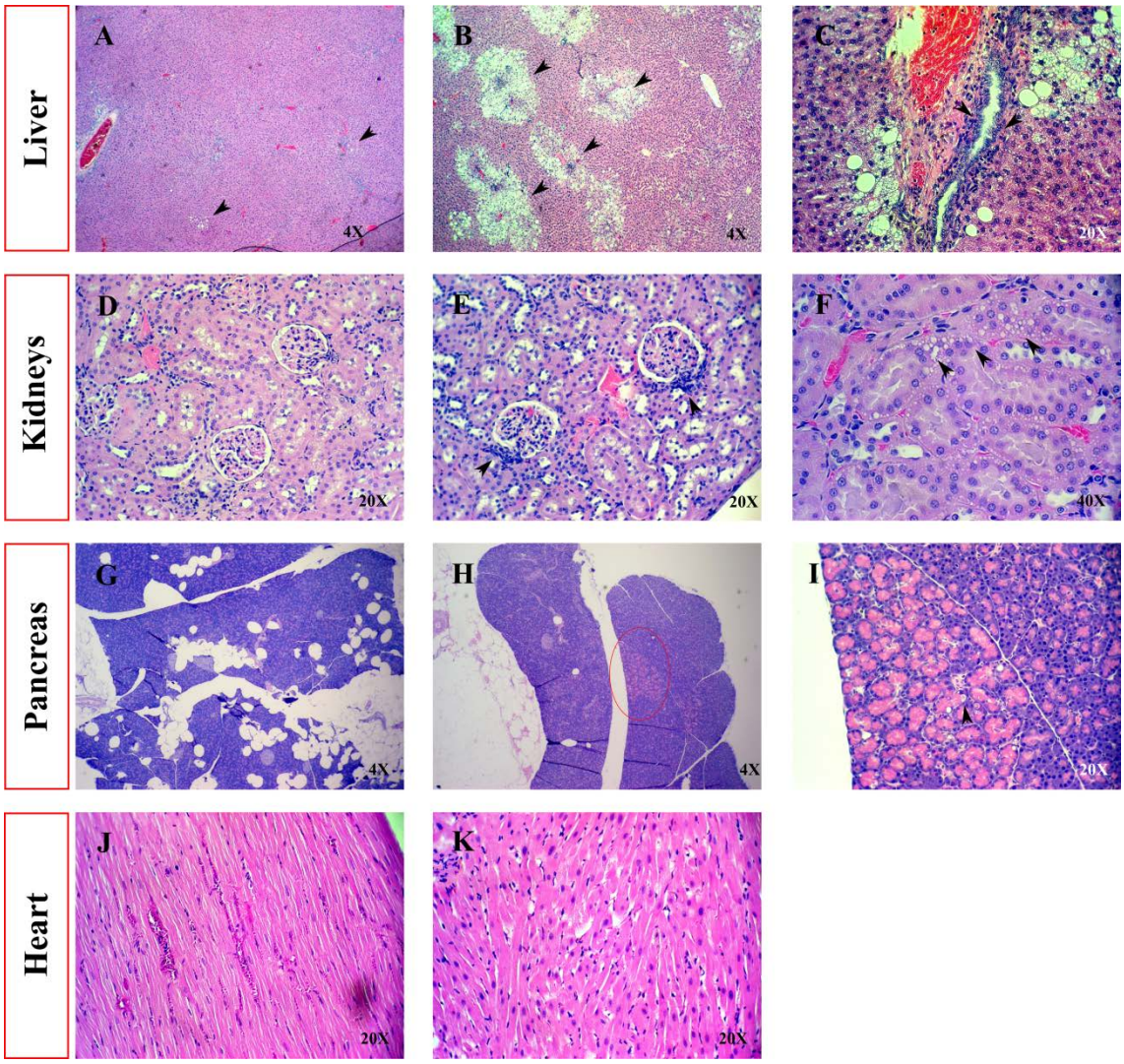

Figure 7.1: Histopathological examination in rats

Pathological findings in 4 organs stained with H&E, Hepatic lobules are presented in A (4X) and B (4X). Black arrows indicate periportal fatty change of hepatocytes in which a mild lesion is found in ND short term study and ND_sham rats (A) while severe degree from HFHS_sham rats is presented in B. Hepatic bile duct at the portal triad is revealed in C (20X) and black arrows indicate the lesion of periportal bile ductular hyperplasia. D (20X) shows normal renal glomeruli and E (20X) shows mild hypercellularity at the glomerular pole indicated by two black arrows. F (40X) shows vacuolation and degeneration of renal tubule. Lobes of pancreas with fatty infiltration is presented in G (4X). Some pink area of pancreas shows degenerative sign (H, 4X), the area inside the red circle was enlarged (I, 20X) showing the degeneration and necrosis of acinar cells, an apoptotic cell is indicated by a black arrow. J (20X) and K (20X) compare myocardial fiber, which is normal from rat fed ND (J) and hypertrophy from HFHS diets (K). The pictures were taken under the objective lens 4X or 20X as stated in the pictures.

Table 7.4 Histopathological changes in four vital organs of the short and long-term animal studies

Organ/pathological descriptions	Short term cohort				Long term cohort				Long term cohort			
	Non-surgical procedure				Sham				Ovariectomy			
	ND	ND+ GSM	HF/HS	HF/HS+ GSM	ND	ND+ GSM	HF/HS	HF/HS+ GSM	ND	ND+ GSM	HF/HS	HF/HS+ GSM
Liver												
-Periportal fatty change of hepatocytes	8	8	33	23	64	50	50	55	100	83	73	82
-Periportal bile ductular hyperplasia	8	0	25	38	18	17	25	27	17	25	36	27
Kidneys												
-Congestion at corticomedullary junction	8	17	42	38	82	91	83	83	83	83	82	73
-Vacuolation/ degeneration of renal tubular epithelium	0	0	33	31	45	45	83	100	50	83	100	82
-Mild hypercellularity of glomerular pole	0	0	17	23	18	18	33	33	42	33	55	91
Heart												
Myocardial hypertrophy	0	0	17	38	0	9	42	45	33	42	82	73
Pancreas												
-Acinar cell degeneration/necrosis	0	0	0	0	36	20	44	42	25	33	18	36
-Fatty infiltration	38	42	75	62	73	100	44	92	75	83	73	64

Data are presented as percentage of animals in each group (n = 9-12) showing the particular lesion. Group: ND=normal control diet, HFHS=high fat/high sugar diet, OVX=ovariectomy, GSM=Greenshell mussel.

Table 7.5 Statistical analysis of histopathological findings from the internal organs

	Age			Diet			GSM			OVX		
Organ/pathological descriptions	26 wks (n = 47)	48 wks (n = 38)	*p*- Value	ND (n = 44)	HFHS (n = 40)	*p*- Value	No GSM (n = 42)	GSM (n = 42)	*p*- Value	Sham (n = 38)	OVX (n = 46)	*p*- Value
Liver												
-Periportal fatty change of hepatocytes	34.64	53.34	**0.000**	44.41	40.40	0.316	43.00	42.00	0.802	37.53	46.61	**0.024**
-Periportal bile ductular hyperplasia	41.64	44.68	0.433	40.09	45.15	0.213	42.50	42.50	1.000	42.55	42.46	0.981
Kidneys												
-Congestion at corticomedullary junction	32.76	55.67	**0.000**	43.82	41.05	0.445	42.50	42.50	1.000	42.76	42.28	0.895
-Vacuolation/ degeneration of renal tubular epithelium	33.23	55.08	**0.000**	36.32	49.30	**0.001**	39.50	45.50	0.139	40.24	44.37	0.310
-Mild hypercellularity of glomerular pole	39.52	47.30	**0.033**	36.91	48.65	**0.010**	41.50	43.50	0.661	36.66	47.33	**0.020**
Heart												
Myocardial hypertrophy	40.83	45.68	0.193	34.05	51.80	**0.000**	41.50	43.50	0.661	35.55	48.24	**0.006**
Pancreas												
-Acinar cell degeneration/necrosis	37.00	50.42	**0.000**	42.41	42.60	0.964	42.00	43.00	0.812	43.26	41.87	0.742
-Fatty infiltration	38.91	48.05	**0.037**	44.86	39.90	0.207	39.50	45.50	0.127	43.66	41.54	0.592

Qualitative data from histopathological examination was summarised in accordance with each effect (age, diet, GSM, and OVX). The data show mean rank calculated by the non-parametric measure. The differences of mean rank between the groups were analysed using Mann-Whitney U test and the p- value was provided at the last column of each effect. Statistical significance was determined at $p<0.05$

7.3.4 Alteration of gut microbial abundance

Table 7.6 demonstrates that the abundance of total bacteria in the rat caecal contents had not changed during the study period between the short term and long term cohort time points; however, significant changes in gut microbial abundance were detected for some particular bacteria. For example, *Lactobacillus acidophilus* had consistently decreased due to feeding HFHS within both cohorts and also between the cohorts (time). *Bifidobacterium* spp. on the other hand was affected by all three factors (HFHS, GSM and OVX). The data show the negative influences of these factors in the long term cohort and a similar trend can be observed for the short term cohort. Interestingly, GSM solely, had a significant effect on the reduction of *Akkermansia muciniphila* which was observed in both cohorts while the opposite effect was detected across the cohorts. Finally, *Bacteroides* spp. were significantly reduced by the effect of HFHS only in the short term cohort while it was insignificant in the long term cohort.

7.3.5 Changes in faecal short chain fatty acids

As shown in Figure 7.2, SCFA were evaluated in the rat caecal contents and the levels were in a range of 1.05-3.01 µg/mL across all groups and cohorts. Total SCFA levels across all groups in the short term rats ranged 2.26-3.01 ng/mL while it seemed to be lower in the long term rats (1.06-1.47ng/mL). However, there were no significant differences in total SCFA levels within the groups of the same cohort or across the cohorts. Despite no significant changes in the total SCFA levels, a particular SCFA, propionic acid, showed significant changes in both cohorts. In the short term cohort, around 8-10% of the SCFA was in the form of propionic acid in ND fed rats but this proportion was reduced by half due to feeding HFHS. A similar trend was also revealed in the long term cohort. Interestingly, inclusion of GSM into the diets had a significant effect increasing propionic acid proportionally. No further significant changes were observed.

Figure 7.3 shows the relationship between propionic acid with the gut microbes. Data were stratified into ND and HFHS and then the propionic acid levels were correlated against the gut microbes. The results indicated that in the ND group, *Akkermansia muciniphila* was negatively correlated with propionic acid. This phenomenon was only detected in the short term cohort.

Table 7.6 Microbial profile in caecal contents of the rats: short term cohort upper table; long term cohort middle table; ANOVA lower table

	ND (n=12)	ND+GSM (n=11)	HF/HS (n=12)	HF/HS+GSM (n=12)	P values
logtotal	11.83±0.17	11.73±0.11	11.56±0.18 *	11.59±0.14	0.579
loglacto	8.41±0.21^{b} *	8.72±0.13^{b} *	7.80±0.13^{a} **	7.95±0.19^{a} ***	0.001
logbifido	7.89±0.38^{b}	6.70±0.28^{ab}	6.84±0.57^{ab}	5.63±0.17^{a}	0.002
logAkker	9.66±0.11^{b} *	9.39±0.10^{ab} *	9.41±0.15^{ab} **	9.05±0.11^{a} *	0.007
logbacteroi	9.61±0.12^{b}	9.20±0.16^{ab}	8.94±0.19^{a} ***	8.69±0.23^{a} *	0.004

	Sham				OVX				
	ND (n=11)	ND+GSM (n=12)	HF/HS (n=12)	HF/HS+GSM (n=12)	ND (n=12)	ND+GSM (n=12)	HF/HS (n=11)	HF/HS+GSM (n=11)	P values
logtotal	12.01±0.08	12.03±0.10	12.04±0.07^{a}	11.51±0.23	11.96±0.10	11.82±0.08	11.78±0.18	11.90±0.09	0.087
loglacto	7.44±0.03	7.82±0.33	6.73±0.33	6.74±0.22	7.10±0.36	8.03±0.61	6.93±0.30	6.66±0.27	0.042
logbifido	7.35±0.18^{b}	7.01±0.25^{bc}	6.74±0.24^{abc}	5.94±0.07^{a}	6.99±0.22^{bc}	6.36±0.24^{ab}	6.28±0.18^{ab}	5.93±0.12^{a}	0
logAkker	9.91±0.05^{b}	9.70±0.08^{ab}	9.93±0.07^{b}	9.47±0.10^{a}	9.80±0.07^{ab}	9.53±0.08^{a}	9.69±0.10^{ab}	9.57±0.12^{ab}	0.001
logbacteroi	9.65±0.07^{bc}	9.39±0.09^{abc}	9.74±0.03^{c}	9.31±0.11^{ab}	9.60±0.05^{bc}	9.18±0.14^{a}	9.46±0.09^{abc}	9.48±0.10^{abc}	0

Statistical analysis by two-way ANOVA with three effects							
	diet	GSM	OVX	diet * GSM	diet * OVX	GSM * OVX	diet * GSM * OVX
logtotal	0.112	0.166	0.688	0.414	0.342	0.213	0.037
loglacto	0.001	0.301	0.983	0.116	0.801	0.804	0.403
logbifido	<0.001	<0.001	0.008	0.684	0.375	0.819	0.19
logAkker	0.317	<0.001	0.124	0.835	0.447	0.193	0.061
logbacteroi	0.517	0.517	0.517	0.517	0.517	0.517	0.517

Caecal contents from the rats were collect at the termination. Later, the quantification of microbial DNA was evaluated using qRT-PCR. Data were present in a Log_{10} scale as mean±SE. Within each cohort, the statistically significant differences across all groups were analysed using One-way ANOVA and p values were reported in the last column. In case there was a significant difference, multiple comparison tests, using Tukey method, was applied and the differences of superscript letters indicated the statistical significance. In the long the cohort, additionally, two-way ANOVA was used to analyse the influence of diet, GSM and ovariectomy (OVX) on the particular bacteria. These three effects were treated as fixed effects in general linear models. The p values were summarized in the table below. All statistical differences were applied at P<0.05. Statistical differences between the cohorts were accessed using Independent T test and asterisk *, **,*** identified significance at P< 0.05, 0.01 and 0.001 respectively. Group: ND=normal control diet, HFHS=high fat/high sugar diet, OVX=ovariectomy, GSM=Greenshell mussel.

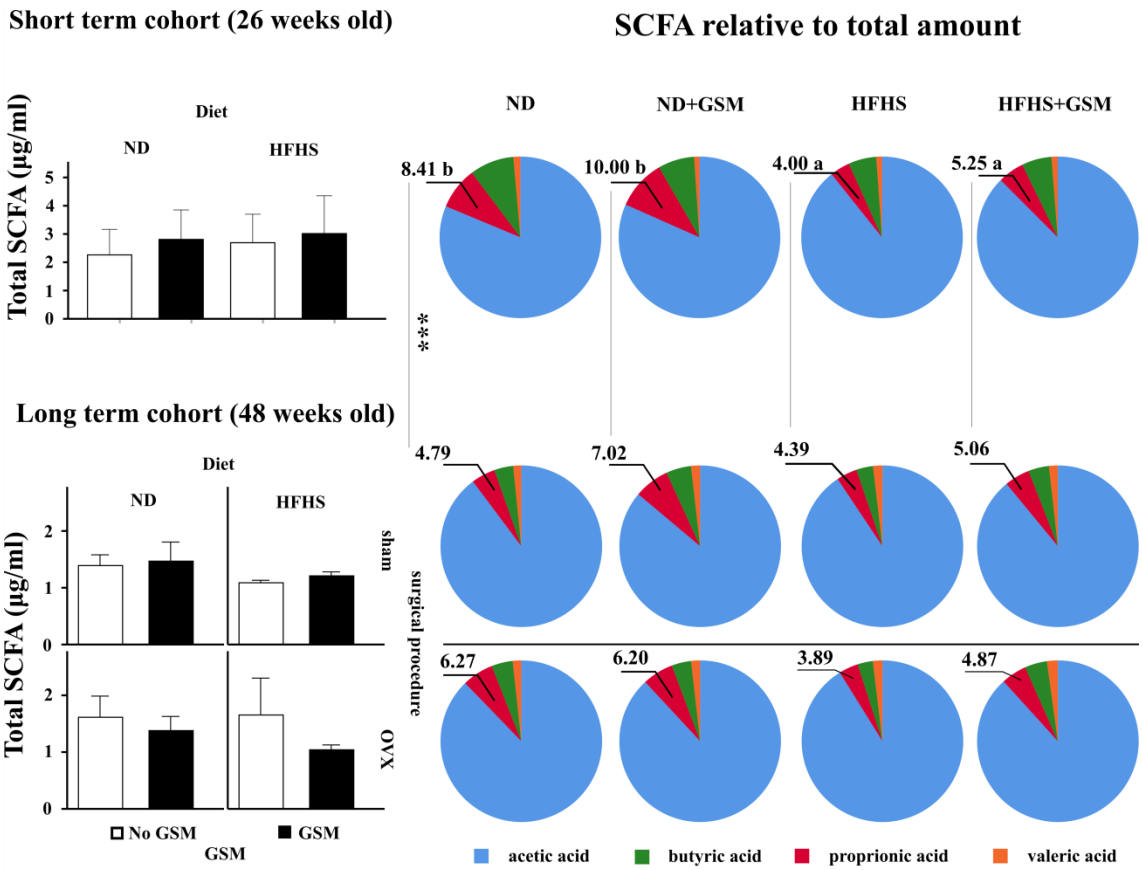

Statistical analysis by two-way ANOVA with three effects

SCFA relative to total amount in the long term cohort	diet	GSM	OVX	diet * GSM	diet * OVX	GSM * OVX	diet * GSM * OVX
Acetic acid	0.071	0.054	0.943	0.774	0.962	0.501	0.193
Proprionic acid	**0.004**	**0.039**	0.834	0.984	0.671	0.327	0.208
Butyric acid	0.301	0.119	0.733	0.496	0.722	0.63	0.262
Valeric acid	0.077	0.288	0.25	0.775	0.405	0.577	0.302

Figure 7.2: Changes of short chain fatty acids in rat caecal contents

The collection of rat caecal contents kept in -80 ºC were measured for short chain fatty acid (SCFA). The total amount (µg/mL) of SCFA in both cohorts is presented by the bar charts. Four types of SCFA were identified and reported as percentage relative to the total SCFA in the pie charts. Within each cohort, the statistically significant differences across all groups were analysed using one-way ANOVA (n=11-12 per group). In case there was a significant difference, multiple comparison tests, using Tukey method, was applied and the differences of superscript letters indicated the statistical significance. In the long the cohort, additionally, two-way ANOVA was used to analyse the influence of diet, GSM and OVX. These three effects were treated as fixed effects in general linear models. The p values were summarized in the table below. All statistical differences were applied at $P<0.05$. Statistical differences between the cohorts were accessed using Independent T test and asterisk *** identified significance at $P< 0.001$. Group: ND=normal control diet, HFHS=high fat/high sugar diet, OVX=ovariectomy, GSM=Greenshell mussel.

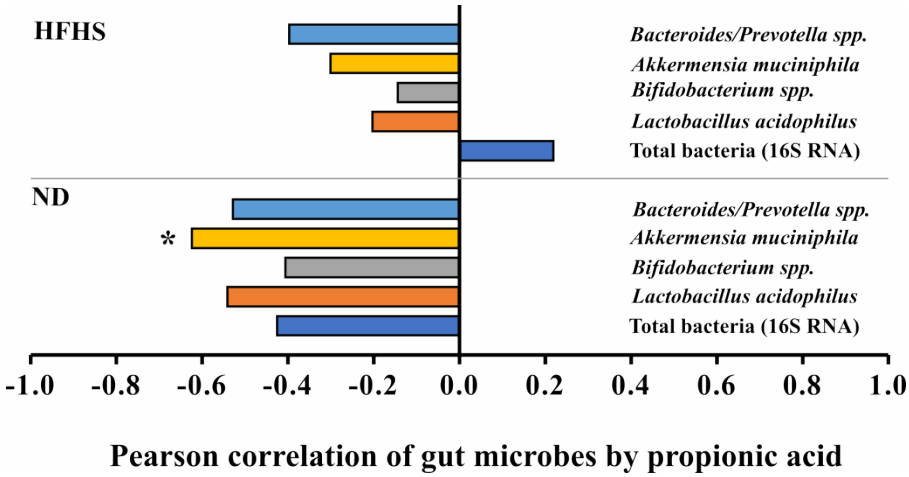

Figure 7.3: Correlation between propionic acid and gut microbes in rat caecal contents

Data from the short term rats were stratified into normal diet (ND), (n=24) and high fat/high sugar diet (HFHS), (n=24) then the correlation of propionic acid against gut microbes was analysed using Pearson method. Asterisk * indicates significant differences at *P value* less than 0.05.

7.4 Discussion

The purpose of this study was to explore the relationship between the MetS-inducing factors and the change in abundance of some beneficial gut microbes in rats. The result indicated that HFHS was the critical factor in the reduction of gut microbiota (as the reduction of caecum weight and caecal contents) especially the groups of bacteria such as *Lactobacillus acidophilus* and *Bifidobacterium* spp. In addition, HFHS affected the reduction of propionic acid in rat caecal contents. Interestingly, inclusion of GSM on the other hand increased the caecum weight and caecal contents which mean the colonization of gut microbes was enhanced. Despite the increased abundance of gut microbiota due to GSM, *Bifdobacterium* spp. and *Akkermansia municiphilla* were relatively decreased and particularly *Akkermansia municiphilla* had a negative correlation with propionic acid.

As the rats in this study were randomised not only by body weight and BMD but also by dispersing littermates – some of whom had been cross-fostered -- as broadly as possible across the test groups, it is unlikely that gut microbiota or other maternal factors played a significant role in the differences observed across groups. Subtle maternal factors could be mitigated by wide-scale cross-fostering pups between litters immediately after birth with tracking, but this requires a method of permanently

identifying individual pups from the age of day 1, and there are no methods that are sufficiently suitable, affordable, and ethical to warrant their use (Wever et al., 2017).

Metabolic syndrome is a cluster of health disorders which are frequently found in obese people associated with the development of hyperglycemia, dyslipidemia, and hypertension. The HFHS-induced obese rats in this study basically had developed metabolic disorders by having an increase in BW, plasma glucose levels, and plasma lipid dysregulation. The increased BW of both obese humans and animals is related to increased fat mass especially visceral fat and obese rats in this study also increased visceral fat (data shown in chapter 4). The accumulation of this fat is associated with insulin resistance and development of T2D (Barzilai et al., 2012) which could be attributed to the augmented production of adipokines and inflammatory cytokines including, leptin, TNF-α, IL-6 and PAI-1 (Barzilai et al., 2012). Another possible complication of increased visceral fat is that the augmented release of free fatty acid circulates into the hepatic portal system and can cause hepatic steatosis (Muzumdar et al., 2008).

In contrast, the increase in liver weight in the long term rats did not correspond with the BW as could be seen in the short term rats. However, liver weight of the long term rats was solely increased by the effect of HFHS but it was reduced by the effect of OVX and advanced age. This occurrence might be because of the additive complications of age and OVX effect on hepatic lesions. The pathological findings in the liver showed the increased percentage of hepatic steatosis in rats due to age, HFHS and OVX. It is possible that fatty changes in hepatocytes were limited to a small degree by the effect of HFHS but it was accelerated by the multiple effects of age and OVX which caused more cell degeneration and apoptosis and eventually liver shrinking.

Many vital organs are also affected by disruptive lipid metabolism and ectopic fat deposition of which the pathological feature called steatosis can be detected in cardiovascular tissue, muscles, kidney, pancreas, and liver (Pi-Sunyer, 2009). Despite no occurrence of steatosis in the heart tissue samples, this study revealed that both OVX rats and HFHS fed rats showed myocardial hypertrophy especially in OVX-rats fed HFHS. Therefore both factors may have an additive effect on hypertension or cardiac disease due to obesity (Woodiwiss et al., 2008; Leopoldo et al., 2010) or it may be a physiological change (Dorn, 2007; Kemi & Ellingsen, 2012) which needs more investigation. The kidneys on the other hand presented mild pathological lesions in

almost of all of the animals and thus this observation was likely due to age rather than a specific treatment such as diet or surgery. This finding is similar to Rangel Silvares et al. (2019) who showed no alteration of renal function in high-fat diet fed rats for 28 weeks but only detectable endothelial dysfunction.

Pancreatic steatosis is less recognized as a consequence of obesity or metabolic syndrome when compared to liver steatosis because of its controversial relationship with T2D and NAFLD (Catanzaro et al., 2016). However, there is a growing interest in using this pathological feature as early detection for metabolic syndrome in animal models. The steatosis in these two organs is different in appearance. Liver steatosis features as intracellular fat accumulation while pancreatic steatosis is histologically visualized by an increased number of adipocytes so called fatty infiltration (Feldman et al., 2016). However, intracellular fat accumulation can occur in the pancreas via the mechanism of fatty replacement resulting in acinar cell degeneration/necrosis (Feldman et al., 2016). Both features were mainly found in the pancreas of the rats in this study. For fatty infiltration, it is unlikely to have any significant importance as a similar feature was detected in all rat groups and cohorts, though highly variable.

Acinar degeneration or necrosis is a pathological feature found in pancreatitis which can be aggravated in rats fed a high fat diet by the TLR4 pathway (Hong et al., 2020). In humans, pancreatitis rising from metabolic conditions is less common when compared with those from alcohol and gallstones however the episodes in cases of metabolic pancreatitis are likely to be more serious and need careful evaluation to prevent life-threatening bouts (Kota et al., 2013). The finding of acinar degeneration/necrosis in this study was consistent in the long term rats but there was no trend observed relating it to diet or OVX. On the other hand, no rats in the short term cohort had this lesion. It is possible that perhaps aged rats had an impairment of their digestive function especially with fat due to the abnormality of exocrine glands in the pancreas. Thus, we postulate that this pathological change may have had some influence on the lipid metabolic dysregulation in the rats.

NAFLD is the characteristic of chronic liver disease found in obesity, insulin resistance and metabolic syndrome (Bedossa et al., 2012). This pathological feature is associated with anthropometric measurements, triglycerides, serum glutamic pyruvic transaminase (SGPT) and serum glutamic oxaloacetic transaminase (SGOT) levels in humans (Patell et al., 2014). A high fat/cholesterol diet can cause the development of

NAFLD in clinical and preclinical studies (Puri et al., 2007; Mells et al., 2015) and could as well in our study. Several clinical studies revealed that patients with NAFLD had a significant increase in blood glucose levels and blood lipid profile (triglyceride, total cholesterol and LDL) (Mahaling et al., 2013; Sookoian & Pirola, 2017) and also in animals (Liu et al., 2016). However, Jensen et al. (2018) study giving Sprague-Darley rats a 16-week high fat diet showed no increase in plasma triglycerides and cholesterol but increased triglycerides and cholesterol were found only in the liver. This means that the circulatory lipids profile might not be a representative parameter for predicting the accumulation of ectopic fat or NAFLD in obese subjects. Although the dysregulation of lipid metabolism in this rat study was detected, some conflicting data still exist. For example, plasma cholesterol was increased in the OVX rats when compared to sham rats which corroborates evidence from postmenopausal women (Ambikairajah et al., 2019) or other OVX-rat studies (Nuttall et al., 1998; Kwon et al., 2008). However, all plasma lipids in this study (triglyceride, cholesterol and HDL) were reduced by the HFHS diet even though HFHS and OVX increased BW and the proportion of NAFLD rats. The alteration in plasma lipid levels cannot be explained solely by the relationship with BW or NAFLD features. We speculate that the result might be compromised by many factors such as the co-occurrence of pancreatitis and the alteration of gut microbiota.

According to the results of the gut bacterial profile, even though there were no significant differences in total bacteria between groups of rats from both cohorts, the abundance of gut microbes was expected to be altered by HFHS due to the significant reduction in caecum and caecal contents weight in HFHS fed rats. Likewise, advanced age seemed to have an impact on the reduction of gut microbiota as mentioned in a previous study (Vemuri et al., 2019). Showing the reduction of beneficial *Lactobacillus* spp. consistently in relation to HFHS and older age could be a characteristic of dysbiosis which has been supported previously by solid evidence (Cani et al., 2012; Clarke et al., 2012; Galvao et al., 2018).

Another group of beneficial bacteria, *Bifidobacterium* spp. was decreased in HFHS fed rats of both cohorts. *Firmicutes* and *Bacteroides* are the most abundant bacteria in animal gut microbiota (Marchesi et al., 2016). The *Firmicutes/Bacteroides* ratio was confirmed as increased in a diet-induced obese rat model with the reduction in *Bifidobacterium spp*. when compared to the lean animals fed a control diet (Patrone et

al., 2012; Ravussin et al., 2012; Collins et al., 2015a). Our study also detected a reduction in *Bacteroides* spp. However, we did not measure the abundance of *Firmicutes*. In a recently reported study, consumption of HFHS not only altered gut bacteria but also changed gut barrier function due to the decrease in epithelial tight junction proteins (occludin) resulting in increased endotoxemia (Parolini, 2019). The increased endotoxemia could induce low-grade inflammation and metabolic disorders (Cani & Delzenne, 2011) via toll-like receptor activation (Shi et al., 2006) and the endocannabinoid system (Muccioli et al., 2010).

Akkermansia muciniphila is a gram negative, anaerobic bacterium found in the gastrointestinal tract of humans and in a number of animal species. It has the ability of utilizing mucin in gut lining as its energy source (Derrien et al., 2004). Many research studies have revealed a beneficial association with *Akkermansia muciniphila* in protecting against obesity, diabetes and metabolic syndrome (Everard et al., 2013; Caesar et al., 2015; Dao et al., 2016). Its abundance was reduced in obese, diabetic and inflammatory bowel disease patients (Cani & de Vos, 2017) and also high fat diet-induced obese and diabetic mice (Everard et al., 2014; Schneeberger et al., 2015; Leal-Díaz et al., 2016; Ojo et al., 2016). Similar to our results from the short term cohort, both HFHS groups (HFHS, HFHS+GSM) had a reduction of *Akkermansia muciniphila* abundance when compared to their diet counterpart, however, this pattern failed to be recognized in the long term rats. Another controversial issue about this microbe is that its abundance increased during aging of the long term cohort while other studies reported a reduction in colonic luminal content during aging in mice (Langille et al., 2014; van der Lugt et al., 2018) and humans (Biagi et al., 2010). However, the same research group later found that its abundance increased in an extreme old age (Biagi et al., 2016). Everard et al. (2014) also showed variable responses of this microbe between different types of diet and models. Therefore, the alteration of *Akkermansia muciniphila* depends on a very intimate relationship with host physiology and diet which is not yet completely understood.

The total amount of bacteria in the gut was not reduced by HFHS but the content of both *Lactobacillus acidophilus* and *Bifidobacterium* spp. was significantly lower while *Akkermansia muciniphila* and *Bacteroides* spp. unchanged. This indicated that other gut bacteria which had not been measured in this study may relatively increase. It is possible that the ratio of *Firmicutes* including *Clostridium coccoide*, *Clostridium*

leptum, *Clostridium clusters XI* and *I*, *Roseburia* spp., *Lactobacillus* spp. may relatively increase in HFHS (Cani et al., 2012; Collin et al., 2015). In addition, the HFHS diet created a specific inflammatory environment in the gut, correlated with an overgrowth of pro-inflammatory *Proteobacteria* such as *Escherichia. coli* (Clarke et al., 2012; Agus et al., 2016).

There is a lack of scientific evidence supporting the impact of GSM on gut microbiota. To date, only one clinical study investigated the relationship of GSM with gut microbes in patients with knee osteoarthritis. Those results showed no significant differences in gut bacteria abundance between the baseline and 12 weeks of GSM administration (3 g/day) however, there was a trend of *Clostridia* spp. reduction which was related to the improvement of gastrointestinal symptom scores and osteoarthritis symptoms (Coulson et al., 2013). This demonstrates the potential for GSM to alter the gut microbial profile in humans. While we did not measure *Clostridia*, our study showed that GSM consistently reduced *Akkermansia muciniphila* abundance in both cohorts. Despite the lack of GSM association with gut microbiota, omega-3 fatty acid in fish oil, which is also prevalent in GSM, has been shown to promote beneficial bacteria such as *Lactobacillus* and *Bifidobacterium* spp. (Ghosh et al., 2013) but to decrease *Helicobacter*, *Clostridiales bacterium*, *Sphingomonadales bacterium*, *Pseudomonas spp*. and *Firmicutes* in rodent models (Yu et al., 2014). In addition, fish oil increased *Akkermansia muciniphila* abundance resulting in a reduction of gut inflammation (David et al., 2014; Derrien et al., 2017). On the contrary, Pusceddu et al. (2015) showed *Akkermansia muciniphila* was dose dependently reduced by EPA/DHA treatment in female rats. Similarly Noriega et al. (2016) reported a case of *Akkermansia muciniphila* reduction in human after 2 weeks of an omega-3 rich diet. Another controversial issue is that *Akkermansia muciniphila* had a negative correlation with propionic acid in the short term rats fed ND. In fact, *Akkermansia muciniphila* should rather have had a correlation with butyric acid as it is a butyrate-producing bacterium and butyrate increased mucin production (Lee et al., 2018). Cani and de Vos (2017) revealed that mucus layer thickness in the gastrointestinal tract lining is a mechanism of gut barrier function which can prevent endotoxemia and metabolic disorders. Hence, increases of *Akkermansia muciniphila* could be beneficial for MetS prevention. Therefore, due to the conflicting data no conclusion can be made whether the reduction of *Akkermansia muciniphila* by GSM effect is beneficial or possibly caused

deterioration in the rats' health. No improvement in blood glucose levels or hepatic steatosis in HFHS rats with GSM could be detected. The relationship between GSM and gut microbes needs further investigation to confirm how GSM may affect the gut microbiota.

In conclusion, this study showed that GSM had some impact on changing the gut bacteria composition resulting in the relative reduction of *Akkermansia muciniphila* however this change had no positive effect on the signs of MetS.

Chapter 8: Discussion

MetOA, a complex subtype of OA, is frequently found in obese people and associated with the presence of hyperglycemia, dyslipidemia, and hypertension. The etiology and pathogenesis of MetOA is not completely understood. It has been hypothesized that the initial pathogenesis of this form of OA arises in subchondral bone area rather than from the surface of articular cartilage as other OA phenotypes (Zhuo et al., 2012). Due to the complex nature of the disease and the difficulty in obtaining an early diagnosis, an increase in the prevalence of contributing health factors such as obesity for several decades, and better diagnostic mechanisms having been recently developed, the prevalence of MetOA is increasing worldwide. This study addressed the potential of reducing MetOA incidence using a nutritional approach employing greenshell mussel. Therefore, for the study *in vitro* assays were conducted using a murine macrophage cell line RAW264.7, in an osteoclast differentiation assay to explore the effect of GSM on the pathological pathways which theoretically have linkages between osteoarthritis and bone health. GSM was furthermore tested in a diet-induced obese rat model; the model in rats and mice recently has been developed and is now wildly use for osteoarthritis research (Collins et al., 2016; Jiang et al., 2020; Koboziev et al., 2020; Friedman et al., 2021).

In addition, the study model also evaluated possible predisposing causes of MetOA and determined that of the factors assessed, age, HFHS, and OVX were the most significant contributors to the development of the disease. Taken together, the data collected from the animal model and in vitro work demonstrated that GSM has protective benefits in bone and joint health and may reduce MetOA development or progression.

8.1 Anti-osteoclastogenesis of GSM lipids

Bone remodeling is a homeostasis mechanism of bone, responsible to endocrine and physical functions in tandem. The equilibrium of osteoblast-mediated bone formation and osteoclast-mediated bone resorption secures bone integrity but excessive osteoclast activity causes deterioration in bone strength, leading to skeletal and mobility disorders (Bertuglia et al., 2016; Chen et al., 2018). Osteoclast differentiation is driven

by RANKL/OPG levels in the bone microenvironment. It is known that osteoblasts regulate the recruitment and activity of osteoclasts through the expression of RANKL and OPG. RANKL is expressed on the osteoblast/ stromal cell surface and binds to a specific receptor (RANK) on the surface of hematopoietic precursor cells to stimulate osteoclast differentiation and maturation in the presence of macrophage colony stimulation factor (M-CSF). OPG, a decoy receptor secreted by osteoblasts, binds RANKL to prevent the activation of RANK and, therefore, to prevent osteoclast differentiation and activation (Cao, 2011). RANKL secreted by osteoblasts directly binds to the RANK receptor on osteoclast precursor cells and initiates the signaling cascade via TRAF6 to activate NFκB and finally stimulate NFATc1 (Boyce et al., 2015). Both pro-inflammatory cytokines, IL-6 and TNF-α can activate RANKL expression in osteoblasts via TLR4 receptors (Campos et al., 2012) and leptin also indirectly manipulates osteoclast differentiation by activating macrophage proliferation, phagocytosis, NK cells and upregulates TNF-α, IL-6, and IL-12 production (Azamar-Llamas et al., 2017). These mediators are related to low-grade inflammation possibly induced by metabolic syndrome. It is also connected to menopause. Lack of estrogen in post-menopausal women results in the expansion of adiposity which highly correlates to increased plasma leptin. Moreover, estradiol has been shown to inhibit IL-6 production *in vitro*, and loss of estrogen by ovariectomy enhanced the number of colony-forming units for granulocytes and macrophages, resulting in an increased osteoclast number in trabecular bone (Jilka et al., 1992). This indicates that osteoclasts numbers may be affected by menopause, potentially distributing to bone-associated diseases and OA; this is discussed in section 8.3.

This *in vitro* study investigated the effect of different fractions of GSM lipids on osteoclast differentiation. The parent fraction of GSM lipid was further separated into polar lipids and non-polar lipids in which the majority of different lipid compositions were triacylglycerol and free fatty acids. A previous study using GSM oil showed anti-inflammatory properties (Whitehouse et al., 1997; McPhee et al., 2007; Treschow et al., 2007; Singh et al., 2008) and similar effect was also revealed with omega-3, especially EPA and DHA (Knott et al., 2011; Komprda, 2012). McPhee et al. (2007) demonstrated that the increased amount of free fatty acids by hydrolysis of triglycerides from GSM oil enhanced the inhibition of the cyclooxygenase activity. The non-polar lipid was rich in free fatty acids and potentially contains higher amounts of omega-3 in free form when

compared with the polar lipid which highly contains triglycerides. Therefore, we postulated that the most active compound in GSM lipid would be PUFA in free form. Although the specific fatty acid had never been tested in this study, it is possible that EPA and DHA may partially involve with this response as these fatty acids are rich in GSM oil and have shown the anti-osteoclastogenic activity (Rahman et al., 2008; Boeyens et al, 2014; Kim et al, 2017; Kasonga et al., 2019). The results showed that the amount of TRAP enzyme and the numbers of TRAP positive cells were significantly reduced by the non-polar lipid fraction and partially reduced by the total lipid fraction at the highest concentration, the latter being relative to the different proportions of non-polar and free fatty acids in its lipid compositions. The property of non-polar lipids to control the actin ring formation is crucial in preventing excessive osteoclast activity. The osteoclast need to adhere to the bone matrix in order to initiate the bone digestive process followed by the release of digestive enzymes (CAII, cathepsin-K and MMP-9) into the pit formed under the osteoclast. The excessive osteoclast activity was mitigated by the non-polar lipid similar to DHA (Boeyens et al., 2014). However, the actual performance of bone resorptive osteoclasts could be measured by the capability of excavating bone matrix which is accessible by resorptive pit formation assay on a bone slide. This assay may be of interesting further studies.

Despite the fact that the high proportion of phospholipids in the polar lipid failed to exhibit the inhibitory effect on this osteoclast differentiation assay, it is still not conclusive whether phospholipids in GSM oil are not bioactives. The difference of their chemical forms between natural and biologically digested form should be considered and a comparison of those should be performed in another experiment to warrant the conclusion.

8.2 Bone mass accrual due to GSM supplementation

The animal study showed that HFHS increased rat's body weights because HFHS provided more kilojoules per gram than the normal diet to rats even though the total feed intake volume of ND groups was higher when compared with HFHS groups. Under the age of 28 weeks, most of bodyweight gain was lean mass especially in ND rats but at the end of the long term cohort (48 weeks old), fat mass was the main portion of weight increase in both ND and HFHS rats. The increased adiposity in the rats generally was attributed to visceral fat (retroperitoneal and perigonadal fat) however in OVX rats fed HFHS which was the most obese group, the acceleration of inguinal fat was more

pronounced than in the sham rats fed the same diet. Moreover, plasma leptin levels showed a highly positive correlation with fat mass as the majority of circulating leptin is produced by fat tissues especially visceral fat (Large et al., 2004). There may be significant differences in bodyweight gain and fat distribution between female and male rats where male rats gain more weight rapidly when compared to the same age and probably attains a higher weight at the end (Collins et al., 2015a).

This chapter had addressed one of the ambiguous issues called the obesity paradox, the controversial relationship between obesity and bone mass. The notion was postulated that obesity can have benefits by increasing bone mineral density (Zhao et al., 2008; Sornay-Rendu et al., 2013; Evans et al., 2015; Yang & Shen, 2015). The result of the current study revealed that the obese rats (HFHS fed rats) with intact ovaries did not show any differences in BMD at any bone sites when compared to the lean rats of the same condition (ND fed rats). However, due to OVX, HFHS rats lost less of their lumbar spine BMD compared to the ND rats. This evidence partly rejects the aforementioned hypothesis but, if extrapolated specifically to postmenopausal women, supports the theory that the expansion of adipocytes in obesity provides an alternative source of estrogen which may have benefits by reducing the rate of bone resorption that is observed after estrogen loss (Rosen & Klibanski, 2009).

The GSM powder contained high amounts of EPA and DHA and inclusion of GSM resulted in an enrichment of those fatty acids into the control diet. Surprisingly, measurement of the fatty acid levels in the diet samples showed that HSHF+GSM had EPA and DHA concentrations three times lower than ND+GSM. The reason might be that the diet samples were prepared and kept in a freezer through the end of the study before analysis. The fatty acids may have been oxidized more rapidly in the HFHS than ND possibly due to the presence of saturated fat in form of lard, which oxidises rapidly. This was an unanticipated finding and, in retrospect, it would have been of interest to collect samples from each diet type on a monthly basis and test the levels of individual fatty acids. However, rats fed these different diets would have acquired similar levels of these fatty acids as the pre-made ND and HSFH diets were freshly mixed with GSM powder for feeding every couple of days and all diets were kept frozen immediately after they were prepared.

Interestingly, inclusion of GSM in the diets resulted in increased BMD of the femur in the short term rats. The increased BMD may be due to the anti-

osteoclastogenesis activity of GSM oil observed in the *in vitro* study, reducing more bone mineral resorption and bone turnover in the rats. Alternatively, DHA and EPA can enhance calcium absorption in duodenum (Haag et al., 2003) and thus the GSM may have elevated calcium store in the rats. In addition, the mineral content in GSM may also contribute more calcium supply for the rats although all diets were calcium-replete. After ovariectomy, rats increased BW rapidly which could be attributed to lean mass within the first 8 weeks however most of the bodyweight gain later was fat mass as can be seen at the end of the study. The post-OVX decrease in estrogen correlated with increased adiposity in the rats and with reduced BMD in the lumbar spine and the femurs; it is known that estrogen regulates appetite and satiety, fat metabolism, and energy utilization (Lizcano & Guzmán, 2014). Estrogen also controls blood calcium levels by bone resorption via upregulating TGF-β to inhibit osteoclast activity (Riggs, 2000) and inhibiting the expression of RANKL (Streicher et al., 2017).

Despite the inhibitory effects of the GSM oil on osteoclast differentiation in cell culture, adding GSM powder in the rat diets failed to significantly reduce bone loss in the OVX rats. In other words, the effect of GSM on bone loss could not counteract the effect of estrogen loss and there are many explanations relating to this issue. It is known that bone health relies on various factors including age, hormones, physical activity, nutrition, and body physiological systems. Bone homeostasis is important to maintain the proper function and strength of bone structure and this is mediated by bone-resorbing osteoclasts and bone-formation osteoblasts (Li et al., 2013). Our *in vitro* study only revealed in one part of the bone resorption process but the bone formation, a crucial role on bone heath, have not been investigated yet. It is possible that if GSM oil had a negative effect on bone formation, then it would compromise the result of this study.

Estrogen plays an important role in bone growth and maturation as well as in the regulation of bone turnover in adult bone. Estrogen has influence on both arms of bone homeostasis. On one arm, it inhibits osteoclast differentiation by inducing osteoclast apoptosis, blocking RANKL/M-CSF-induced activator protein-1-dependent transcription through a reduction of c-jun activity, and suppressing RANKL expression on osteoblasts (Khosla et al, 2012). The results could limit the bone resorption activity. On the other arm, estrogen has been shown to inhibit osteoblast apoptosis by activating the Src/Shc/ERK signaling pathway (Kousteni et al., 2001) and downregulation of JNK,

which alters the activity of a number of transcription factors, including Elk-1, CCAAT enhancer binding protein-β (C/EBPβ), cyclic adenosine monophosphate-response element binding protein (CREB), and c-Jun/cFos (Kousteni et al., 2003). Therefore, estrogen deficiency causes the excessive osteoclast activity and reduces bone formation. Loss of BMD at all bone sites in this animal study should be attributed to both processes and also the various factors mentioned above; however, the *in vitro* study only revealed the inhibitory effect of GSM oil on osteoclasts. Hence, the effect of GSM oil in the rat diets may not be efficient to prevent bone loss from reduced bone formation. In addition, the abrupt loss of estrogen due to ovariectomy in our experiment could have a severe effect on bone loss and thus the mild therapeutic effect of GSM may not be able to deter the consequence of estrogen loss. Moreover, it is possible that the free fatty acids in GSM diets may not reach the effective concentration of the GSM oil at bone tissue as indicated in the *in vitro* study. The amount of the GSM powder included in the rat diet was adequate for providing n-3LCPUFAs as a daily dose recommended in humans; however, the high metabolic rate of rats may accelerate elimination resulting in reduced peak concentrations of the GSM active compounds in blood stream. Thus, the measurement of the bioactives distribution should be monitored in future studies to ensure that the minimum level of 3LCPUFAs can be reached in blood circulation and bone tissue.

8.3 Early signal of osteoarthritis prevention

Early detection of MetOA is crucial to prevent progressive cartilage erosion but the lack of correlation between clinical signs and joint pathological lesions has hampered the early diagnosis of patients. Thus, a specific biomarker for predicting early onset of the MetOA pathogenesis is of paramount importance. However, the pathogenesis of MetOA is still inconclusive; whether it is initiated at the cartilage surface or subchondral bone. One theory is that a group of endogenous proteins called alarmins arising from cartilage damage can activate joint inflammation via various receptors (Oppenheim & Yang, 2005). Another notion proposes that increased bone remodeling in subchondral bone and changed microarchitecture in this area introduce inflammatory mediators to the cartilage layer leading to cartilage damage (Goldring & Goldring, 2016). The crosstalk communication between these layers is evident (Lajeunesse & Reboul, 2003; Bellido et al., 2010) and pathological lesions such as

osteophyte formation, bone remodeling, subchondral sclerosis, and attrition can be detected before cartilage degradation is detected (Intema et al., 2010).

The short term cohort, fed for 14 weeks, focused on this early event of MetOA, whereas the long term cohort, fed 36 weeks, focused on later events, in order to assess the effects of whole GSM on two stages of MetOA progression. A study (Collins et al., 2015a) using male rats in a diet-induced obesity model for 28 weeks reported more severe pathological features compared to our study including severe obesity, obvious cartilage destruction, and high concentrations of pro-inflammatory cytokines in both blood and synovial fluid. This study fed rats with a diet containing a higher concentration of fat. Therefore, the difference with the Collins trial may be due to testosterone in male rats combined with a higher-energy diet, both of which would influence progression and severity of MetOA (Ma et al., 2007). Our studies using female rats and a diet with less fat than the Collins group used, may have slowed the rate of progression of joint disease by comparison. However, the model of this study and the two time points selected were sufficient to provide evidence of GSM both before and after frank joint damage was visible.

Plasma pro-inflammatory cytokines (TNF-α, IL-6, IL-1β, and IL-10) in the present study were present in low concentrations with no significant difference between groups which is similar to a study done by Collins et al. (2015a). On the contrary, plasma leptin was increased significantly in rats fed HFHS and had a positive correlation with BW. In fact, it was highly correlated with fat mass rather than lean mass as leptin is produced by adipocytes, especially white adipocytes, that contribute the most to leptin in blood circulation (Large et al., 2004). Leptin is an initiator for systemic and local inflammation in obesity. Leptin activates toll-like receptor 4 (TLR-4) on innate immune cells such as macrophages and natural killer (NK) cells, resulting in an upregulation of cell proliferation, phagocytosis function, and production of TNF-α, IL-6, IL-1β, and IL-12 (Azamar-Llamas et al., 2017). The increases of those pro-inflammatory cytokines cause upregulation of RANKL expression in osteoblasts (Campos et al., 2012) which eventually induces excessive osteoclast activity (Tamura et al., 1993; Jilka et al., 1992). Although there was no evidence of pro-inflammatory cytokines to support systemic low-grade inflammation in this rat study, many chronic diseases caused by low-grade inflammation such as rheumatoid arthritis, inflammatory bowel disease, atopic dermatitis, psoriasis, and asthma also have been revealed to have

an absence or minimum concentrations of those markers (Calder et al., 2013), although they may be present in synovial fluid. In addition, elderly people who were expected to have low-grade inflammation did not have increased serum inflammatory marker levels but rather an increase in the production of IL-1β, IL-6, and TNF-α in *ex vivo* culture by mononuclear white blood cells activated with phytohemagglutinin (PHA) plus phorbol myristate acetate (PMA) (Fagiolo et al., 1993; Pietschmann et al., 2003). Thus, low-grade chronic inflammation may not be reflected by changes in serum pro-inflammatory cytokines, but may instead demonstrate changes in discrete microenvironments both in cell function and soluble factors. In the current study, we could not conclusively demonstrate that low-grade inflammation was successfully established, although the elevation of leptin and plasma glucose indicates probable initiation of a metabolic disorder.

Despite the fact that most of the knee joints in the short term rats appeared histologically normal, plasma CTX-II, which is the degradation product of type-II collagen of articular cartilage, was increased in HFHS-fed rats by approximately 50% although this did not reach statistical significance. Interestingly this augmented CTX-II was significantly reduced in the HFHS-fed rats supplemented with GSM compared to HFHS alone. This finding provides further evidence that GSM can reduce the rate of degradation in cartilage metabolism and therefore may provide some protection against OA. The absence of changes in inflammatory markers suggests that the GSM's effects may be localized to the joint microenvironment. There was evidence indicating that circulatory CTX-II detection is sensitive and thus measurable levels can likely be identified prior to a cartilage lesion being detectable histologically. This is supported by a study using a papain-induced osteoarthritis rat model, in which a significant increase of serum CTX-II was detected within a day after inducing papain into the knee joints; CTX-II plateaued at week 2 and remained constant until the study concluded at week 4 (Khan et al., 2014). Similarly, Murat et al. (2007) also used the papain model and observed that CTX-II increased within 1 week, but significant changes in the Mankin scores of the knee joints did not occur until week 4. Thus, in the rat there is consensus that CTX-II increases significantly prior to the cartilage lesion becoming explicit. It may be possible to confirm the protective effect of GSM on cartilage using chondrocyte explant culture models. An *in vitro* model revealed the explant chondrocyte triggered by pro-inflammatory cytokines released high amount of CTX-II in culture media (Caterall

et al., 2013). Testing with this model may provide a clear cut view of the cartilaginous protective effect of GSM.

The results of rats in this short term cohort showed promising effects of GSM on OA prevention and also corroborates previous animal studies using GSM oils in a chemical-induced arthritis model (Whitehouse et al., 1997). However, it remains inconclusive whether this initial OA prevention could be attributed to anti-inflammatory property or anti-osteoclastogenesis which was for the first time reported for GSM in our study. This context will be discussed in the next section.

8.4 Preventive effects of GSM against osteoarthritis

The development of MetOA in humans is a chronic deterioration process and involves multiple causes. The short-term rat study provided significant information about reduced CTX-II in GSM-fed rats which is promising for early and mild OA prevention. The long term cohort was to evaluate if GSM could protect against a more severe OA in postmenopausal women and simultaneously, if estrogen deficiency affects the development of OA.

The result revealed that both ovariectomy and HFHS had cumulative effects on BW increase which was highly correlated with plasma leptin levels and leptin gene expression in perigonadal fat but ovariectomy independently caused increases of adiponectin and MCP-1. In addition, OVX also had more impact on the rats' hyperglycaemia than HFHS. However, the development of OA in Sprague-Dawley rats was not a single factor of estrogen deficiency; it depended on multiple factors including age, HFHS, and OVX to damaged articular cartilage structure as can be seen in the knee joint scores. Therefore, a multiple phenotype of OA is considered to be afflicting the rats in this study.

There has been a controversy about circulatory levels and inflammatory effects of adiponectin in obesity (Stofkova, 2009). Our study revealed that adiponectin was less sensitive in responding to the increased BW or body fat but ovariectomy significantly elevated adiponectin. Increased adiponectin can result in inducing NOS2, IL-6, MMP-3, MMP-9 and MCP-1 expression in chondrocytes (Lago et al., 2008) which corroborates with our result of increased MCP-1 in plasma. Therefore, this study postulates that adiponectin may behave as an inflammatory mediator rather than anti-inflammatory and activates MCP-1.

MCP-1, a chemokine produced by adipocytes, macrophages, and endothelial cells, can regulate macrophage polarization and infiltration, insulin sensitivity and lipid metabolism (Nio et al., 2012). Hence, it causes local inflammation involved in arteriosclerosis and coronary heart disease (Kanda et al., 2006) and may play a role in osteoarthritis as its presence is strongly correlated with this disorder. Interestingly, plasma MCP-1 theoretically is associated with adiposity (Kouyama et al., 2007) but our data revealed that MCP-1 was modified by the effect of ovariectomy, not obesity. The male rats in Collins et al. (2015a) study gained even more weight than our female rats, but no change in plasma MCP-1 levels was detected. This evidence is perhaps pointing out that MCP-1 is distinctly different in the female and might be a crucial modulator of MetOA in post-menopausal women; if so, then it could be used as a biomarker to diagnose or monitor disease progression in this population. It may also be of interest to determine whether drugs that target MCP-1 are more potent against this specific OA phenotype.

Similar to our study, in the male rat study (Collins et al., 2015a) the pro-inflammatory cytokines in the blood circulation were not elevated in diet-induced obese rats when compared to normal control rats. Most of the inflammatory markers increased in the obese rats' plasma were chemokines. However, most of pro-inflammatory cytokines were found to be significantly increased in the synovial fluid of the rat knee joints. Our study on the other hand detected extremely low to undetectable concentrations of pro-inflammatory cytokines in PBS-lavage synovial fluids of all knee joints (data not shown). This might be because of the high dilution factor of PBS in the procedure, as collection of synovial fluid from rat knees is a very technically challenging and imprecise procedure. However, we cannot rule out that the cytokines were absent from the joint cavity. In addition, we could not detect the signs of joint effusion in any of the rat groups; so exacerbated inflammation events in the joint cavity were not expected

Another hypothesis is that the pathogenesis of cartilage lesions due to metabolic syndrome in this study was activated from inside out because of the excessive osteoclast activity in the subchondral bone area. The DXA scans from all bone sites that were measured also revealed a decline of bone mineral density in OVX rats. If osteoclasts were involved with the early pathogenesis of MetOA in this study then the reduction of the knee pathological scores in OVX-rat-fed HFHS due to inclusion of GSM

theoretically could be attributed to its anti-osteoclastogenesis activity as supported by the *in vitro* study and the increase in BMD in the short term rats. However, this study was not able to identify osteoclasts in subchondral bone area. Our histopathological slides of the knee joints were stained with safranin-O which is sufficient for examining cartilage. To investigate the modification of osteoclast activity in the knee joints, it was needed to stain for the TRAP enzyme in osteoclasts and use immunohistochemistry to assess the concentration and movement of proteins involving in osteoclast differentiation and functions such as RANKL, OPG, MMP-9, Cathepsin K etc. In addition, data from microCT scans of the knee joints could provide the three dimensional structure in subchondral bone area and especially, quantifying the bone matrix in that specific region, providing solid evidence.

Interestingly, plasma concentrations of CTX-II, the cartilage degradation marker, did not correlate with the pathological changes in knee joints in the long term rats. In a matching study, we did detect a significant increase of CTX-II in younger rats correlating with obesity and the initiation of Met-OA. A similar study showed that serum CTX-II dramatically increased in OVX rats within 3 weeks of surgery, then declined to the baseline level six weeks after OVX (Oestergaard et al., 2006). Likewise, Høegh-Andersen et al. (2004) monitored serum CTX-II in 5-month-old ovariectomised rats and found that CTX-II transiently increased by approximately 50% within 2 weeks after surgery and then declined afterwards to 50% below baseline at week 8. CTX-II in the sham rats also declined to the same level of the OVX rats. This indicates that the sensitivity of serum CTX-II as a cartilage marker is of less value in rats older than 6 months. This ambiguity is likely due to the limitation of the model, as mature rats retain growth plate function. Therefore, we conclude that the CTX-II data in the short-term cohort rats in this study correctly demonstrated a significant protective effect of GSM; however, the lack of effect of GSM on CTX-II in the long-term cohort cannot reliably be interpreted to mean that GSM was ineffective. To carry out future long-term studies in animal models with CTX-II being a primary outcome, it would be advisable to use a different species that does not present this confounding factor.

8.5 Influence of GSM on gut microbes

Microbes in gastrointestinal tracts have an important role in an animal's digestive system and other physiological functions (Marchesi et al., 2016). The gut ecosystem and composition are associated with diet and can be linked to many diseases including

obesity, T2D, cancer, metabolic syndrome, and osteoarthritis (Turnbaugh et al., 2006; Collins et al., 2015b; Sun & Kato, 2016; Berthelot et al., 2019). A growing body of evidence reveals that modulation of gut microbes showed improvement of metabolic syndrome (Lee et al., 2018), bone loss (Ohlsson et al., 2014) and osteoarthritis (So et al., 2011). To understand the influence of gut microbes on the development of diseases and preventive effect of GSM in this study therefore, caecal contents of the rats were collected at the end of the study and some beneficial bacteria were evaluated.

The result of our rat model is similar to other studies in which HSHS-fed rats increased bodyweight, adiposity, plasma glucose levels in association with a reduction of the beneficial bacteria *Lactobacillus acidophilus* and *Bifidobacterium* spp. (Ley et al., 2005; Patrone et al., 2012; Ravussin et al., 2012). Reduction of the beneficial bacterial composition was relative to an increase in endotoxin-producing bacteria. This can activate low-grade inflammation and metabolic disorders by disrupting the gut barrier function and the activation of TLR-4 by LPS (Cani & Delzenne, 2011). Furthermore, the change in gut microbiota composition or gut dysbiosis can cause hepatic steatosis (non-alcoholic fatty liver diseases) which is related to obesity, T2D, and MetS. The increase of *Fimicutes/Bacteroides* ratio and *Escherichia coli* were evident as a gut microbiome signature for this pathological feature, (Grabherr et al., 2019; Jasirwan et al., 2019). The occurrence of hepatic steatosis in this study was explicit in rats on HFHS and even more pronounced in longer feeding and in OVX rats. However, our data are not available to relate this pathological feature to the particular gut microbiome signature but this striking evidence can confirm the existence of MetS in our rats.

There is evidence showing that *Lactobacillus* spp. are associated with decreased bone resorption via reducing TRAP5 and RANKL, and increasing OPG expression and BMD in OVX rodents (Rodrigues et al., 2012; Britton et al., 2014; Ohlsson et al., 2014). However, the OVX rats in our study did not have altered *Lactobacillus acidophilus* abundance but altered *Bifidobacterium* instead. Feeding GSM increased bone mineral density in femurs in the short term cohort but there was no significant change in *Lactobacillus acidophilus* in the rats. Therefore, evidence is still lacking to support the relationship of *Lactobacillus acidophilus* with bone health.

The relationship between gut microbes and OA has been revealed in an arthritis rat model which showed that *Lactobacillus. casei* reduced pain, cartilage destruction, and lymphocyte infiltration (So et al., 2011). Some studies proposed that particular

bacteria directly activate OA such as *Streptococococus* spp. (Boer et al., 2019) and *Mycoplasma synoviae* in chicken (Dušanić et al., 2009). As the OA in this rat study was based on a multiple phenotype in which its pathogenesis was compromised by various factors, it is difficult to measure the direct influence of gut bacteria on OA development.

Despite the lack of a strong relationship of gut microbes with the pathological changes in rats, adding GSM into the diet resulted in the significant reduction of *Akkermansia muciniphila* and this change had an inverse correlation with propionic acid. *Akkermansia muciniphila* has been recognized as a beneficial bacterium. Its abundance was reduced in obese, diabetic and inflammatory bowel disease patients (Cani & de Vos, 2017) and also high fat diet-induced obese and diabetic mice (Everard et al., 2014; Schneeberger et al., 2015; Ojo et al., 2016). On the contrary, our result showed it was increased by the effect of HFHS. To date, there was only one clinical study showing a mild relationship of GSM with gut microbiota, specifically with the reduction of *Clostridia* spp. (Coulson et al., 2013). Our study revealed a significant effect of GSM on *Akkermansia muciniphila* but lacks corroboration. The ambiguity in gut microbiota warrants further intensive investigation.

Table 8.1 shows a summary of the main findings in this study. To sum up, the study found that the non-polar lipid fraction of GSM lipids exerted anti-osteoclastogenesis in osteoclast differentiation assay which can reduce excessive bone resorption. This property may be involved with the increase of femur BMD in the short term rats and the protective effects on OA induced by metabolic syndrome. However, GSM powder did not improve any metabolic profiles in the rats, given the notion that the preventive effects of GSM on OA was not exhibited solely by its anti-inflammatory activity but also the anti-osteoclastogenesis which could mitigate or retard the early pathogenesis in subchondral bone area due to the bone-resorptive osteoclasts. In relation to gut microbiota, the results showed that the alteration of gut microbiota mostly depended on diet, for instance, HFHS reduced beneficial bacteria (*Lactobacillus acidophilus* and *Bifidobacterium* spp.) and GSM reduced the proportion of *Akkermansia muciniphila* in caecal contents. However, there is lack of evidence to support the specific relation of gut microbiota to particular diseases. The influence of GSM on gut microbiota needs more research done to provide further insights. . Finally, this animal model revealed that MCP-1 might be useful as a biomarker to detect MetOA in post-menopausal women.

8.6 Conclusion

To sum up based on the two objectives of this thesis; the hypothesis is that omega-3 fatty acid in GSM could exert an anti-inflammatory activity to prevent MetOA in rats in which chronic low-grade inflammation may initiate the pathological mechanism through bone remodeling in subchondral bone area. This study demonstrates that GSM may alleviate MetOA in rats by showing the reduction of severity in knee joint pathology. The main bioactives or the therapeutic actions of GSM are not clearly defined although many studies postulated that n-3 LC-PUFAs especially DHA and EPA in GSM exert the anti-inflammatory activity. However, the results of this study were unable to strongly support or reject evidence of previous studies or our hypothesis. The MetOA rats in this study presented with obvious MetS criteria including increased plasma adipokines (leptin and adiponectin), elevation of plasma MCP-1, dysregulation of glucose and lipid metabolism, and gut dysbiosis; however we could not detect the critical mediators of inflammation status, pro-inflammatory cytokines, in blood circulation or knee joint of the rats.

It is possible that the nature of low-grade inflammation leading to MetS itself is variable, irregular or present in very low concentrations as which the sensitivity of the assay kits used in this study was out of that limit. The other significant inflammatory marker, MCP-1, was elevated in the rats that underwent ovariectomy but inclusion of GSM failed to reduce this marker in blood circulation. On one hand, this probably means that the anti-inflammatory activity of GSM did not affect the course of MetS; however, only one marker can not be a reliable representative for the state of low-grade inflammation in the whole body. It needs more evidence of other inflammatory markers before making further conclusions. On the other hand, the reduction of knee joint severity by inclusion of GSM in rat diet without association with the anti-inflammatory property may point out that besides GSM oil and especially n-3 LC-PUFAs exerting potent anti-inflammation, other elements in GSM meat such as proteins, carbohydrates and minerals may exert other bioactive functions to protect the rat knee joint from developing MetOA. Furthermore, if the absence of pro-inflammatory cytokines in blood circulation and synovial fluid are valid findings, it may partially explain the idea that the pathogenesis of MetOA is in fact developed from inside the subchondral bone layer, rather the arising from endogenous proteins called “alarmin” in the milieu of a joint

cavity. Thus, if this is correct, MetOA should be reviewed as a disease of bone and joints rather than the joint itself alone.

This study unravelled a new biological activity of GSM relating to this context using an osteoclast differentiation assay. Despite unidentified species of fatty acids, free fatty acids of non-polar lipid GSM can inhibit differentiation of macrophage cell lines into osteoclasts. Theoretically, the reduction of bone resorption may shift the balance of bone homeostasis and leads to a net increase of bone mass in animals. This can be seen in animals of the short term cohort as the young rats significantly increased the right femur BMD; however, the animal study used whole GSM meat while the in vitro study used GSM oil and therefore the effect on the increased BMD in rats may not solely be attributed to the GSM oil as proteins, minerals and other elements are possibly involved. However, the in vitro study revealed that at least one composition of GSM with a crucial mode of action may be responsible for the increase of BMD in those rats. Despite the effect of GSM on a slightly increased BMD in young animals, GSM failed to mitigate bone loss in OVX rats of the long term cohort. The findings reveals that consuming of GSM might not be beneficial to post-menopausal women on bone loss; however, the effect of GSM on increasing peak bone mass may beneficial to young subjects in adolescence as high peak bone mass in women shows reduced risks of osteoporosis for the future.

The results of this study also demonstrated that MetOA in female rats was not possible to be induced by a single factor but it was caused by multi-factorial factors including aging, obesity, and estrogen loss. As can be seen in the study, the long term rats fed HFHS became obese and metabolically abnormal but showed few changes of knee joint pathology. But with ovariectomy aggravating more weight gain, metabolic disorders and reduced bone mass resulted in the obvious OA lesions at knee joints. The model seems to reflect the OA situation in women. Certainly, aging, health decline, tissue deterioration and menopause are inevitable but it is diet, obesity and metabolic disorders are modifiable factors that can be controlled to hamper or delay the development of OA. This message is simple but crucial in social communications to inform the public. With factual and clear messaging, it should be possible to induce sufficient lifestyle changes that will result in reducing the rate of OA incidence globally.

There are also some limitations in this study. First of all, both the animal model and the in vitro model are relevant to OA studies; however to extrapolate the data from

these studies into the human context should be performed with awareness because of interspecies discrepancies including bone growth, fat distribution and characteristics of menopause. Ovary intact rats typically experience irregular estrous cycles (called estropause) at the age of 9-12 months but mature ovulatory follicles are possibly present in rats of that age (Koebele & Bimonte-Nelson, 2016). The ovariectomised rat model is not an identical condition to menopause in older women. The post-menopausal women have a long transitional period of sex hormone irregularity before having complete ovarian failure while the OVX rats have abrupt loss of sex hormone when they are in young age. Next, our in vitro model revealed only bone resorption activities of osteoclasts however, bone is regulated by both bone resorption and bone formation processes therefore it could be more accurately estimation if both processes were assessed.

Due to the wide scope of this study, it was less likely to address all relationships of those multifactorial factors with the pathological conditions. There are other interesting test assays and methods which were not performed in this study but that information may provide more insight of GSM's biological activities or better ideas of OA pathological mechanisms. CPR, one of the relevant markers indicating low-grade inflammation should be included in the inflammatory panel assay. Estrogen levels should be monitored in order to confirm the advantage of increased adiposity as an alternative source for estrogen in the OVX rats leading to increased BMD at the right femur. As for the decline of CTX-II levels in aged rats, it is not reliable to compare the data between different ages of rats, and therefore more than one cartilage marker should be considered such as COMP, aggrecan neoepitope, etc. Other species of laboratory animals which may represent similarity of epiphyseal plate closure as humans may be a better model choice. High sensitivity ELISA assays for pro-inflammatory and anti-inflammatory cytokines may increase the possibility of detecting those analytes; however, the obstacles of those cytokines are not only in very low concentrations but also highly variable and possibly changeable during the course of inflammation; therefore, it may not have much advantages of using those test kits which are expensive and time consuming. Measuring protein synthesis of those cytokines at cellular levels may provide more critical evidence of low-grade inflammation for further studies which should include the detection of cytokine mRNA in fat tissues, articular cartilage, synovial membrane, and liver. In addition, the event of oxidative stress should be

covered. Furthermore, despite the facts that bone mineral density is related to bone strength and that it has been used for predicting fracture in clinical practice,t BMD is not equivalent to bone strength as the strength also depends on microarchitecture of bone. Therefore, the mechanical testing on a particular bone site should be performed in parallel; otherwise a quantitative measurement of the microscopic structure of bone using microcomputed tomography can be an alternative. Tracking specific cells or markers relating to OA pathogenesis at knee joints could highlight the critical events and elucidate more about the pathological mechanism of MetOA.

Finally, the results of this study showed that GSM meat alleviated OA lesions without improving the metabolic conditions. Therefore, the anti-inflammatory property of GSM lipid may not have a direct effect on OA prevention but other components including proteins, carbohydrates or minerals may exert a different therapeutic action at local areas including cartilage, bone or joint surrounding tissues. The future animal studies could be designed for an acute induction of OA or include spontaneous models such as guinea pigs, and the different components of GSM meat should be tested to specify the compositions which are really effective.

Table 8.1 Result summary- The metabolic inducing factors cause a disease cluster and the preventive effects of GSM indicated

❶ = a mild and transient effect shown in the short term cohort but no effect in ovariectomised rats

❷ = reduction of sCTX-II in the short term cohort; inconclusive data in the long term cohort

NA = not assess; ? = inconclusive

			MetOA in rats		
			Age	HFHS	OVX
Effects	Obesity	**Increased bodyweight**			
		Lean mass	Yes	No	Yes (early onset)
		Fat mass	Yes	Yes	Yes (late onset)
	Bone loss	**Loss of bone mass**			
		Clinical levels (BMD)	No	No	Yes
		Cell levels (osteoclasts)	-	-	-
	Osteo-arthritis	Cartilage deterioration			
		Systemic levels (sCTX-II)	?	Yes (clinically significant)	?
		Macroscopic levels (increased histopathological lesions)	Yes (collective)	Yes (collective)	Yes (collective)
	Metabolic syndrome	**Low grade inflammation**			
		Systemic levels	↑Leptin	↑Leptin	↑ Leptin, adiponectin, MCP-1
		Local levels (synovial fluid)	?	?	?
		Dysregulation of glucose metabolism			
		Systemic levels	NA	↑glucose	↑ HbA1c
		Dysregulation of lipid metabolism			
		Systemic levels	NA	↓HDL	↑cholesterol
		Local levels (hepatosteatosis)	↑frequency	↑frequency	↑frequency
		Gut dysbiosis			
		Lactobacillus acidophilus	↓	↓	No
		Bifidobacterium spp.	No	↓	↓
		Akkermansia muciniphila	↑	No	No

❶ ❷ ↓

Preventive effects of GSM

References

Abdelhamid, A., Hooper, L., Sivakaran, R., Hayhoe, R. P. G., Welch, A., Abdelhamid, A., . . . Winstanley, L. (2019). The relationship between Omega-3, Omega-6 and total polyunsaturated fat and musculoskeletal health and functional status in adults: a systematic review and meta-analysis of RCTs. *Calcified Tissue International, 105*(4), 353-372.

Agus, A., Denizot, J., Thévenot, J., Martinez-Medina, M., Massier, S., Sauvanet, P., . . . Barnich, N. (2016). Western diet induces a shift in microbiota composition enhancing susceptibility to Adherent-Invasive E. coli infection and intestinal inflammation. *Scientific Reports, 6*, 19032-19032.

Al-Lahham, S. a. H., Peppelenbosch, M. P., Roelofsen, H., Vonk, R. J., & Venema, K. (2010). Biological effects of propionic acid in humans; metabolism, potential applications and underlying mechanisms. *Biochimica et Biophysica Acta (BBA) - Molecular and Cell Biology of Lipids, 1801*(11), 1175-1183.

Alberti, K. G., Eckel, R. H., Grundy, S. M., Zimmet, P. Z., Cleeman, J. I., Donato, K. A., . . . Smith, S. C., Jr. (2009). Harmonizing the metabolic syndrome: a joint interim statement of the International Diabetes Federation Task Force on Epidemiology and Prevention; National Heart, Lung, and Blood Institute; American Heart Association; World Heart Federation; International Atherosclerosis Society; and International Association for the Study of Obesity. *Circulation, 120*(16), 1640-1645.

Ambikairajah, A., Walsh, E., & Cherbuin, N. (2019). Lipid profile differences during menopause: a review with meta-analysis. *Menopause, 26*(11), 1327-1333.

Amoako, A. O., & Pujalte, G. G. A. (2014). Osteoarthritis in young, active, and athletic individuals. *Clinical medicine insights. Arthritis and musculoskeletal disorders, 7*, 27-32.

Ansar, W., & Ghosh, S. (2016). Inflammation and Inflammatory Diseases, Markers, and Mediators: Role of CRP in Some Inflammatory Diseases. *Biology of C Reactive Protein in Health and Disease*, 67-107.

Ashley, D. T., O'Sullivan, E. P., Davenport, C., Devlin, N., Crowley, R. K., McCaffrey, N., . . . O'Gorman, D. J. (2011). Similar to adiponectin, serum levels of osteoprotegerin are associated with obesity in healthy subjects. *Metabolism: Clinical and Experimental, 60*(7), 994-1000.

Attur, M., Krasnokutsky, S., Statnikov, A., Samuels, J., Li, Z., Friese, O., . . . Abramson, S. B. (2015). Low-Grade Inflammation in Symptomatic Knee Osteoarthritis: Prognostic Value of Inflammatory Plasma Lipids and Peripheral Blood Leukocyte Biomarkers. *Arthritis & Rheumatology, 67*(11), 2905-2915.

Audet, M., & Stevens, R. C. (2019). Emerging structural biology of lipid G protein-coupled receptors. *Protein science : a publication of the Protein Society, 28*(2), 292-304.

Azamar-Llamas, D., Hernandez-Molina, G., Ramos-Avalos, B., & Furuzawa-Carballeda, J. (2017). Adipokine contribution to the pathogenesis of osteoarthritis. *Mediators Inflamm, 2017*, 1-26.

Bao, J.-p., Chen, W.-p., Feng, J., Hu, P.-f., Shi, Z.-l., & Wu, L.-d. (2010). Leptin plays a catabolic role on articular cartilage. *Molecular Biology Reports, 37*(7), 3265-3272.

Bao, M., Zhang, K., Wei, Y., Hua, W., Gao, Y., Li, X., & Ye, L. (2020). Therapeutic potentials and modulatory mechanisms of fatty acids in bone. *Cell Proliferation, 53*(2), e12735-

Baquero, F., & Nombela, C. (2012). The microbiome as a human organ. *Clinical Microbiology and Infection, 18*, 2-4.

Barboza, E., Hudson, J., Chang, W.-P., Kovats, S., Towner, R. A., Silasi-Mansat, R., . . . Griffin, T. M. (2017). Profibrotic Infrapatellar Fat Pad Remodeling Without M1 Macrophage Polarization Precedes Knee Osteoarthritis in Mice With Diet-Induced Obesity. *Arthritis & Rheumatology, 69*(6), 1221-1232.

Barzilai, N., Huffman, D. M., Muzumdar, R. H., & Bartke, A. (2012). The Critical Role of Metabolic Pathways in Aging. *Diabetes, 61*(6), 1315-1322.

Bas, S., Finckh, A., Puskas, G. J., Suva, D., Hoffmeyer, P., Gabay, C., & Lübbeke, A. (2014). Adipokines correlate with pain in lower limb osteoarthritis: different associations in hip and knee. *International Orthopaedics, 38*(12), 2577-2583.

Batiste, D. L., Kirkley, A., Laverty, S., Thain, L. M. F., Spouge, A. R., & Holdsworth, D. W. (2004). Ex vivo characterization of articular cartilage and bone lesions in a rabbit ACL transection model of osteoarthritis using MRI and micro-CT. *Osteoarthritis and Cartilage, 12*(12), 986-996.

Bedossa, P., Poitou, C., Veyrie, N., Bouillot, J.-L., Basdevant, A., Paradis, V., . . . Clement, K. (2012). Histopathological algorithm and scoring system for evaluation of liver lesions in morbidly obese patients. *Hepatology, 56*(5), 1751-1759.

Bellido, M., Lugo, L., Roman-Blas, J. A., Castañeda, S., Caeiro, J. R., Dapia, S., . . . Herrero-Beaumont, G. (2010). Subchondral bone microstructural damage by increased remodelling aggravates experimental osteoarthritis preceded by osteoporosis. *Arthritis Research & Therapy, 12*(4), R152-R152.

Berthelot, J.-M., Sellam, J., Maugars, Y., & Berenbaum, F. (2019). Cartilage-gut-microbiome axis: a new paradigm for novel therapeutic opportunities in osteoarthritis. *RMD Open, 5*(2), 10-37.

Bertuglia, A., Lacourt, M., Girard, C., Beauchamp, G., Richard, H., & Laverty, S. (2016). Osteoclasts are recruited to the subchondral bone in naturally occurring post-traumatic equine carpal osteoarthritis and may contribute to cartilage degradation. *Osteoarthritis and Cartilage, 24*(3), 555-566.

Bettica, P., Cline, G., Hart, D. J., Meyer, J., & Spector, T. D. (2002). Evidence for increased bone resorption in patients with progressive knee osteoarthritis: Longitudinal results from the Chingford study. *Arthritis & Rheumatism, 46*(12), 3178-3184.

Biagi, E., Franceschi, C., Rampelli, S., Severgnini, M., Ostan, R., Turroni, S., . . . Candela, M. (2016). Gut Microbiota and Extreme Longevity. *Current Biology, 26*(11), 1480-1485.

Biagi, E., Nylund, L., Candela, M., Ostan, R., Bucci, L., Pini, E., . . . De Vos, W. (2010). Through ageing, and beyond: gut microbiota and inflammatory status in seniors and centenarians. *PLoS One, 5*(5), e10667-e10667.

Bidwell, J. P., Yang, J., & Robling, A. G. (2008). Is HMGB1 an osteocyte alarmin? *Journal of Cellular Biochemistry, 103*(6), 1671-1680.

Bierer, T. L., & Bui, L. M. (2002). Improvement of arthritic signs in dogs fed green-lipped mussel (Perna canaliculus). *Journal of Nutrition, 132*(6 Suppl 2), 1634s-1636s.

Bijlsma, J. W., Berenbaum, F., & Lafeber, F. P. (2011). Osteoarthritis: an update with relevance for clinical practice. *Lancet, 377*(9783), 2115-2126.

Bligh, E. G., & Dyer, W. J. (1959). A rapid method of total lipid extraction and purification. *Canadian Journal of Biochemistry and Physiology, 37*(8), 911-917.

Blüher, M. (2019). Obesity: global epidemiology and pathogenesis. *Nature Reviews Endocrinology, 15*(5), 288-298.

Boer, C. G., Radjabzadeh, D., Medina-Gomez, C., Garmaeva, S., Schiphof, D., Arp, P., . . . van Meurs, J. B. J. (2019). Intestinal microbiome composition and its relation to joint pain and inflammation. *Nat Commun, 10*(1), 4881.

Boeyens, J. C., Deepak, V., Chua, W. H., Kruger, M. C., Joubert, A. M., & Coetzee, M. (2014). Effects of omega3- and omega6-polyunsaturated fatty acids on RANKL-induced osteoclast differentiation of RAW264.7 cells: a comparative in vitro study. *Nutrients, 6*(7), 2584-2601.

Bolland, M. J., Grey, A. B., Ames, R. W., Horne, A. M., Gamble, G. D., & Reid, I. R. (2006). Fat mass is an important predictor of parathyroid hormone levels in postmenopausal women. *Bone, 38*(3), 317-321.

Bondeson, J., Wainwright, S. D., Lauder, S., Amos, N., & Hughes, C. E. (2006). The role of synovial macrophages and macrophage-produced cytokines in driving aggrecanases, matrix metalloproteinases, and other destructive and inflammatory responses in osteoarthritis. *Arthritis Research & Therapy, 8*(6), R187-R199.

Bos, G., Snijder, M. B., Nijpels, G., Dekker, J. M., Stehouwer, C. D. A., Bouter, L. M., . . . Jansen, H. (2005). Opposite contributions of trunk and leg fat mass with plasma lipase activities: The Hoorn Study. *Obesity Research, 13*, 1817-1823.

Boselli, E., Grob, K., & Lercker, G. (2000). Determination of furan fatty acids in extra virgin olive oil. *Journal of Agricultural and Food Chemistry, 48*(7), 2868-2873.

Botter, S. M., van Osch, G. J. V. M., Clockaerts, S., Waarsing, J. H., Weinans, H., & van Leeuwen, J. P. T. M. (2011). Osteoarthritis Induction Leads to Early and Temporal Subchondral Plate Porosity in the Tibial Plateau of Mice An In Vivo Microfocal Computed Tomography Study. *Arthritis And Rheumatism, 63*, 2690-2699.

Bowes, M. A., McLure, S. W., Wolstenholme, C. B., Vincent, G. R., Williams, S., Grainger, A., & Conaghan, P. G. (2016). Osteoarthritic bone marrow lesions almost exclusively colocate with denuded cartilage: a 3D study using data from the Osteoarthritis Initiative. *Annals of the Rheumatic Diseases, 75*(10), 1852-1857.

Boyce, B. F., Yan, X., Jinbo, L., Lianping, X., & Zhenqiang, Y. (2015). NF-κB-Mediated Regulation of Osteoclastogenesis. *Endocrinology & Metabolism, 30*(1), 35-44.

BrahmaNaidu, P., Nemani, H., Meriga, B., Mehar, S. K., Potana, S., & Ramgopalrao, S. (2014). Mitigating efficacy of piperine in the physiological derangements of high fat diet induced obesity in Sprague Dawley rats. *Chem Biol Interact, 221*, 42-51.

Brenna, J. T., Salem, N., Sinclair, A. J., & Cunnane, S. C. (2009). α-Linolenic acid supplementation and conversion to n-3 long-chain polyunsaturated fatty acids in humans. *Prostaglandins, Leukotrienes and Essential Fatty Acids, 80*(2), 85-91.

Brien, S., Prescott, P., Coghlan, B., Bashir, N., & Lewith, G. (2008). Systematic review of the nutritional supplement Perna Canaliculus (green-lipped mussel) in the treatment of osteoarthritis. *QJM: An International Journal of Medicine, 101*(3), 167-167.

Briggs, A. M., Cross, M. J., Hoy, D. G., Sanchez-Riera, L., Blyth, F. M., Woolf, A. D., & March, L. (2016). Musculoskeletal health conditions represent a global threat

to healthy aging: a report for the 2015 world health organization world report on ageing and health. *The Gerontologist*(2), 243-255.

Britton, R. A., Irwin, R., Quach, D., Schaefer, L., Zhang, J., Lee, T., . . . McCabe, L. R. (2014). Probiotic L. reuteri treatment prevents bone loss in a menopausal ovariectomised mouse model. *Journal of Cellular Physiology, 229*(11), 1822-1830.

Brunner, A. M., Henn, C. M., Drewniak, E. I., Lesieur-Brooks, A., Machan, J., Crisco, J. J., & Ehrlich, M. G. (2012). High dietary fat and the development of osteoarthritis in a rabbit model. *Osteoarthritis and Cartilage, 20*(6), 584-592.

Bui, L. M., & Bierer, T. L. (2003). Influence of green lipped mussels (Perna canaliculus) in alleviating signs of arthritis in dogs. *Vet Ther, 4*(4), 397-407.

Burguera, B., Hofbauer, L. C., Thomas, T., Gori, F., Evans, G. L., Khosla, S., . . . Turner, R. T. (2001). Leptin reduces ovariectomy-induced bone loss in rats. *Endocrinology and Metabolism Clinics of North America, 142*, 3546-3553.

Burri, L., Hoem, N., Banni, S., & Berge, K. (2012). Marine omega-3 phospholipids: metabolism and biological activities. *International Journal of Molecular Sciences, 13*(11), 15401-15419.

Burr, D. B. (2004). Anatomy and physiology of the mineralized tissues: Role in the pathogenesis of osteoarthrosis. *Osteoarthritis and Cartilage, 12*, 20-30.

Burr, D. B., & Gallant, M. A. (2012). Bone remodelling in osteoarthritis. *Nature Reviews Rheumatology, 8*, 665-673.

Caesar, R., Tremaroli, V., Kovatcheva-Datchary, P., Cani, Patrice D., & Bäckhed, F. (2015). Crosstalk between Gut Microbiota and Dietary Lipids Aggravates WAT Inflammation through TLR Signaling. *Cell Metabolism, 22*(4), 658-668.

Cai, A., Hutchison, E., Hudson, J., Kawashima, Y., Komori, N., Singh, A., . . . Griffin, T. M. (2014). Metabolic enrichment of omega-3 polyunsaturated fatty acids does not reduce the onset of idiopathic knee osteoarthritis in mice. *Osteoarthritis and Cartilage, 22*(9), 1301-1309.

Calder, P. C., Ahluwalia, N., Albers, R., Bosco, N., Bourdet-Sicard, R., Haller, D., . . . Zhao, J. (2013). A consideration of biomarkers to be used for evaluation of inflammation in human nutrition. *British journal of nutrition, 109*(1), 34-45.

Calder, P. C., Bosco, N., Bourdet-Sicard, R., Capuron, L., Delzenne, N., Doré, J., . . . Visioli, F. (2017). Health relevance of the modification of low grade inflammation in ageing (inflammageing) and the role of nutrition. *Ageing Research Reviews, 40*, 95-119.

Campos, R. M., de Piano, A., da Silva, P. L., Carnier, J., Sanches, P. L., Corgosinho, F. C., . . . Nascimento, C. M. (2012). The role of pro/anti-inflammatory adipokines on bone metabolism in NAFLD obese adolescents: Effects of long-term interdisciplinary therapy. *Endocrine, 42*, 146–156.

Cani, P. D., Amar, J., Iglesias, M. A., Poggi, M., Knauf, C., Bastelica, D., . . . Burcelin, R. (2007). Metabolic Endotoxemia Initiates Obesity and Insulin Resistance. *Diabetes, 56*(7), 1761-1777.

Cani, P. D., Bibiloni, R., Knauf, C., Waget, A., Neyrinck, A. M., Delzenne, N. M., & Burcelin, R. (2008). Changes in Gut Microbiota Control Metabolic Endotoxemia-Induced Inflammation in High-Fat Diet–Induced Obesity and Diabetes in Mice. *Diabetes, 57*(6), 1470-1481.

Cani, P. D., & de Vos, W. M. (2017). Next-Generation Beneficial Microbes: The Case of Akkermansia muciniphila. *Frontiers in Microbiology, 8*(1765), 1-15.

Cani, P. D., & Delzenne, N. M. (2011). The gut microbiome as therapeutic target. *Pharmacology & Therapeutics, 130*(2), 202-212.

Cani, P. D., Osto, M., Geurts, L., & Everard, A. (2012). Involvement of gut microbiota in the development of low-grade inflammation and type 2 diabetes associated with obesity. *Gut Microbes, 3*(4), 1-15.

Cao, J. J. (2011). Effects of obesity on bone metabolism. *Journal of Orthopaedic Surgery and Research, 6*(1), 30.

Catanzaro, R., Cuffari, B., Italia, A., & Marotta, F. (2016). Exploring the metabolic syndrome: Nonalcoholic fatty pancreas disease. *World journal of gastroenterology, 22*(34), 7660-7675.

Catterall, J. B., Hsueh, M. F., Stabler, T. V., McCudden, C. R., Bolognesi, M., Zura, R., . . . Kraus, V. B. (2012). Protein Modification by Deamidation Indicates Variations in Joint Extracellular Matrix Turnover. *Journal of Biological Chemistry, 287*, 4640-4651.

Caughey, D. E., Grigor, R. R., Caughey, E. B., Young, P., Gow, P. J., & Stewart, A. W. (1983). Perna canaliculus in the treatment of rheumatoid arthritis. *European Journal of Rheumatology and Inflammation, 6*(2), 197-200.

Chambers, E. S., Morrison, D. J., & Frost, G. (2015). Control of appetite and energy intake by SCFA: what are the potential underlying mechanisms? *Proceedings of the Nutrition Society, 74*(3), 328-336.

Chandran, M., Phillips, S. A., Ciaraldi, T., & Henry, R. R. (2003). Adiponectin: More Than Just Another Fat Cell Hormone? *Diabetes Care, 26*(8), 2442-2450.

Chen, D., Shen, J., Zhao, W., Wang, T., Han, L., Hamilton, J. L., & Im, H. J. (2017). Osteoarthritis: toward a comprehensive understanding of pathological mechanism. *Bone Research, 5*, 16044.

Chen, J., Bao, C., Cho, S. H., & Lee, H. J. (2017). Green lipped mussel oil complex suppresses lipopolysaccharide stimulated inflammation via regulating nuclear factor-kappa B and mitogen activated protein kinases signaling in RAW264.7 murine macrophages. *Food Science and Biotechnology, 26*, 815-822.

Chen, X., Li, X., Zhai, X., Zhi, X., Cao, L., Qin, L., & Su, J. (2018). Shikimic Acid Inhibits Osteoclastogenesis in Vivo and in Vitro by Blocking RANK/TRAF6 Association and Suppressing NF-κB and MAPK Signaling Pathways. *Cellular Physiology and Biochemistry, 51*(6), 2858-2871.

Cheng, H., Hao, B., Sun, J., & Yin, M. (2018). C-Terminal Cross-Linked Telopeptides of Type II Collagen as Biomarker for Radiological Knee Osteoarthritis: A Meta-Analysis. *Cartilage*, 1947603518798884.

Chi-Ho, L., John Hon-Kei, L., Curtise Kin-Cheung, N., Janice, M., Yoki Kwok-Chu, B., Man-Sau, W., & Samuel Chun-Lap, L. (2009). Pain Controlling and Cytokine-regulating Effects of Lyprinol, a Lipid Extract of Perna Canaliculus, in a Rat Adjuvant-induced Arthritis Model. *Evidence-based Complementary & Alternative Medicine (eCAM), 6*(2), 239-245.

Chin, K.-Y., & Ima-Nirwana, S. (2017). The Effects of Testosterone Deficiency and Its Replacement on Inflammatory Markers in Rats: A Pilot Study. *International Journal Of Endocrinology And Metabolism, 15*(1), e43053-e43053.

Cho, I., Yamanishi, S., Cox, L., Methé, B. A., Zavadil, J., Li, K., . . . Blaser, M. J. (2012). Antibiotics in early life alter the murine colonic microbiome and adiposity. *Nature, 488*(7413), 621-626.

Cho, S. H., Jung, Y. B., Seong, S. C., Park, H. B., Byun, K. Y., Lee, D. C., . . . Son, J. H. (2003). Clinical efficacy and safety of Lyprinol, a patented extract from New Zealand green-lipped mussel (Perna Canaliculus) in patients with osteoarthritis of the hip and knee: a multicenter 2-month clinical trial. *European Annals of Allergy and Clinical Immunology, 35*(6), 212-216.

Christensen, R., Bartels, E. M., Astrup, A., & Bliddal, H. (2007). Effect of weight reduction in obese patients diagnosed with knee osteoarthritis: a systematic review and meta-analysis. *Annals of the Rheumatic Diseases, 66*(4), 433-439.

Cicuttini, F. M., Baker, J. R., & Spector, T. D. (1996). The association of obesity with osteoarthritis of the hand and knee in women: a twin study. *The Journal of Rheumatology, 23*(7), 1221-1226.

Clark, A. G., Jordan, J. M., Vilim, V., Renner, J. B., Dragomir, A. D., Luta, G., & Kraus, V. B. (1999). Serum cartilage oligomeric matrix protein reflects osteoarthritis presence and severity - The Johnston county osteoarthritis project. *Arthritis And Rheumatism, 42*, 2356-2364.

Clarke, S. F., Murphy, E. F., Nilaweera, K., Ross, P. R., Shanahan, F., O'Toole, P. W., & Cotter, P. D. (2012). The gut microbiota and its relationship to diet and obesity. *Gut Microbes, 3*(3), 186-198.

Cobb, C. S., & Ernst, E. (2006). Systematic review of a marine nutriceutical supplement in clinical trials for arthritis: the effectiveness of the New Zealand green-lipped mussel Perna canaliculus. *Clinical Rheumatology, 25*(3), 275-284.

Coggon, D., Reading, I., Croft, P., McLaren, M., Barrett, D., & Cooper, C. (2001). Knee osteoarthritis and obesity. *International journal of obesity and related metabolic disorders : journal of the International Association for the Study of Obesity, 25*(5), 622-627.

Collins, K. H., Paul, H. A., Reimer, R. A., Seerattan, R. A., Hart, D. A., & Herzog, W. (2015a). Relationship between inflammation, the gut microbiota, and metabolic osteoarthritis development: studies in a rat model. *Osteoarthritis and Cartilage, 23*(11), 1989-1998.

Collins, K. H., Reimer, R. A., Seerattan, R. A., Herzog, W., & Hart, D. A. (2016). Response to diet-induced obesity produces time-dependent induction and progression of metabolic osteoarthritis in rat knees. *Journal of Orthopaedic Research, 34*(6), 1010-1018.

Collins, K. H., Reimer, R. A., Seerattan, R. A., Leonard, T. R., & Herzog, W. (2015b). Using diet-induced obesity to understand a metabolic subtype of osteoarthritis in rats. *Osteoarthritis and Cartilage, 23*(6), 957-965.

Collin-Osdoby, P., & Osdoby, P. (2012). RANKL-mediated osteoclast formation from murine RAW 264.7 cells. *Methods Mol Biol*, 816, 187-202.

Compston, J. (2015). Obesity and fractures in postmenopausal women. *Current Opinion in Rheumatology, 27*(4), 414-419.

Compston, J. E., Watts, N. B., Chapurlat, R., Cooper, C., Boonen, S., Greenspan, S., . . . Siris, E. S. (2011). Obesity is not protective against fracture in postmenopausal women: GLOW. *The American Journal of Medicine, 124*(11), 1043-1050.

Cook, J. L., Hung, C. T., Kuroki, K., Stoker, A. M., Cook, C. R., Pfeiffer, F. M., . . . Stannard, J. P. (2014). Animal models of cartilage repair. *Bone Joint Res, 3*(4), 89-94.

Cooke, P. S., & Naaz, A. (2004). Role of estrogens in adipocyte development and function. *Experimental Biology and Medicine, 229*, 1127-1135.

Cornier, M. A., Dabelea, D., Hernandez, T. L., Lindstrom, R. C., Steig, A. J., Stob, N. R., . . . Eckel, R. H. (2008). The metabolic syndrome. *Endocrine Reviews, 29*(7), 777-822.

Cornish, J., MacGibbon, A., Lin, J.-M., Watson, M., Callon, K. E., Tong, P. C., . . . Reid, I. R. (2008). Modulation of Osteoclastogenesis by Fatty Acids. *Endocrinology & Metabolism, 149*, 5688-5695.

Coulson, S., Butt, H., Vecchio, P., Gramotnev, H., & Vitetta, L. (2013). Green-lipped mussel extract (Perna canaliculus) and glucosamine sulphate in patients with knee osteoarthritis: therapeutic efficacy and effects on gastrointestinal microbiota profiles. *Inflammopharmacology, 21*(1), 79-90.

Coulson, S., Vecchio, P., Gramotnev, H., & Vitetta, L. (2012). Green-lipped mussel (Perna canaliculus) extract efficacy in knee osteoarthritis and improvement in gastrointestinal dysfunction: a pilot study. *Inflammopharmacology, 20*(2), 71-76.

Covington, D. K., Briscoe, C. A., Brown, A. J., & Jayawickreme, C. K. (2006). The G-protein-coupled receptor 40 family (GPR40-GPR43) and its role in nutrient sensing. *Biochemical Society Transactions, 34*(Pt 5), 770-773.

Cox, L. M., Yamanishi, S., Sohn, J., Alekseyenko, A. V., Leung, J. M., Cho, I., . . . Blaser, M. J. (2014). Altering the intestinal microbiota during a critical developmental window has lasting metabolic consequences. *Cell, 158*(4), 705-721.

Crowder, M. K., Seacrist, C. D., & Blind, R. D. (2017). Phospholipid regulation of the nuclear receptor superfamily. *Adv Biol Regul, 63*, 6-14.

Culemann, S., Grüneboom, A., Nicolás-Ávila, J. Á., Weidner, D., Lämmle, K. F., Rothe, T., . . . Krönke, G. (2019). Locally renewing resident synovial macrophages provide a protective barrier for the joint. *Nature, 572*(7771), 670-675.

Cummings, J. H., Pomare, E. W., Branch, W. J., Naylor, C. P., & Macfarlane, G. T. (1987). Short chain fatty acids in human large intestine, portal, hepatic and venous blood. *Gut, 28*(10), 1221-1227.

Dagher, P. C., Egnor, R. W., Taglietta-Kohlbrecher, A., & Charney, A. N. (1996). Short-chain fatty acids inhibit cAMP-mediated chloride secretion in rat colon. *American Journal of Physiology-Cell Physiology, 271*(6), C1853-C1860.

Dao, M. C., Everard, A., Aron-Wisnewsky, J., Sokolovska, N., Prifti, E., Verger, E. O., . . . Clément, K. (2016). Akkermansia muciniphila and improved metabolic health during a dietary intervention in obesity: relationship with gut microbiome richness and ecology. *Gut, 65*(3), 426-436.

David, L. A., Maurice, C. F., Carmody, R. N., Gootenberg, D. B., Button, J. E., Wolfe, B. E., . . . Turnbaugh, P. J. (2014). Diet rapidly and reproducibly alters the human gut microbiome. *Nature, 505*(7484), 559-563.

De Laet, C., Kanis, J. A., Odén, A., Johanson, H., Johnell, O., Delmas, P., . . . Tenenhouse, A. (2005). Body mass index as a predictor of fracture risk: A meta-analysis. *Osteoporosis International: With other Metabolic Bone Diseases, 16*(11), 1330-1340.

de Visser, H. M., Kozijn, A. E., Pouran, B., van Rijen, M. H., Weinans, H., Mastbergen, S. C., . . . Lafeber, F. P. J. G. (2017). Metabolic dysregulation accelerates injury-induced joint degeneration, driven by local inflammation; an in vivo rat study. *Journal of Orthopaedic Research*, (237)12, 1-10.

Dellorto, D. (2012). Global report: Obesity bigger health crisis than hunger. Retrieved May, 30 2020 from https://edition.cnn.com/2012/12/13/health/global-burden-report/index.html

Denoble, A. E., Huffman, K. M., Stabler, T. V., Kelly, S. J., Hershfield, M. S., McDaniel, G. E., . . . Kraus, V. B. (2011). Uric acid is a danger signal of increasing risk for osteoarthritis through inflammasome activation. *Proceedings of the National Academy of Sciences, 108*(5), 2088-2093.

Derrien, M., Belzer, C., & de Vos, W. M. (2017). Akkermansia muciniphila and its role in regulating host functions. *Microbial Pathogenesis, 106*, 171-181.

Derrien, M., Vaughan, E. E., Plugge, C. M., & de Vos, W. M. (2004). Akkermansia muciniphila gen. nov., sp. nov., a human intestinal mucin-degrading bacterium. *International Journal of Systematic and Evolutionary Microbiology, 54*(5), 1469-1476.

Di Iorio, A., Ferrucci, L., Sparvieri, E., Cherubini, A., Volpato, S., Corsi, A., . . . Paganelli, R. (2003). Serum IL-1β levels in health and disease: a population-based study. 'The InCHIANTI study'. *Cytokine, 22*(6), 198-205.

Dimitri, P., Bishop, N., Walsh, J. S., & Eastell, R. (2012). Obesity is a risk factor for fracture in children but is protective against fracture in adults: A paradox. *Bone, 50*(2), 457-466.

Ding, M. (2010). Microarchitectural adaptations in aging and osteoarthrotic subchondral bone issues. *Acta Orthopaedica, 81*(sup340), 1-53.

Dinh, K. M., Kaspersen, K. A., Mikkelsen, S., Pedersen, O. B., Petersen, M. S., Thørner, L. W., . . . Erikstrup, C. (2019). Low-grade inflammation is negatively associated with physical Health-Related Quality of Life in healthy individuals: Results from The Danish Blood Donor Study (DBDS). *PLoS One, 14*(3), e0214468-e0214468.

DiPatrizio, N. V. (2016). Endocannabinoids in the Gut. *Cannabis and cannabinoid research, 1*(1), 67-77.

Dobenecker, B., Beetz, Y., & Kienzle, E. (2002). A placebo-controlled double-blind study on the effect of nutraceuticals (chondroitin sulfate and mussel extract) in dogs with joint diseases as perceived by their owners. *Journal of Nutrition, 132*(6 Suppl 2), 1690s-1691s.

Dorn, G. W. (2007). The Fuzzy Logic of Physiological Cardiac Hypertrophy. *Hypertension, 49*(5), 962-970.

Drincic, A. T., Armas, L. A. G., Van Diest, E. E., & Heaney, R. P. (2012). Volumetric Dilution, Rather Than Sequestration Best Explains the Low Vitamin D Status of Obesity. *Obesity, 20*, 1444-1448.

Drosatos-Tampakaki, Z., Drosatos, K., Siegelin, Y., Gong, S., Khan, S., Van Dyke, T., . . . Schulze-Späte, U. (2014). Palmitic acid and DGAT1 deficiency enhance osteoclastogenesis, while oleic acid-induced triglyceride formation prevents it. *Journal of Bone and Mineral Research, 29*(5), 1183-1195.

Duan, P., & Bonewald, L. F. (2016). The role of the wnt/β-catenin signaling pathway in formation and maintenance of bone and teeth. *Int J Biochem Cell Biol, 77*, 23-29.

Duncan, S. H., Barcenilla, A., Stewart, C. S., Pryde, S. E., & Flint, H. J. (2002). Acetate utilization and butyryl coenzyme A (CoA):acetate-CoA transferase in butyrate-producing bacteria from the human large intestine. *Applied and Environmental Microbiology, 68*(10), 5186-5190.

Dušanić, D., Berčič, R. L., Cizelj, I., Salmič, S., Narat, M., & Benčina, D. (2009). Mycoplasma synoviae invades non-phagocytic chicken cells in vitro. *Veterinary Microbiology, 138*(1), 114-119.

Eason, C. T., Adams, S. L., Puddick, J., Romanazzi, D., Miller, M. R., King, N., . . . Packer, M. A. (2018). Greenshell™ Mussels: A Review of Veterinary Trials and Future Research Directions. *Veterinary Sciences, 5*(2), 1-9.

Ebina, K., Oshima, K., Matsuda, M., Fukuhara, A., Maeda, K., Kihara, S., . . . Shimomura, I. (2009). Adenovirus-mediated gene transfer of adiponectin reduces the severity of collagen-induced arthritis in mice. *Biochemical and Biophysical Research Communications, 378*(2), 186-191.

El Maghraoui, A., Rezqi, A., El Mrahi, S., Sadni, S., Ghozlani, I., & Mounach, A. (2014). Osteoporosis, vertebral fractures and metabolic syndrome in postmenopausal women. *BMC Endocrine Disorders, 14*, 93.

Elliott, A. L., Kraus, V. B., Luta, G., Stabler, T., Renner, J. B., Woodard, J., . . . Jordan, J. M. (2005). Serum hyaluronan levels and radiographic knee and hip osteoarthritis in African Americans and Caucasians in the Johnston County Osteoarthritis Project. *Arthritis & Rheumatism, 52*(1), 105-111.

Ellulu, M. S., Patimah, I., Khaza'ai, H., Rahmat, A., & Abed, Y. (2017). Obesity and inflammation: the linking mechanism and the complications. *Archives of medical science : AMS, 13*(4), 851-863.

Eun-Young, K., Su-Kyung, S., Yun-Young, C., Un Ju, J., Eunjung, K., Taesun, P., . . . Myung-Sook, C. (2012). Time-course microarrays reveal early activation of the immune transcriptome and adipokine dysregulation leads to fibrosis in visceral adipose depots during diet-induced obesity. *BMC Genomics, 13*(1), 450-465.

Evans, A. L., Paggiosi, M. A., Eastell, R., & Walsh, J. S. (2015). Bone density, microstructure and strength in obese and normal weight men and women in younger and older adulthood. *Journal of Bone and Mineral Research, 30*, 920-928.

Everard, A., Belzer, C., Geurts, L., Ouwerkerk, J. P., Druart, C., Bindels, L. B., . . . Cani, P. D. (2013). Cross-talk between Akkermansia muciniphila and intestinal epithelium controls diet-induced obesity. *Proceedings Of The National Academy Of Sciences Of The United States Of America, 110*(22), 9066-9071.

Everard, A., Lazarevic, V., Gaïa, N., Johansson, M., Ståhlman, M., Backhed, F., . . . Cani, P. D. (2014). Microbiome of prebiotic-treated mice reveals novel targets involved in host response during obesity. *The ISME journal, 8*(10), 2116-2130.

Fagiolo, U., Cossarizza, A., Scala, E., Fanales-Belasio, E., Ortolani, C., Cozzi, E., . . . Paganelli, R. (1993). Increased cytokine production in mononuclear cells of healthy elderly people. *European Journal Of Immunology, 23*(9), 2375-2378.

Fain, J. N., Buehrer, B., Tichansky, D. S., & Madan, A. K. (2008). Regulation of adiponectin release and demonstration of adiponectin mRNA as well as release by the non-fat cells of human omental adipose tissue. *International Journal of Obesity, 32*(3), 429-435.

Fantuzzi, G. (2008). Adiponectin and inflammation: Consensus and controversy. *Journal of Allergy and Clinical Immunology, 121*(2), 326-330.

Fassio, A., Idolazzi, L., Rossini, M., Gatti, D., Adami, G., Giollo, A., & Viapiana, O. (2018). The obesity paradox and osteoporosis. *Eating and Weight Disorders - Studies on Anorexia, Bulimia and Obesity, 23*(3), 293-302.

Feldman, M., Friedman, L. S., & Brandt, L. J. (2016). *Sleisenger and Fordtran's Gastrointestinal and Liver Disease* (10 ed.). Philadelphia: Elsevier.

Felson, D. T., Zhang, Y., Hannan, M. T., & Anderson, J. J. (1993). Effects of weight and body mass index on bone mineral density in men and women: the Framingham study. *J Bone Miner Res, 8*, 567–573.

Ferrandiz, M. L., Terencio, M. C., Ruhi, R., Verges, J., Montell, E., Torrent, A., & Alcaraz, M. J. (2014). Influence of age on osteoarthritis progression after anterior cruciate ligament transection in rats. *Exp Gerontol, 55*, 44-48.

Ferrari, M., Fornasiero, M. C., & Isetta, A. M. (1990). MTT colorimetric assay for testing macrophage cytotoxic activity in vitro. *Journal of Immunological Methods, 131*(2), 165-172.

Ferreira, M. R., Alvarez, S. M., Illesca, P., Giménez, M. S., & Lombardo, Y. B. (2018). Dietary Salba ameliorates the adipose tissue dysfunction of dyslipemic insulin-

resistant rats through mechanisms involving oxidative stress, inflammatory cytokines and peroxisome proliferator-activated receptor γ. *European Journal of Nutrition, 57*(1), 83-94.

Filková, M., Šenolt, L., Braun, M., Hulejová, H., Pavelková, A., Šléglová, O., . . . Pavelka, K. (2009). Serum hyaluronic acid as a potential marker with a predictive value for further radiographic progression of hand osteoarthritis. *Osteoarthritis and Cartilage, 17*(12), 1615-1619.

Firestein, G. S. (2003). Evolving concepts of rheumatoid arthritis. *Nature, 423*(6937), 356-361.

Foell, D., Wittkowski, H., & Roth, J. (2007). Mechanisms of Disease: a 'DAMP' view of inflammatory arthritis. *Nature Clinical Practice Rheumatology, 3*(7), 382-390.

Fonseca, H., Powers, S. K., Gonalves, D., Santos, A., Mota, M. P., & Duarte, J. A. (2012). Physical inactivity is a major contributor to ovariectomy-induced sarcopenia. *International Journal of Sports Medicine, 33*(4), 268-278.

Forouzanfar, M. H., Afshin, A., Alexander, L. T., Anderson, H. R., Bhutta, Z. A., Biryukov, S., . . . Murray, C. J. L. (2016). Global, regional, and national comparative risk assessment of 79 behavioural, environmental and occupational, and metabolic risks or clusters of risks: a systematic analysis for the Global Burden of Disease Study 2015. *The Lancet, 388*(10053), 1659-1724.

Francin, P.-J., Guillaume, C., Humbert, A.-C., Pottie, P., Netter, P., Mainard, D., & Presle, N. (2011). Association between the chondrocyte phenotype and the expression of adipokines and their receptors: Evidence for a role of leptin but not adiponectin in the expression of cartilage-specific markers. *Journal of Cellular Physiology, 226*(11), 2790-2797.

Fredrik, B., Hao, D., Ting, W., Lora, V. H., Gou Young, K., Andras, N., . . . Jeffrey, I. G. (2004). The Gut Microbiota as an Environmental Factor That Regulates Fat Storage. *Proceedings Of The National Academy Of Sciences Of The United States Of America, 101*(44), 15718.

Friedman, B., Corciulo, C., Castro, C. M., & Cronstein, B. N. (2021). Adenosine A2A receptor signaling promotes FoxO associated autophagy in chondrocytes. *Sci Rep, 11*(1), 968.

Funaki, Y., Hasegawa, Y., Okazaki, R., Yamasaki, A., Sueda, Y., Yamamoto, A., . . . Shimizu, E. (2018). Resolvin E1 Inhibits Osteoclastogenesis and Bone Resorption by Suppressing IL-17-induced RANKL Expression in Osteoblasts and RANKL-induced Osteoclast Differentiation. *Yonago Acta Medica, 61*, 8-18.

Galvao, C. F., Xavier, V. F., Marcin, G. Ł., Boroni Moreira, A. P., Usuda Prado Rocha, D. M., de Cássia Gonçalves Alfenas, R., . . . Alfenas, R. d. C. G. (2018). Impact of dietary fat on gut microbiota and low-grade systemic inflammation: mechanisms and clinical implications on obesity. *International Journal of Food Sciences & Nutrition, 69*(2), 125-143.

Graber, D. R., Jones, W. J., & Johnson, J. A. (1995). Human and ecosystem health: the environment-agriculture connection in developing countries. *J Agromedicine, 2*(3), 47-64.

Garnero, P., Conrozier, T., Christgau, S., Mathieu, P., Delmas, P. D., & Vignon, E. (2003). Urinary type II collagen C-telopeptide levels are increased in patients with rapidly destructive hip osteoarthritis. *Annals of the Rheumatic Diseases, 62*, 939-943.

Gérard, K., & Mathieu, F. (2012). The contribution of bone to whole-organism physiology. *Nature*(7381), 314-324.

Ghosh, S., DeCoffe, D., Brown, K., Rajendiran, E., Estaki, M., Dai, C., . . . Gibson, D. L. (2013). Fish oil attenuates omega-6 polyunsaturated fatty acid-induced dysbiosis and infectious colitis but impairs LPS dephosphorylation activity causing sepsis. *PLoS One, 8*(2), e55468.

Gibson, S., & Gibson, R. G. (1998). The treatment of arthritis with a lipid extract of Perna canaliculus: a randomised trial. *Complimentary Therapies in Medine, 6*, 122-126.

Gibson, S. L. (2000). The effect of a lipid extract of the New Zealand green-lipped mussel in three cases of arthritis. *Journal of Alternative and Complementary Medicine, 6*(4), 351-354.

Goldring, S. R., & Goldring, M. B. (2016). Changes in the osteochondral unit during osteoarthritis: structure, function and cartilage-bone crosstalk. *Nature Reviews Rheumatology, 12*, 632-644.

Grabherr, F., Grander, C., Effenberger, M., Adolph, T. E., & Tilg, H. (2019). Gut Dysfunction and Non-alcoholic Fatty Liver Disease. *Frontiers in Endocrinology,* 10(611), 1-9.

Gregor, M. F., & Hotamisligil, G. S. (2011). Inflammatory mechanisms in obesity. *Annual Review of Immunology, 29*, 415-445.

Griffin, T. M., & Guilak, F. (2008). Why is obesity associated with osteoarthritis? Insights from mouse models of obesity. *Biorheology, 45*, 387-398.

Griffin, T. M., Huebner, J. L., Kraus, V. B., & Guilak, F. (2009). Extreme obesity due to impaired leptin signaling in mice does not cause knee osteoarthritis. *Arthritis and Rheumatism, 60*(10), 2935-2944.

Grundy, S. M., Cleeman, J. I., Daniels, S. R., Donato, K. A., Eckel, R. H., Franklin, B. A., . . . Costa, F. (2005). Diagnosis and management of the metabolic syndrome: an American Heart Association/National Heart, Lung, and Blood Institute Scientific Statement. *Circulation, 112*(17), 2735-2752. 10.

Guenther, M., James, R., Marks, J., Zhao, S., Szabo, A., & Kidambi, S. (2014). Adiposity distribution influences circulating adiponectin levels. *Translational Research, 164*(4), 270-277.

Guri, A. J., & Bassaganya-Riera, J. (2011). Systemic effects of white adipose tissue dysregulation and obesity related inflammation. *Obesity, 19*, 689–700.

Haag, M., Magada, O. N., Claassen, N., Böhmer, L. H., & Kruger, M. C. (2003). Omega-3 fatty acids modulate ATPases involved in duodenal Ca absorption. *Prostaglandins, Leukotrienes and Essential Fatty Acids (PLEFA), 68*(6), 423-429.

Haissam, A. S., Allal, O., Ganesh, V. H., & Md Mizanur, R. (2019). Bone Benefits of Fish Oil Supplementation Depend on its EPA and DHA Content. *Nutrients*(11), 2701-2711.

Ham, K. D., & Carlson, C. S. (2004). Effects of Estrogen Replacement Therapy on Bone Turnover in Subchondral Bone and Epiphyseal Metaphyseal Cancellous Bone of Ovariectomised Cynomolgus Monkeys. *Journal of Bone and Mineral Research, 19*(5), 823-829.

Heidemann, C., Schulze, M. B., & Franco, O. H. (2008). Dietary patterns and risk of mortality from cardiovascular disease, cancer, and all causes in a prospective cohort of women. *Circulation, 118*, 230-237.

Hernandez-Morante, J. J., Milagro, F., Gabaldon, J. A., Martinez, J. A., Zamora, S., & Garaulet, M. (2006). Effect of DHEA-sulfate on adiponectin gene expression in adipose tissue from different fat depots in morbidly obese humans. *European journal of endocrinology, 155*(4), 593-600.

Hirasawa, A., Tsumaya, K., Awaji, T., Katsuma, S., Adachi, T., Yamada, M., . . . Tsujimoto, G. (2005). Free fatty acids regulate gut incretin glucagon-like peptide-1 secretion through GPR120. *Nature Medicine, 11*, 90-94.

Ho, A. Y. Y., & Kung, A. W. C. (2005). Determinants of peak bone mineral density and bone area in young women. *Journal of Bone and Mineral Metabolism, 23*, 470-475.

Høegh-Andersen, P., Tankó, L. B., Andersen, T. L., Lundberg, C. V., Mo, J. A., Heegaard, A.-M., . . . Christgau, S. (2004). Ovariectomised rats as a model of postmenopausal osteoarthritis: validation and application. *Arthritis Research & Therapy, 6*(2), R169-R180.

Holmes, C., Cunningham, C., Zotova, E., Woolford, J., Dean, C., Kerr, S., . . . Perry, V. H. (2009). Systemic inflammation and disease progression in Alzheimer disease. *Neurology, 73*(10), 768-774.

Hong, Y.-p., Yu, J., Su, Y.-r., Mei, F.-c., Li, M., Zhao, K.-l., . . . Wang, W.-x. (2020). High-Fat Diet Aggravates Acute Pancreatitis via TLR4-Mediated Necroptosis and Inflammation in Rats. *Oxidative Medicine and Cellular Longevity, 2020*, 8172714, 1-11.

Hosnijeh, F. S., Siebuhr, A. S., Uitterlinden, A. G., Oei, H. G., Hofman, A., Karsdal, M. A., . . . van Meurs, B. J. (2016). Association between biomarkers of tissue inflammation and progression of osteoarthritis: evidence from the Rotterdam study cohort. *Arthritis Research & Therapy, 18*(1), 81-91.

Howe, P., Buckley, J., & Meyer, B. (2007). Long-chain omega-3 fatty acids in red meat. *Nutrition & Dietetics, 64*(4), 135-139.

Huskisson, E. C., Scott, J., & Bryans, R. (1981). Seatone is ineffective in rheumatoid arthritis. *British Medical Journal (Clinical Research Ed.), 282*(6273), 1358-1359.

Hwang, D. K., & Choi, H. J. (2010). The relationship between low bone mass and metabolic syndrome in Korean women. *Osteoporos. Int., 21*(3), 425–431.

Hwang, H. S., & Kim, H. A. (2015). Chondrocyte Apoptosis in the Pathogenesis of Osteoarthritis. *International Journal of Molecular Sciences, 16*(11), 26035-26054.

Ilich, J. Z., Kelly, O. J., Kim, Y., & Spicer, M. T. (2014). Low-grade chronic inflammation perpetuated by modern diet as a promoter of obesity and osteoporosis. *Archives of Industrial Hygiene & Toxicology / Arhiv za Higijenu Rada I Toksikologiju, 65*(2), 139-148.

Inadera, H. (2008). The usefulness of circulating adipokine levels for the assessment of obesity-related health problems. *International Journal of Medical Sciences, 5*, 248-262.

Intema, F., Hazewinkel, H. A. W., Gouwens, D., Bijlsma, J. W. J., Weinans, H., Lafeber, F. P. J. G., & Mastbergen, S. C. (2010). In early OA, thinning of the subchondral plate is directly related to cartilage damage: results from a canine ACLT-meniscectomy model. *Osteoarthritis and Cartilage, 18*(5), 691-698.

Itoh, Y., Kawamata, Y., Harada, M., Kobayashi, M., Fujii, R., Fukusumi, S., . . . Shinohara, T. (2003). Free fatty acids regulate insulin secretion from pancreatic B cells through GPR40. *Nature, 422*(6928), 173-183.

Janusz, M. J., Little, C. B., King, L. E., Hookfin, E. B., Brown, K. K., & Heitmeyer, S. A. (2004). Detection of aggrecanase- and MMPgenerated catabolic neoepitopes in the rat iodoacetate model of cartilage degeneration. *Osteoarthritis Cartilage, 12*, 720-728.

Jasirwan, C. O. M., Lesmana, C. R. A., Hasan, I., Sulaiman, A. S., & Gani, R. A. (2019). The role of gut microbiota in non-alcoholic fatty liver disease: pathways of mechanisms. *Bioscience of microbiota, food and health, 38*(3), 81-88.

Jensen, V. S., Hvid, H., Damgaard, J., Nygaard, H., Ingvorsen, C., Wulff, E. M., . . . Fledelius, C. (2018). Dietary fat stimulates development of NAFLD more potently than dietary fructose in Sprague–Dawley rats. *Diabetology & Metabolic Syndrome, 10*(1), 4-8.

Jiang, M., He, J., Gu, H., Yang, Y., Huang, Y., Xu, X., & Liu, L. (2020). Protective effect of resveratrol on obesity-related osteoarthritis via alleviating JAK2/STAT3 signaling pathway is independent of SOCS3. *Toxicology and Applied Pharmacology, 388*, 114871.

Jiao, Q., Wei, L., Chen, C., Li, P., Wang, X., Li, Y., . . . Wei, X. (2016). Cartilage oligomeric matrix protein and hyaluronic acid are sensitive serum biomarkers for early cartilage lesions in the knee joint. *Biomarkers, 21*(2), 146-151.

Jilka, R. L., Hangoc, G., Girasole, G., Passeri, G., Williams, D. C., Abrams, J. S., . . . Manolagas, S. C. (1992). Increased osteoclast development after estrogen loss: mediation by interleukin-6. *Science, 257*(5066), 88-91.

Jimenez, P. A., Glasson, S. S., & Trubetskoy, O. V. (1997). Spontaneous osteoarthritis in Dunkin Hartley guinea pigs: histologic, radiologic, and biochemical changes. *Lab Anim Sci, 47*, 598-601.

Johnston, I. G., & Williams, B. P. (2016). Evolutionary Inference across Eukaryotes Identifies Specific Pressures Favoring Mitochondrial Gene Retention. *Cell Systems, 2*(2), 101-111.

Jordan, K. M., Syddall, H. E., Garnero, P., Gineyts, E., Dennison, E. M., Sayer, A. A., . . . Arden, N. K. (2006). Urinary CTX-II and glucosyl-galactosyl-pyridinoline are associated with the presence and severity of radiographic knee osteoarthritis in men. *Annals of the Rheumatic Diseases, 65*(7), 871-877.

Kadowaki, T., & Yamauchi, T. (2005). Adiponectin and Adiponectin Receptors. *Endocrine Reviews, 26*(3), 439-451.

Kahveci, D., & Xu, X. (2011). Repeated hydrolysis process is effective for enrichment of omega 3 polyunsaturated fatty acids in salmon oil by Candida rugosa lipase. *Food Chemistry, 129*(4), 1552-1558.

Kamei, N., Tobe, K., Suzuki, R., Ohsugi, M., Watanabe, T., Kubota, N., . . . Kadowaki, T. (2006). Overexpression of Monocyte Chemoattractant Protein-1 in Adipose Tissues Causes Macrophage Recruitment and Insulin Resistance. *Journal of Biological Chemistry, 281*(36), 26602-26614.

Kanda, H., Tateya, S., & Tamori, Y. (2006). MCP-1 contributes to macrophage infiltration into adipose tissue, insulin resistance, and hepatic steatosis in obesity,. *Journal of Clinical Investigation, 116*(6), 1494-1505.

Kaneko, S., Satoh, T., Chiba, J., Ju, C., Inoue, K., & Kagawa, J. (2000). Interleukin–6 and interleukin–8 levels in serum and synovial fluid of patients with osteoarthritis. *Cytokines, Cellular & Molecular Therapy, 6*(2), 71-79.

Kang, S. J., Choi, B. R., Kim, S. H., Yi, H. Y., Park, H. R., Kim, D. C., . . . Lee, Y. J. (2015). Dried Pomegranate Potentiates Anti-Osteoporotic and Anti-Obesity Activities of Red Clover Dry Extracts in Ovariectomised Rats. *Nutrients, 7*(4), 2622-2647.

Karsdal, M. A., Byrjalsen, I., Alexandersen, P., Bihlet, A., Andersen, J. R., Riis, B. J., . . . Christiansen, C. (2015). Treatment of symptomatic knee osteoarthritis with oral salmon calcitonin: results from two phase 3 trials. *Osteoarthritis and Cartilage, 23*(4), 532-543.

Karsdal, M. A., Leeming, D. J., Dam, E. B., Henriksen, K., Alexandersen, P., Pastoureau, P., . . . Christiansen, C. (2008). Should subchondral bone turnover be targeted when treating osteoarthritis? *Osteoarthritis and Cartilage, 16*(6), 638-646.

Karuppal, R. (2017). Current concepts in the articular cartilage repair and regeneration. *Journal of Orthopaedics, 14*(2), A1-A3.

Karvonen-Gutierrez, C. A., Harlow, S. D., Mancuso, P., Jacobson, J., Mendes de Leon, C. F., & Nan, B. (2013). Association of leptin levels with radiographic knee osteoarthritis among a cohort of midlife women. *Arthritis Care & Research, 65*(6), 936-944.

Kasonga, A. E., Kruger, M. C., & Coetzee, M. (2019). Free fatty acid receptor 4-β-arrestin 2 pathway mediates the effects of different classes of unsaturated fatty acids in osteoclasts and osteoblasts. *Biochimica et Biophysica Acta (BBA) - Molecular and Cell Biology of Lipids, 1864*(3), 281-289.

Ke, X., Jin, G., Yang, Y., Cao, X., Fang, R., Feng, X., & Lei, B. (2015). Synovial Fluid HMGB-1 Levels are Associated with Osteoarthritis Severity. *Clínica y Laboratorio, 61*(7), 809-818.

Kelley, D. E., Thaete, F. L., Troost, F., Huwe, T., & Goodpaster, B. H. (2000). Subdivisions of subcutaneous abdominal adipose tissue and insulin resistance. *American Journal Of Physiology-Endocrinology And Metabolism, 278*, 941-948.

Kemi, O. J., & Ellingsen, Ø. (2012). Cardiac Hypertrophy, Physiological. In F. C. Mooren (Ed.), *Encyclopedia of Exercise Medicine in Health and Disease* (pp. 171-175). Berlin, Heidelberg: Springer Berlin Heidelberg.

Kemp, G. J., Birrell, F., Clegg, P. D., Cuthbertson, D. J., De Vito, G., van Dieën, J. H., . . . Mathers, J. C. (2018). Developing a toolkit for the assessment and monitoring of musculoskeletal ageing. *Age and Ageing, 47*(4), 1-19.

Khan, H. M., Ashraf, M., Hashmi, A. S., Ahmad, M.-u.-D., & Anjum, A. A. (2014). Relationship between Disease Activity and Circulating Level of Collagen II C-Telopeptide Fragments in Papain Induced Osteoarthritis Rat Model. *Pakistan Veterinary Journal, 34*(1), 92-95.

Khan, N. M., Clifton, K. B., Lorenzo, J., Hansen, M. F., & Drissi, H. (2020). Comparative transcriptomic analysis identifies distinct molecular signatures and regulatory networks of chondroclasts and osteoclasts. *Arthritis Research & Therapy*, 22(1), 1-14.

Khosla, S., Oursler, M. J., & Monroe, D. G. (2012). Estrogen and the skeleton. *Trends in endocrinology and metabolism: TEM, 23*(11), 576-581.

Kim, H. J., Ohk, B., Yoon, H. J., Kang, W. Y., Seong, S. J., Kim, S. Y., & Yoon, Y. R. (2017). Docosahexaenoic acid signaling attenuates the proliferation and differentiation of bone marrow-derived osteoclast precursors and promotes apoptosis in mature osteoclasts. *Cellular Signalling, 29*, 226-232.

Kim, J. H., & Kim, N. (2014). Regulation of NFATc1 in Osteoclast Differentiation. *Journal of bone metabolism, 21*(4), 233-241.

Kimura, I., Ichimura, A., Ohue-Kitano, R., & Igarashi, M. (2020). Free Fatty Acid Receptors in Health and Disease. *Physiological Reviews, 100*(1), 171-210.

King, L. K., March, L., & Anandacoomarasamy, A. (2013). Obesity & osteoarthritis. *Indian Journal of Medical Research, 138*(2), 185-193.

Kinjo, M., Setoguchi, S., & Solomon, D. H. (2007). Bone mineral density in adults with the metabolic syndrome: Analysis in a population-based U.S. sample. *J. Clin. Endocrinol. Metab., 92*, 4161–4164.

Kloppenburg, M., & Berenbaum, F. (2020). Osteoarthritis year in review 2019: epidemiology and therapy. *Osteoarthritis and Cartilage, 28*(3), 242-248.

Knott, L., Avery, N. C., Hollander, A. P., & Tarlton, J. F. (2011). Regulation of osteoarthritis by omega-3 (n-3) polyunsaturated fatty acids in a naturally occurring model of disease. *Osteoarthritis Cartilage, 19*(9), 1150-1157.

Knowles, H. J., Moskovsky, L., Thompson, M. S., Grunhen, J., Cheng, X., & Kashima, T. G. (2012). Chondroclasts are mature osteoclasts which are capable of cartilage matrix resorption. *Virchows Arch, 461*, 205-210.

Koboziev, I., Scoggin, S., Gong, X., Mirzaei, P., Zabet-Moghaddam, M., Yosofvand, M., . . . Moustaid-Moussa, N. (2020). Effects of Curcumin in a Mouse Model of Very High Fat Diet-Induced Obesity. *Biomolecules, 10*(10), 1368.

Koebele, S. V., & Bimonte-Nelson, H. A. (2016). Modeling menopause: The utility of rodents in translational behavioral endocrinology research. *Maturitas, 87*, 5-17.

Komprda, T. (2012). Eicosapentaenoic and docosahexaenoic acids as inflammation-modulating and lipid homeostasis influencing nutraceuticals: A review. *Journal of Functional Foods, 4*(1), 25-38.

Kopp, H. P., Krzyzanowska, K., Mohlig, M., Spranger, J., Pfeiffer, A. F. H., & Schernthaner, G. (2005). Effects of marked weight loss on plasma levels of adiponectin, markers of chronic subclinical inflammation and insulin resistance in morbidly obese women. *International Journal of Obesity, 29*, 766-771.

Kota, S. K., Krishna, S. V. S., Lakhtakia, S., & Modi, K. D. (2013). Metabolic pancreatitis: Etiopathogenesis and management. *Indian Journal of Endocrinology and Metabolism, 17*(5), 799-805.

Kousteni S, Bellido T, Plotkin LI, O'Brien CA, Bodenner DL, Han L, Han K, DiGregorio GB, Katzenellenbogen JA, Katzenellenbogen BS, Roberson PK, Weinstein RS, Jilka RL, Manolagas SC. (2001). Nongenotropic, sex-nonspecific signaling through the estrogen or androgen receptors: dissociation from transcriptional activity. *Cell, 104*, 719–730.

Kousteni S, Han L, Chen JR, Almeida M, Plotkin LI, Bellido T, Manolagas SC. (2003). Kinase-mediated regulation of common transcription factors accounts for the bone-protective effects of sex steroids. *J Clin Invest, 111*, 1651–1664.

Kouyama, K., Miyake, K., Zenibayashi, M., & et al. (2007). Association of serum MCP-1 concentration and MCP-1 polymorphism with insulin resistance in Japanese individuals with obese type 2 diabetes. *Kobe Journal of Medical Sciences, 53*(6), 345–354,.

Kraus, V. B., Blanco, F. J., Englund, M., Karsdal. M.A, & Lohmander, L. S. (2015). Call for standardized definitions of osteoarthritis and risk stratification for clinical trials and clinical use. *Osteoarthritis Cartilage, 23*(8), 1233-1241.

Krautkramer, K. A., Kreznar, J. H., Romano, K. A., Vivas, E. I., Barrett-Wilt, G. A., Rabaglia, M. E., . . . Denu, J. M. (2016). Diet-Microbiota Interactions Mediate Global Epigenetic Programming in Multiple Host Tissues. *Molecular Cell, 64*(5), 982-992.

Kris-Etherton, P. M., Innis, S. M., Assocition, A. D., & Canada, D. O. (2007). Position of the American Dietetic Association and Dietitians of Canada: dietary fatty acids. *Journal of the American Dietetic Association, 109*(9), 1599-1611.

Kruger, M. C., & Morel, P. C. H. (2016). Experimental control for the ovariectomised rat model: Use of sham versus nonmanipulated animal. *Journal of Applied Animal Welfare Science, 19*(1), 73-80.

Kruger, M. C., & Schollum, L. M. (2005). Is docosahexaenoic acid more effective than eicosapentaenoic acid for increasing calcium bioavailability? *Prostaglandins, Leukotrienes and Essential Fatty Acids (PLEFA), 73*(5), 327-334.

Kuyinu, E. L., Narayanan, G., Nair, L. S., & Laurencin, C. T. (2016). Animal models of osteoarthritis: classification, update, and measurement of outcomes. *Journal of Orthopaedic Surgery & Research, 11*, 1-27.

Kwon, H.-y., Rhyu, M.-r., & Lee, Y.-J. (2008). *The Effects of Cirsium japonicum on Lipid Profile in Ovariectomised Rats*.

Lago, R., Gomez, R., Otero, M., Lago, F., Gallego, R., Dieguez, C., . . . Gualillo, O. (2008). A new player in cartilage homeostasis: adiponectin induces nitric oxide synthase type II and pro-inflammatory cytokines in chondrocytes. *Osteoarthritis Cartilage, 16*, 1101-1109.

Lajeunesse, D., & Reboul, P. (2003). Subchondral bone in osteoarthritis: a biologic link with articular cartilage leading to abnormal remodeling. *Current Opinion in Rheumatology, 15*(5), 628-633.

Lampropoulou-Adamidou, K., Lelovas, P., & Karadimas, E. V. (2014). Useful animal models for the research of osteoarthritis. *Eur J Orthop Surg Traumatol, 24*(3), 263–271.

Langille, M. G., Meehan, C. J., Koenig, J. E., Dhanani, A. S., Rose, R. A., Howlett, S. E., & Beiko, R. G. (2014). Microbial shifts in the aging mouse gut. *Microbiome, 2*(1), 50-50.

Large, V., Peroni, O., Letexier, D., Ray, H., & Beylot, M. (2004). Metabolism of lipids in human white adipocyte. *Diabetes and Metabolism, 30*(4), 294-309.

Layé, S., Nadjar, A., Joffre, C., & Bazinet, R. P. (2018). Anti-inflammatory effects of omega-3 fatty acids in the brain: Physiological mechanisms and relevance to pharmacology. *Pharmacological Reviews, 70*(1), 12-38.

Leal-Díaz, A. M., Noriega, L. G., Torre-Villalvazo, I., Torres, N., Alemán-Escondrillas, G., López-Romero, P., . . . Tovar, A. R. (2016). Aguamiel concentrate from Agave salmiana and its extracted saponins attenuated obesity and hepatic steatosis and increased Akkermansia muciniphila in C57BL6 mice. *Scientific Reports, 6*(1), 34242.

Lee, H., Lee, Y., Kim, J., An, J., Lee, S., Kong, H., . . . Kim, K. (2018). Modulation of the gut microbiota by metformin improves metabolic profiles in aged obese mice. *Gut Microbes, 9*(2), 155-165.

Lee, Y. H., Song, G. G., & Bae, S. C. (2012). Omega-3 Polyunsaturated Fatty Acids and the Treatment of Rheumatoid Arthritis: A Meta-analysis. *Archives of Medical Research, 43*(5), 356-362.

Lelovas, P. P., Xanthos, T. T., Thoma, S. E., Lyritis, G. P., & Dontas, I. A. (2008). The laboratory rat as an animal model for osteoporosis research. *Comparative Medicine, 58*(5), 424-430.

Leopoldo, A. S., Sugizaki, M. M., Lima-Leopoldo, A. P., do Nascimento, A. F., Luvizotto, R. d. A. M., de Campos, D. H. S., . . . Cicogna, A. C. (2010). Cardiac remodeling in a rat model of diet-induced obesity. *The Canadian journal of cardiology, 26*(8), 423-429.

Lewinson, D., & Silbermann, M. (1992). Chondroclasts and endothelial cells collaborate in the process of cartilage rsorption. *The Anatomical Record,* 233, 504-514.

Ley, R. E., Backhed, F., Turnbaugh, P., Lozupone, C. A., Knight, R. D., & Gordon, J. I. (2005). Obesity alters gut microbial ecology. *Proc Natl Acad Sci U S A, 102*(31), 11070-11075.

Li, C., Rui, C., Hua, W., & Fengxia, L. (2015). Mechanisms Linking Inflammation to Insulin Resistance. *International Journal of Endocrinology, 2015* (508409), 1-10

Li, G., Yin, J., Gao, J., Cheng, T. S., Pavlos, N. J., Zhang, C., & Zheng, M. H. (2013). Subchondral bone in osteoarthritis: insight into risk factors and microstructural changes. *Arthritis Research & Therapy, 15*, 223.

Liebertha, l. J., Sambamurthy, N., & Scanzello, C. R. (2015). Inflammation in joint injury and post-traumatic osteoarthritis. *Osteoarthritis Cartilage, 23*, 1825-1834.

Little, C. B., & Zaki, S. (2012). What constitutes an ‘‘animal model of osteoarthritis’’: the need for consensus? *Osteoarthritis Cartilage, 20*(4), 261–267.

Litwic, A., Edwards, M. H., Dennison, E. M., & Cooper, C. (2013). Epidemiology and burden of osteoarthritis. *British Medical Bulletin, 105*, 185-199.

Liu, J., Han, L., Zhu, L., & Yu, Y. (2016). Free fatty acids, not triglycerides, are associated with non-alcoholic liver injury progression in high fat diet induced obese rats. *Lipids in Health and Disease, 15*(1), 27-37.

Liu, X., Machado, G. C., Eyles, J. P., Ravi, V., & Hunter, D. J. (2018). Dietary supplements for treating osteoarthritis: a systematic review and meta-analysis. *British Journal of Sports Medicine, 52*(3), 167-175.

Lizcano, F., & Guzmán, G. (2014). Estrogen Deficiency and the Origin of Obesity during Menopause. *BioMed research international, 2014*, 757461-757461.

Lofvall, H., Newbould, H., Karsdal, M. A., Dziegiel, M. H., Richter, J., Henriksen, K., & Thudium, C. S. (2018). Osteoclasts degrade bone and cartilage knee joint compartments through different resorption processes. *Arthritis Research & Therapy, 20*, 1564-1575

Logar, D. B., Komadina, R., Preželj, J., Ostanek, B., Trošt, Z., & Marc, J. (2007). Expression of bone resorption genes in osteoarthritis and in osteoporosis. *Journal of Bone and Mineral Metabolism, 25*(4), 219-225.

Louis, P., Young, P., Holtrop, G., & Flint, H. J. (2010). Diversity of human colonic butyrate-producing bacteria revealed by analysis of the butyryl-CoA:acetate CoA-transferase gene. *Environmental Microbiology, 12*(2), 304-314.

Lovejoy, J. C., Champagne, C. M., de Jonge, L., Xie, H., & Smith, S. R. (2008). Increased visceral fat and decreased energy expenditure during the menopausal transition. *International Journal of Obesity, 32*(6), 949-958.

Lu, Y., Ho, C. S., Liu, X., Chua, A. N., Wang, W., McIntyre, R. S., & Ho, R. C. (2017). Chronic administration of fluoxetine and pro-inflammatory cytokine change in a rat model of depression. *PLoS One, 12*(10), 1-14.

Lubkowska, A., Dobek, A., Mieszkowski, J., Garczynski, W., & Chlubek, D. (2014). Adiponectin as a Biomarker of Osteoporosis in Postmenopausal Women: Controversies. *Disease Markers*, 1-14.

Lutz, T. A., & Woods, S. C. (2012). Overview of animal models of obesity. *Current Protocols in Pharmacology, 58*, 1-22.

Lyons, T. J., McClure, S. F., Stoddart, R. W., & McClure, J. (2006). The normal human chondro-osseous junctional region: evidence for contact of uncalcified cartilage with subchondral bone and marrow spaces. *BMC Musculoskeletal Disorders, 7*, 52-52.

Ma, H. L., Blanchet, T. J., Peluso, D., Hopkins, B., Morris, E. A., & Glasson, S. S. (2007). Osteoarthritis severity is sex dependent in a surgical mouse model. *Osteoarthritis and Cartilage, 15*(6), 695-700.

Mabey, T., Honsawek, S., Tanavalee, A., Yuktanandana, P., Wilairatana, V., & Poovorawan, Y. (2016). Plasma and synovial fluid inflammatory cytokine profiles in primary knee osteoarthritis. *Biomarkers, 21*(7), 639-644.

Magna, M., & Pisetsky, D. S. (2014). The role of HMGB1 in the pathogenesis of inflammatory and autoimmune diseases. *Molecular medicine (Cambridge, Mass.), 20*(1), 138-146.

Mahaling, D. U., Basavaraj, M. M., & Bika, A. J. (2013). Comparison of lipid profile in different grades of non-alcoholic fatty liver disease diagnosed on ultrasound. *Asian Pacific Journal of Tropical Biomedicine, 3*(11), 907-912.

Malfait, A. M. (2016). Osteoarthritis year in review 2015: biology. *Osteoarthritis Cartilage, 24*(1), 21-26.

Mankin, H. J., Dorfman, H., Lippiello, L., & Zarins, A. (1971). Biochemical and metabolic abnormalities in articular cartilage from osteo-arthritic human hips. II. Correlation of morphology with biochemical and metabolic data. *J Bone Joint Surg Am, 53*(3), 523-537.

Manolopoulos, K. N., Karpe, F., & Frayn, K. N. (2010). Gluteofemoral body fat as a determinant of metabolic health. *International Journal of Obesity, 34*, 949-959.

Marchesi, J. R., Adams, D. H., Fava, F., Hermes, G. D. A., Hirschfield, G. M., Hold, G., . . . Hart, A. (2016). The gut microbiota and host health: a new clinical frontier. *Gut, 65*(2), 330-339.

Marino, S., Logan, J. G., Mellis, D., & Capulli, M. (2014). Generation and culture of osteoclasts. *BoneKEy reports, 3*, 570-570.

Mastaglia, S. R., Pellegrini, G. G., Mandalunis, P. M., Gonzales Chaves, M. M., Friedman, S. M., & Zeni, S. N. (2006). Vitamin D insufficiency reduces the protective effect of bisphosphonate on ovariectomy-induced bone loss in rats. *Bone, 39*(4), 837-844.

McCoy, A. (2015). Animal models of osteoarthritis: Comparisons and key considerations. *Veterinary Pathology, 52*(5), 803-818.

McPhee, S., Hodges, L. D., Wright, P. F. A., Wynne, P. M., Kalafatis, N., Harney, D. W., & Macrides, T. A. (2007). Anti-cyclooxygenase effects of lipid extracts from the New Zealand green-lipped mussel, Perna canaliculus. *Comparative Biochemistry and Physiology, Part B, 146*, 346-356.

Meijer, B., Gearry, R. B., & Day, A. S. (2012). The role of S100A12 as a systemic marker of inflammation. *International journal of inflammation, 2012*, 907078-907078.

Meirow, Y., & Baniyash, M. (2017). Immune biomarkers for chronic inflammation related complications in non-cancerous and cancerous diseases. *Cancer Immunol Immunother, 66*, 1089-1101.

Mells, J. E., Fu, P. P., Kumar, P., Smith, T., Karpen, S. J., & Anania, F. A. (2015). Saturated fat and cholesterol are critical to inducing murine metabolic syndrome with robust nonalcoholic steatohepatitis. *J Nutr Biochem, 26*(3), 285-292.

Messina, O. D., Vidal Wilman, M., & Vidal Neira, L. F. (2019). Nutrition, osteoarthritis and cartilage metabolism. *Aging Clinical and Experimental Research, 31*(6), 807.

Meulenbelt, I., Kloppenburg, M., Kroon, H. M., Houwing-Duistermaat, J. J., Garnero, P., & Hellio Le Graverand, M. P. (2006). Urinary CTX-II levels are associated with radiographic subtypes of osteoarthritis in hip, knee, hand, and facet joints in subject with familial osteoarthritis at multiple sites: the GARP study. *Ann Rheum Dis, 65*, 360-365.

Meyer, E. G., Baumer, T. G., Slade, J. M., Smith, W. E., & Haut, R. C. (2008). Tibiofemoral Contact Pressures and Osteochondral Microtrauma during Anterior Cruciate Ligament Rupture Due to Excessive Compressive Loading and Internal

Torque of the Human Knee. *The American Journal of Sports Medicine, 36*(10), 1966-1977.
Miller, M. R., Kruger, M. C., Wynne, C., Waaka, D., Li, W., Frampton, C., . . . Eason, C. (2020). Bioavailability of Orally Administered Active Lipid Compounds from four Different Greenshell™ Mussel Formats. *Marine Drugs, 18*(11), 524.
Miller, M., Perry, N., Burgess, E., & Marshall, S. (2011a). Regiospecific Analyses of Triacylglycerols of Hoki (Macruronus novaezelandiae) and Greenshell™ Mussel (Perna canaliculus). *Journal of the American Oil Chemists' Society (JAOCS), 88*(4), 509-516.
Miller, M. R., Pearce, L., & Bettjeman, B. I. (2014a). Detailed Distribution of Lipids in Greenshell™ Mussel (Perna canaliculus). *Nutrients, 6*(4), 1454-1474.
Miller, M. R., Perry, N., Burgess, E., & Marshall, S. (2011b). Regiospecific analyses of triacylglycerols of hoki (Macruronus novaezelandiae) and Greenshell™ mussel (Perna canaliculus). *Journal of the American Oil Chemists Society, 88*, 509-515.
Miller, R. E., Miller, R. J., & Malfait, A.-M. (2014b). Osteoarthritis joint pain: the cytokine connection. *Cytokine, 70*(2), 185-193.
Mitchell, N. S., Catenacci, V. A., Wyatt, H. R., & Hill, J. O. (2011). Obesity: Overview of an Epidemic. *Psychiatric Clinics of North America, 34*(4), 717-732.
Mobasheri, A., Bay-Jensen, A. C., van Spil, W. E., Larkin, J., & Levesque, M. C. (2017). Osteoarthritis Year in Review 2016: biomarkers (biochemical markers). *Osteoarthritis and Cartilage, 25*(2), 199-208.
Montague, C. T., Farooqi, I. S., Whitehead, J. P., Soos, M. A., Rau, H., Wareham, N. J., . . . O'Rahilly, S. (1997). Congenital leptin deficiency is associated with severe early-onset obesity in humans. *Nature, 387*(6636), 903-908.
Morrisette-Thomas, V., Cohen, A. A., Fülöp, T., Riesco, É., Legault, V., Li, Q., . . . Ferrucci, L. (2014). Inflamm-aging does not simply reflect increases in pro-inflammatory markers. *Mechanisms of Ageing and Development, 139*, 49-57.
Morrison, D. J., & Preston, T. (2016). Formation of short chain fatty acids by the gut microbiota and their impact on human metabolism. *Gut Microbes, 7*(3), 189-200.
Muccioli, G. G., Naslain, D., Bäckhed, F., Reigstad, C. S., Lambert, D. M., Delzenne, N. M., & Cani, P. D. (2010). The endocannabinoid system links gut microbiota to adipogenesis. *Molecular Systems Biology, 6*, 392-392.
Mulet, T., Picó, C., Oliver, P., & Palou, A. (2003). Blood leptin homeostasis: sex-associated differences in circulating leptin levels in rats are independent of tissue leptin expression. *The International Journal of Biochemistry & Cell Biology, 35*(1), 104-110.
Murat, N., Karadam, B., Ozkal, S., Karatosun, V., & Gidener, S. (2007). [Quantification of papain-induced rat osteoarthritis in relation to time with the Mankin score]. *Acta Orthopaedica et Traumatologica Turcica, 41*(3), 233-237.
Muzumdar, R., Allison, D. B., Huffman, D. M., Ma, X., Atzmon, G., Einstein, F. H., . . . Barzilai, N. (2008). Visceral adipose tissue modulates mammalian longevity. *Aging Cell, 7*(3), 438-440.
National Institutes of Health. (2020). Omega-3 fatty Acids: Fact sheet for health professionals. Retrieved May, 05 2020 from https://ods.od.nih.gov/factsheets/Omega3FattyAcids-HealthProfessional/
Nefla, M., Berenbaum, F., Jacques, C., & Holzinger, D. (2016). The danger from within: Alarmins in arthritis. *Nature Reviews Rheumatology, 12*(11), 669-683.
Neumann, E., Junker, S., Schett, G., Frommer, K., & Müller-Ladner, U. (2016). Adipokines in bone disease. *Nature Reviews Rheumatology, 12*(5), 296-302.

Nio, Y., Yamauchi, T., Iwabu, M., & et al. (2012). Monocyte chemoattractant protein-1 (MCP-1) deficiency enhances alternatively activated M2 macrophages and ameliorates insulin resistance and fatty liver in lipoatrophic diabetic A-ZIP transgenic mice. *Diabetologia Croatica, 55*(12), 3350–3358.

Noble, B.S., Peet, N., Stevens, H.Y., Brabbs, A., Mosley, J.R. (2003). Mechanical loading: biphasic osteocyte survival and targeting of osteoclasts for bone destruction in rat cortical bone. *Am J Physiol Cell Physiol, 284*, 934–943.

Noriega, B. S., Sanchez-Gonzalez, M. A., Salyakina, D., & Coffman, J. (2016). Understanding the Impact of Omega-3 Rich Diet on the Gut Microbiota. *Case Rep Med, 2016*, 3089303.

Norling, L. V., & Perretti, M. (2013). The role of omega-3 derived resolvins in arthritis. *Current Opinion in Pharmacology, 13*(3), 476-481.

Nuttall, M. E., Bradbeer, J. N., Stroup, G. B., Nadeau, D. P., Hoffman, S. J., Zhao, H., . . . Gowen, M. (1998). Idoxifene: A Novel Selective Estrogen Receptor Modulator Prevents Bone Loss and Lowers Cholesterol Levels in Ovariectomised Rats and Decreases Uterine Weight in Intact Rats. *Endocrinology, 139*(12), 5224-5234.

Odamaki, T., Kato, K., Sugahara, H., Hashikura, N., Takahashi, S., Xiao, J.-z., . . . Osawa, R. (2016). Age-related changes in gut microbiota composition from newborn to centenarian: a cross-sectional study. *BMC Microbiology, 16*(1), 90-99.

Oestergaard, S., Sondergaard, B. C., Hoegh-Andersen, P., Henriksen, K., Qvist, P., Christiansen, C., . . . Karsdal, M. A. (2006). Effects of ovariectomy and estrogen therapy on type II collagen degradation and structural integrity of articular cartilage in rats - Implications of the time of initiation. *Arthritis And Rheumatism, 54*, 2441-2451.

Oh, D. Y., Talukdar, S., Bae, E. J., Imamura, T., Morinaga, H., Fan, W., . . . Olefsky, J. M. (2010). GPR120 Is an Omega-3 Fatty Acid Receptor Mediating Potent Anti-inflammatory and Insulin-Sensitizing Effects. *Cell, 142*(5), 687-698.

Ohashi, K., Parker, J. L., Ouchi, N., Higuchi, A., Vita, J. A., Gokce, N., . . . Walsh, K. (2010). Adiponectin Promotes Macrophage Polarization toward an Anti-inflammatory Phenotype. *Journal of Biological Chemistry, 285*(9), 6153-6160.

Ohlsson, C., Engdahl, C., Fåk, F., Andersson, A., Windahl, S. H., Farman, H. H., . . . Sjögren, K. (2014). Probiotics protect mice from ovariectomy-induced cortical bone loss. *PLoS One, 9*(3), 92368-92368.

Ojo, B., El-Rassi, G. D., Payton, M. E., Perkins-Veazie, P., Clarke, S., Smith, B. J., & Lucas, E. A. (2016). Mango Supplementation Modulates Gut Microbial Dysbiosis and Short-Chain Fatty Acid Production Independent of Body Weight Reduction in C57BL/6 Mice Fed a High-Fat Diet. *The Journal of Nutrition, 146*(8), 1483-1491.

Oppenheim, J. J., & Yang, D. (2005). Alarmins: chemotactic activators of immune responses. *Current Opinion in Immunology, 17*(4), 359-365.

Ouchi, N., Kihara, S., Arita, Y., Okamoto, Y., Maeda, K., Kuriyama, H., . . . Matsuzawa, Y. (2000). Adiponectin, an Adipocyte-Derived Plasma Protein, Inhibits Endothelial NF-κB Signaling Through a cAMP-Dependent Pathway. *Circulation, 102*(11), 1296-1301.

Parisi, L., Gini, E., Baci, D., Tremolati, M., Fanuli, M., Bassani, B., . . . Mortara, L. (2018). Macrophage polarization in chronic inflammatory diseases: killers or builders? *Journal of Immunology Research, 1*, 25.

Parolini, C. (2019). Effects of fish n-3 pufas on intestinal microbiota and immune system. *Mar Drugs, 17*(6), 374.

Patell, R., Dosi, R., Joshi, H., Sheth, S., Shah, P., & Jasdanwala, S. (2014). Non-Alcoholic Fatty Liver Disease (NAFLD) in Obesity. *J Clin Diagn Res, 8*(1), 62-66.

Patrone, V., Ferrari, S., Lizier, M., Lucchini, F., Minuti, A., Tondelli, B., . . . Callegari, M. L. (2012). Short-term modifications in the distal gut microbiota of weaning mice induced by a high-fat diet. *Microbiology, 158*(4), 983-992

Pearson, M. J., Herndler-Brandstetter, D., Tariq, M. A., Nicholson, T. A., Philp, A. M., Smith, H. L., . . . Lord, J. M. (2017). IL-6 secretion in osteoarthritis patients is mediated by chondrocyte-synovial fibroblast cross-talk and is enhanced by obesity. *Sci Rep, 7*(1), 3451-3461.

Pelletier, J. P., Boileau, C., Brunet, J., Boily, M., Lajeunesse, D., Reboul, P., . . . Laufer, S. (2004). The inhibition of subchondral bone resorption in the early phase of experimental dog osteoarthritis by licofelone is associated with a reduction in the synthesis of MMP-13 and cathepsin K. *Bone, 34*(3), 527-538.

Petersen, K. K., Siebuhr, A. S., Graven-Nielsen, T., Simonsen, O., Boesen, M., Gudbergsen, H., . . . Arendt-Nielsen, L. (2016). Sensitization and Serological Biomarkers in Knee Osteoarthritis Patients With Different Degrees of Synovitis. *The Clinical Journal of Pain, 32*(10), 841-848.

Pietschmann, P., Gollob, E., Brosch, S., Hahn, P., Kudlacek, S., Willheim, M., . . . Tragl, K. H. (2003). The effect of age and gender on cytokine production by human peripheral blood mononuclear cells and markers of bone metabolism. *Experimental Gerontology, 38*(10), 1119-1127.

Pingali, P. L. (2012). Green Revolution: Impacts, limits, and the path ahead. *Proceedings of the National Academy of Sciences, 109*(31), 12302-12308.

Pitroda, A. P., Harris, S. S., & Dawson-Hughes, B. (2009). The association of adiposity with parathyroid hormone in healthy older adults. *Endocrine, 36*(2), 218-228.

Pollard, B., Guilford, W. G., Ankenbauer-Perkins, K. L., & Hedderley, D. (2006). Clinical efficacy and tolerance of an extract of green-lipped mussel (Perna canaliculus) in dogs presumptively diagnosed with degenerative joint disease. *N Z Vet J, 54*(3), 114-118.

Poole, A. R., Ionescu, M., Swan, A., & Dieppe, P. A. (1994). Changes in cartilage metabolism in arthritis are reflected by altered serum and synovial-fluid levels of the cartilage proteoglycan aggrecan - implications for pathogenesis. *Journal of Clinical Investigation, 94*, 25-33.

Poulet, B., Westerhof, T. A., & Hamilton, R. W. (2013). Spontaneous osteoarthritis in Str/ort mice is unlikely due to greater vulnerability to mechanical trauma. *Osteoarthritis Cartilage, 21*, 756-763.

Pradhan, A. (2007). Obesity, metabolic syndrome, and type 2 diabetes: inflammatory basis of glucose metabolic disorders. *Nutrition Review, 65*(2), 152-156.

Pranprawit, A., Wolber, F. M., Heyes, J. A., Molan, A. L., & Kruger, M. C. (2013). Short-term and long-term effects of excessive consumption of saturated fats and/or sucrose on metabolic variables in Sprague Dawley rats: a pilot study. *Journal Of The Science Of Food And Agriculture, 93*(13), 3191-3197.

Prieto-Alhambra, D., Premaor, M. O., Fina Avilés, F., Hermosilla, E., Martinez-Laguna, D., Carbonell-Abella, C., . . . Díez-Pérez, A. (2012). The association between fracture and obesity is site-dependent: A population-based study in postmenopausal women. *Journal of Bone and Mineral Research, 27*(2), 294-300.

Priyadarshini, M., Wicksteed, B., Schiltz, G. E., Gilchrist, A., & Layden, B. T. (2016). SCFA Receptors in Pancreatic β Cells: Novel Diabetes Targets? *Trends in endocrinology and metabolism: TEM, 27*(9), 653-664.

Punia, S., Sandhu, K. S., Siroha, A. K., & Dhull, S. B. (2019). Omega 3-metabolism, absorption, bioavailability and health benefits–A review. *PharmaNutrition, 10*, 100162.

Puri, P., Baillie, R. A., Wiest, M. M., Mirshahi, F., Choudhury, J., Cheung, O., . . . Sanyal, A. J. (2007). A lipidomic analysis of nonalcoholic fatty liver disease. *Hepatology, 46*(4), 1081-1090.

Pusceddu, M. M., El Aidy, S., Crispie, F., O'Sullivan, O., Cotter, P., Stanton, C., . . . Dinan, T. G. (2015). N-3 Polyunsaturated Fatty Acids (PUFAs) Reverse the Impact of Early-Life Stress on the Gut Microbiota. *PLoS One, 10*(10), 139721-139721.

Ràfols, M. E. (2014). Adipose tissue: Cell heterogeneity and functional diversity. *Endocrinol Nutr., 61*(2), 100-112.

Rahman, M. M., Bhattacharya, A., & Fernandes, G. (2008). Docosahexaenoic acid is more potent inhibitor of osteoclast differentiation in RAW 264.7 cells than eicosapentaenoic acid. *Journal of Cellular Physiology*, 214(1), 201-209.

Rajaei, E., Mowla, K., Ghorbani, A., Bahadoram, S., Bahadoram, M., & Dargahi-Malamir, M. (2015). The Effect of Omega-3 Fatty Acids in Patients With Active Rheumatoid Arthritis Receiving DMARDs Therapy: Double-Blind Randomized Controlled Trial. *Global journal of health science, 8*(7), 18-25.

Ranasinghe, P., Mathangasinghe, Y., Jayawardena, R., Hills, A. P., & Misra, A. (2017). Prevalence and trends of metabolic syndrome among adults in the asia-pacific region: a systematic review. *BMC Public Health, 17*(1), 101-111.

Rangel Silvares, R., Nunes Goulart da Silva Pereira, E., Eduardo Ilaquita Flores, E., Lino Rodrigues, K., Ribeiro Silva, A., Gonçalves-de-Albuquerque, C. F., & Daliry, A. (2019). High-fat diet-induced kidney alterations in rats with metabolic syndrome: endothelial dysfunction and decreased antioxidant defense. *Diabetes, metabolic syndrome and obesity : targets and therapy, 12*, 1773-1781.

Ravn, P., Cizza, G., Bjarnason, N. H., Thompson, D., Daley, M., & Wasnich, R. D. (1999). Lowbody mass index is an important risk factor for low bone mass and increased bone loss in early postmenopausalwomen. Early postmenopausal intervention cohort (EPIC) study group. . *J Bone Miner Res, 14*, 1622-1627.

Ravussin, Y., Koren, O., Spor, A., LeDuc, C., Gutman, R., Stombaugh, J., . . . Leibel, R. L. (2012). Responses of gut microbiota to diet composition and weight loss in lean and obese mice. *Obesity (Silver Spring), 20*(4), 738-747.

Reid, I. R. (2010). Fat and bone. *Archives of Biochemistry and Biophysics, 503*, 20-27.

Reverchon, M., Rame, C., Bertoldo, M., & Dupont, J. (2014). Adipokines and the Female Reproductive Tract. *International Journal of Endocrinology, 2014*, 1-10.

Richette, P., Poitou, C., Garnero, P., Vicaut, E., Bouillot, J., Lacorte, J. M., . . . Chevalier, X. (2011). Benefits of massive weight loss on symptoms, systemic inflammation and cartilage turnover in obese patients with knee osteoarthritis. *Annals of Rheumatic Diseases*(1), 139-149.

Richter, M., Trzeciak, T., Owecki, M., Pucher, A., & Kaczmarczyk, J. (2015). The role of adipocytokines in the pathogenesis of knee joint osteoarthritis. *International Orthopaedics, 39*(6), 1211-1217.

Riggs, B. L. (2000). The mechanisms of estrogen regulation of bone resorption. *The Journal of clinical investigation, 106*(10), 1203-1204.

Rittenberg, D., & Bloch, K. (1945). The utilization of acetic acid for the synthesis of fatty acids. *Journal of Biological Chemistry, 160*, 417-424.

Rizkalla, G., Reiner, A., Bogoch, E., & Poole, A. R. (1992). Studies of the articular cartilage proteoglycan aggrecan in health and osteoarthritis. Evidence for molecular heterogeneity and extensive molecular changes in disease. *The Journal of clinical investigation, 90*(6), 2268-2277.

Roberts, S., Weightman, B., Urban, J., & Chappell, D. (1986). Mechanical and biochemical properties of human articular cartilage in osteoarthritic femoral heads and in autopsy specimens. *Journal of Bone and Joint Surgery - Series B, 68*(2), 278-288.

Robling, A. G., Castillo, A. B., & Turner, C. H. (2006). Biomechanical and molecular regulation of bone remodeling. *Annu Rev Biomed Eng, 8*, 455-498.

Rodrigues, F. C., Castro, A. S., Rodrigues, V. C., Sérgio, A. F., Edimar, F. F., Tânia, T. O., . . . Célia, L. F. (2012). Yacon Flour and Bifidobacterium longum Modulate Bone Health in Rats. *Journal of Medicinal Food, 15*(7), 664-670.

Rolauffs, B., Williams, J. M., Aurich, M., Grodzinsky, A. J., Kuettner, K. E., & Cole, A. A. (2010). Proliferative remodeling of the spatial organization of human superficial chondrocytes distant from focal early osteoarthritis. *Arthritis And Rheumatism, 62*(2), 489-498.

Rosaria, M., Maria, P., Giuseppina Mattace, R., Emanuela, E., Anna, C., Anna, N., . . . Raffaele, D. C. (2004). Estrogen and raloxifene modulate leptin and its receptor in hypothalamus and adipose tissue from ovariectomised rats. *Endocrinology*(7), 3115.

Rosen, C. J., & Klibanski, A. (2009). Bone, fat, and body composition: evolving concepts in the pathogenesis of osteoporosis. *Am. J. Med., 122*, 409–414.

Rousseau, J. C., & Garnero, P. (2012). Biological markers in osteoarthritis. *Bone, 51*(2), 265-277.

Roy, E. J., & Wade, G. N. (1977). Role of food intake in estradiol-induced body weight changes in female rats. *Hormones and Behavior, 8*(3), 265-274.

Ruiz-Lopez, N., Usher, S., Sayanova, O. V., Napier, J. A., & Haslam, R. P. (2015). Modifying the lipid content and composition of plant seeds: engineering the production of LC-PUFA. *Applied Microbiology and Biotechnology, 99*, 143-154.

Ruse, M., Lambert, A., Robinson, N., Ryan, D., Shon, K.-J., & Eckert, R. L. (2001). S100A7, S100A10, and S100A11 Are Transglutaminase Substrates. *Biochemistry, 40*(10), 3167-3173. 10.

Säämänen, A. M., Hyttinen, M., & Vuorio, E. (2007). Analysis of arthritic lesions in the Del1 mouse: a model for osteoarthritis. *Methods in Molecular Medicine, 136*, 283–302.

Saini, R. K., & Keum, Y.-S. (2018). Omega-3 and omega-6 polyunsaturated fatty acids: Dietary sources, metabolism, and significance — A review. *Life Sciences, 203*, 255-267.

Saklayen, M. G. (2018). The Global Epidemic of the Metabolic Syndrome. *Current Hypertension Reports, 20*(2), 12-12.

Salazar, N., Arboleya, S., Valdés, L., Stanton, C., Ross, P., Ruiz, L., . . . de Los Reyes-Gavilán, C. G. (2014). The human intestinal microbiome at extreme ages of life. Dietary intervention as a way to counteract alterations. *Frontiers in genetics, 5*, 406-406.

Saltzman, E. T., Thomsen, M., Hall, S., & Vitetta, L. (2017). Perna canaliculus and the Intestinal Microbiome. *Marine Drugs, 15*(7), 1-13.

Scharstuhl, A., Vitters, E. L., Van der Kraan, P. M., & Van den Berg, W. B. (2003). Reduction of osteophyte formation and synovial thickening by adenoviral overexpression of transforming growth factor b/bone morphogenetic protein inhibitors during experimental osteoarthritis. *Arthritis Rheumatology, 48*, 3442-3451.

Schemmel, R., Mickelsen, O., & Mostosky, U. (1970). Influence of body weight, age, diet and sex on fat depots in rats. *Anatomical Record, 166*(3), 437-447.

Scheppach, W. (1994). Effects of short chain fatty acids on gut morphology and function. *Gut, 35*(1), 35-38.

Schneeberger, M., Everard, A., Gómez-Valadés, A. G., Matamoros, S., Ramírez, S., Delzenne, N. M., . . . Cani, P. D. (2015). Akkermansia muciniphila inversely correlates with the onset of inflammation, altered adipose tissue metabolism and metabolic disorders during obesity in mice. *Scientific Reports, 5*(1), 16643.

Scott, D., Chandrasekara, S. D., Laslett, L. L., Cicuttini, F., Ebeling, P. R., & Jones, G. (2016). Associations of sarcopenic obesity and dynapenic obesity with bone mineral density and incident fractures over 5-10 years in community-dwelling older adults. *Calcified Tissue International, 99*, 30-42.

Scott, D., Daly, R. M., Sanders, K. M., & Ebeling, P. R. (2015). Fall and fracture risk in sarcopenia and dynapenia with and without obesity: The role of lifestyle interventions. *Current Osteoporosis Reports, 13*, 235-244.

Scott, K. P., Martin, J. C., Campbell, G., Mayer, C.-D., & Flint, H. J. (2006). Whole-genome transcription profiling reveals genes up-regulated by growth on fucose in the human gut bacterium "Roseburia inulinivorans". *Journal of Bacteriology, 188*(12), 4340-4349.

Sekar, S., Shafie, S. R., Prasadam, I., Crawford, R., Panchal, S. K., Brown, L., & Xiao, Y. (2017). Saturated fatty acids induce development of both metabolic syndrome and osteoarthritis in rats. *Scientific Reports, 7* , 46457.

Senftleber, N. K., Nielsen, S. M., Andersen, J. R., Bliddal, H., Tarp, S., Lauritzen, L., . . . Christensen, R. (2017). Marine Oil Supplements for Arthritis Pain: A Systematic Review and Meta-Analysis of Randomized Trials. *Nutrients, 9*(1), 42-52.

Sheu, A., & Diamond, T. (2016). Bone mineral density: testing for osteoporosis. *Australian prescriber, 39*(2), 35-39.

Shi, H., Kokoeva, M. V., Inouye, K., Tzameli, I., Yin, H., & Flier, J. S. (2006). TLR4 links innate immunity and fatty acid-induced insulin resistance. *The Journal of clinical investigation, 116*(11), 3015-3025.

Shinmei, M., Ito, K., Matsuyama, S., Yoshihara, Y., & Matsuzawa, K. (1993). Joint fluid carboxyterminal type II procollagen peptide as a marker of cartilage collagen biosynthesis. *Osteoarthritis Cartilage, 1*, 121-128.

Shoelson, S. E., Lee, J., & Goldfine, A. B. (2006). Inflammation and insulin resistance. *The Journal of clinical investigation, 116*(7), 1793-1801.

Sigit, F. S., Tahapary, D. L., Trompet, S., Sartono, E., Willems van Dijk, K., Rosendaal, F. R., & de Mutsert, R. (2020). The prevalence of metabolic syndrome and its association with body fat distribution in middle-aged individuals from Indonesia and the Netherlands: a cross-sectional analysis of two population-based studies. *Diabetology & Metabolic Syndrome, 12*(1), 2-10.

Singh, M., Hodges, L. D., Wright, P. F. A., Cheah, D. M. Y., Wynne, P. M., Kalafatis, N., & Macrides, T. A. (2008). The CO2-SFE crude lipid extract and the free fatty acid extract from Perna canaliculus have anti-inflammatory effects on

adjuvant-induced arthritis in rats. *Comparative Biochemistry and Physiology Part B: Biochemistry and Molecular Biology, 149*(2), 251-258.

Siriarchavatana, P., Kruger, M. C., Miller, M. R., Tian, H. S., & Wolber, F. M. (2019). The Preventive Effects of Greenshell Mussel (Perna canaliculus) on Early-Stage Metabolic Osteoarthritis in Rats with Diet-Induced Obesity. *Nutrients, 11*(7), 1601.

Sjögren, K., Engdahl, C., Henning, P., Lerner, U. H., Tremaroli, V., Lagerquist, M. K., . . . Ohlsson, C. (2012). The gut microbiota regulates bone mass in mice. *Journal of bone and mineral research : the official journal of the American Society for Bone and Mineral Research, 27*(6), 1357-1367.

Smith, S. R., Lovejoy, J. C., Greenway, F., Ryan, D., deJonge, L., de la Bretonne, J., . . . Bray, G. A. (2001). Contributions of total body fat, abdominal subcutaneous adipose tissue compartments, and visceral adipose tissue to the metabolic complications of obesity. *Metabolism-Clinical And Experimental, 50*, 425-435.

Snijder, M. B., Visser, M., Dekker, J. M., Goodpaster, B. H., Harris, T. B., Kritchevsky, S. B., . . . for the Health, A. B. C. S. (2005). Low subcutaneous thigh fat is a risk factor for unfavourable glucose and lipid levels, independently of high abdominal fat. The Health ABC Study. *Diabetologia: Clinical and Experimental Diabetes and Metabolism, 48*(2), 301.

So, J.-S., Song, M.-K., Kwon, H.-K., Lee, C.-G., Chae, C.-S., Sahoo, A., . . . Im, S.-H. (2011). Lactobacillus casei enhances type II collagen/glucosamine-mediated suppression of inflammatory responses in experimental osteoarthritis. *Life Sciences, 88*(7), 358-366.

Sonnenburg, J. L., Xu, J., Leip, D. D., Chen, C.-H., Westover, B. P., Weatherford, J., . . . Gordon, J. I. (2005). Glycan Foraging in Vivo by an Intestine-Adapted Bacterial Symbiont. *Science, 307*(5717), 1955-1959.

Sookoian, S., & Pirola, C. J. (2017). Systematic review with meta-analysis: risk factors for non-alcoholic fatty liver disease suggest a shared altered metabolic and cardiovascular profile between lean and obese patients. *Alimentary Pharmacology and Therapeutics, 46*(2), 85-95.

Sornay-Rendu, E., Boutroy, S., Vilayphiou, N., Claustrat, B., & Chapurlat, R. D. (2013). In obese postmenopausal women, bone microarchitecture and strength are not commensurate to greater body weight: The os des femmes de lyon (OFELY) study. *Journal of Bone and Mineral Research, 28*, 1679-1687.

Sowers, M., Lachance, L., Jamadar, D., Hochberg, M. C., Hollis, B., Crutchfield, M., & Jannausch, M. L. (1999). The associations of bone mineral density and bone turnover markers with osteoarthritis of the hand and knee in pre- and perimenopausal women. *Arthritis & Rheumatism, 42*(3), 483-489.

Steppan, C. M., Crawford, D. T., Chidsey-Frink, K. L., Ke, H., & Swick, A. G. (2000). Leptin is a potent stimulator of bone growth in ob/ob mice. *Regul Pept, 92*(1-3), 73-78.

Stofkova, A. (2009). Leptin and adiponectin: from energy and metabolic dysbalance to inflammation and autoimmunity. *Endocrine Regulations, 43*(4), 157-168.

Streicher, C., Heyny, A., Andrukhova, O., Haigl, B., Slavic, S., Schüler, C., . . . Erben, R. G. (2017). Estrogen Regulates Bone Turnover by Targeting RANKL Expression in Bone Lining Cells. *Scientific Reports, 7*(1), 6460.

Suganami, T., Mieda, T., Itoh, M., Shimoda, Y., Kamei, Y., & Ogawa, Y. (2007). Attenuation of obesity-induced adipose tissue inflammation in C3H/HeJ mice carrying a Toll-like receptor 4 mutation. *Biochemical and Biophysical Research Communications, 354*(1), 45-49.

Sun, A. R., Panchal, S. K., Friis, T., Sekar, S., Crawford, R., Brown, L., . . . Prasadam, I. (2017). Obesity-associated metabolic syndrome spontaneously induces infiltration of pro-inflammatory macrophage in synovium and promotes osteoarthritis. *PLoS One, 12*(8), 1-22.

Sun, J., & Kato, I. (2016). Gut microbiota, inflammation and colorectal cancer. *Genes & Diseases, 3*(2), 130-143.

Suri, S., Gill, S. E., Massena de Camin, S., Wilson, D., McWilliams, D. F., & Walsh, D. A. (2007). Neurovascular invasion at the osteochondral junction and in osteophytes in osteoarthritis. *Annals of the Rheumatic Diseases, 66*(11), 1423-1428.

Suri, S., & Walsh, D. A. (2012). Original Full Length Article: Osteochondral alterations in osteoarthritis. *Bone, 51*, 204-211.

Tamura, T., Udagawa, N., Takahashi, N., Miyaura, C., Tanaka, S., Yamada, Y., . . . et, a. (1993). Soluble interleukin-6 receptor triggers osteoclast formation by interleukin 6. *Proceedings Of The National Academy Of Sciences Of The United States Of America, 90*(24), 11924-11928.

Tang, X., Liu, G., Kang, J., Hou, Y., Jiang, F., Yuan, W., & Shi, J. (2013). Obesity and risk of hip fracture in adults: a meta-analysis of prospective cohort studies. *PLoS One, 8*(4), 55077-55077.

Taniguchi, N., Yoshida, K., Ito, T., Tsuda, M., Mishima, Y., Furumatsu, T., . . . Asahara, H. (2007). Stage-specific secretion of HMGB1 in cartilage regulates endochondral ossification. *Molecular and Cellular Biology, 27*(16), 5650-5663.

Tat, S. K., Amiable, N., Pelletier, J.-P., Boileau, C., Lajeunesse, D., Duval, N., & Martel-Pelletier, J. (2009a). Modulation of OPG, RANK and RANKL by human chondrocytes and their implication during osteoarthritis. *Rheumatology (Oxford), 48*, 1482-1490.

Tat, S. K., Pelletier, J.-P., Velasco, C. R., Padrines, M., & Martel-Pelletier, J. (2009b). New Perspective in Osteoarthritis: The OPG and RANKL System as a Potential Therapeutic Target? *The Keio Journal of Medicine, 58*(1), 29-40.

Tazoe, H., Otomo, Y., Kaji, I., Tanaka, R., Karaki, S. I., & Kuwahara, A. (2008). Roles of short-chain fatty acids receptors, gpr41 and gpr43 on colonic functions. *Journal of Physiology and Pharmacology, 59*, 251-262.

Teichtahl, A. J., Wluka, A. E., Proietto, J., & Cicuttini, F. M. (2005). Obesity and the female sex, risk factors for knee osteoarthritis that may be attributable to systemic or local leptin biosynthesis and its cellular effects. *Medical Hypotheses, 65*, 312-315.

Teitelbaum, J. E., & Allan Walker, W. (2001). Review: The role of omega 3 fatty acids in intestinal inflammation. *Journal of Nutritional Biochemistry, 12*(1), 21-32.

Teitelbaum, S. L. (2000). Bone resorption by osteoclasts. *Science (New York, N.Y.), 289*(5484), 1504-1508.

Thierry, T., Francesca, G., Sundeep, K., Michael D, J., Bartolome, B., & B Lawrence, R. (1999). Leptin acts on human marrow stromal cells to enhance differentiation to osteoblasts and to inhibit differentiation to adipocytes. *Endocrinology*(4), 1630.

Thijssen, E., van Caam, A., & van der Kraan, P. M. (2014). Obesity and osteoarthritis, more than just wear and tear: pivotal roles for inflamed adipose tissue and dyslipidaemia in obesity-induced osteoarthritis. *Rheumatology, 54*(4), 588-600.

Tortosa-Caparrós, E., Marín, F., Orenes-Piñero, E., & Navas-Carrillo, D. (2017). Anti-inflammatory effects of omega 3 and omega 6 polyunsaturated fatty acids in

cardiovascular disease and metabolic syndrome. *Critical Reviews in Food Science and Nutrition, 57*(16), 3421-3429.

Toth, M. J., Tchernof, A., Sites, C. K., & Poehlman, E. T. (2000). Menopause-related changes in body fat distribution. *Ann N Y Acad Sci, 904*, 502-506.

Treschow, A. P., Hodges, L. D., Kalafatis, N., Macrides, T. A., Wright, P. F. A., & Wynne, P. M. (2007). Novel anti-inflammatory ω-3 PUFAs from the New Zealand green-lipped mussel, Perna canaliculus. *Comparative Biochemistry and Physiology - B Biochemistry and Molecular Biology, 147*(4), 645-656.

Turnbaugh, P. J., Ley, R. E., Mahowald, M. A., Magrini, V., Mardis, E. R., & Gordon, J. I. (2006). An obesity-associated gut microbiome with increased capacity for energy harvest. *Nature, 444*(7122), 1027-1031.

Vadacca, M., Margiotta, D. P. E., Navarini, L., & Afeltra, A. (2011). Leptin in immuno-rheumatological diseases. *Cellular & Molecular Immunology, 8*(3), 203-212.

Vaidya, H. B., Gangadaran, S., & Cheema, S. K. (2017a). An obesogenic diet enriched with blue mussels protects against weight gain and lowers cholesterol levels in C57BL/6 mice. *Nutr Res, 46*, 31-37.

Vaidya, H. B., Gangadaran, S., & Cheema, S. K. (2017b). A high fat-high sucrose diet enriched in blue mussels protects against systemic inflammation, metabolic dysregulation and weight gain in C57BL/6 mice. *Food Research International, 100*(Pt 2), 78-85.

Van der Lugt, B., Rusli, F., Lute, C., Lamprakis, A., Salazar, E., Boekschoten, M. V., . . . Steegenga, W. T. (2018). Integrative analysis of gut microbiota composition, host colonic gene expression and intraluminal metabolites in aging C57BL/6J mice. *Aging, 10*(5), 930-950.

Van Heerden, B., Kasonga, A., Kruger, M. C., & Coetzee, M. (2017). Palmitoleic Acid Inhibits RANKL-Induced Osteoclastogenesis and Bone Resorption by Suppressing NF-κB and MAPK Signalling Pathways. *Nutrients, 9*(5), 441.

Van Spil, W. E., Welsing, P. M. J., Bierma-Zeinstra, S. M. A., Bijlsma, J. W. J., Roorda, L. D., Cats, H. A., & Lafeber, F. P. J. G. (2015). The ability of systemic biochemical markers to reflect presence, incidence, and progression of early-stage radiographic knee and hip osteoarthritis: data from CHECK. *Osteoarthritis and Cartilage, 23*(8), 1388-1397.

Vandeweerd, J.-M., Coisnon, C., Clegg, P., Cambier, C., Pierson, A., Hontoir, F., . . . Buczinski, S. (2012). Systematic Review of Efficacy of Nutraceuticals to Alleviate Clinical Signs of Osteoarthritis. *Journal of Veterinary Internal Medicine, 26*(3), 448-456.

Vanwanseele, B., Lucchinetti, E., & Stussi, E. (2002). The effects of immobilization on the characteristics of articular cartilage: current concepts and future directions. *Osteoarthritis Cartilage, 10*, 408-419.

Vemuri, R., Gundamaraju, R., Shinde, T., Perera, A. P., Basheer, W., Southam, B., . . . Eri, R. (2019). Lactobacillus acidophilus DDS-1 Modulates Intestinal-Specific Microbiota, Short-Chain Fatty Acid and Immunological Profiles in Aging Mice. *Nutrients, 11*(6), 1297.

Villafuerte, B. C., Fine, J. B., Bai, Y., Zhao, W., Fleming, S., & DiGirolamo, M. (2000). Expressions of Leptin and Insulin-Like Growth Factor-I Are Highly Correlated and Region-Specific in Adipose Tissue of Growing Rats. *Obesity Research, 8*(9), 646-655.

Viney, M., & Riley, E. M. (2017). The Immunology of Wild Rodents: Current Status and Future Prospects. *Frontiers in Immunology, 8*, 1481-1481.

Vista, E. S., & Lau, C. S. (2011). What about supplements for osteoarthritis? A critical and evidenced-based review. *International Journal of Rheumatic Diseases, 14*(2), 152-158.

Vogel, H. G., & Vogel, W. H. (1997). *Drug Discovery and Evaluation : Pharmacological Assays*: Springer Berlin Heidelberg.

von Muhlen, D., Safii, S., Jassal, S. K., Svartberg, J., & Barrett-Connor, E. (2007). Associations between the metabolic syndrome and bone health in older men and women: the Rancho Bernardo study. *Osteoporos. Int., 18*(10), 1337–1344.

Wakimoto, T., Kondo, H., Nii, H., Kimura, K., Egami, Y., Oka, Y., . . . Abe, I. (2011). Furan fatty acid as an anti-inflammatory component from the green-lipped mussel Perna canaliculus. *Proceedings Of The National Academy Of Sciences Of The United States Of America, 108*(42), 17533-17537.

Wakitani, S., Okabe, T., Kawaguchi, A., Nawata, M., & Hashimoto, Y. (2009). Highly sensitive ELISA for determining serum keratan sulphate levels in the diagnosis of OA. *Rheumatology, 49*(1), 57-62.

Wall, R., Ross, R. P., Stanton, C., & Fitzgerald, G. F. (2010). Fatty acids from fish: The anti-inflammatory potential of long-chain omega-3 fatty acids. *Nutrition Reviews, 68*(5), 280-289.

Walsh, D. A., Bonnet, C. S., Turner, E. L., Wilson, D., Situ, M., & McWilliams, D. F. (2007). Angiogenesis in the synovium and at the osteochondral junction in osteoarthritis. *Osteoarthritis and Cartilage, 15*(7), 743-751.

Walsh, D. A., McWilliams, D. F., Turley, M. J., Dixon, M. R., Fransès, R. E., Mapp, P. I., & Wilson, D. (2010). Angiogenesis and nerve growth factor at the osteochondral junction in rheumatoid arthritis and osteoarthritis. *Rheumatology (Oxford, England), 49*(10), 1852-1861.

Wannamethee, S. G., Whincup, P. H., Rumley, A., & Lowe, G. D. (2007). Inter-relationships of interleukin-6, cardiovascular risk factors and the metabolic syndrome among older men. *Journal of Thrombosis and Haemostasis, 5*(8), 1637-1643.

Wauquier, F., Philippe, C., Léotoing, L., Mercier, S., Davicco, M.-J., Lebecque, P., . . . Wittrant, Y. (2013). The free fatty acid receptor G protein-coupled receptor 40 (GPR40) protects from bone loss through inhibition of osteoclast differentiation. *The Journal Of Biological Chemistry, 288*(9), 6542-6551.

Weisberg, S. P., Hunter, D., Huber, R., Lemieux, J., Slaymaker, S., Vaddi, K., . . . Ferrante, A. W., Jr. (2006). CCR2 modulates inflammatory and metabolic effects of high-fat feeding. *The Journal of clinical investigation, 116*(1), 115-124.

Wen, C., Lu, W. W., & Chiu, K. Y. (2014). Importance of subchondral bone in the pathogenesis and management of osteoarthritis from bench to bed. *Journal of Orthopaedic Translation, 2*, 16-25.

Wever, K. E., Geessink, F. J., Brouwer, M. A. E., Tillema, A., & Ritskes-Hoitinga, M. (2017). A systematic review of discomfort due to toe or ear clipping in laboratory rodents. *Lab Anim, 51*(6), 583-600.

Whitehouse, M. W., Macrides, T. A., Kalafatis, N., Betts, W. H., Haynes, D. R., & Broadbent, J. (1997). Anti-inflammatory activity of a lipid fraction (Lyprinol) from the NZ green-lipped mussel. *Inflammopharmacology, 5*(3), 237-246.

Whiting, S. J., Vatanparast, H., Baxter-Jones, A., Faulkner, R. A., Mirwald, R., & Bailey, D. A. (2004). Factors that affect bone mineral accrual in the adolescent growth spurt. *Journal of Nutrition, 134*, 696-700.

Wilhelmi, G., & Faust, R. (1976). Suitability of the C57 black mouse as an experimental animal for the study of skeletal changes due to ageing, with special reference to osteo-arthrosis and its response to tribenoside. *Pharmacology, 14*, 289-296.

Wollam, J., & Antebi, A. (2011). Sterol Regulation of Metabolism, Homeostasis, and Development. *Annual Review of Biochemistry, 80*(1), 885-916.

Wong, I. P. L., Zengin, A., Herzog, H., & Baldock, P. A. (2008). Central regulation of bone mass. *Seminars in Cell & Developmental Biology, 19*(5), 452-458.

Wong, S. K., Chin, K.-Y., Suhaimi, F. H., Ahmad, F., & Ima-Nirwana, S. (2018). Effects of metabolic syndrome on bone mineral density, histomorphometry and remodelling markers in male rats. *PLoS One, 13*(2), e0192416.

Woodiwiss, A. J., Libhaber, C. D., Majane, O. H., Libhaber, E., Maseko, M., & Norton, G. R. (2008). Obesity promotes left ventricular concentric rather than eccentric geometric remodeling and hypertrophy independent of blood pressure. *American Journal of Hypertension, 21*(10), 1144-1151.

Woolf, A. D., & Pfleger, B. (2003). Burden of major musculoskeletal conditions. *Bulletin of the World Health Organization, 81*(9), 646-656.

World Health Organization. (2006). BMI classification, global database on body mass index. Retrieved March, 28 2019 from http://www.who.int/bmi/index.jsp.

World Health Organization. (2020, 1 April 2020). Obesity and overweight. Retrieved April, 04 2020 from https://www.who.int/news-room/fact-sheets/detail/obesity-and-overweight.

Wortsman, J., Matsuoka, L. Y., Chen, T. C., Lu, Z., & Holick, M. F. (2000). Decreased bioavailability of vitamin D in obesity [corrected] [published erratum appears in AM J CLIN NUTR 2003 May;77(5):1342]. *American Journal of Clinical Nutrition, 72*(3), 690-693.

Wu, W., Billinghurst, R. C., Pidoux, I., Antoniou, J., Zukor, D., Tanzer, M., & Poole, A. R. (2002). Sites of collagenase cleavage and denaturation of type II collagen in aging and osteoarthritic articular cartilage and their relationship to the distribution of matrix metalloproteinase 1 and matrix metalloproteinase 13. *Arthritis & Rheumatism, 46*(8), 2087-2094.

Xiong, J., Onal, M., Jilka, R. L., Weinstein, R. S., Manolagas, S. C., & O'Brien, C. A. (2011). Matrix-embedded cells control osteoclast formation. *Nature Medicine, 17*, 1235-1262.

Xu, F., Du, Y., Hang, S., Chen, A., Guo, F., & Xu, T. (2013). Adipocytes regulate the bone marrow microenvironment in a mouse model of obesity. *Mol. Med. Rep., 8*, 823-828.

Xu, H., Barnes, G. T., Yang, Q., Tan, G., Yang, D., Chou, C. J., . . . Chen, H. (2003). Chronic inflammation in fat plays a crucial role in the development of obesity-related insulin resistance. *The Journal of clinical investigation, 112*(12), 1821-1830.

Yammani, R. R., Carlson, C. S., Bresnick, A. R., & Loeser, R. F. (2006). Increase in production of matrix metalloproteinase 13 by human articular chondrocytes due to stimulation with S100A4: Role of the receptor for advanced glycation end products. *Arthritis & Rheumatism, 54*(9), 2901-2911.

Yang, S., & Shen, X. (2015). Association and relative importance of multiple obesity measures with bone mineral density: the National Health and Nutrition Examination Survey 2005-2006. *Archives Of Osteoporosis, 10*, 1-10.

Yaturu, S., Humphrey, S., Landry, C., & Jain, S. K. (2009). Decreased bone mineral density in men with metabolic syndrome alone and with type 2 diabetes. *Medical Science Monitor, 15*, 5-9.

Yu, H. N., Zhu, J., Pan, W. S., Shen, S. R., Shan, W. G., & Das, U. N. (2014). Effects of fish oil with a high content of n-3 polyunsaturated fatty acids on mouse gut microbiota. *Archives of Medical Research, 45*(3), 195-202.

Zawadzki, M., Janosch, C., & Szechinski, J. (2013). Perna canaliculus lipid complex PCSO-524 demonstrated pain relief for osteoarthritis patients benchmarked against fish oil, a randomized trial, without placebo control. *Marine Drugs*, 11(6), 1920-1935.

Zenobia, C., & Hajishengallis, G. (2015). Basic biology and role of interleukin-17 in immunity and inflammation. *Periodontology 2000, 69*(1), 142-159.

Zhao, G., Nyman, M., & Jonsson, J. A. (2006). Rapid determination of short-chain fatty acids in colonic contents and faeces of humans and rats by acidified water-extraction and direct-injection gas chromatography. *Biomedical Chromatography, 20*, 674-682.

Zhao, L.-J., Jiang, H., Papasian, C. J., Maulik, D., Drees, B., Hamilton, J., & Deng, H.-W. (2008). Correlation of obesity and osteoporosis: Effect of fat mass on the determination of osteoporosis. *Journal of Bone and Mineral Research, 23*, 17-29.

Zhao, L. J., Liu, Y. J., Liu, P. Y., Hamilton, J. L., Recker, R. R., & Deng, H. W. (2007). Relationship of obesity with osteoporosis. *J. Clin. Endocrinol. Metab., 92*, 1640–1646.

Zhao, X., Dong, Y., Zhang, J., Li, D., Hu, G., Yao, J., . . . Li, H. (2016). Leptin changes differentiation fate and induces senescence in chondrogenic progenitor cells. *Cell Death & Disease, 7*(4), e2188-e2188.

Zhen, G., Wen, C., Jia, X., Li, Y., Crane, J. L., Mears, S. C., & al., e. (2013). Inhibition of TGF-b signaling in mesenchymal stem cells of subchondral bone attenuates osteoarthritis. *Nat Med, 19*, 704-712.

Zhou, S., Thornhill, T. S., Meng, F., Xie, L., Wright, J., & Glowacki, J. (2016). Influence of osteoarthritis grade on molecular signature of human cartilage. *Journal of Orthopaedic Research, 34*(3), 454-462.

Zhuo, Q., Yang, W., Chen, J., & Wang, Y. (2012). Metabolic syndrome meets osteoarthritis. *Nature reviews. Rheumatology, 8*(12), 729-737.

Zhou, Y., Xu, Q., Dong, Y., Zhu, S., Song, S., & Sun, S. (2017). Supplementation of Mussel Peptides Reduces aging Phenotype, Lipid Deposition and Oxidative Stress in D-Galactose-Induce Aging Mice. *J Nutr Health Aging, 21*(10), 1314-1320.

Appendices

Appendix A: Thesis output

Publication

Siriarchavatana P, Kruger MC, Miller MR, Tian HS, Wolber FM. The preventive effects of greenshell mussel (*Perna canaliculus*) on early-stage metabolic osteoarthritis in rats with diet-induced obesity. Nutrients. 2019;11(7):1601. doi:10.3390/nu11071601.

Siriarchavatana, P., Kruger, M. C., Miller, M. R., Tian, H., & Wolber, F. M. (2020). Effects of Greenshell Mussel (*Perna canaliculus*) intake on pathological markers of multiple phenotypes of osteoarthritis in rats. *Applied Sciences, 10*(17), 6131. doi: 10.3390/app10176131.

Conferences

Siriarchavatana P, Kruger MC, Miller MR, Tian HS, Wolber FM. Protective Effects of Green Shelled Mussels in Osteoarthritis. Proceedings 2019, 8, 50; doi:10.3390/proceedings2019008050, 2018 Annual Meeting of the Nutrition Society of New Zealand, 28-30th November 2018, Massey University, East Precint, Albany, Auckland.

Siriarchavatana, P; Kruger, M.C.; Wolber, F.M. (2019). Correlation between body condition score and body composition in a rat model for obesity research. 2019, NZ Branch Winter Conference, 3-4 July 2019, Massey University, Palmerston North, New Zealand

Siriarchavatana, P; Kruger, M.C.; Miller, M.R.; Tian, H.; Wolber, F.M. (2019). Protective effects of green shelled mussels in osteoarthritis. Foodomics 2019 Annual Meeting of the Nutrition Society of New Zealand, 9-11 April 2019, Cordis Hotel, Auckland.

Siriarchavatana, P; Kruger, M.C.; Miller, M.R.; Tian, H.; Wolber, F.M. (2020). Consumption of greenshell mussel increases acquisition of lean mass and bone mineral density in rats. World Congress on Oil &Fats 2020, 9-12 February 2020, International Convention Centre, Sydney, Australia

Addendum

This manuscript was produced at the beginning of the study. However, its content was not related to the main thesis, therefore this manuscript was excluded from the structure of the thesis and not intend for justification.

Correlation between body condition score and body composition in a rat model for obesity research

Parkpoom Siriarchavatana1, Marlena C. Kruger2, 3, and Frances M. Wolber1 ,4 *

1 School of Food and Advanced Technology, Massey University, Palmerston North, New Zealand; 2 School of Health Sciences, Massey University, Palmerston North, New Zealand; 3 Riddet Centre of Research Excellence, Massey University, Palmerston North, New Zealand; 4 Centre for Metabolic Health Research, Massey University, Palmerston North, New Zealand

* Correspondence: F.M.Wolber@massey.ac.nz

Running title: Body condition scoring in obese rats

Abstract

The incidences of obesity-associated chronic diseases are increasing worldwide. Research into the causes of obesity as well as potential treatments has highlighted the crucial role of preclinical studies using animal models. Rats are one of the most widely used species in obesity research. However, even with decades of research in both genetically obese rats and diet-induced obese rat models, definitive criteria to practically classify levels of obesity in the rat are not well established. The current study proposes new criteria modified from body condition score (BCS) using an animal health monitoring system. The modified criteria were tested and compared with body composition from dual energy X-ray absorptiometry scans and selected adipose tissue weights. The results showed that the modified body condition scale was highly correlated with fat deposition in the rat body, particularly the visceral and inguinal fat pads. Both pads were closely related to changes in some specific landmarks used for the scale determination. These finding should extrapolate to obese rats in other models, with the advantage that data classified in BCS can pair the animal data with human body mass index. This will enhance the value of information from preclinical studies to design and predict outcomes of subsequent human clinical trials.

Abbreviations: BC, body condition; DXA, Dual energy X-ray absorptiometry; BCS, body condition score; HFHS, high-fat-high-sugar

Introduction

Animal models play a crucial role in obesity research to unravel the complicated causes of obesity, which include usually polygenic rather than monogenic and include genetics, lifestyle, physiological disorders, aging, menopause and diet.[1, 11, 15, 19] They are also a useful tool to demonstrate efficacy of pharmaceutical agents and treatments of obesity. However, there are limited measures to monitor changes in body adiposity in animals. Body weight, body scans and body condition scoring each have both advantages and disadvantages.

Body weight is routinely used as a part of laboratory animal husbandry. It is possible to generate consistent data if the practice has been done accurately. However, weight gain will not correlate with body adiposity when confounding factors such tumor mass, organ enlargement or intraperitoneal fluid accumulation are present.[8] In addition, factors such as

sex, age, body frame size, and pregnancy status can change the reference weight.[24] In addition, body weight alone cannot be used as a measurement of obesity because obesity is determined by the ratio of weight and height as body mass index (BMI) in humans. Moreover, body weight cannot be used to compare the degree of obesity across different species of animals.

Dual energy X-ray absorptiometry (DXA) is widely used to assess body composition as well as bone mineral density in human research. By utilizing two levels of X-ray energy the scanner is able to segregate body fat mass from lean mass, thus providing a more accurate adiposity measurement than body weight alone can.[20] However, DXA scanners are rarely available in most animal facilities.

Body condition scoring has been successfully used in health monitoring programs of various animal species such as cows,[14] cats,[23] sheep,[9] and non-human primates 4 as well as of laboratory animals. Body condition scoring is a subjective technique of evaluating body fat distribution performed by estimating the body contour and palpating through the bony protuberances along the lumbar spine, hips and tail. For rodents, the criteria of this technique has been established only for mice but it should apply for use in rats as well, based on the fact that both species have fat pad distribution in the same pattern.[2] Body condition (BC) scales for mice normally range from 1-5 with one score increments.[6] The midrange score of 3 represents the optimal condition; lower scores represent poor condition and higher scores represent excessive fat deposition.

This 5-level score is appropriate and practical for routine health monitoring but not for obesity classification in research. This is because the experimental animals, which are genetically modified obese rats or rats with diet-induced obesity, tend to put on more weight much more quickly than normal rats. Thus, there is no strong evidence to support the reliability of standard BC scoring for obesity research, and there are no published data describing whether the fat distribution pattern in experimentally obese rats is similar to normal rats. It was speculated that body weight of the rats in this study would be higher than the normative value of rat's body weight. Therefore, the aim of this study was to establish and optimize a BC scoring system for obese rats by comparing data on the rats' physical condition with the information from DXA scans. To accomplish this, the standard mouse BC scale was modified into a 1-5 scale with half-score increments, and each score was provided with a new description.

Materials and methods

Animals

The animals examined in this study were also used to investigate the effects of mussel meat on obesity-induced osteoarthritis rats. The groups of the animals were determined by the influential factors on obesity (high fat-high sugar diets and/or ovariectomy). Only data from this project related to the objective of this article are reported here. Ninety six female SD rats with eight-week age were obtained from the small animal production unit of Massey University, Palmerston North, New Zealand and the experiment was carried on in the same animal facility. The animal room environment was set at 22±1°C, 45-55% humidity and 12/12 hour light-dark cycle throughout the study. One week acclimatization period was provided before initiating the study.

The rats were singly housed in conventional cages with heat-treated aspen-chip bedding. To maintain the social behavior of the animals, clear hard-plastic cages (RE Walters, Australia) with high-top wire lids were used so that the rats could stand upright and visualize each other. Food, water, and general health status was checked and recorded daily. Body weights were measured weekly using a 2-digit balance (Sartorius, USA).

The rats received standard chow diets until 12 weeks old before being introduced to the experimental diets. Filtered water in nipple bottles was provided ad lib. Clean water bottles, cages and fresh bedding were provided weekly, with the cages and other equipment cleaned using a mechanical cage washer with the last-step-heating process to eliminate cross contamination. The room and floor were cleaned daily and sanitized weekly with disinfectant. The facility is compliant with Massey University and New Zealand laboratory animal welfare standards. This animal study was approved by Massey University Animal Ethics Committee (protocol number MUAEC approval 16/112), and met or exceeded all laboratory animal care and welfare standards for New Zealand.

Experimental procedure

Ninety six female rats age 12 weeks were equally allocated (n=24) into these test groups: (1) normal diet; (2) normal diet plus mussel meat; (3) High fat-high sugar diet (HFHS); (4) HFHS plus mussel meat. Normal diets contained 5% sucrose, 5% soy oil, and; HFHS diets contained 30% sucrose, 15% soy oil, 15% lard, and 15% casein-based protein (Specialty Feeds, Glen Forrest, Western Australia), and fed the test diet for 36-38 weeks. At the age of 20 weeks old, half of each group (12 of 24 rats) was assigned to ovariectomy procedure as described by Kruger and Morel. 10 At the end of the study, BC was scored by one examiner prior to performing DXA scans. Rats were deeply anesthetized with 50ul/100 g body weight of a cocktail composed of 0.5 ml ketamine + 0.2 ml acepromazine + 0.1 ml xylazine and 0.2 ml sterile water, administered via intraperitoneal route using a 25 g hypodermic needle and 1ml-syringe. This provided an adequate immobilization for DXA scanning within 30 mins. After humane euthanasia via exsanguination and induction of pneumothorax, all fat pads were harvested separately and weighed during the necropsy process using a 3-digit balance.

Body condition scoring

Data from three rats were excluded on the advice of the attending veterinarian as the consequences of a hernia from an incomplete wound closure, an overgrown tumor and weight loss/failure to thrive. A total of 93 female rats aged 48-50 weeks old were assessed. In accordance with the objective of obesity classification, the scale here is only determined from 2.5-5 (normal condition to obesity). The categories below normal conditions (underweight) are not described here due to the lack of such cases in this study.

<u>Score 2.5</u> Rat is lean

- Segmentation of vertebral column easily palpable
- Thin flesh cover over dorsal pelvis, small amount of subcutaneous fat
- Sacrum, iliac crest and ischial tuberosity are prominent.
- Segmentation of caudal vertebrae is palpable.

Score 3.0 Rat is well-conditioned
- Segmentation of vertebral column easily palpable
- Moderate subcutaneous fat store over pelvis.
- Sacrum, iliac crest and ischial tuberosity are palpable with pressure
- Spinous process of caudal vertebrae palpable

Score 3.5 Rat is slightly overweight.
- Segmentation of vertebral column palpable with pressure
- Sacrum, iliac crest and ischial tuberosity are not palpable
- Spinous process of caudal vertebrae is not palpable
- Moderate fat store around pubis-tail base (V-shaped bottom)

Score 4.0 Rat is overweight.
- Segmentation of vertebral column palpable with pressure
- Sacrum, iliac crest and ischial tuberosity are not palpable
- Spinous process of caudal vertebrae is not palpable
- Overwhelming fat store around pubis-tail base (U-shaped bottom)
- Moderate subcutaneous fat around flanks

Score 4.5 Rat is obese
- Segmentation of vertebral column is not palpable
- Sacrum, iliac crest and ischial tuberosity are not palpable
- Spinous process of caudal vertebrae is not palpable
- Overwhelming fat store around pubis-tail base (U-shaped bottom)
-Overwhelming subcutaneous fat around flanks

Score 5.0 Rat is extremely obese
- Segmentation of vertebral column is not palpable
- Sacrum, iliac crest and ischial tuberosity are not palpable
- Spinous process of caudal vertebrae is not palpable
- Overwhelming fat store around pubis-tail base (U-shaped bottom)
- Overwhelming subcutaneous fat covers all scapular region

Data analysis

Body weight, fat depots and body composition measurements from DXA scan were pooled across all experimental groups and categorized into each BCS (2.5, 3.0, 3.5, 4.0, 4.5 and 5.0). Pearson correlation was used to evaluate the relationship between body weight or BCS with the body composition from DXA scans. Means were calculated and plotted into graphs for visualizing the fitness of curves. The statistics software IBM SPSS (version 24) was used to analyze all data in this study. A p-value <0.5 was considered statistically significant.

Results

The purpose of the main experiment was to investigate the effects of various factors driving obesity. The data were obtained to determine how the information from BCS may be of benefit in animal studies of obesity research. As can be seen in Figure 1, >50% of the sham rats on the normal formula diet group were scored 3.5 (slightly overweight). Including mussel meat in the normal diet shifted the proportion of animals in the overweight category with a score of 4.0 from <10% to >40%, although the proportion of rats in the well-conditioned category (score of 3.0) did not change as this is known that outbred stock rats are composed

of diet resistant group and obesity prone group. 5, 12 A HFHS diet, as expected, induced obesity as the almost 60% expansion of the score 4.0 and introduced another one-upper score (4.5) into this group; we have previously shown that a HFHS diet is more effective than high sugar diet alone on inducing obesity with metabolic syndrome. [16] Once again, adding mussel meat into HFHS diet caused a further increase in obese rats (score 4.5) to 50%. This information shows that both a HFHS diet and the inclusion of mussel meat have an influence on weight gain.

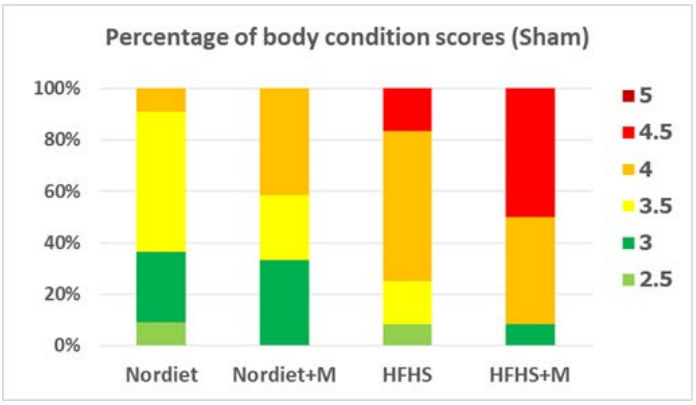

Figure 1: Percentage of body condition scores (sham)
The effects of high-fat-high sugar diet and of mussel meat on obesity incidence in ovary intact rats. Normal diet (Nordiet), normal diet plus mussel meat (Nordiet+M), High-fat-high-sugar diet (HFHS), and high-fat-high-sugar diet plus mussel meat (HFHS+M).

Data from the ovariectomized rats (Figure 2) showed a similar pattern between normal and HFHS diets but with an even more intensified obese condition. The intact rats in both normal diet groups showed no scores above 4.0 but up to 20% of the ovariectomized rats on the same diets were in two upper scores. The combination of ovariectomy and HFHS diet further exacerbated the condition, with all animals falling into the overweight, obese, or extremely obese categories. Interestingly, the inclusion of mussel meat in the diets of ovariectomized rats slightly reduced, rather than increasing, the proportion of obese (4.5-5 score) rats.

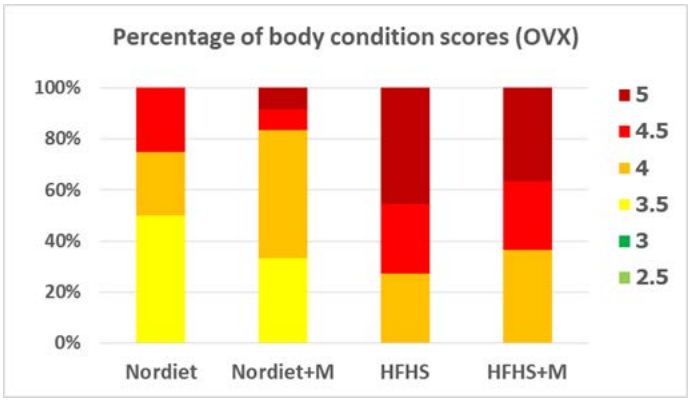

Figure 2: Percentage of body condition scores (OVX)
The effects of high-fat-high sugar diet and of mussel meat on obesity incidence in ovariectomized rats. Normal diet (Nordiet), normal diet plus mussel meat (Nordiet+M), High-fat-high-sugar diet (HFHS), and high-fat-high-sugar diet plus mussel meat (HFHS+M).

The lowest body weight of the rats were 320 g and the highest was 843.4 g. Only 10 rats (11%) were scored 2.5 and 3, which would be defined as the optimal condition, with mean weights of 322.20 g ±3.11 and 356.02 g ±13.41 respectively (Table 1). The next two categories (3.5 and 4.0) accounted for 59% of the population and covered the body weight range of 409.3-615.00 g. These two categories indicate the rats were overweight. The remaining 30% of the population occupied the two uppermost categories (4.5-5.0) and were obese (weight range=559.40-843.40 g).

Body condition score		**Body and fat pad weight (3-digit balance)**				
		Body weight (g)	**Visceral fat (g)**	**Inguinal fat (g)**	**Scapular brown fat (g)**	**Visceral: inguinal ratio**
2.5	mean±SD	322.20±3.11	22.83±4.67	4.34±0.22	0.67±0.05	5.26
(n=2)	min-max	320.00-324.40	19.53-26.14	4.19-4.51	0.64-0.71	
3	mean±SD	356.02±13.41	24.07±4.10	7.04±1.73	0.83±0.15	3.41
(n=8)	min-max	331.00-375.40	20.07-33.32	4.16-9.90	0.57-1.08	
3.5	mean±SD	444.98±25.81	35.64±7.97	12.35±4.57	0.92±0.16	2.88
(n=21)	min-max	409.30-493.00	24.79-51.65	5.95-20.69	0.69-1.31	
4	mean±SD	523.84±53.33	48.52±10.46	20.37±5.30	1.14±0.22	2.38
(n=34)	min-max	448.00-615.00	29.71-67.31	3.96-28.23	0.84-1.83	
4.5	mean±SD	623.11±37.62	63.15±10.29	29.66±8.99	1.10±0.23	2.13
(n=18)	min-max	559.40-685.00	50.25-83.87	4.00-46.74	0.72-1.63	
5.0	mean±SD	725.21±69.74	73.95±12.81	46.87±7.82	1.14±0.22	1.57
(n=10)	min-max	628.30-843.40	62.37-96.17	35.39-64.30	0.79-1.47	

Table 1: Distribution of body weights and fat deposits by body condition score
SD = standard deviation

The visceral fat including retroperitoneal and epididymal fat pad was harvested from the abdominal cavity while inguinal and subscapular brown fat pad were dissected from subcutaneous fat tissue. Inguinal fat covers the dorsolumbar region to the gluteal region. 3 Subscapular brown fat, a butterfly-like shaped pad brown in color, is fitted in between the scapulae and underneath the subscapular white fat tissue. The visceral fat pad, which was the major white fat pad examined, accounted for 7-10% of total body weight in rats across BC 2.5-5.0 (Table 1). Inguinal fat was smaller and more variable, contributing 1.34-6.45% of body weight across BC 2.5-5.0. Subscapular brown fat pads were very small by comparison. The ratio of visceral fat to inguinal fat varied, with a mean ratio of 5.26:1 in BC 2.5 and 1.57:1 in BC 5.0.

DXA scans (Table 2) showed that mean percent body fat increased consecutively from 36.56% in BC 2.5 to 64.35% in BC 5.0. Table 3 shows the correlations of body weight or BCS with body composition. Generally, it was highly correlated with all parameters except lean mass and subscapular fat. Body weight measured using a standard balance matched the total mass measured by DXA scan (Pearson correlation value 0.999).

Body condition score		DXA scan measurement			
		Fat mass (g)	Lean mass (g)	Total mass (g)	% fat
2.5	mean±SD	115.26±0.23	200.00±6.89	315.26±6.65	36.56±0.84
(n=2)	min-max	115.09-115.43	195.13-204.88	310.56-319.97	35.97-37.14
3	mean±SD	131.67±14.05	220.38±12.52	352.05±13.24	37.36±3.27
(n=8)	min-max	118.15-163.34	202.64-238.72	330.89-374.31	33.65-44.63
3.5	mean±SD	195.14±33.04	243.11±18.97	438.25±26.53	44.32±5.58
(n=21)	min-max	139.04-246.01	210.38-278.70	394.95-483.73	33.33-53.90
4	mean±SD	271.46±43.42	248.73±28.02	520.20±54.03	52.00±4.80
(n=34)	min-max	187.65-346.07	200.35-306.19	438.39-614.51	40.26-59.91
4.5	mean±SD	375.39±32.46	245.94±21.71	621.33±38.18	60.38±3.01
(n=18)	min-max	326.37-426.25	212.57-289.02	558.75-683.23	55.61-65.67
5	mean±SD	462.67±75.51	252.85±23.81	715.53±74.55	64.35±4.93
(n=10)	min-max	325.63-584.36	217.94-296.20	621.83-842.20	52.37-69.38

Table 2: Distribution of body composition by DXA scans into body condition score
SD = standard deviation

	BC score		Body weight	
	Pearson Correlation	Significance	Pearson Correlation	Significance
BC score	1		0.921	< 0.001
Body weight	0.921	< 0.001	1	
Fat mass	0.919	< 0.001	0.974	< 0.001
Lean mass	0.316	0.002	0.447	< 0.001
Total mass	0.921	< 0.001	0.999	< 0.001
% fat	0.882	< 0.001	0.877	< 0.001
Visceral fat	0.84	< 0.001	0.945	< 0.001
Inguinal fat	0.851	< 0.001	0.876	< 0.001
Subscapular brown fat	0.443	< 0.001	0.509	< 0.001

Table 3: Correlations of BCS and body weight with body composition and fat pad weight

Similarly, BCS showed a high correlation with total mass (0.921) as well as other parameters. The five most highly correlated parameters were fat mass, total mass, percent fat, visceral fat and inguinal fat. Only lean mass and subscapular fat were less well correlated. As shown in Figures 3A, 3B and 3C, the correlation curves of BCS with total mass or fat mass or percent fat fitted a near-perfect linear regression, except at the lowest score of 2.5. While this may indicate a poor correlation between the parameters at this score it is more likely due to insufficient sample size and thus requires further investigation. Conversely, lean mass and BCS showed a steep slope in the lower scores (2.5, 3.0 and 3.5) but a horizontal line in the three uppermost scores, indicating that lean mass proportionally increased under conditions of normal weight but not obesity.

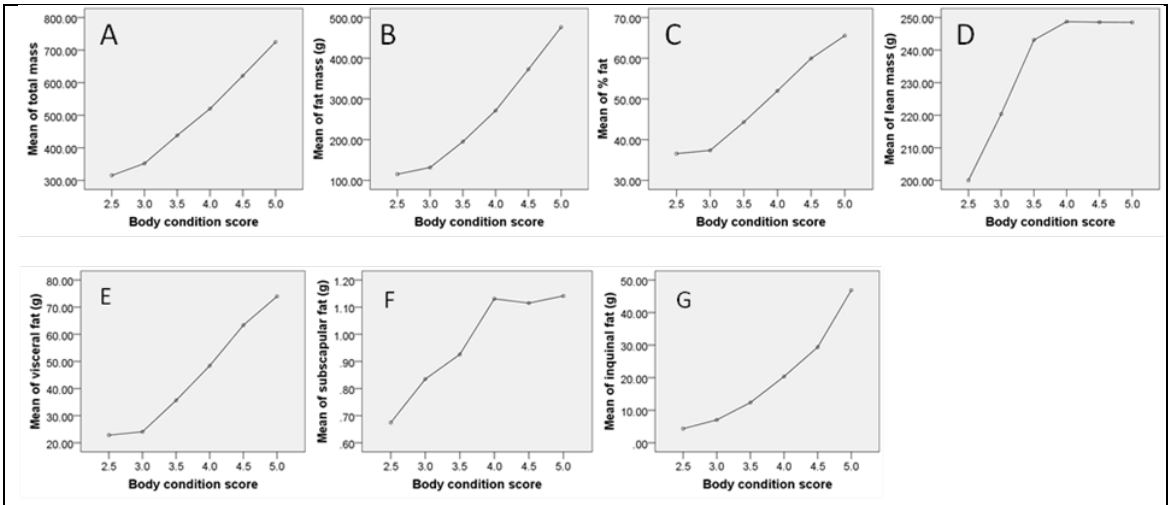

Figure 3: Relationship between body composition and body condition score. Curves show relative trends of body condition score with various parameters of body composition from DXA scans (A) total mass, (B) fat mass, (C) percent fat and (D) lean mass and with individual fat pads (E) visceral fat, (F) subscapular brown fat and (G) inguinal fat.

Visual evidence of the correlation between subcutaneous fat and obesity are shown in a set of photographs (Figure 4), in which the red line demarcates the junction of rat's costal arch and upper abdomen. In BC 2.5, this line was obviously prominent with the abrupt recession of the abdomen. The line was less dominant, with smooth recession of the abdomen, in BC 3.0. From BC 3.5 onward, the recession of abdomen was replaced with abdominal contents due to expansion of visceral fat. A second anatomical landmark, used to discriminate BC 3.5 from 4.0, was at the tail base. This region was covered with subcutaneous fat tissue, which was connected to the inguinal fat pad. As fat volume increased, the contour of this region changed from a V shape to a U shape. The third landmark was the lateral abdominal line, visible as a straight line and running parallel along the body frame in BC 4.0. This line shifted outward at BC 4.5. The final landmark, near the scapular region, was used to identify BC 5 as the subcutaneous fat at this site overwhelmed the normal body contours.

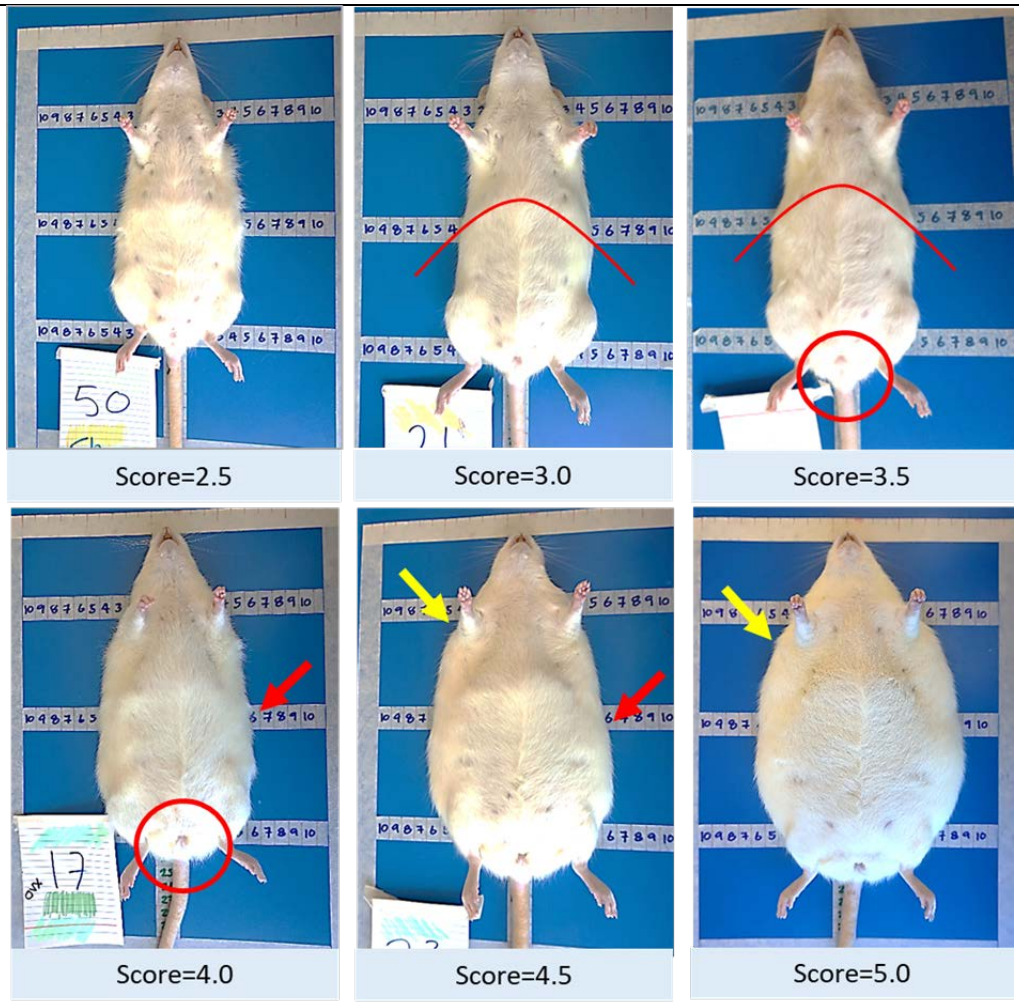

Figure 4: Characterization of the rat body to match body condition score. Changing body contours spanning BC 2.5 - 5.0 by specific landmark: Red arcing lines labels the costal arch; red circles show the tail base area; red arrows indicate the lateral abdominal line; yellow arrows indicate subcutaneous fat around the scapular area.

Discussion

Body condition scoring has conventionally been using in laboratory rat health monitoring, with the grading protocol standardized from normal rats. According to the laboratory animal guideline, the normative value of adult rat body weight is 250-300 g in females and 300-500 g in males.[7] However, the body weight of obese rats in the current study far exceeded those values. Therefore, the previous criteria do not cover the upper limit of obese rat weight. Indeed, if the BCS for routine health monitoring had been applied in to the animals in the current study, all of those with a body weight >500 g would have been scored in category[5]. These data would be too skewed to represent a normal distribution. Therefore, a new set of body scoring criteria are needed for obese rat models.

One possible solution is to stratify body weight into many levels of interval scales; however, body weight alone is still not an ideal measure to explain obesity due to numerous confounding factors. We found that the higher body weight did not always result in a higher score using the BCS criteria described above, as obesity is a factor of fat distribution. The aim of this study was to modifying the BCS criteria to better fit obesity rat research. These findings may extrapolate to and be used with current BCS in animal health monitoring programs, which have a reliable justification in normal-weight animals.

The approach used in the current study was to adjust and modify the standard scores to be proportionally dependent on body weight, body composition or fat distribution pattern of rat body. Our findings demonstrated that body weight measured using conventional animal scales and body mass calculated from DXA scans (total mass) were highly correlated (Pearson correlation =0.999). Thus, as the two methods are comparable in term of accuracy and precision, interpretation of other tissue fractions from DXA scans in vivo should be reliable as those made by physical weighing ex vivo. DXA scans provides the information of whole body fat mass, lean mass, total mass and percent fat while weighing on scales gives more detail about the different fractions of fat tissue. Each method can stand alone, but each also complements the other.

The visceral fat harvested in the current study consisted of the combination of epididymal fat and retroperitoneal fat from the abdominal cavity, whereas the two subcutaneous fat pads harvested and assessed separately were the inguinal white fat and subscapular brown fat. The result showed that both BCS and body weight had an equivalent correlation with those parameters; body weight had a slightly higher correlation coefficient with most parameters, except for percent fat (BCS=0.882 vs body weight=0.877).

Comparison of visceral, inguinal, and subscapular fat pads showed that visceral and inguinal fat increased at the same rate as total fat mass and percent fat. In particular, the curve correlating inguinal fat and BCS fitted the trend line across the spectrum, from the lowest point (BC 2.5) to extreme obesity (BC 5.0). Interestingly, the ratio of visceral/inguinal fat was reduced as BCS increased. Moreover, visceral fat only increased ~4 fold from BC 2.5-5.0 while inguinal fat increased ~10 fold. This suggests that subcutaneous fat bore a greater responsibility than visceral fat in the weight gain observed in the obese rats, and verified the study hypothesis that the distribution pattern of subcutaneous fat in particular could be used fat to classify the levels of obesity in rats and other animals.

In contrast to the white adipose tissue deposits, the change in subscapular brown fat pad weight was irregular and did not demonstrate a proportional increase at the higher scores (4.0-5.0). This corroborates other published studies that show subscapular brown fat is not linked with overall body fat deposition.[18, 22] This is due to the fact that brown adipose tissue's function is to metabolize fatty acid to generate heat.[17, 25]

Weight ranges in humans are defined by body mass index (BMI), which is a value derived from the relation of weight and height. The World Health Organization has divided human BMI into four major categories; underweight (<18.5), normal weight (18.5-24.9), over weight (25-29.9) and obese (>30),[27] with variations based on ethnicity or country. For example, Hong Kong defines BMI 25-30 as "overweight-moderate obese"[27] while Japan categorizes four levels of obesity.[21] This demonstrates the necessity of adjusting BMI ranges to fit individual populations.

BMI categories are associated with defined health risks. Overweight and underweight people have higher mortality rates than those of normal weight.[26] Similarly, high BMI subjects have a greater incidence of type 2 diabetes.[13] These examples support the

importance of including BMI in public health data. Further, information from preclinical studies that mimic the general human population is useful in epidemiological prediction modelling.

The HFHS diet in the current study increased the obese population. Similarly, ovariectomy in rats, mimicking the post-menopausal period in women, dramatically impacted obesity frequency. The combination of both factors demonstrated an additive effect. The BCS of the current study runs from BC 2.5 to 5.0, which spans the spectrum from normal weight to obese. These BCS scales could be stratified into three categories to match the human body ranges: normal weight (BCS 2.5-3.0), overweight (3.5-4.0) and obese (4.5-5.0). This would provide a visual and measurable prediction about the independent and combined consequences of consuming HFHS diet and of estrogen loss, which drive the healthy normal weight population (light-dark green zone) into obese population (light-dark red zone).

In conclusion, this study demonstrates the relationship between a HFHS diet and menopause on obesity development. The modified BC scales with clear landmark scoring parameters correlated significantly with visceral and inguinal fat pads weights; the only exception was the poor correlation between the score and the visceral fat pad normal weight animals, possibly due to insufficient sample size. The limitation of this study is that the range of BCS did not cover underweight populations. However, for rat obesity studies, the BCS presented in this study present an alternative method to identify and categorize overweight and obese animals that is both cost-effective and non-invasive.

Acknowledgement

This study was partially funded by a grant from the New Zealand Ministry of Primary Industries High Value Nutrition research program and was carried out as a collaboration between Massey University, Cawthron Institute, and Sanford Ltd. Massey University also provided financial support through a doctoral scholarship. The authors thank Anne Broomfield and Corrin Hulls for the main responsibility in surgical procedure and DXA scanning; Gabrielle Plimmer and Shampa De for supporting in necropsy.

References

1. Archer E, Lavie CJ, Hill JO. 2018. The Contributions of 'Diet', 'Genes', and Physical Activity to the Etiology of Obesity: Contrary Evidence and Consilience. Progress in Cardiovascular Diseases 61:89-102.
2. Chilliard Y. 1993. Dietary fat and adipose tissue metabolism in ruminants, pigs, and rodents: a review. J Dairy Sci 76:3897-3931.
3. Chusyd DE, Wang D, Huffman DM, Nagy TR. 2016. Relationships between Rodent White Adipose Fat Pads and Human White Adipose Fat Depots. Front nutr 3:10-10.
4. Clingerman KJ, Summers L. 2012. Validation of a body condition scoring system in rhesus macaques (Macaca mulatta): inter- and intrarater variability. J Am Assoc Lab Anim Sci 51:31-36.
5. Collins KH, Reimer RA, Seerattan RA, Herzog W, Hart DA. 2016. Response to diet-induced obesity produces time-dependent induction and progression of metabolic osteoarthritis in rat knees. J Orthop Res 34:1010-1018.
6. Foltz CJ, Ullman-Cullere M. 1999. Guidelines for assessing the health and condition of mice. Lab Animal 28:28-32.
7. Fox JG. 2015. Laboratory animal medicine. [electronic resource], Third edition ed. Elsevier.
8. Hickman DL, Swan M. 2010. Use of a Body Condition Score Technique to Assess Health Status in a Rat Model of Polycystic Kidney Disease. J Am Assoc Lab Anim Sci 49:155-159.

9. Keinprecht H, Pichler M, Pothmann H, Huber J, Iwersen M, Drillich M. 2016. Short term repeatability of body fat thickness measurement and body condition scoring in sheep as assessed by a relatively small number of assessors. Small Rumin Res 139:30-38.
10. Kruger MC, Morel PCH. 2016. Experimental Control for the Ovariectomized Rat Model: Use of Sham Versus Nonmanipulated Animal. J Appl Anim Welf Sci 19:73-80.
11. Leeners B, Geary N, Tobler PN, Asarian L. 2017. Ovarian hormones and obesity. Hum Reprod Update 23:300-321.
12. Levin BE, Hogan SUE, Sullivan AC. 1989. Initiation and perpetuation of obesity and obesity resistance in rats. Am J Physiol Regul Integr Comp Physiol 25:R766.
13. Lim JS, Lee DH, Park JY, Jin SH, Jacobs DR. 2007. A strong interaction between serum gamma-glutamyltransferase and obesity on the risk of prevalent type 2 diabetes: results from the Third National Health and Nutrition Examination Survey. Clin Chemist 53:1092-1098.
14. O'Boyle N, Corl CM, Gandy J, Sordillo LM. 2006. Relationship of body condition score and oxidant stress to tumor necrosis factor expression in dairy cattle. Vet Immunol Immunopathol 113:297-304.
15. Pradhan A. 2007. Obesity, metabolic syndrome, and type 2 diabetes: inflammatory basis of glucose metabolic disorders. Nutr Rev 65:S152-156.
16. Pranprawit A, Wolber FM, Heyes JA, Molan AL, Kruger MC. 2013. Short-term and long-term effects of excessive consumption of saturated fats and/or sucrose on metabolic variables in Sprague Dawley rats: a pilot study. J Sci Food Agri 93:3191-3197.
17. Ràfols ME. 2014. Adipose tissue: Cell heterogeneity and functional diversity. Endocrinol Nutr 61:100-112.
18. Reed DR, Duke FF, Ellis HK, Rosazza MR, Lawler MP, Alarcon LK, Tordoff MG. 2011. Body fat distribution and organ weights of 14 common strains and a 22-strain consomic panel of rats. Physiol Behav 103:523-529.
19. Ross SE, Flynn JI, Pate RR. 2016. What is really causing the obesity epidemic? A review of reviews in children and adults. J Sports Sci 34:1148-1153.
20. Rothney MP, Brychta RJ, Schaefer EV, Chen KY, Skarulis MC. 2009. Body composition measured by dual-energy X-ray absorptiometry half-body scans in obese adults. Obesity (Silver Spring) 17:1281-1286.
21. Shiwaku K, Anuurad E, Enkhmaa B, Nogi A, Kitajima K, Shimono K. 2004. Overweight Japanese with body mass indexes of 23.0-24.9 have higher risks for obesity-associated disorders: a comparison of Japanese and Mongolians. Int J Obes Relat Metab Disord 28:152-158.
22. Tatsuhiro M, Hiroyuki T, Hiroo S, Masashige S. 2002. Body fat accumulation is greater in rats fed a beef tallow diet than in rats fed a safflower or soybean oil diet. Asia Pac J Clin Nutr:302.
23. Teng KT, McGreevy PD, Toribio J-ALML, Raubenheimer D, Kendall K, Dhand NK. 2018. Strong associations of nine-point body condition scoring with survival and lifespan in cats. J Feline Med Surg 20:1110-1118.
24. Ullman-Cullere MH, Foltz CJ. 1999. Body condition scoring: A rapid and accurate method for assessing health status in mice. Lab Anim Sci 49:319-323.
25. Warner A, Kjellstedt A, Carreras A, Böttcher G, Xiao-Rong P, Seale P, Oakes N, Lindén D. 2016. Activation of β3-adrenoceptors increases in vivo free fatty acid uptake and utilization in brown but not white fat depots in high-fat-fed rats. Am J Physiol Endocrinol Metab 311:E901-E910.
26. Whitlock G, Lewington S, Sherliker P, Clarke R, Emberson J, Halsey J, Qizilbash N, Collins R, Peto R. 2009. Body-mass index and cause-specific mortality in 900 000 adults: collaborative analyses of 57 prospective studies. Lancet 373:1083-1096.
27. World Health Organization. 2004. Appropriate body-mass index for Asian populations and its implications for policy and intervention strategies. The Lancet 363:157-163.

Documents: Third party copyright

SPRINGER NATURE LICENSE
TERMS AND CONDITIONS

Apr 01, 2020

This Agreement between Massey University ("You") and Springer Nature ("Springer Nature") consists of your license details and the terms and conditions provided by Springer Nature and Copyright Clearance Center.

License Number	4800400708312
License date	Apr 01, 2020
Licensed Content Publisher	Springer Nature
Licensed Content Publication	Nature Reviews Rheumatology
Licensed Content Title	Changes in the osteochondral unit during osteoarthritis: structure, function and cartilage–bone crosstalk
Licensed Content Author	Steven R. Goldring et al
Licensed Content Date	Sep 22, 2016
Type of Use	Thesis/Dissertation
Requestor type	academic/university or research institute
Format	print and electronic
Portion	figures/tables/illustrations
Number of figures/tables/illustrations	1
High-res required	no

Appendix B: Supplementary data

Table A1: cytotoxicity assessment of GSM oil using cell viability assay (MTT)

	Concentration	Total lipid		polar lipid		Non-polar lipid	
		1 day	6 days	1 day	6 days	1 days	6 days
Morphological change score	Vehicle control (0.1% DMSO)	0	0	0	0	0	0
	10 % DMSO	4	4	4	4	4	4
	64 µg/ml	1	3	1	3	1	3
	32 µg/ml	1	2	1	2	1	2
	16 µg/ml	0	1	0	1	0	1
	8 µg/ml	0	1	0	0	0	0
	4 µg/ml	0	0	0	0	0	0
	2 µg/ml	0	0	0	0	0	0
	1 µg/ml	0	0	0	0	0	0
Percentage of cell viability	Vehicle control (0.1% DMSO)	100	100	100	100	100	100
	10 % DMSO	9.01 ±0.7	20.76 ±1.3	9.01 ±0.7	20.76 ±1.3	9.01 ±0.7	20.76 ±1.3
	64 µg/ml	71.78 ±8.0	56.82 ±29.4	72.4 ±3.5	45.07 ±18.7	76.99 ±2.0	30.00 ±9.4
	32 µg/ml	79.66 ±7.1	68.20 ±32.0	83.62 ±5.8	70.05 ±45.3	81.14 ±1.8	97.09 ±8.3
	16 µg/ml	99.49 ±27.0	95.34 ±6.6	97.29 ±7.71	91.37 ±4.4	100.6 ±6.9	85.71 ±9.1
	8 µg/ml	113.6 ±8.4	109.84 ±32.5	112.7 ±10.9	105.87 ±15.8	95.47 ±16.1	112.49 ±8.8
	4 µg/ml	148.00 ±24.5	108.94 ±21.4	125.00 ±3.0	77.03 ±26.5	103.90 ±31.5	88.01 ±18.7
	2 µg/ml	122.70 ±14.5	106.14 ±11.9	124.6 ±18.3	107.57 ±8.1	100.7 ±0.7	72.11 ±21.0
	1 µg/ml	109.7 ±10.4	104.44 ±27.0	109.3 ±13.8	118.68 ±20.4	NA	101.38 ±13.5

Score 0 = no changes (none); score 1 = slightly change, few cell affected (slightly toxic); score 2 = mild changes, some cells round/spindle shaped (mild toxic); score 3 = moderate changes, many cells round/spindle shaped (moderately toxic); score 4 = severe changes, about all cells show morphological change (severely toxic)

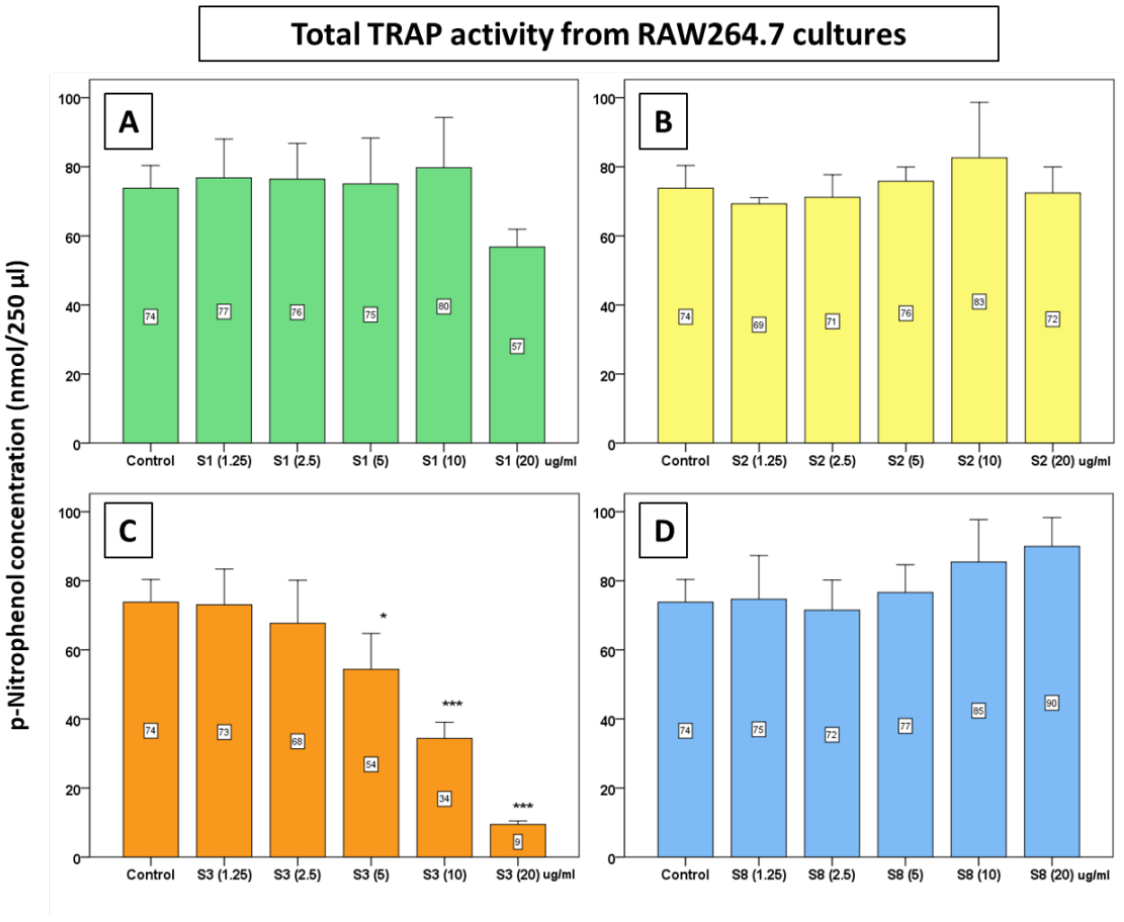

Figure A1: The inhibitory effect of the GSM extracts on osteoclast differentiation (pilot study)
The GSM extracts were incubated with the culture for 5 days in various concentrations then the supernatants were collected for the enzymatic activity measurement. The subsequent OD values from the assay were calculated into p-Nitrophenol concentration. The bar graphs and error bar represent the mean of concentration and standard deviation respectively. Image A, B, C and D show the results from GSM extracts number 1, 2, 3 and 8 respectively. Oneway-ANOVA method and Least significant differences are used to test the statistical significance. The asterisk *, **, *** mean the p value at 0.05, 0.01 and 0.001 respectively. S1 = total lipid; S2 = polar lipid; S3 = non-polar lipid., S8 = carbohydrate part of GSM meat

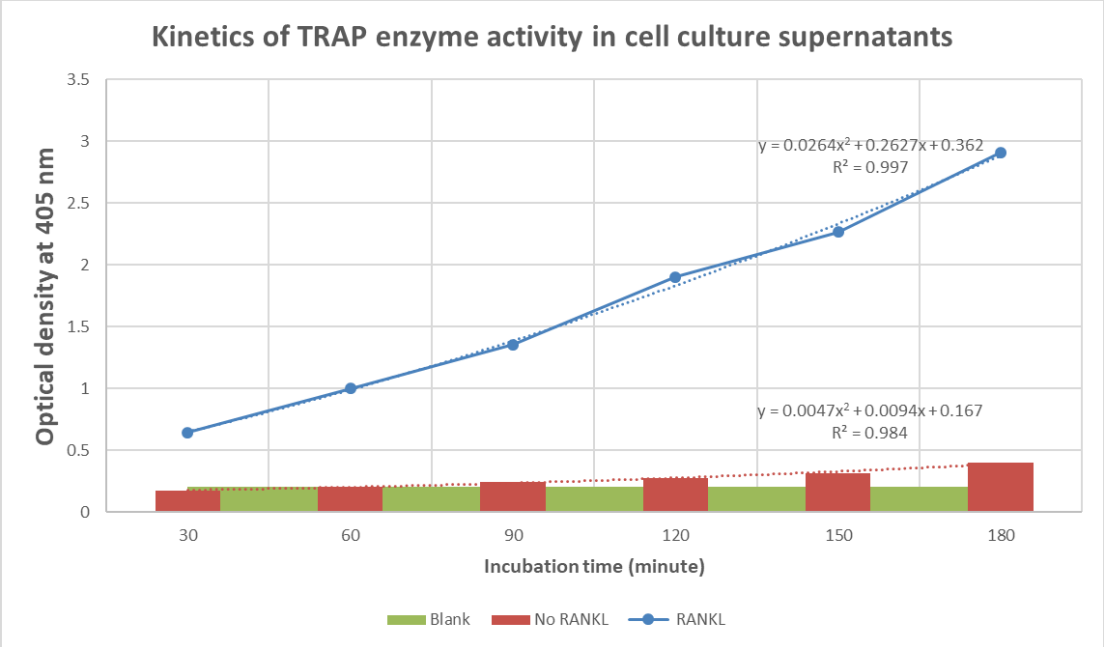

Figure A2: Kinetics of TRAP enzyme activity in cell culture supernatants
The pool samples of controls (no GSM extract) from previous TRAP assay were used to conduct this experiment. The samples were incubated with TRAP reagent in different durations ranging from 30 mins to 180 mins. The control sample which received RANKL is represented in the blue line while the control sample without RANKL is showed in red bars. The equation and coefficient value are present above their graph. The new culture media was used as a blank and show in green color.

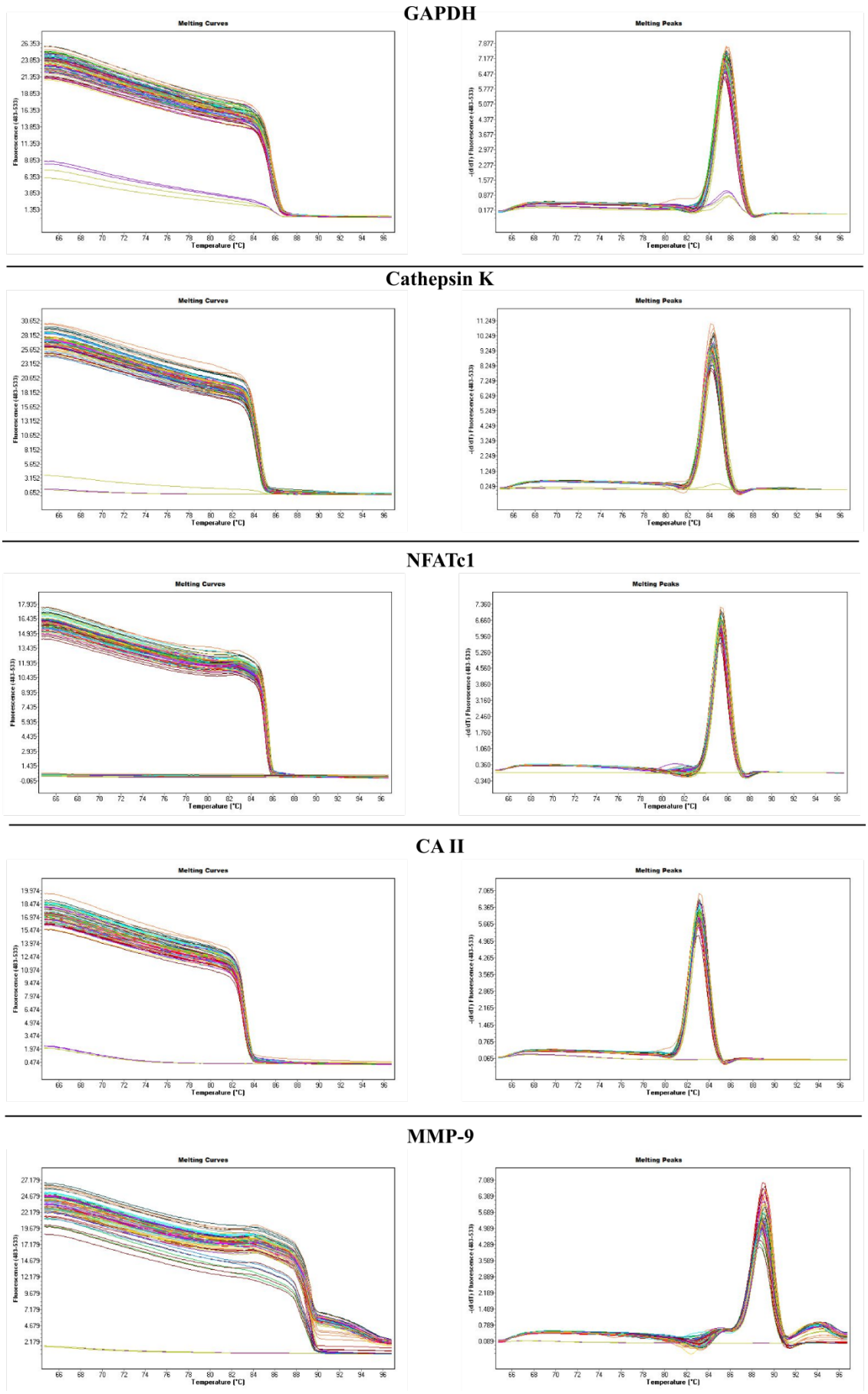

Figure A3: Melting curve and melting peak of gene expression from the osteoclast cultures were evaluated at the end of the RT-PCR process.

Table A2: Correlation of body weight or leptin with bone mineral density (data related to Figure 4.6)

ND_Sham

		Body weight	Body fat mass	Body lean mass	Leptin (ng/ml)	whole body BMD	Right femur BMD	lumbar spine BMD
Body weight	Pearson Correlation	1	.857**	.731*	0.549	.902**	.854**	.831**
	Sig. (2-tailed)		0.001	0.011	0.080	0.000	0.001	0.002
	N	11	11	11	11	11	11	11
Body fat mass	Pearson Correlation	.857**	1	0.300	.776**	.615*	.722*	.624*
	Sig. (2-tailed)	0.001		0.369	0.005	0.044	0.012	0.040
	N	11	11	11	11	11	11	11
Body lean mass	Pearson Correlation	.731*	0.300	1	0.027	.877**	.644*	.688*
	Sig. (2-tailed)	0.011	0.369		0.937	0.000	0.033	0.019
	N	11	11	11	11	11	11	11
Leptin (ng/ml)	Pearson Correlation	0.549	.776**	0.027	1	0.328	0.330	0.221
	Sig. (2-tailed)	0.080	0.005	0.937		0.325	0.321	0.513
	N	11	11	11	11	11	11	11
Whole body BMD	Pearson Correlation	.902**	.615*	.877**	0.328	1	.855**	.857**
	Sig. (2-tailed)	0.000	0.044	0.000	0.325		0.001	0.001
	N	11	11	11	11	11	11	11
Right femur BMD	Pearson Correlation	.854**	.722*	.644*	0.330	.855**	1	.875**
	Sig. (2-tailed)	0.001	0.012	0.033	0.321	0.001		0.000
	N	11	11	11	11	11	11	11
Lumbar spine_BMD	Pearson Correlation	.831**	.624*	.688*	0.221	.857**	.875**	1
	Sig. (2-tailed)	0.002	0.040	0.019	0.513	0.001	0.000	
	N	11	11	11	11	11	11	11

Table A2 (continue)

ND_OVX								
		Body weight	Body fat mass	Body lean mass	Leptin (ng/ml)	whole body BMD	Right femur BMD	lumbar spine BMD
Body weight	Pearson Correlation	1	.966**	.634*	.878**	0.502	.700*	0.081
	Sig. (2-tailed)		0.000	0.027	0.000	0.096	0.011	0.803
	N	12	12	12	12	12	12	12
Body fat mass	Pearson Correlation	.966**	1	0.430	.954**	0.553	.696*	0.206
	Sig. (2-tailed)	0.000		0.163	0.000	0.062	0.012	0.522
	N	12	12	12	12	12	12	12
Body lean mass	Pearson Correlation	.634*	0.430	1	0.212	0.306	0.555	-0.150
	Sig. (2-tailed)	0.027	0.163		0.508	0.334	0.061	0.641
	N	12	12	12	12	12	12	12
Leptin (ng/ml)	Pearson Correlation	.878**	.954**	0.212	1	0.403	0.542	0.188
	Sig. (2-tailed)	0.000	0.000	0.508		0.194	0.069	0.559
	N	12	12	12	12	12	12	12
Whole body BMD	Pearson Correlation	0.502	0.553	0.306	0.403	1	.758**	.721**
	Sig. (2-tailed)	0.096	0.062	0.334	0.194		0.004	0.008
	N	12	12	12	12	12	12	12
Right femur BMD	Pearson Correlation	.700*	.696*	0.555	0.542	.758**	1	0.333
	Sig. (2-tailed)	0.011	0.012	0.061	0.069	0.004		0.291
	N	12	12	12	12	12	12	12
Lumbar spine_BMD	Pearson Correlation	0.081	0.206	-0.150	0.188	.721**	0.333	1
	Sig. (2-tailed)	0.803	0.522	0.641	0.559	0.008	0.291	
	N	12	12	12	12	12	12	12

Table A2 (continue)

ND+GSM_ Sham								
		Body weight	Body fat mass	Body lean mass	Leptin (ng/ml)	whole body BMD	Right femur BMD	lumbar spine BMD
Body weight	Pearson Correlation	1	.910**	0.571	.937**	0.549	0.512	-0.211
	Sig. (2-tailed)		0.000	0.052	0.000	0.065	0.089	0.511
	N	12	12	12	11	12	12	12
Body fat mass	Pearson Correlation	.910**	1	0.198	.863**	0.457	0.202	-0.410
	Sig. (2-tailed)	0.000		0.517	0.001	0.116	0.507	0.164
	N	12	12	12	11	12	12	12
Body lean mass	Pearson Correlation	0.571	0.198	1	.630*	0.337	.621*	0.146
	Sig. (2-tailed)	0.052	0.517		0.038	0.261	0.024	0.634
	N	12	12	12	11	12	12	12
Leptin (ng/ml)	Pearson Correlation	.937**	.863**	.630*	1	0.348	0.393	-0.396
	Sig. (2-tailed)	0.000	0.001	0.038		0.294	0.232	0.228
	N	11	11	11	11	11	11	11
Whole body BMD	Pearson Correlation	0.549	0.457	0.337	0.348	1	0.372	0.445
	Sig. (2-tailed)	0.065	0.116	0.261	0.294		0.210	0.128
	N	12	12	12	11	12	12	12
Right femur BMD	Pearson Correlation	0.512	0.202	.621*	0.393	0.372	1	0.510
	Sig. (2-tailed)	0.089	0.507	0.024	0.232	0.210		0.075
	N	12	12	12	11	12	12	12
Lumbar spine_BMD	Pearson Correlation	-0.211	-0.410	0.146	-0.396	0.445	0.510	1
	Sig. (2-tailed)	0.511	0.164	0.634	0.228	0.128	0.075	
	N	12	12	12	11	12	12	13

Table A2 (continue)

ND+GSM_OVX								
		Body weight	Body fat mass	Body lean mass	Leptin (ng/ml)	whole body BMD	Right femur BMD	lumbar spine BMD
Body weight	Pearson Correlation	1	.949**	0.270	.840**	.624*	0.252	0.229
	Sig. (2-tailed)		0.000	0.395	0.001	0.030	0.429	0.475
	N	12	12	12	12	12	12	12
Body fat mass	Pearson Correlation	.949**	1	-0.039	.904**	.581*	0.186	0.064
	Sig. (2-tailed)	0.000		0.903	0.000	0.047	0.563	0.843
	N	12	12	12	12	12	12	12
Body lean mass	Pearson Correlation	0.270	-0.039	1	-0.140	0.291	0.320	.597*
	Sig. (2-tailed)	0.395	0.903		0.664	0.359	0.311	0.040
	N	12	12	12	12	12	12	12
Leptin (ng/ml)	Pearson Correlation	.840**	.904**	-0.140	1	0.422	0.033	0.045
	Sig. (2-tailed)	0.001	0.000	0.664		0.172	0.919	0.889
	N	12	12	12	12	12	12	12
Whole body BMD	Pearson Correlation	.624*	.581*	0.291	0.422	1	.700*	0.429
	Sig. (2-tailed)	0.030	0.047	0.359	0.172		0.011	0.164
	N	12	12	12	12	12	12	12
Right femur BMD	Pearson Correlation	0.252	0.186	0.320	0.033	.700*	1	.681*
	Sig. (2-tailed)	0.429	0.563	0.311	0.919	0.011		0.015
	N	12	12	12	12	12	12	12
Lumbar spine_BMD	Pearson Correlation	0.229	0.064	.597*	0.045	0.429	.681*	1
	Sig. (2-tailed)	0.475	0.843	0.040	0.889	0.164	0.015	
	N	12	12	12	12	12	12	12

Table A2 (continue)

HFHS_sham								
		Body weight	Body fat mass	Body lean mass	Leptin (ng/ml)	whole body BMD	Right femur BMD	lumbar spine BMD
Body weight	Pearson Correlation	1	.959**	.629*	.823**	0.516	.732**	0.210
	Sig. (2-tailed)		0.000	0.028	0.001	0.086	0.007	0.513
	N	12	12	12	12	12	12	12
Body fat mass	Pearson Correlation	.959**	1	0.393	.881**	0.382	.641*	0.237
	Sig. (2-tailed)	0.000		0.206	0.000	0.221	0.025	0.459
	N	12	12	12	12	12	12	12
Body lean mass	Pearson Correlation	.629*	0.393	1	0.214	.645*	.657*	0.078
	Sig. (2-tailed)	0.028	0.206		0.504	0.024	0.020	0.811
	N	12	12	12	12	12	12	12
Leptin (ng/ml)	Pearson Correlation	.823**	.881**	0.214	1	0.197	0.374	0.269
	Sig. (2-tailed)	0.001	0.000	0.504		0.539	0.231	0.398
	N	12	12	12	12	12	12	12
Whole body BMD	Pearson Correlation	0.516	0.382	.645*	0.197	1	.716**	0.370
	Sig. (2-tailed)	0.086	0.221	0.024	0.539		0.009	0.236
	N	12	12	12	12	12	12	12
Right femur BMD	Pearson Correlation	.732**	.641*	.657*	0.374	.716**	1	0.353
	Sig. (2-tailed)	0.007	0.025	0.020	0.231	0.009		0.261
	N	12	12	12	12	12	12	12
Lumbar spine_BMD	Pearson Correlation	0.210	0.237	0.078	0.269	0.370	0.353	1
	Sig. (2-tailed)	0.513	0.459	0.811	0.398	0.236	0.261	
	N	12	12	12	12	12	12	12

Table A2 (continue)

HFHS_OVX								
		Body weight	Body fat mass	Body lean mass	Leptin (ng/ml)	whole body BMD	Right femur BMD	lumbar spine BMD
Body weight	Pearson Correlation	1	.990**	.723*	.787**	0.260	.640*	0.420
	Sig. (2-tailed)		0.000	0.012	0.007	0.439	0.034	0.198
	N	11	11	11	10	11	11	11
Body fat mass	Pearson Correlation	.990**	1	.655*	.805**	0.187	0.596	0.369
	Sig. (2-tailed)	0.000		0.029	0.005	0.581	0.053	0.264
	N	11	11	11	10	11	11	11
Body lean mass	Pearson Correlation	.723*	.655*	1	0.224	0.485	.777**	0.372
	Sig. (2-tailed)	0.012	0.029		0.534	0.130	0.005	0.260
	N	11	11	11	10	11	11	11
Leptin (ng/ml)	Pearson Correlation	.787**	.805**	0.224	1	0.102	0.419	0.532
	Sig. (2-tailed)	0.007	0.005	0.534		0.778	0.229	0.114
	N	10	10	10	10	10	10	10
Whole body BMD	Pearson Correlation	0.260	0.187	0.485	0.102	1	.654*	.609*
	Sig. (2-tailed)	0.439	0.581	0.130	0.778		0.029	0.047
	N	11	11	11	10	11	11	11
Right femur BMD	Pearson Correlation	.640*	0.596	.777**	0.419	.654*	1	.785**
	Sig. (2-tailed)	0.034	0.053	0.005	0.229	0.029		0.004
	N	11	11	11	10	11	11	11
Lumbar spine_BMD	Pearson Correlation	0.420	0.369	0.372	0.532	.609*	.785**	1
	Sig. (2-tailed)	0.198	0.264	0.260	0.114	0.047	0.004	
	N	11	11	11	10	11	11	11

Table A2 (continue)

HFHS+ GSM_ sham								
		Body weight	Body fat mass	Body lean mass	Leptin (ng/ml)	whole body BMD	Right femur BMD	lumbar spine BMD
Body weight	Pearson Correlation	1	.911**	0.540	.771**	0.440	.873**	0.054
	Sig. (2-tailed)		0.000	0.057	0.002	0.132	0.000	0.861
	N	12	12	12	12	12	12	12
Body fat mass	Pearson Correlation	.911**	1	0.155	.922**	0.143	.724**	-0.183
	Sig. (2-tailed)	0.000		0.612	0.000	0.642	0.005	0.549
	N	12	12	12	12	12	12	12
Body lean mass	Pearson Correlation	0.540	0.155	1	-0.052	.765**	.635*	.563*
	Sig. (2-tailed)	0.057	0.612		0.866	0.002	0.020	0.045
	N	12	12	12	12	12	12	12
Leptin (ng/ml)	Pearson Correlation	.771**	.922**	-0.052	1	-0.039	.603*	-0.308
	Sig. (2-tailed)	0.002	0.000	0.866		0.898	0.029	0.307
	N	12	12	12	12	12	12	12
Whole body BMD	Pearson Correlation	0.440	0.143	.765**	-0.039	1	.695**	.818**
	Sig. (2-tailed)	0.132	0.642	0.002	0.898		0.008	0.001
	N	12	12	12	12	12	12	12
Right femur BMD	Pearson Correlation	.873**	.724**	.635*	.603*	.695**	1	0.440
	Sig. (2-tailed)	0.000	0.005	0.020	0.029	0.008		0.132
	N	12	12	12	12	12	12	12
Lumbar spine_BMD	Pearson Correlation	0.054	-0.183	.563*	-0.308	.818**	0.440	1
	Sig. (2-tailed)	0.861	0.549	0.045	0.307	0.001	0.132	
	N	12	12	12	12	12	12	12

Table A2 (continue)

HFHS+ GSM_ OVX								
		Body weight	Body fat mass	Body lean mass	Leptin (ng/ml)	whole body BMD	Right femur BMD	lumbar spine BMD
Body weight	Pearson Correlation	1	.962**	0.345	.734**	-0.111	0.470	-0.129
	Sig. (2-tailed)		0.000	0.299	0.007	0.744	0.145	0.706
	N	12	11	11	12	11	11	11
Body fat mass	Pearson Correlation	.962**	1	0.094	.879**	-0.205	0.316	-0.298
	Sig. (2-tailed)	0.000		0.783	0.000	0.545	0.344	0.373
	N	11	11	11	11	11	11	11
Body lean mass	Pearson Correlation	0.345	0.094	1	0.146	0.386	.759**	.684*
	Sig. (2-tailed)	0.299	0.783		0.668	0.242	0.007	0.020
	N	11	11	11	11	11	11	11
Leptin (ng/ml)	Pearson Correlation	.734**	.879**	0.146	1	-0.214	0.222	-0.271
	Sig. (2-tailed)	0.007	0.000	0.668		0.528	0.512	0.420
	N	12	11	11	12	11	11	11
Whole body BMD	Pearson Correlation	-0.111	-0.205	0.386	-0.214	1	0.556	.621*
	Sig. (2-tailed)	0.744	0.545	0.242	0.528		0.076	0.042
	N	11	11	11	11	11	11	11
Right femur BMD	Pearson Correlation	0.470	0.316	.759**	0.222	0.556	1	.673*
	Sig. (2-tailed)	0.145	0.344	0.007	0.512	0.076		0.023
	N	11	11	11	11	11	11	11
Lumbar spine_BMD	Pearson Correlation	-0.129	-0.298	.684*	-0.271	.621*	.673*	1
	Sig. (2-tailed)	0.706	0.373	0.020	0.420	0.042	0.023	
	N	11	11	11	11	11	11	11

Table A3: Summary_Rat body weight

Age (weeks)	**Short term cohort ----- Body weight**								ANOVA P value
	Group								
	ND (n=12)		ND+GSM (n=11)		HFHS (n=12)		HFHS+GSM (n=12)		
	Mean	SE	Mean	SE	Mean	SE	Mean	SE	
Feeding--- Standard pellet chow									
4	98.32	4.35	94.87	4.79	96.86	2.92	99.77	3.38	0.85
5	135.20	4.15	135.58	4.78	134.71	3.54	137.96	3.45	0.94
6	167.37	4.39	166.12	6.23	164.31	2.87	168.45	5.39	0.94
7	196.60	4.79	194.77	6.60	194.48	3.86	191.93	6.08	0.94
8	220.09	5.25	215.06	6.88	216.59	3.86	213.46	7.17	0.86
9	237.84	5.80	233.29	7.85	232.83	4.29	235.85	7.44	0.94
10	255.94	6.69	257.37	10.24	255.59	5.05	252.28	8.78	0.97
11	264.56	6.32	262.13	9.71	257.66	4.84	259.13	8.77	0.91
12	277.14	8.24	280.47	10.48	280.78	6.53	276.28	9.43	0.98
Feeding changed----Experimental diets based on the groups, DXA I									
13	287.44	8.47	283.83	10.43	284.67	6.17	286.40	10.02	0.99
14	289.58	9.06	292.81	10.74	309.00	8.25	308.22	11.06	0.37
15	297.24	9.21	293.00	11.32	319.13	8.66	322.65	11.73	0.11
16	295.95	8.29	303.24	13.04	329.26	9.80	333.49	13.07	0.05
17	306.17	8.76	312.66	14.03	342.01	10.47	349.17	14.45	0.03
18	309.00	8.69	313.22	14.27	344.78	11.09	349.79	15.25	0.04
19	314.04	9.59	316.95	14.65	349.77	11.62	352.08	16.48	0.08
DXA II									
20	316.11	8.93	327.34	14.69	357.92	12.69	359.10	17.53	0.06
21	319.81	8.55	328.52	14.72	360.70	12.46	369.35	18.19	0.03
22	325.08	9.29	336.23	14.88	370.98	12.60	380.85	18.94	0.02
23	329.92	9.96	338.77	15.25	376.13	13.09	386.64	20.16	0.02
24	335.21	11.23	344.42	15.15	385.12	13.64	388.17	20.69	0.03
25	337.51	11.27	350.12	15.34	394.71	13.82	402.28	22.25	0.01
26	343.71	11.74	351.85	15.38	400.89	14.56	411.71	24.03	0.01
DXA III, End of the study									

Table A3: Summary_Rat body weight (continue)

Ages weeks	**Long term cohort—Body weight**																ANOVA P values
	Sham								Ovariectomy (OVX)								
	ND (n=12)		ND+GSM (n=12)		HFHS (n=12)		HFHS+GSM (n=12)		ND (n=12)		ND+GSM (n=12)		HFHS (n=11)		HFHS+GSM (n=12)		
	Mean	SE	Mean	SE	Mean	SE	Mean	SE	Mean	SE	Mean	SE	Mean	SE	Mean	SE	
Feeding--- Standard pellet chow																	
4	103.42	4.37	96.32	3.95	97.34	3.43	97.70	3.66	97.68	4.59	102.10	4.34	101.81	5.88	100.85	3.78	0.895
5	137.45	4.92	126.62	9.84	134.02	3.67	133.03	4.57	131.37	5.47	136.76	4.20	140.49	6.66	135.28	3.71	0.823
6	168.91	5.24	172.98	5.12	171.16	4.36	167.13	4.82	169.93	4.68	176.37	5.70	173.17	7.23	170.70	3.49	0.943
7	191.72	6.51	194.15	5.43	199.63	5.23	194.29	5.11	191.85	6.38	194.54	5.85	195.49	6.15	197.98	3.96	0.975
8	222.83	9.16	223.78	5.41	228.58	6.03	225.49	6.30	223.25	7.61	215.09	5.20	222.20	6.33	228.78	4.92	0.876
9	233.62	8.07	234.93	5.02	240.10	6.53	236.05	6.14	235.27	6.81	234.73	6.90	233.87	6.20	242.93	5.19	0.966
10	259.45	9.88	259.94	5.92	263.88	6.23	261.68	5.64	257.53	7.02	255.50	6.86	258.62	5.64	265.38	5.94	0.977
11	268.48	9.80	267.71	5.92	272.06	6.92	269.57	6.60	265.74	6.87	265.88	8.06	269.44	6.98	272.78	6.63	0.996
12	273.73	8.53	276.06	6.20	280.84	7.01	281.62	7.54	275.64	8.20	267.37	8.96	276.51	7.93	280.70	6.41	0.911
	Feeding changed----Experimental diets based on the groups, DXA I																
13	284.78	8.81	286.02	6.50	288.43	7.18	287.86	6.74	285.14	6.97	281.62	7.54	288.71	8.13	290.98	6.33	0.993
14	292.40	9.15	297.28	7.04	316.51	8.49	318.23	6.98	293.45	8.22	292.41	8.52	313.51	7.50	308.65	5.53	0.047
15	297.04	10.76	303.38	7.66	332.06	10.94	336.20	7.79	300.56	7.92	297.80	9.68	330.22	7.93	332.14	9.75	0.001
16	303.34	10.14	308.48	7.41	340.90	11.55	350.70	8.74	315.13	11.18	302.63	10.25	343.47	9.71	342.12	10.92	0.001
17	311.31	11.12	316.02	7.72	355.41	11.72	362.17	9.81	312.66	7.78	310.67	11.50	354.95	10.63	350.27	11.27	0.000
18	315.08	10.62	318.89	8.43	357.47	11.84	368.85	9.92	318.01	8.36	312.98	11.14	361.44	11.72	357.15	11.55	0.000
19	317.54	11.40	325.25	8.80	358.09	11.83	375.70	10.78	321.04	8.35	319.75	14.63	366.56	12.16	361.53	11.91	0.000
	DXA II, Ovariectomy																
20	317.30	10.82	325.39	8.69	365.21	12.28	380.91	10.97	320.58	7.72	316.68	11.37	372.09	13.61	365.50	11.78	0.000
21	318.71	11.12	332.70	15.62	326.40	39.66	385.24	10.65	326.02	8.18	329.80	12.20	392.37	8.43	371.08	12.13	0.000
22	317.88	11.41	324.98	8.17	357.67	11.97	377.52	10.82	330.18	8.03	336.94	11.85	386.50	12.69	370.13	11.21	0.000
23	318.72	11.36	329.69	8.27	360.08	13.07	383.97	12.64	345.79	8.28	360.15	12.60	408.25	13.39	378.82	12.43	0.000
24	325.05	11.30	335.18	8.83	372.31	12.17	390.72	12.78	369.01	8.50	374.91	12.99	428.58	14.27	410.57	11.28	0.000
25	328.32	11.66	340.03	9.98	382.38	13.05	401.92	12.44	383.87	9.07	381.18	13.35	441.94	15.09	427.29	13.14	0.000
26	333.93	11.93	343.18	9.88	377.10	13.15	407.41	11.95	392.57	9.12	383.26	14.28	447.29	16.34	436.15	14.48	0.000
	DXA III																

Table A3: Summary: Rat body weight (continue)

Ages weeks	**Long term cohort—Body weight**																ANOVA P values
	Sham								Ovariectomy (OVX)								
	ND		ND+GSM		HFHS		HFHS+GSM		ND		ND+GSM		HFHS		HFHS+GSM		
	Mean	SE	Mean	SE	Mean	SE	Mean	SE	Mean	SE	Mean	SE	Mean	SE	Mean	SE	
27	333.92	12.06	343.72	9.88	388.36	12.83	415.88	12.48	392.23	9.85	386.70	15.15	459.18	17.62	447.43	15.33	0.000
28	335.54	12.40	349.75	9.63	397.77	13.73	422.59	12.54	403.13	11.05	394.58	15.24	470.91	17.97	458.34	14.92	0.000
29	342.41	12.73	352.75	9.99	407.18	14.99	429.26	13.08	413.28	11.41	401.39	15.80	482.28	19.01	476.57	19.59	0.000
30	343.23	12.85	358.12	10.51	413.03	14.89	437.60	13.80	417.45	11.41	405.71	16.30	494.27	20.58	487.74	19.07	0.000
31	347.53	12.65	360.08	10.32	420.21	15.30	442.52	14.27	424.07	12.22	410.80	16.71	500.90	21.13	492.61	20.11	0.000
32	347.86	12.73	366.38	11.19	423.89	15.84	454.72	15.24	426.62	12.55	415.78	16.63	507.18	21.94	501.75	20.92	0.000
33	353.37	12.86	369.99	12.51	427.15	16.82	457.45	16.80	430.48	11.84	420.23	17.16	514.27	22.73	506.06	21.17	0.000
34	355.18	13.20	374.65	12.66	430.98	17.14	460.36	16.58	430.44	12.03	424.98	17.68	522.56	23.50	516.83	22.08	0.000
35	360.05	12.93	378.05	12.73	438.90	17.38	467.38	15.87	437.70	11.85	428.31	17.62	530.62	24.02	521.13	22.10	0.000
36	364.95	13.19	383.05	12.63	445.26	17.38	477.78	15.50	445.29	12.80	431.18	18.07	538.98	24.26	527.46	21.47	0.000
37	364.51	14.06	387.87	13.54	453.28	18.77	485.12	17.03	444.09	12.99	439.03	18.17	546.80	25.18	534.20	22.39	0.000
38	367.96	14.35	387.28	13.96	459.10	19.05	490.02	18.00	449.28	13.02	440.64	18.87	550.26	26.75	536.64	22.21	0.000
39	375.30	14.68	391.70	14.63	470.14	20.51	501.59	18.44	453.66	13.44	446.01	18.90	559.31	27.39	546.50	22.14	0.000
40	379.18	14.60	399.90	14.71	477.25	21.22	508.00	18.69	464.63	14.25	452.68	19.00	571.46	28.95	554.48	21.73	0.000
	(n=11)		(n=12)		(n=12)		(n=12)		(n=12)		(n=12)		(n=11)		(n=12)		
41	379.98	16.05	402.05	14.84	484.58	22.49	514.48	18.37	467.30	14.17	453.22	20.08	575.85	29.11	565.76	22.99	0.000
42	382.25	15.35	406.62	15.66	492.18	22.90	523.39	18.42	469.26	14.01	462.30	19.73	585.85	29.52	574.63	24.56	0.000
43	386.87	15.79	414.17	16.13	499.42	23.99	530.59	18.13	474.06	14.27	467.30	19.81	593.21	30.12	580.99	25.03	0.000
44	389.69	17.04	412.11	16.17	505.87	24.65	542.62	18.93	482.23	15.12	472.39	20.50	600.09	30.33	590.00	25.93	0.000
45	395.25	17.62	415.41	16.34	509.87	25.07	550.69	20.12	486.67	16.38	475.48	21.06	606.99	31.34	593.50	26.46	0.000
46	396.33	17.69	415.73	18.06	519.28	25.20	558.18	20.56	488.49	17.00	484.85	21.06	613.56	31.64	601.28	28.16	0.000
47	397.89	17.56	421.49	17.52	529.58	26.55	567.62	21.52	493.02	18.24	482.32	21.84	621.75	32.44	609.86	28.71	0.000
48	403.89	17.30	428.18	18.05	535.38	27.16	578.15	21.78	499.20	18.56	488.27	22.36	633.35	34.01	619.05	29.34	0.000
	(n=9)		(n=9)		(n=8)		(n=12)		(n=9)		(n=9)		(n=10)		(n=8)		
49	397.78	19.24	441.30	24.11	537.58	40.61	584.99	23.04	513.76	24.44	508.96	30.16	617.31	30.55	624.29	33.45	0.000
	(n=5)		(n=5)		(n=3)		(n=6)		(n=4)		(n=7)		(n=7)		(n=5)		
50	395.94	24.43	454.50	38.44	491.33	86.23	603.97	25.91	497.40	40.58	487.20	25.92	640.03	40.43	636.86	48.14	0.000
	DXA IV, End of the study																

Table A4: Summary: Data from DXA scans

		Rats short term cohort											
		Percent change T2-T1				Percent change T3-T1				P values			
		ND (n=12)	ND+GSM (n=12)	HFHS (n=12)	HFHS+GSM (n=12)	ND (n=12)	ND+GSM (n=12)	HFHS (n=12)	HFHS+GSM (n=12)	Time	Time* Diet	Time* GSM	Time* Diet* GSM
WB_mass Fat	mean	104.42[a]	105.11[a]	242.09[b]	244.35[b]	164.13[a]	189.72[a]	421.83[b]	375.07[b]	<0.001	<0.001	0.337	0.057
	SE	14.72	17.05	32.09	15.06	29.23	27.92	51.35	27.48				
WB_mass Lean	mean	5.58[a]	10.85[b]	7.93[ab]	4.49[a]	13.35[a]	16.90[a]	13.77[a]	17.02[a]	<0.001	0.160	0.790	0.003
	SE	0.77	1.98	1.42	0.97	1.81	2.34	1.82	1.89				
WB_mass total	mean	15.42[a]	20.57[a]	31.40[b]	34.38[b]	28.42[a]	34.96[a]	54.51[b]	62.11[b]	<0.001	<0.001	0.314	0.330
	SE	1.67	2.33	2.38	2.58	3.45	3.00	3.77	5.24				
WB_ % fat	mean	75.76[a]	68.92[a]	157.57[b]	156.75[b]	101.14[a]	112.48[a]	232.89[b]	193.91[b]	<0.001	0.058	0.127	0.011
	SE	10.61	12.09	21.17	10.61	18.06	17.60	28.53	14.95				
WB_ BMC	mean	26.50[a]	30.51[a]	37.16[b]	39.62[b]	38.35[a]	45.04[a]	56.65[b]	60.44[b]	<0.001	<0.001	0.568	0.747
	SE	1.30	2.25	1.63	2.28	3.03	3.36	1.97	2.56				
WB_ BMD	mean	10.89[a]	11.51[a]	11.55[a]	13.04[a]	13.00[a]	14.93[a]	15.51[a]	15.74[a]	<0.001	0.880	0.483	0.210
	SE	0.58	0.89	0.64	0.88	1.25	1.20	0.70	1.02				
LF_ BMC	mean	25.45[a]	28.41[a]	27.85[a]	29.63[a]	35.90[a]	42.36[a]	39.41[a]	43.81[a]	<0.001	0.852	0.276	0.757
	SE	2.16	1.89	1.50	1.79	3.56	2.87	2.01	2.52				
LF_ BMD	mean	14.45[a]	13.94[a]	12.52[a]	14.68[a]	17.29[ab]	19.97[ab]	15.96[a]	20.85[b]	<0.001	0.817	0.059	0.734
	SE	1.61	0.94	1.67	1.06	1.87	1.31	1.88	1.26				
RF_ BMC	mean	24.87[a]	29.04[a]	28.23[a]	29.15[a]	35.26[a]	39.72[ab]	40.05[ab]	45.05[b]	<0.001	0.212	0.502	0.164
	SE	1.74	2.16	1.93	1.99	3.06	2.43	2.65	2.35				
RF_ BMD	mean	12.01[a]	13.32[ab]	15.28[b]	14.74[ab]	15.89[a,b]	19.79[b]	17.18[a]	22.06[b]	<0.001	0.334	0.001	0.076
	SE	1.05	1.01	1.21	1.03	1.39	1.61	1.42	1.23				
LS_ BMC	mean	26.75[a]	26.17[a]	28.78[a]	25.81[a]	34.59[a]	39.54[a]	39.76[a]	40.24[a]	<0.001	0.594	0.139	0.912
	SE	2.80	2.40	1.73	2.77	3.38	4.24	2.89	4.42				
LS_ BMD	mean	12.42[a]	12.23[a]	12.92[a]	11.47[a]	14.98[a]	17.56[a]	16.83[a]	15.52[a]	<0.001	0.775	0.475	0.537
	SE	1.74	1.14	1.28	1.59	2.05	1.65	1.69	2.42				

(Data in relation to Figure 4.3, 4-4 of Chapter 4)

Table A4: Summary: Data from DXA scans (continue)

		Rats long term cohort (sham)											
		Percent change T2-T1				Percent change T3-T1				Percent change T4-T1			
		ND (n=12)	ND+GSM (n=12)	HFHS (n=12)	HFHS+GSM (n=12)	ND (n=12)	ND+GSM (n=12)	HFHS (n=12)	HFHS+GSM (n=12)	ND (n=12)	ND+GSM (n=12)	HFHS (n=12)	HFHS+GSM (n=12)
WB_mass Fat	mean	83.94^{a}	95.74^{a}	225.15^{b}	276.93^{b}	86.99^{A}	118.39^{A}	298.44^{B}	355.69^{B}	334.61^{Z}	405.05^{Z}	787.69^{X}	960.63^{X}
	SE	12.53	11.74	22.05	28.95	16.31	17.64	31.33	48.44	45.78	59.89	81.44	117.02
WB_mass Lean	mean	7.45	8.69	7.06	8.73	14.82^{A}	12.41^{AB}	7.55^{B}	8.85^{AB}	5.39	5.54	6.95	8.47
	SE	1.89	1.53	0.78	1.17	2.67	1.88	1.05	1.37	2.78	2.78	2.10	1.48
WB_mass total	mean	18.31^{a}	19.99^{a}	32.66^{b}	39.41^{b}	24.50^{A}	26.83^{A}	41.62^{B}	48.07^{B}	50.74^{Z}	56.65^{Z}	97.85^{X}	117.05^{X}
	SE	1.60	1.55	2.31	2.10	2.19	2.01	3.17	2.98	5.10	4.27	7.46	7.81
WB_ % fat	mean	55.07^{a}	63.66^{a}	144.23^{b}	168.50^{b}	49.67^{A}	72.51^{A}	179.17^{B}	203.06^{B}	185.55^{Z}	221.94^{ZX}	344.14^{XC}	377.30^{C}
	SE	9.57	10.50	14.90	17.87	12.09	14.54	18.62	27.29	25.75	35.14	33.06	41.02
WB_ BMC	mean	27.12^{a}	27.91^{a}	37.17^{b}	43.65^{b}	34.91^{A}	36.93^{AB}	45.20^{BC}	52.80^{C}	59.62^{Z}	61.95^{Z}	82.08^{X}	89.31^{X}
	SE	1.57	1.29	2.05	1.94	2.08	2.03	2.67	3.22	3.79	3.37	4.62	5.16
WB_ BMD	mean	11.40^{ab}	10.57^{ab}	9.91^{a}	13.46^{b}	12.97^{AB}	13.07^{AB}	10.77^{A}	14.94^{B}	15.73	14.89	14.61	16.33
	SE	1.12	0.65	1.11	0.76	1.29	0.87	1.06	0.60	1.16	0.95	1.20	0.91
LF_ BMC	mean	24.68	24.64	26.75	31.01	31.08	32.42	33.63	34.80	38.39	41.81	42.69	43.03
	SE	2.35	1.78	2.34	1.20	2.69	2.31	2.71	2.64	3.67	2.07	3.61	2.82
LF_ BMD	mean	12.42	12.03	12.34	11.83	15.33	15.22	16.41	14.50	15.00	15.91	16.42	15.58
	SE	1.19	1.14	1.51	1.25	2.00	1.56	1.55	1.26	1.66	1.20	1.86	1.43
RF_ BMC	mean	24.88	28.47	25.35	29.52	32.03	35.49	29.91	35.29	39.63	44.27	41.28	44.08
	SE	2.33	1.86	2.38	1.70	3.25	2.32	2.27	1.64	4.73	2.68	3.57	2.22
RF_ BMD	mean	12.21	12.67	10.97	11.35	15.11	15.66	12.77	14.03	15.75	16.99	14.23	14.84
	SE	1.59	1.30	1.27	1.07	1.89	1.70	1.49	1.32	2.16	1.49	2.08	1.25
LS_ BMC	mean	25.10	24.04	22.55	30.55	31.06	32.37	27.39	37.56	40.53	37.86	36.48	40.60
	SE	3.11	2.02	3.50	3.62	4.22	2.39	3.38	3.72	4.99	2.18	4.08	5.02
LS_ BMD	mean	11.06	9.92	9.45	12.33	13.51	13.02	10.26	14.00	14.21	12.39	10.31	10.59
	SE	1.87	1.06	2.14	1.84	2.53	1.15	2.03	1.69	2.68	0.86	2.28	2.10

(Data in relation to Figure 4.3, 4-4 of Chapter 4)

Table A4: Summary: Data from DXA scans (continue)

		Rats long term cohort (OVX)											
		Percent change T2-T1				Percent change T3-T1				Percent change T4-T1			
		ND (n=12)	ND+GSM (n=12)	HFHS (n=11)	HFHS+GSM (n=12)	ND (n=12)	ND+GSM (n=12)	HFHS (n=11)	HFHS+GSM (n=12)	ND (n=12)	ND+GSM (n=12)	HFHS (n=11)	HFHS+GSM (n=12)
WB_mass Fat	mean	121.78^{ab}	102.91^{a}	220.93^{c}	193.48^{bc}	171.79^{A}	175.78^{A}	362.08^{B}	280.59^{AB}	709.49^{ZX}	644.59^{Z}	996.12^{X}	891.49^{ZX}
	SE	18.49	13.33	28.76	22.77	29.55	16.04	44.50	28.28	85.28	44.86	107.61	79.81
WB_mass Lean	mean	7.65	7.21	7.00	8.21	31.69^{B}	24.50^{AB}	17.20^{A}	22.20^{A}	3.29	3.87	1.92	5.80
	SE	0.80	1.52	1.68	1.07	1.89	2.46	2.85	1.67	1.18	2.06	3.31	2.00
WB_mass total	mean	21.02^{a}	19.53^{a}	35.68^{b}	33.68^{b}	47.70^{AB}	43.39^{A}	63.45^{C}	57.57^{BC}	88.00^{Z}	83.97^{Z}	135.83^{X}	127.68^{X}
	SE	1.77	1.64	3.55	2.36	2.45	2.22	5.08	3.08	4.18	5.55	11.80	7.60
WB_ % fat	mean	81.93^{a}	69.11^{a}	133.43^{ab}	118.51^{b}	81.86^{A}	92.05^{A}	178.68^{B}	141.13^{AB}	328.88	303.18	357.20	338.88
	SE	13.64	9.42	15.46	15.28	17.87	10.33	21.16	17.15	43.10	18.48	27.90	37.36
WB_ BMC	mean	28.61^{a}	28.80^{a}	40.84^{b}	39.77^{b}	42.85^{A}	41.80^{A}	53.48^{B}	50.44^{AB}	74.46^{Z}	70.33^{ZX}	91.96^{XC}	87.90^{C}
	SE	2.00	1.81	2.97	1.52	2.81	1.73	4.23	2.05	4.24	2.93	5.92	3.11
WB_ BMD	mean	10.88	14.17	11.14	12.42	10.27	12.59	10.08	10.80	12.92	12.96	12.92	11.44
	SE	0.99	1.38	1.23	1.11	1.17	1.20	1.14	1.33	1.49	1.22	1.65	1.25
LF_ BMC	mean	26.13	30.25	29.30	30.51	28.88	30.92	32.28	29.25	26.83	29.69	37.74	28.16
	SE	2.06	2.04	3.05	2.38	2.78	1.97	3.25	2.74	3.72	3.01	4.46	3.96
LF_ BMD	mean	10.92	12.43	11.96	12.12	9.91	10.35	11.44	9.90	2.62	3.90	9.17	4.72
	SE	1.24	1.37	1.90	1.54	1.38	1.29	2.35	1.79	1.88	1.28	2.79	2.57
RF_ BMC	mean	25.49	28.43	26.85	30.33	28.87	31.23	33.55	28.59	29.72	29.57	37.13	30.77
	SE	2.09	2.18	3.00	2.14	2.85	2.73	3.89	2.88	3.27	3.27	4.57	3.70
RF_ BMD	mean	11.76	14.12	10.75	14.28	9.40	11.20	11.34	9.84	4.07	5.36	8.41	7.01
	SE	1.28	1.49	1.41	1.47	1.46	1.44	1.66	1.48	1.67	1.58	1.82	2.42
LS_ BMC	mean	22.47	27.20	25.03	31.75	26.79	28.04	25.05	28.86	19.86	14.24	27.63	26.08
	SE	3.60	2.15	3.62	1.81	3.01	3.75	4.74	2.58	4.93	3.50	4.45	3.25
LS_ BMD	mean	8.06	12.18	10.10	13.39	6.92	7.97	6.71	9.00	-1.66	-4.22	1.44	0.96
	SE	1.65	1.31	2.15	1.04	1.67	1.65	2.54	1.03	2.56	1.98	2.10	1.71

(Data in relation to Figure 4.3, 4-4 of Chapter 4)

Table A4: Summary: Data from DXA scans (continue)

	DXA data_ Long term cohort_ statistical analysis_ Repeated Measure method							
	time	time * diet	time * extract	time * condition	time * diet * extract	time * diet * condition	time * extract * condition	time * diet * extract * condition
WB_mass Fat	<0.001	<0.001	0.693	<0.001	0.464	0.040	0.098	0.508
WB_mass Lean	<0.001	<0.001	0.105	<0.001	0.004	0.327	0.586	0.344
WB_mass total	<0.001	<0.001	0.367	<0.001	0.825	0.561	0.112	0.519
WB_ % fat	<0.001	<0.111	0.829	0.001	0.337	0.009	0.482	0.620
WB_ BMC	<0.001	0.050	0.007	<0.001	0.992	0.015	0.272	0.768
WB_ BMD	<0.001	0.483	0.002	<0.001	0.640	0.692	0.185	0.370
LF_ BMC	<0.001	0.448	0.073	<0.001	0.018	0.251	0.197	0.807
LF_ BMD	<0.001	0.066	0.339	<0.001	0.287	0.244	0.409	0.679
RF_ BMC	<0.001	0.264	0.115	<0.001	0.250	0.757	0.128	0.376
RF_ BMD	0.001	0.143	0.134	<0.001	0.281	0.149	0.125	0.280
LS_ BMC	<0.001	0.050	0.007	<0.001	0.992	0.015	0.272	0.768
LS_ BMD	<0.001	0.347	0.003	<0.001	0.866	0.015	0.231	0.527

(Data in relation to Figure 4.3, 4-4 of Chapter 4)

Table A5: Summary: Rat fat pads from dissection

		Short term cohort				Long term cohort (sham)				Long term cohort (OVX)			
		26 weeks old (non-surgery)				48 weeks old (sham)				48 weeks old (OVX)			
		ND (n=12)	ND+GSM (n=12)	HFHS (n=12)	HFHS +GSM (n=12)	ND (n=12)	ND+GSM (n=12)	HFHS (n=11)	HFHS +GSM (n=12)	ND (n=12)	ND+GSM (n=12)	HFHS (n=11)	HFHS +GSM (n=11)
Body weight	mean	343.71	351.85	400.89	411.71	395.94	454.500	491.33	603.97	497.40	487.20	640.03	636.86
	SE	11.74	15.38	14.560	24.03	24.43	38.44	86.23	25.91	40.58	25.92	40.43	48.14
Fat tissues													
Retroperitoneal	mean	9.05	10.99	19.29	18.81	18.22	18.72	32.84	35.46	26.38	24.02	38.97	39.86
	SE	1.08	1.63	1.45	1.47	1.72	1.79	3.17	2.36	2.18	2.39	2.88	3.74
Epididymal	mean	8.80	8.75	15.32	17.90	13.45	13.43	21.52	24.87	17.40	16.54	26.02	21.11
	SE	0.84	0.92	1.52	1.65	1.52	1.27	1.43	1.70	1.06	1.50	2.14	1.61
Inguinal	mean	5.23	4.70	7.95	10.71	8.29	11.17	17.76	25.22	19.49	19.22	36.57	36.95
	SE	0.80	1.25	1.14	2.34	0.99	1.58	2.48	1.83	1.83	2.62	3.49	4.02
Interscapular	mean	0.83	0.90	0.97	1.10	0.86	1.05	1.15	1.26	0.92	1.03	1.00	1.06
	SE	0.05	0.06	0.05	0.09	0.05	0.05	0.08	0.07	0.04	0.07	0.06	0.05
Total fat	mean	23.91	25.34	43.53	48.52	40.83	44.37	73.28	86.81	64.19	60.80	102.56	98.99
	SE	2.18	3.70	3.43	4.88	3.71	4.34	6.25	5.00	4.52	5.64	7.91	8.51

Statistical analysis by repeated measure method

	Between 26 weeks old (non-surgery) and 48 weeks old (sham)							Between 48 weeks old (sham) and 48 weeks old (OVX)						
	diet	GSM	Time	diet * extract	diet * Time	GSM* Time	diet *GSM * Time	diet	GSM	OVX	diet * GSM	diet * OVX	GSM* OVX	diet * GSM * OVX
Body weight	<0.001	0.72	0.72	0.043	0.546	0.108	0.72	0.003	0.018	0.42	0.764	0.998	0.041	0.126
Fat tissues														
Retroperitoneal	<0.001	0.404	<0.001	0.958	0.017	0.763	0.409	<0.001	0.822	0.001	0.464	0.690	0.531	0.879
Perigonadal	<0.001	0.138	<0.001	0.130	0.329	0.842	0.851	<0.001	0.578	0.078	0.878	0.152	0.041	0.094
Inguinal	<0.001	0.009	<0.001	0.097	0.002	0.087	0.784	<0.001	0.139	<0.001	0.458	0.11	0.148	0.576
Interscapular	<0.001	0.011	0.007	0.931	0.436	0.580	0.424	<0.001	0.010	0.082	0.501	0.033	0.480	0.788
Total_fat	<0.001	0.059	<0.001	0.273	0.011	0.388	0.603	<0.001	0.543	<0.001	0.555	0.920	0.150	0.541

(Data in relation to Figure 4.2 of Chapter 4)

Table A6: Summary: Short chain fatty acid levels in rat caecal contents

Short term rats

	ND (n=13)	ND+GSM (n=11)	HFHS (n=12)	HFHS+GSM (n=11)	P values
Acetic acid (µg/ml)	1.88±0.43	2.42±0.52	2.47±0.51	2.77±0.67	0.683
Proprionic acid (ng/ml)	160.26±18.26[b]***	212.81±22.91[b]	77.74±13.02[a]	92.39±10.74[a]	<0.001
Buteric acid (ng/ml)	188.37±35.78**	145.38±21.34	115.44±12.94	120.31±14.59	0.126
Valeric acid (ng/ml)	26.26±1.27[b]***	22.55±0.82[a]	23.24±0.78[ab]	23.87±0.80[ab]	0.047
TotalSCFA (µg/ml)	2.26±0.45	2.80±0.52	2.69±0.51	3.01±0.67	0.779

Long term rats

	Sham				OVX				
	ND (n=11)	ND+GSM (n=13)	HFHS (n=12)	HFHS+GSM (n=13)	ND (n=12)	ND+GSM (n=12)	HFHS (n=11)	HFHS+GSM (n=10)	P values
Acetic acid (µg/ml)	1.25±0.18	1.31±0.33	0.96±0.04	1.07±0.07	1.45±0.37	1.23±0.25	1.56±0.65	0.93±0.09	0.836
Proprionic acid (ng/ml)	60.11±9.04[abcd]	78.79±6.11[cd]	45.32±3.73[ab]	59.42±7.90[abcd]	83.41±9.10[bcd]	73.43±6.70[d]	37.98±5.70[a]	49.70±6.35[abc]	<0.001
Buteric acid (ng/ml)	51.38±10.51	55.94±6.82	36.76±3.67	50.53±14.50	53.82±8.28	44.70±5.20	30.27±4.75	44.55±7.34	0.396
Valeric acid (ng/ml)	20.05±0.64	20.65±0.73	19.94±0.64	20.79±0.84	21.74±0.96	20.99±0.62	20.22±0.66	21.34±0.85	0.689
TotalSCFA (µg/ml)	1.39±0.19	1.47±0.34	1.06±0.05	1.21±0.07	1.61±0.38	1.38±0.25	1.65±0.65	1.05±0.10	0.811

Statistical analysis by two-way ANOVA with three effects

	diet	GSM	OVX	diet * GSM	diet * OVX	GSM * OVX	diet * GSM * OVX
Acetic acid	0.663	0.662	0.383	0.199	0.117	1.316	0.284
Proprionic acid	0.000	0.061	0.842	0.310	0.110	0.125	0.181
Buteric acid	0.085	0.085	0.085	0.085	0.085	0.085	0.085
Valeric acid	0.583	0.583	0.583	0.583	0.583	0.583	0.583
TotalSCFA	0.326	0.458	0.545	0.702	0.762	0.232	0.629

(Data in relation to Figure 7.2 of Chapter 7)